

**SEDIMENTLOGY AND GEOCHEMISTRY OF THE
LIMESTONE SUCCESSIONS OF THE LOWER
MEMBER OF THE QULQULA FORMATION,
KURDISTAN REGION, NE-IRAQ**

**A THESIS
SUBMITTED TO THE COLLEGE OF SCIENCE, UNIVERSITY
OF SULAIMANI, IN PARTIAL FULFILLMENT OF THE
REQUIRMENTS FOR THE DEGREE OF DOCTORATE OF
PHILOSOPHY IN
GEOLOGY**

BY

Sardar Mohammad Raza

M.Sc. in Geochemistry, Baghdad University, (2000)

Supervised by:

Dr. Habib Rasheed Habib

Professor

Dr. Kamal Haji Karim

Assistant Professor

February, (2009) (A.D)

Rebandan, 2708 (KU)



رَبَّنَا كُنَّا بِمَسْرِ النَّبِيِّ رَاكِبَةً وَهِيَ
سَرَّاءُ نَحْنُ نَحْنُ مَا نَحْنُ مَا نَحْنُ مَا نَحْنُ مَا نَحْنُ

لَنَا بِمَسْرِ النَّبِيِّ رَاكِبَةً وَهِيَ
سَرَّاءُ نَحْنُ نَحْنُ مَا نَحْنُ مَا نَحْنُ مَا نَحْنُ

بِسْمِ اللَّهِ الرَّحْمَنِ الرَّحِيمِ



Supervisor Certification

We certify that this thesis (**Sedimentology and Geochemistry of Limestone Successions of the Lower Member of the Qulqula Formation, Kurdistan Region, NE-Iraq**) is prepared under our supervision at the University of Sulaimani, College of Science, Department of Geology as a partial requirement for the degree of Doctorate of Philosophy in Geology.

Signature: 

Supervisor: Habib Rasheed Habib

Title: Professor

Address: University of Baghdad
College of Science
Department of Geology

Date: 15 / 2 / 2009

Signature: 

Supervisor: . Kamal Haji Karim

Title: Assistant Professor

Address: University of Sulaimani
College of Science
Department of Geology

Date: 15 / 2 / 2009

In the view of the available recommendations, I forward the thesis for debate by the examining committee

Signature: 

Supervisor: *Dr. Kamal Haji Karim / Assistant Professor*

**Head of the Departmental Committee
on Graduate Studies in Geology**

Date: 15 / 2 / 2009

Approved by the Council of the College of Science

Signature:

Name: *Dr. Parekhan M. Abdul-Rahman*

Title: *Assistant Professor*

Date: 15 / 2 / 2009

Linguistic Evaluation Certification

I hereby certify that this thesis has been read and checked and after indicating all the grammatical and spelling mistakes; the thesis was given again to the candidate to make the adequate corrections. After the second reading, I found that the candidate corrected the indicated mistakes. Therefore, I certify that this thesis is free from mistakes.


Name: *Fenik M. Ghahur*


Signature: *[Handwritten Signature]*


Date: *22/10* / 2008


English Department /College of Languages/ Sulaimani University


We, the examining committee, hereby certify that we have read this thesis and examined the student in its contents and whatever relevant to it and, in our opinion; it is adequate with " " standing for the Doctorate of Philosophy in Geology.

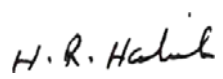
Signature: 
Name: **Dr. Basim Abdulkhaliq Al-Qayim**
Title: *Professor*
Address: *University of Sulaimani*
Date: *15 / 2 / 2009*
(Chairman)


Signature: 
Name: **Dr. Mazin Yousif Tamr Agha**
Title: *Professor*
Address: *University of Salahadeen*
Date: *15 / 2 / 2009*
(Member)

Signature: 
Name: **Dr. Sabah Ahmed Ismail**
Title: *Assistante Professor*
Address: *University of Kirkuk*
Date: *15 / 2 / 2009*
(Member)

Signature: 
Name: **Dr. A. Z. Tamin**
Title: *Expert*
Address: *State Company of Geological Survey and Mining*
Date: *15 / 2 / 2009*
(Member)

Signature: 
Name: **Dr. Habib Rashid Habib**
Title: *Assistante Professor*
Address: *University of Salahadeen*
Date: *15 / 2 / 2009*
(Member)

Signature: 
Name: **Dr. Habib Rashid Habib**
Title: *Professor*
Address: *University of Baghdad*
Date: *15 / 2 / 2009*
(Supervisor and Member)

Signature: 
Name: **Dr. Kamal Haji Karim**
Title: *Assistant Professor*
Address: *University of Sulaimani*
Date: *15 / 2 / 2009*
(Supervisor and Member)

Dedicated To:

***The Soul of my
Father, Mother and My Brother***

***My wife
and
Who Search for the Truth***

ACKNOWLEDGEMENTS

I am deeply indebted to Dr. Habib Rashid Habib and Dr. Kamal Haji Karim for their undertaking the task of supervising this thesis and offering many suggestions and corrections during all stages of the work in the field and lab. My best thanks to the dean of the College of Science (Dr. Parykhan Mohamad Abdulrahman) and also the head of the Department of Geology for their generous support including equipments facilities that offered to this work.

I would like to express my gratitude to the university presidency for providing the financial support for transportation (during fieldwork) and printing the draft and final copy of this work.

I would like to express, from my heart and soul, thanks to my wife for her patience during the whole period of my study helping in drawing and typing, and also best special thanks to my nephew Rezhan Jameel and to Mr. Musheer Mustafa for their considerable assistance in field work and Dr. Yousif Osman for his support in analyzing MPA in Japan.

Sardar

October, 2008

ABSTRACT

The lower member of Qulqula Formation is exposed in the Thrust Zone, North East of Iraq (Kurdistan Region) near the Iraqi-Iranian border. The lower part consists of alternation of more than four detrital limestone successions each more than 25m thick, which alternate with thick intervals of bedded chert and calcareous shale. These limestone successions are studied sedimentologically and geochemically in five outcrop sections. These sections are Dostadara, Kaolos, Type section, Tawella, and Gali. The limestones successions are mainly of distinctly bedded and show coarse grain lithology of shallow marine origin. All successions are mainly composed of low diversity allochems and facies such as, grainstone and packstone of one or the mixture of the allochems such as peloids, ooids, intraclasts and bioclasts which are suffered from different degrees of micritization, and there is a little of wackstone and mudstone.

The middle parts of the studied area (Dostadara and Gali sections) have more thickness and contain coarser grains than the other sections. The Tawella section consists mostly of pelloid while the Type section (near Qulqula village) is only one that contains algal boundstone. The cement material consists mostly of blocky cement and minor amount of matrix (lime mud).

The lower part of Qulqula Formation overlies the Balambo and Kometan Formations and a conglomerate bed 0.2–2 m thick separates the two formations. In the present study, the lower boundary is considered as tectonic and the existed conglomeratic bed is studied and inferred that it belongs to Tanjero Formation. It is discovered that, with the conglomerate, slices of the Shiranish Formation occurs below the lower part of the Qulqula Formation.

This conglomerate is about 35 Km nearly continuously in the field, from Said Sadiq town to Chuwarta town. At 6Km to the east of Chuwarta town, the conglomeratic bed combines with the conglomerate beds of the lower part of Tanjero Formation (Maastrichtian). The lithology of the conglomeratic bed is similar to the conglomerate of the Tanjero Formation; both of them consist, lithologically, of variegated chert and limestone clasts. Therefore, the two conglomerates have the same age and origin. The only difference is that the conglomerate of Tanjero Formation is characterized by better roundness and sorting than the concerned conglomerate in present study. The difference is attributed to more closeness to the sources area. The occurrence of Shiranish Formation and conglomeratic bed of Tanjero Formation below Qulqula Formation is attributed to thrusting of the Formation on them. The Upper boundary of the formation shows tectonic contact with different stratigraphical units of younger ages. These younger units are such as Red Bed Series, Tanjero Formation and Quaternary sediments (Bamo Conglomerate) thrust or slid over the Qulqula Formation.

The depositional environment was high energy normal marine shallow platform of ramp setting. The facies analyses indicated that the middle part of the studied area Koalos, Dostadara and Gali sections were deposited in the mid-ramp while the Type section and Tawella sections are deposited in inner and outer ramp respectively. Generally the environment becomes shallower from extreme South East toward extreme North West, but vertically becomes shallower in the middle part. The tectonic setting consisted of extensional basin which is developed during the late phase of the Neo-Tethysis opening.

The result of the chemical analyses also aids that the four successions have the same origin which all of them detached from one succession and separated into more than four successions by reverse or thrust faulting. This is because the geochemical analyses did not give strong anomaly that enable researcher to give them different origins.

The XRD analyses of the bulk and insoluble residues samples showed that the main mineral compositions of the limestone successions (according to abundance) are calcite with little Mg-Calcite, Quartz and Kolinite.

The presence of apatite mineral in Type Locality and Dostadara (1st Ridge) is confirmed by MPA.

The cluster analysis of all limestone beds of all studied sections, which includes 60 samples with 18 geochemical variables, explains 3 main groups: Limestone content, clay with I.R. content and trace elements.

Factor Analysis from all localities included in this study revealed seven factors affecting the total number of samples which is 60 samples; the main factor is carbonate factor which includes the presence of kaolinite mineral.

Another main factor indicating the presence of phosphate grains or apatite in the studied rocks and also there are indications of recrystallization, Mg-Calcite and diagenesis.

LIST OF CONTENTS	
Chapter One: INTRODUCTION	
Subject	Page
1.1. Preface.....	1
1.2. Location and Geomorphology.....	1
1.3. Geological Setting.....	3
1.4- Previous Studies.....	6
1.5. Aim of the Study	9
1.6. Studied Sections.....	9
1.6.1. Sections of Central or Middle Part of the Studied Area (MP)	9
1.6.2. Section of the Southeastern Part.....	10
1.6.3. Section of the Northwestern Part.....	10
1.7. Methodology.....	10
Chapter Two: STRATIGRAPHY AND SEDIMENTOLOGY	
2.1. Introduction.....	16
2-2. Lithology of the Lower Part of the Formation.....	16
2.2.1. Conglomeratic Bed at the Base of the Lower part as Lower Boundary of the Formation....	17
2.2.2. Limestone Successions at the Lower Member of the Formation	19
2.3. Criteria for Finding the Top and Bottom (Way Up) of the Limestone Members.....	24
2.3.1. Rip-up Clasts.....	25
2.3.2. Cross Lamination.....	25
2.3.3. Graded Bedding.....	25
2.3.4. Channel Gutter (Small Channels)	27
2.4. Upper Boundaries of the Formation.....	28
2.4.1. Upper Boundary at the Northwest Part of the Studied Area (NP)	30
2.4.2. In the Area between Nalparez and Tawella Towns	31
2.4.2.1. Thick Bedded Conglomerate.....	31
2.4.2.2. Separate Bocks of Conglomerate.....	31
2.4.2.3. Slipped Bedded Bocks.....	31
2.4.2.4. In the Penjween Area.....	32
2.4.2.5. In the Area at the Northwest of Halabja Town.....	32
2.5. Cyclicity Indicators in Qulqula Formation	32
2.5.1. Signals of Cyclicity.....	32
2.5.2. Reason of Cyclicity and Time Relation between Lithologies.....	33
2-6- Origin of the Chert nodules and beds in the Qulqula Formation.....	34
2.6.1. Origin of Chert Nodules.....	34
2.6.2. Origin of Bedded Cherts.....	36
Chapter Three: MICROFACIES ANALYSES	
3.1. Introduction.	40
3.2. Lithofacies Variation.....	40
3.3. The Microfacies of the Limestone Successions.....	41
3.3.1. Grainstone Microfacies.....	41
3.3.1.1. Lithoclasts Grainstone.....	41
3.3.1.2. Bioclastic Grainstone.....	44
3.3.1.3. Peloidal Grainstone	45
3.3.1.4. Oo-Pelloidal Grainstone.....	48
3.3.2. Rudstone Facies.....	51
3.3.3. Bindstone Lithofacies.....	52
3.3.4. Floatstone Facies.....	54
3.3.5. Mudstone Microfacies.....	54
3.3.6. Chert Nodules Bearing Lime Wackestone Submicrofacies....	55

3.3.7. Intraclastic Wackstone.....	55
3.4. Environment of Deposition....	59
3.4.1. Rimmed Versus Ramp Platform.....	60
3.4.2. Source Area.....	61
Chapter Four: GEOCHEMISTRY	
4.1. Introduction.....	64
4.2. Analytical procedure....	65
4.2.1. Determination of Major and Trace Elements...	65
4.2.2. Separation of Insoluble Residue Contents.....	65
4.2.3. The Loss On Ignition	65
4.2.4. Micro Probe Analyses (MPA).....	66
4.3. X-Ray Diffraction Analyses.....	67
4.3.1. Bulk Sample Mineral Composition.....	67
4.3.2. Mineral Content of The Insoluble Residue.....	67
4.4. Major Oxides Geochemistry.....	69
4.5. Trace Element Geochemistry.....	85
4.6. Statistics and Data Analysis.....	95
4.6.1. Preface.....	95
4.6.2. Precision and Accuracy.....	96
4.6.3. Cluster and Factor Analyses.....	99
Conclusions.....	112
References.	114

APPENDIXES

<u>Title</u>	<u>Page</u>
Appendix (A): Major oxide, Trace Element and Insoluble Residue content in the limestone bulk and insoluble residue samples from Qulqula Fm.....	127
Appendix (B): XRD patterns of some black limestone powder bulk and insoluble residue samples illustrating the diffraction maximum pattern of Calcite and little Kaolinite & Quartz.....	136

LIST OF FIGURES		
Fig. No.	Title	Page
Fig(1.1):	Location and geological map of studied area , showing studied section.....	3
Fig(1.2):	Tectonic map of Iraq showing the location of the studied area which consists of three parts.....	5
Fig(1.3):	The studied are divided to several graben and horsts (Karim, et al, 2007).....	6
Fig(1.4A):	Location and geological map of central part of the studied area (the NW part).....	13
Fig(1.4B):	Geological map of the Central part of the studied area (SE complementary part).....	14
Fig(1.5):	Geological map of the northeastern part of the studied area showing outcrop of Qulqula Formation and the sampled section (solid black line).....	15
Fig(2.1):	Texture (A) and lithology (B) of the conglomerate bed between Balambo and Qulqula formation, near Kaolos and Dostadara Villages.....	18
Fig(2.2):	The conglomerate bed at the base of Qulqula Formation exposed 1 Km north of Kaolos village, 6 Km north of Said Sadiq Town.	18
Fig(2.3):	Qulqula Formation is overlying both Shiranish Formation and Tanjero Formation due to thrusting (reverse faulting), at 1km west of Harmella Village (8km west of Chwarta Town).	20
Fig(2.4):	The enlarged area in the black parallelogram in the previous photo shows Qulqula Formation overlying Shiranish Formation due to thrusting (reverse faulting), at 1km west of Harmella Village (8km west of Chuwarta Town).	20
Fig(2.5):	Relation between Qulqula Conglomerate and Avroman Formation at the area between Kaolos Village and Tawella Town.....	21
Fig(2.6):	Part of the P1 (succession one) showing white weathering colour (fresh black or dark grey), type of bedding with chert nodules (ch), at 2km to the north of Dostadara Village, on the peak of Qalay Kurre mountain.	21
Fig (2.7):	Stratigraphic column of the Dostadara Village sections.	22
Fig (2.8):	Four limestone successions at the lower part of Qulqula Formation, west of Dostadara Village.....	23
Fig (2.9):	Dostadara Village geologic cross section, passing directly by the west of Village.....	23
Fig (2.10):	Rip up clast found in the limestone member at 6Km to the south of Razila Village at 30km to the north of Said Sadiq Town.	24
Fig (2.11):	Cross lamination in the limestone of the succession one near Harmela Village, 12km east of Chuwarta Town.	26
Fig(2.12):	Graded Bedding and Cross Lamination in the conglomerate at the base of Qulqula Formation at the area between Kaolos and Chuarta area 2km to the southwest of Dostadra village.	27
Fig (2.13):	Gutter Cast Graded Bedding and Cross Lamination in the studied limestone succession at the lower part of Qulqula Formation at the area between Kaolos and Chuarta area 2km to the Southwest of Dostadara Village.....	28
Fig (2.14):	Thin section photos of the sharp contact between bottom and top (wackstone and peloidal grainstone respectively) of two limestone layer of the Dostadara.....	28
Fig (2.15):	Position of the Qulqula and Conglomerate Formations within Tectonic Scenario of Northeastern Iraq.	29
Fig (2.16):	Angular unconformity between Red Bed Series and Qulqula Formation at Northwest of Qaladiza Town.....	30
Fig (2.17):	Angular unconformity between Red Bed Series and Qulqula Formation at Northwest of Qaladiza Town.....	30
Fig (2.18):	Resting of alluvium fan sediment (Quaternary) on Qulqula Formation at northern boundary of Sharazoor plain.....	31
Fig (2.19):	A) Alternation of marl laminae and with limestone beds, B: Alternation of marl and silicious shale at the middle part of the formation.....	33
Fig (2.20):	Cutting of the laminae of a Cross Lamination by Chert Nodules in the limestone succession of Qulqula Formation.	35
Fig (2.21):	Cutting of the Laminae of a Cross Lamination by Chert Nodules in the limestone succession of Qulqula Formation.	36

Fig (2.22): Occurrence of Chert Nodules in sandy limestone (lime sandstone) in the limestone succession of Qulqula Formation.....	36
Fig (3.1): Classification (Dunham, 1962) for carbonate rocks	40
Fig (3.2): A) Well rounded different lithoclast (dark colour) with bioclasts. B) Different lithoclast (dark colour) with bioclasts.....	42
Fig (3.3): A) Badly sorted different lithoclast. B) Subangular lithoclasts with foramoniferas whole skeletons.....	43
Fig (3.4): well rounded different lithoclast and bioclasts showing different degrees of micritization..Sample 2Dos-15a.....	43
Fig (3.5): Well rounded different lithoclast and bioclasts showing different degrees of micritization. 2Dos-15b.....	43
Fig (3.6): A: Intensely micritized lithoclasts with one longitudinal section of green algae(c) and superficial ooids(s). B: Badly sorted bioclasts (possibly pelecypods) with lithoclasts.....	44
Fig (3.7): Longitudinal section of Tetrataxid inflata (Bottom Right) and some other foram clasts and lithoclasts.....	45
Fig (3.8):Some foram clasts (as a colony), lithoclasts and superficial ooids.....	45
Fig (3.9): Different origins of peloids (Reijers and Hsu, 1986) which can be applied on the constituents of limestones of the Qulqula Formation.....	47
Fig (3.10): Peloidal grainstone Sample: 2Dos-8a.....	47
Fig (3.11): Peloid gainstone cut by two fracture that are filled with spary calcite.....	47
Fig (3.12): Peloid Grainstone contains biserial foram at the right side with spary calcite cement (white).....	48
Fig (3.13): Ooids-peloids grainstone which composed of spherical and oblate (B) superficial ooids. The oblate voids are formed around bioclasts. Some unknown origin peloids are can be seen.....	50
Fig (3.14): Ooids- Peloids grainstone which composed of spherical superficial ooids. with partially micritized lihoclasts.	51
Fig (3.15): Conglomeratic limestone (rudstone) of the P1 at 2km southeast of Harmella Village.....	52
Fig (3.16): Green algal encrustation as bindstone facies.	53
Fig (3.17): Oncoids and green algal by separate encrustation.....	53
Fig (3.18): A) Lithoclastic-peloidal Grainstone in which the peloidal show some race of superficial ooids. Type Section, S.N.7a. Peloidal with phosphatic grain..	54
Fig (3.19): Mudstone Lithofacies.....	54
Fig (3.20): Rip-up Clasts (Conglomerate) in the P1 2km Southwest of Dostadara Village.	56
Fig (3.21): Rip-up Clasts (as Floatstone Facies) in the P1 4Km Northeast of Haji Mamand Village.	56
Fig. (3.22A) Distribution of the Lithofacies and microfacies in the limestone successions of the Dostadara section.....	57
Fig. (3.22B) Distribution of the Lithofacies and microfacies in of the limestone successions of the Gali, Kaolos Tawella and Type Locality sections(only the digested samples are indicated).	58
Fig(3.23A): Depositional environment of the limestone successions of the Qulqula Formation as a ramp on the Jurassic extension platform (on the half graben). X1, X2, X3, X4, and X5: are representing the locations of Tawella, Kaolos Dotadara, Gali and Type section respectively.....	61
Fig.(3.23B): Possible tectonic setting (extension platform margin) of the upper Jurassic showing ramp platform on the southwestern side of the Neo-Tethys on which the limestone successions of Qulqula Formation are deposited.....	62
Fig.(3.24): Tectonic and environment of Qulqula Radiolarite Formation with in the tectonic Senario of Phanerozoic by (Numan, 1997).....	62
Fig (3.25): Basinal and tectonic setting of Cretaceous formations in which position of the Qulqula Formation is indicated as equivalent of Balambo Formation. A) (Karim, 2004), B and C) (Taha, (2008), D) (Ameen, 2008).	63

Fig. (4.1) Distribution of clay mineral in marine environment (Potter et al,1980) which show that Kaolinite (the only clay mineral in the present study) is deposited in shallow water environments.	68
Fig (4.2): Frequency diagrams of CaO and MgO content in limestones of the studied sections.....	69
Fig (4.3): In all sections the CaO content is a mirror of content MgO as it shown in these four graphs. (UL) is CaO% in limestone successions; (UR) is CaO% in other sections; (BL) is MgO% in limestone successions and (BR) is MgO% in other sections.....	70
Fig (4.4A): MgO and I.R. content in limestones of the studied sections.	71
Fig (4.4B): Frequency diagrams of Al ₂ O ₃ and SiO ₂ content in limestones of the studied sections..	76
Fig (4.5): SiO ₂ and Al ₂ O ₃ contents (abnormal distribution) in all studied sections. (UL) is SiO ₂ % in limestone successions; (UR) is SiO ₂ % in other sections; (BL) is Al ₂ O ₃ % in limestone successions and (BR) is Al ₂ O ₃ % in other sections.	76
Fig (4.6): Frequency diagrams of Fe ₂ O ₃ and Na ₂ O content in limestones of the studied sections.	80
Fig (4.7): Fe ₂ O ₃ and Na ₂ O contents show the distribution in all studied sections. (UL) is Fe ₂ O ₃ % in limestone successions; (UR) is Fe ₂ O ₃ % in other sections; (BL) is Na ₂ O% in limestone successions and (BR) is Na ₂ O% in other sections.	80
Fig (4.8): Frequency diagrams of K ₂ O and MnO content in limestones of the studied sections.....	81
Fig(4.9) K ₂ O and MnO contents shows the distribution in all studied sections. (UL) is K ₂ O% in limestone successions; (UR) is K ₂ O% in other sections; (BL) is MnO% in limestone successions and (BR) is MnO% in other sections.	82
Fig (4.10): Frequency diagrams of P ₂ O ₅ content in limestones of the studied sections.....	84
Fig (4.11): P ₂ O ₅ contents show the distribution in all studied sections (L) is P ₂ O ₅ % in limestone successions and (R) is P ₂ O ₅ % in other sections.	84
Fig(4.12): Frequency diagrams of Sr and Co content in limestones of the studied sections.....	86
Fig (4.13): Sr and Co contents show the distribution in all studied sections. (UL) is Sr% in limestone successions; (UR) is Sr% in other sections; (BL) is Co% in limestone successions and (BR) is Co% in other sections.	86
Fig (4.14): Frequency diagrams of Cu and Ni content in limestones of the studied sections.....	89
Fig (4.15): Cu and Ni contents show the distribution in all studied sections. (UL) is Cu% in limestone successions; (UR) is Cu% in other sections; (BL) is Ni% in limestone successions and (BR) is Ni% in other sections.	89
Fig (4.16): Frequency diagrams of Pb and Zn content in limestones of the studied sections.....	92
Fig (4.17): Pb and Zn contents show the distribution in all studied sections. (UL) is Pb% in limestone successions; (UR) is Pb% in other sections; (BL) is Zn% in limestone successions and (BR) is Zn% in other sections.	92
Fig (4.18): Frequency diagrams of Cr content in limestones of the studied sections.....	94
Fig (4.19): P ₂ O ₅ contents show the distribution in all studied sections (L) is Cr% in limestone successions and (R) is Cr% in other sections.	94
Fig(4.20): Cluster Analyses (R-Mode)of geochemical variables of all limestones in the five studied sections.....	100
Fig(4.21): Cluster analyses (Q-Mode) of geochemical variables of all Sections.....	101
Fig (4.22): Result of the study of geochemistry, sedimentology and stratigraphy as applied on straigraphic column of the Dostadara and Gali sections which shows that the four successions are derived from one due to thrust faulting.	106
Fig (4.23): Result of the study of geochemistry, sedimentology and stratigraphy as applied on straigraphic column of Kaolos section which shows that the two successions are derived from one succession due to thrust faulting.	107
Fig(4.24): Result of the study of geochemistry, sedimentology and stratigraphy as applied on straigraphic cross section of the Lower Part of the Qulqula Formation of Dostadara and Gali sections which shows that the two successions are derived from one succession due to thrust or reverse faulting.	108
Fig. (4.25) Distribution of the major oxides and miner elements (including traces) of the limestone successions of the Gali and Kaolos sections (only the digested samples are indicated).....	109
Fig. (4.26) Distribution of the major oxides and miner elements (including traces) of the limestone successions of the Dostadara and type locality sections.	110

LIST OF TABLES		
Table No.	Title	Page
	Table (1-1): The location and distance of the selected samples in the studied section.....	12
	Table (2.1): seven hypotheses proposed for the origin of bedded radiolarian cherts.....	37
	Table (3-1): Lithofacies variation of the Qulqula Formation according to their frequency in the successions.....	42
	Table (4.1): MPA of Type-8 sample in Type-Locality section shows that the typical mineral is typical Apatite.....	66
	Table (4-2); Showing Coefficient of Variation, Ranges, Mean content and Standard Deviation of geochemical analyses in bulk samples of the Dostadara Ridges.....	72
	Table (4-3); Showing Coefficient of Variation, Ranges, Mean content and Standard Deviation of geochemical analyses in bulk samples of the Type Locality, Kaolos. Kaols-Z and Gali sections.....	73
	Table (4-4): Correlation coefficient between the geochemical variables of all samples	74
	Tables (4-5): Shows the $\text{SiO}_2 / \text{Al}_2\text{O}_3$ ratio in the bulk samples from the six traverses.....	78
	Table (4-6) shows a comparison between the Fe_2O_3 , Mn, Ni, Zn and Sr content of limestone beds of the studied sections, with some other published data.....	87
	Table (4-7):- Standard Deviation and Precision (C.V%) of all samples for CaCO_3 and MgCO_3 which were analysed by Calcimetry and AAS.	97
	Table (4-8): - Results of analytical accuracy of Fe_2O_3 , Mn and Sr contents in limestone of all studied sections.	98
	Table (4-9) Rotated Factor Loading for all Studied Section Samples.....	104

CHAPTER ONE

INTRODUCTION

1-1- Preface

The Qulqula Formation was first mentioned by Bolton, (1955) and gave more detailed definitions in (1958). The formation is a unit of the Qulqula Group which includes Qulqula Radiolarian and Qulqula Conglomerate formations. This former formation is underlying the Qulqula Conglomerate Formation. It consists of thick successions of bedded chert, shale and siliceous limestone (Buday, 1980; Jassim and Goff, 2006). They also mentioned that the contacts of the formation are hard to be determined because of complex structure of the outcrop areas which are marked by intense folding, faulting and thrusting.

Field study showed that the lower part of the Qulqula Formation, in the studied area, is widely exposed throughout the Thrust Zone and complete sections are exposed, usually forming successions, along the southwestern side of Avroman and Qandil mountain in addition to northeastern side of Kurra Kazahaw (Fig 1.1) (Karim, 2003).

The age and stratigraphic position of this group is controversial because of insufficient studies and complex structure of the occurrence area (Karim, 2003). In present study, the limestone successions of the Lower part of the Qulqula Formation are selected, for detail study geochemically and sedimentologically.

These successions consist of black limestone successions that are located at the lower part of the formation. The number of these successions are more than four which discussed by Karim, (2003).

1.2. Location and Geomorphology

The studied area is located within Sulaimani Government in northeastern Iraq near the border with Iran. It stretches as a narrow belt from southeast of the Halabja town to Qandil mountain toe at the northwest which has length of more than 150kms (Fig.1.1). This area located between latitudes ($36^{\circ} 41' 23''$ and $35^{\circ} 25' 48''$) to the north and longitudes ($45^{\circ} 10' 04''$ and $46^{\circ} 20' 41''$) to the east. In the studied area the formation crops out in four localities as follows from southeast to northwest:

1-Avroman-Halabja outcrops (southeastern part of the studied area: SP) which exposed between Shinarwe and Avroman mountains from south and north respectively. At the east and west, the area is bounded by Iraqi-Iranian border and both Khurmal and Ahmad Awa towns respectively. This area includes Halabja, Tawella and Biyara Towns. The outcrops, in this area, are extensive and not covered. In this area the thickness of the limestone successions has intermediated thickness which ranges between 7–15m (Fig. 1.1)

2-Surren mountain toe outcrops which begin from east of Khurmal town and ends near Kaolos village at the northwest. The outcrop areas are narrow covered intermittently by Quaternary limestone conglomerate. These conglomerates are studied in detail by Baziany, (2006). The limestone successions are so thin that they do not form any successions or even they are difficult to be recognized.

3- Kaolos-Basine outcrops: Central part of the study area: (CP) which extends from Kaolos village, at the southeast to the Basine town at the northwest. The well exposed outcrops are available which have the width and length of 20 and 50km respectively. The limestone successions are well developed and each succession has the thickness of about 25m.

4-Qandil mountain toe outcrops: northwestern part of the studied area: (NP) which is located at the lower slope of southwestern side of Qandil Mountain. The outcrops, in this area, are similar to that of Surren mountain toe. The type locality of the Qulqula Formation is located in this area near Qulqula gorge at left side of Marado stream. The limestone successions are mostly siliceous and recrystallized.

The studied area now covered by high mountains which is trending northwest–southeast .In the same direction and between these mountains there are narrow or wide subsequent (strike) valleys. The mountains and valleys are dissected by; at least, two long consequent valleys and tens of smaller ones. The large valleys are Little Zab and Diala river valleys.

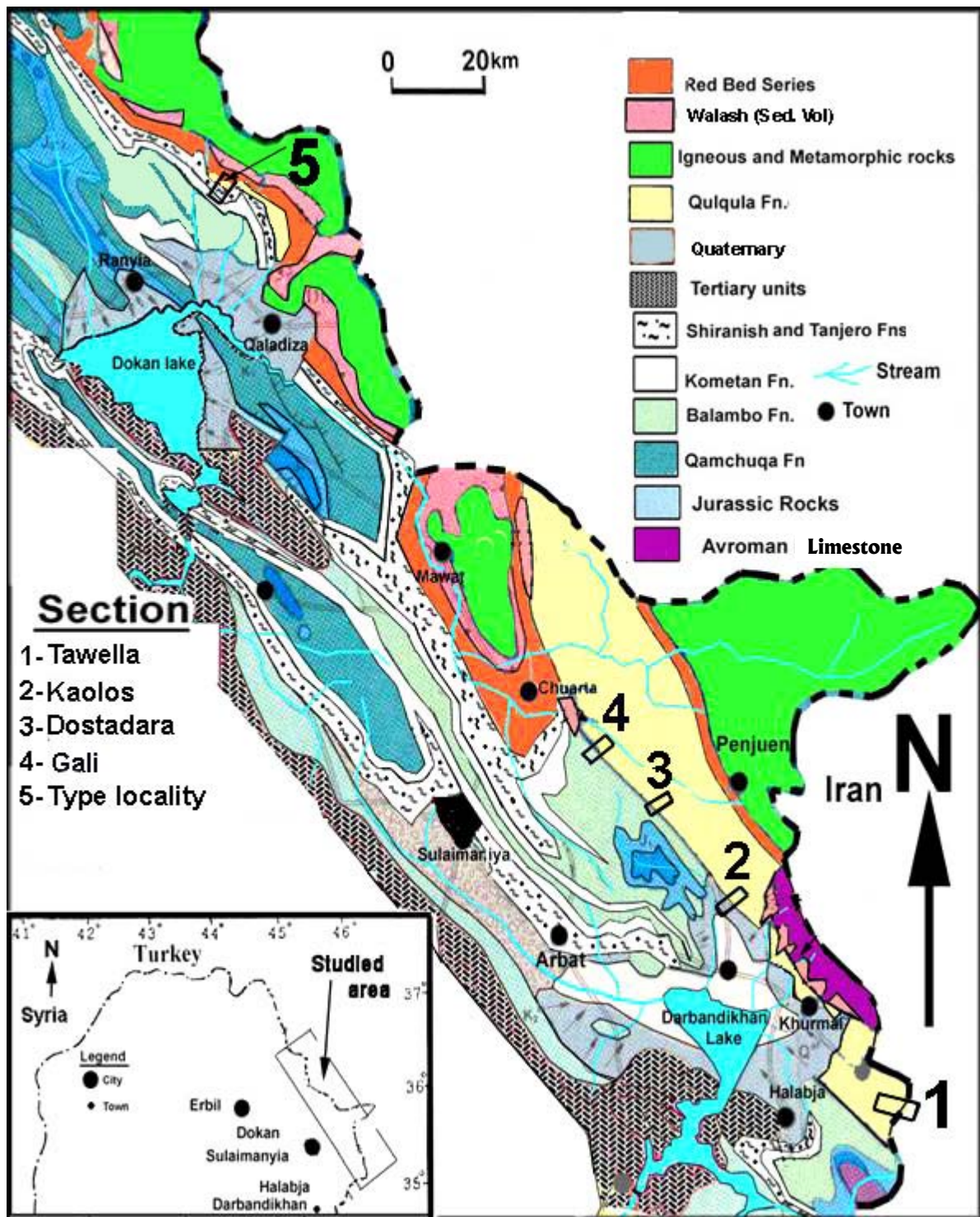


Fig.1.1: Location and geological map of studied area from Sissakian, et al., (2000), showing studied section.

1-3-Geological Setting

The studied area is located within the western part of Zagros Fold-Thrust Belt, which is developed from the basin fill of the Neo-Tethys and deformations that accompanied colliding of the Iranian and Arabian plates. Dunnington, (1958) believed that the thrust zone has developed during the Alpine Orogeny which started from Upper Cretaceous time and continued through the Tertiary where it is accentuated

during the Pliocene time. He added that the regional structure of the area trends with the Zagros, NW-SE direction, though several changes in the direction have been recorded (Fig.1.2). Structurally, the studied area is located within the Thrust Zones (Buday and Jassim, 1987). The same authors, in their tectonic subdivision of Iraq put the studied area in the Qulqula-Khuakurk Subzone. The area is characterized by obscured anticlines and synclines which have been stacked together as very thick and tight successions which were overturned toward southwest. Most of these structures suffered from thrusting, therefore, Stocklin, (1968) called the studied area "Crushed Zone" this is because it is highly deformed on large scale and small scale, even one can see fracture, fault and fold under polarizing microscope. According to Karim, (2003); Karim and Surdashy, (2005), Baziany, (2006), the deformation and development of the studied area mainly began from Campanian. They added that at this age the continental part of Iranian and Arabian plate is collided with Iranian and a Foreland basin is formed. By continuous advancing (thrusting) of the foreland and hinterland of the Iranian plate the sediments inside the basin is progressively deformed and accumulated as accretionary prism. The deformations and sedimentation were continuous until the end of Tertiary, by which the studied area gained the present geological setting which is now highly modified by weathering and erosion.

The studied area consists, at least, of four large horsts which are separated by three grabens (Fig.1.3). The first horst is located in the area around Halabja town while the second one is located in the north east of Sulaimani city in the area between Said Sadiq and Chuarta towns. On this horst, the Jurassic rocks are exposed near the northeastern boundary (Fig.1.3). This horst is bounded by two transverse normal faults from northwest and southeast. The former fault is described by Karim, (2005) which is located in the east of Chuwarta town while the latter is found in this study, and it passes through Said Sadiq town and Kaolos village. The third horst is located between Mawat and Qaladiza towns.

The grabens are consisting of low lands (plains) such as Sharazoor plain (eastern part), Mawat and Chuwarta low lands and Sangasar Plain. In this area, the Qulqula Formation acts as thrust fault inside the graben while is perform as reverse faults on the horsts (Karim *et al*, 2007) (Fig.1.3).

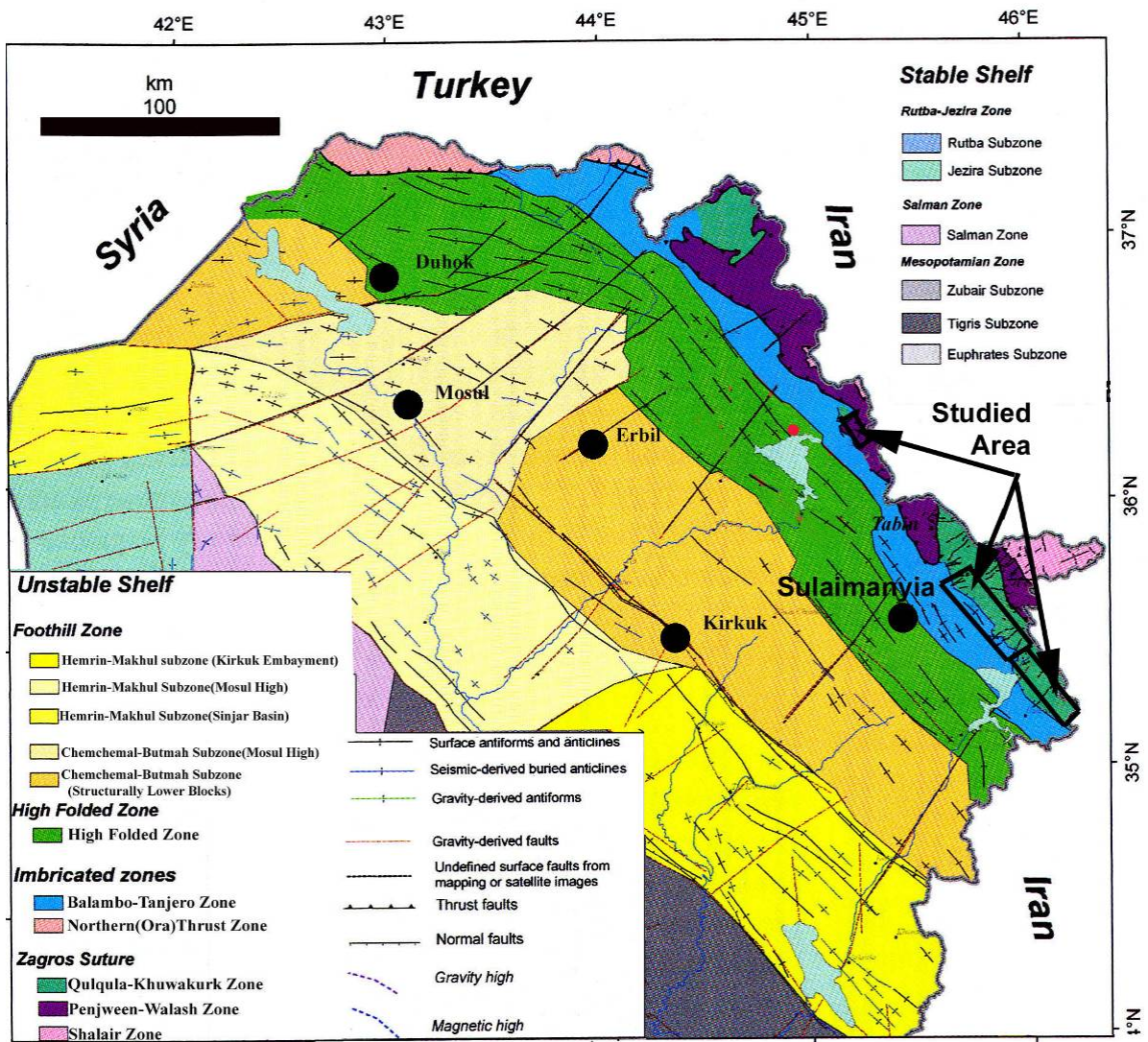


Fig.1.2: Tectonic map of Iraq Jassim and Goff, (2006) showing the location of the studied area which consist of three parts (northwestern, central and southeastern parts)

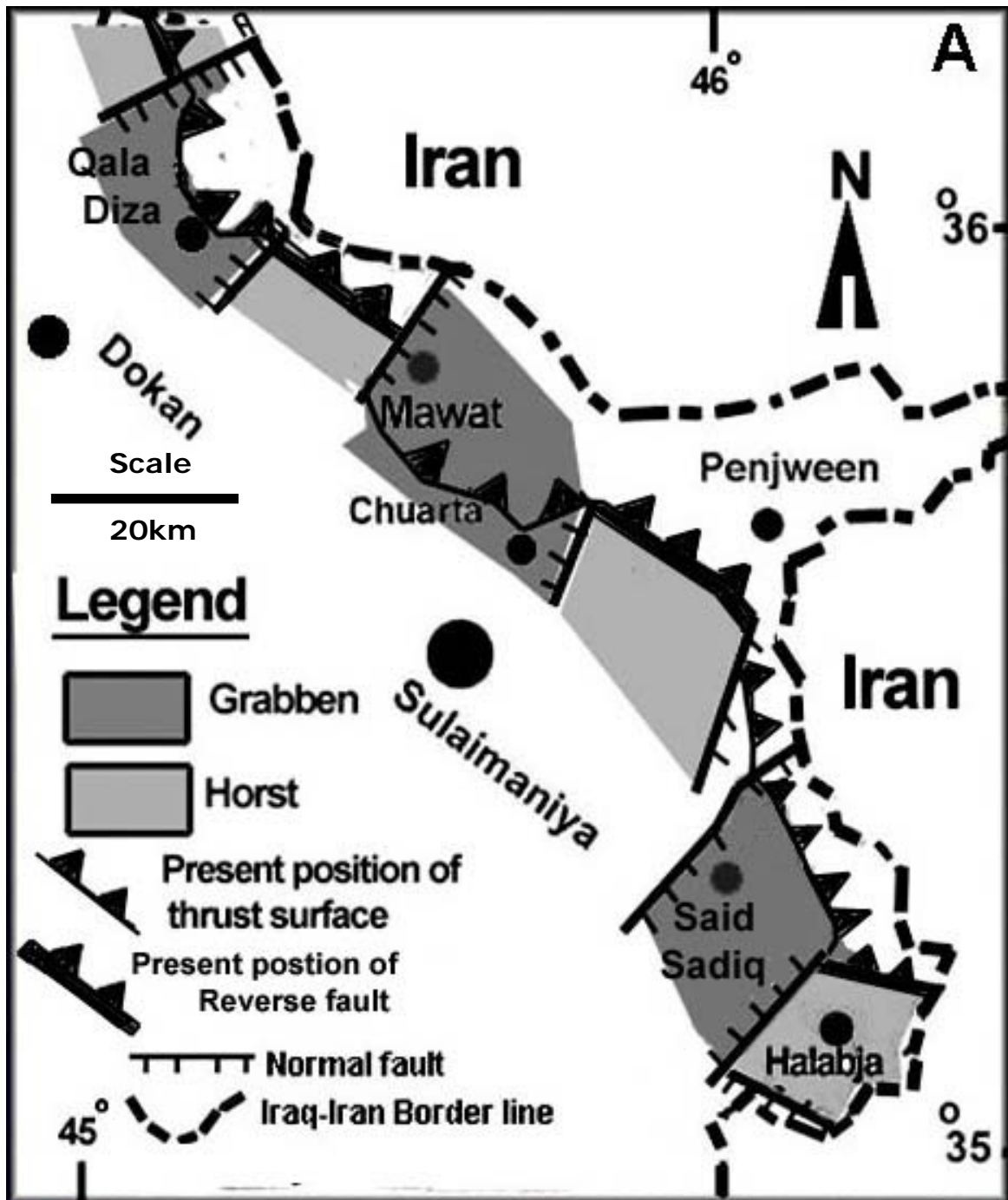


Fig.1.3: The studied area divided to several grabens and horsts (Karim et al, 2007).

1.4. Previous Studies

According to Buday, (1980), the Qulqula Formation was described by Bolton in (1955), but a more precise definition and description was given by the same author in (1958). The only available description on lithology, stratigraphy and age of the formation is that of the Buday (op. cit.) who mentioned that the type area lies in the

Qulqula gorge. Parson, (1957) described briefly radiolarite in the same area of distribution of Qulqula Formation in the area between Chuarta and Penjween towns. He mentioned that this rock consist of chert and shale with subordinate limestone. He added that the limestone is dark grey on fresh surfaces but weather to light grey and contain many thin bands of black chert.

Waddington, (1955) supposed that the formation is older than Jurassic. Karim, (1975) inferred the age of Albian to Cenomanian from foraminifera study. (Jassim *et al.*, (1984) used the term “Qulqula Radiolarian Series” and they divided this Series into two Formations:

- 1- Qulqula Formation. (Aptian–Albian).
- 2- Qulqula Conglomerate Formation (Cenomanian).

They also cited that the sequence that is overlying the Qulqula Formation is the Qulqula Conglomerates Formation, which is composed of thick limestone conglomerates and cherty grit, interbedded with grey marly shales, chert and detrital limestone. The thickness of this sequence is 1200m. Buday and Suk, (1980), in Jassim *et al.*, (1984), divided the Series, on the basis of the character of its limestone and the biostratigraphy, into four units, these are:

- 1-Tithonian–Berriasian unit. 2-Valanginian–Lower Aptian unit.
- 3-Upper Albian–Cenomanian unit. 4-Cenomanian unit.

Jassim *et al.*, op. cit), mentioned that the Cenomanian unit is the equivalent to the Qulqula Conglomerate Formation. They added that it is composed of conglomerate interbedded with chert and limestone and the fragments in the conglomerate were studied in some details by Buday and Suk, (1980). They also mentioned that at least up to 75% of fragments in some locations belongs to the Avroman limestone, the rest belong to the older limestone and chert of the sequence of the Qulqula itself .They cited that the unit is characterized by the following fossils: Ovalviolina sp., Hemicyclina sigali, Hedbergella washitensis, Hedbergella sp., Thalmaninella ticineusis, Dicyclina sp., and pelagic crinoids.

Nunna *et al.*, (1981), studied the area around the Kaolos proposed dam project where Qulqula Formation is exposed. They mentioned that Qulqula Series can be classified into Lower Qulqula Formation (Aptian-Albian) and an upper Conglomerate Formation (Cenomanian). They added that tectonism is affected the formation during the Middle Cretaceous which is folding them intensely and leading to the development of an orogeny. Buday and Jassim, (1987) used “Qulqula Formation” instead of “Qulqula Formation” which is also, for simplicity, followed in this paper.

These two authors reported thrusting of Qulqula on Balambo Formation for about 15kms recently, depending on allochthony, Numan, (1997) put Balambo and Qulqula Formations in two far separated trench-like basins, at both sides of spreading mid-oceanic ridges. Sissakian, (1997) has shown the formation on the geological map of the Arbeel and Mahabad Quadrangles area (scale: 1:250000). On this map the formation covered about 5km² and exposed at front of the outcrop of Qulqula Formation (Fig.1.5). Karim, (2003), cited that Qulqula Formation (Qulqula Formation) was deposited in a subduction trench forming an accretionary prism during the colliding of the Iranian and Arabian plates. Karim, (2004) has mentioned occurrence of partially metamorphosed outcrop of Qulqula Formation in the Shelair Phyllite (Qandil metamorphic Group).

Sissakian, (2005) mentioned that the Qulqula Group comprised of Qulqula Formation and Qulqula Conglomerate Formation. This latter formation is overlying the Qulqula Formation in a gradation condition. Al-Barzinjy, (2005), mentioned that the lithology of the Red Bed Series is mostly derived from Qulqula Group and Ophiolites. Karim, (2004) wrote about close relation of Qulqula Conglomerate Formation with conglomerate of lower sequence of Tanjero Formation.

Karim, (2003) found and discussed a conglomerate bed in detail for the first time at the base of Qulqula Formation. The conglomerate crops out between Chuarta and Said Sadiq towns as a bed of about (20-40)cm thick. This conglomerate is located above the Balambo Formation. According to this author the conglomerate consists of different types of subrounded to angular chert and limestone pebbles and boulders. Sissakian, (2005) used series instead of group and indicated the environment of the upper part of the Series (Qulqula Conglomerate Formation) as Marine Eugeosynclinal (flysch type), with age of Cenomanian-Santonian.

Baziany, (2006) studied in detail the Qulqula Conglomerate Formation which overlies Qulqula Formation. He found an angular unconformity between the two Formations at type section and Basine area. He mentioned that the age of Qulqula Conglomerate Formation is Paleocene-Eocene. He further added that the rocks of Upper Cretaceous are missing on the unconformity. From the study of the type section, Karim and Baziany, (2007) proposed to abandon the Qulqula Conglomerate Formation and remove it from stratigraphy of Iraq because it is equivalent to Red Bed Series. Baziany and Karim, (2007) have studied the Qulqula Conglomerate Formation in the Halabja–Avroman area and showed that this formation is not exist in this area.

1.5. Aims of the Study

1. The purpose of the present work is to establish depositional environment and paleogeographic setting of the limestones successions of the Qulqula Formation through facies analysis and geochemistry.

2. The study of the geochemical and sedimentological variations within and between the four limestone successions in five sections with a possible interpretation of the depositional environment as another purpose of the present study. This includes distribution of the major and some trace elements in the bulk samples and their separated insoluble residues

3. This study tries to see if the four successions are repetition of single succession by imbrications and faulting (thrusting) or they are different successions which are related to different time and space.

1.6-Studied Sections.

Five sections are selected for detailed study of the Lower part of the Qulqula Radilarian Formation. As previously mentioned, the studied area consists of very long belt in the Thrust Zone which includes three discontinuous parts (see section 2.1 and fig.1.2). According to these parts, the sampled sections are grouped as follows:

1-6-1. Sections of Central or Middle Part of the Studied Area (MP)

Kaolos Section

This section is located directly in the south of Kaolos village, in the extreme southeastern of the middle part of studied area, about 15 Km to the north of Said Sadiq town at latitude N $35^{\circ} 29' 13.89''$ and longitude E $45^{\circ} 52' 1.47''$ (Fig. 1.2 and 1.4A). This section consists of two successions which have less thickness than others in which each is about 15m thick...

Dostadara Section

This section is located nearly in the middle part of this area, directly to the west of Dostadara village, about 12 Km to the northeast of Barzinja town (Fig. 1.2 and 1.4A). Located at latitude N $35^{\circ} 34' 47.33''$ and longitude E $45^{\circ} 46' 45.63''$. This section consists of four successions, each one of average 25m thickness.

Gali Section

This section is located about 1Km to the east of the Chuwarta Town, at the extreme northeastern part of the middle part of studied area (Fig.1.2 and 1.4B). Located at latitude $35^{\circ} 38' 54.08''$ and longitude $45^{\circ} 41' 13.67''$. Dostadara and Gali section consist of four successions each more than 25 thick).

1.6.2- Section of the Southeastern Part

Tawella Section

It is located at latitude $35^{\circ} 25' 48''$ and longitude $46^{\circ} 02' 41''$, at the 15km northeast of Halabja town (Fig.1.1). The section is located directly to the east of Tawela town at the extreme southeastern end of the studied area. In this area only one succession is sampled because the other succession located near the border of Iran.

1.6.3- Section of the Northwestern Part

Type Section (Qulqula Gorge)

It is located at latitude $36^{\circ} 21' 23''$ and longitude $45^{\circ} 10' 04''$, at the upstream of Kulkula gogre stream at the toe of Qandil mountain, 17km to the north of Qala Diza town (Fig.1.2). In this section only one succession is exposed which is about 15m thick.

1.7. Methodology

1- Reconnaissance survey of all areas of the occurrence of the formation to find the distribution of the outcrops of the formation. For this, topographic map of 1: 50000 and Google Earth Satellite image are used. The three dimension images are compared with the topographic and geologic maps.

2- Collection of available literature that concerns the formation.

3- Selection of suitable outcrop sections for sampling and description, this includes (type of lithology, vertical and lateral change), distinguishing sedimentary structures and stratigraphic relation of the formation with surrounding formations. The samples are taken in regular interval of about 1.5m, but in the monotonous intervals the sample spacing is increased

4- After removing the weathered parts, 118 fresh samples (point samples) were carefully collected from the five sections which were taken perpendicular to the strike of strat, table (1.1). The samples were broken into smaller pieces and were saved for petrographic examination under polarized and stereoscopic microscopes and small

portion of each rock sample was used to make a 150 thin section for the microscopic study. The samples are taken with large hammer (1.5kgs) in order to obtain samples free from weathering and secondary calcite and silica mineralization. As the chert nodules in the limestone successions are secondary, therefore, the samples that contain chert nodules are neglected during chemical analysis.

5- The samples were collected to represent the limestone beds within the studied formation. The distance between the samples (apparent thickness) is measured by a measuring tape, the angle of the tilted beds is measured by a compass and the true thickness between the samples is derived from the apparent thickness and the dip. The position of the samples in the sections is fixed in table (1.1).

6- Another fraction was used for the preparation of the sample powder, after breaking the rock sample into small grains using a hammer. The grains are pulverized into powder by porcelain mortar. The powder then passed through a 180 mesh sieve and stored in glass bottle.

7- Sixty bulk samples were prepared, the power (about 0.5 gram) were used for chemical analyses to determine various major oxide and trace elements.

8- Thirteen samples were taken from powder and dissolved in acetic acid for the preparation of insoluble residue samples for major oxide and trace element analyses.

9- Twenty selected bulk and IR samples were selected for X-Ray analyses, six for insoluble residue samples and two of them were heated to 550°C,

10- Statistical analyses (cluster and factor analyses) of the elements for correlation between the elements of each succession in one side and with the limestone of the other sections.

Table(1-1): The location and distance of the selected samples in the studied section

Dostadara Section								Gali Section		Tawella Section		Type Locality Section		Kaolos Section	
1 st Ridge	Distance in M	2 nd Ridge	Distance in M	3 rd Ridge	Distance in M	4 th Ridge	Distance in M		Distance in M		Distance in M		Distance in M	1 st Ridge	Distance in Meter
1Dos-5	Bottom	2Dos-1	Bottom	3Dos-1	Bottom	4Dos-1	Bottom	1G	Bottom	Taw-1	Bottom	Type-1	Bottom	Kolz-1	Bottom
1Dos-6	1.5	2Dos-2	5	3Dos-2	2	4Dos-2	2	2G		Taw-2	10	Type-2	3	Kol-2	2
1Dos-7	1.5	2Dos-3	2	3Dos-3	2	4Dos-3	3.5	3G	4	Taw-3	3	Type-3	3	Kol-3	4
1Dos-8	1	2Dos-4	2	3Dos-4	1.5	4Dos-4	2	4G	3	Taw-4	4	Type-4	2.5 Top	Kol-4	10
1Dos-9	1.5	2Dos-5	2	3Dos-5	3	4Dos-5	3.5	5G	2	Taw-5	5 Top	Type Locality-2	Distance in Meters	Kol-5	5
1Dos-10	2	2Dos-6	1.5	3Dos-6	2	4Dos-6	2	6G	5			Type-5	Bottom	Kol-6	5
1Dos-11	1	2Dos-7	3	3Dos-7	1.5	4Dos-7	2	7G	4			Type-6	4	Kol-7	4
1Dos-12	1	2Dos-8	2	3Dos-8	2	4Dos-8	3	8G	0			Type-7	2	Kol-8	10
1Dos-13	1	2Dos-9	2	3Dos-9	2	4Dos-9	3.5	9G	5			Type-8	2	Kol-9	6 Top
1Dos-14	1	2Dos-10	1.5	3Dos-10	2	4Dos-10	4.5	10G	5			Type-9	2.5	2 nd Ridge	
1Dos-15	1	2Dos-11	1	3Dos-11	3	4Dos-11	2	11G	5			Type-10	2.5	Kolz-2	2
1Dos-16	1.5	2Dos-12	2	3Dos-12	2	4Dos-12	2	12G	4			Type-11	2	Kolz-5	5
1Dos-17	1.5	2Dos-13	1.5	3Dos-13	4	4Dos-13	2	13G	2			Type-12	3 Top	Kolz-7	7
1Dos-18	1.5	2Dos-14	2	3Dos-14	3	4Dos-14	3 Top	14G	0					Kolz-9	5
1Dos-19	2	2Dos-15	1.5	3Dos-15	8 Top			15G	6					Kolz-12	3
1Dos-20	1	2Dos-16	2.5					16G	3					Kolz-14	6
1Dos-21	2	2Dos-17	1.5 Top					17G	3					Kolz-17	9
1Dos-22	6 Top														
Total Exposed Thickness in meter	28		33		38		35		51		22		26.5		83

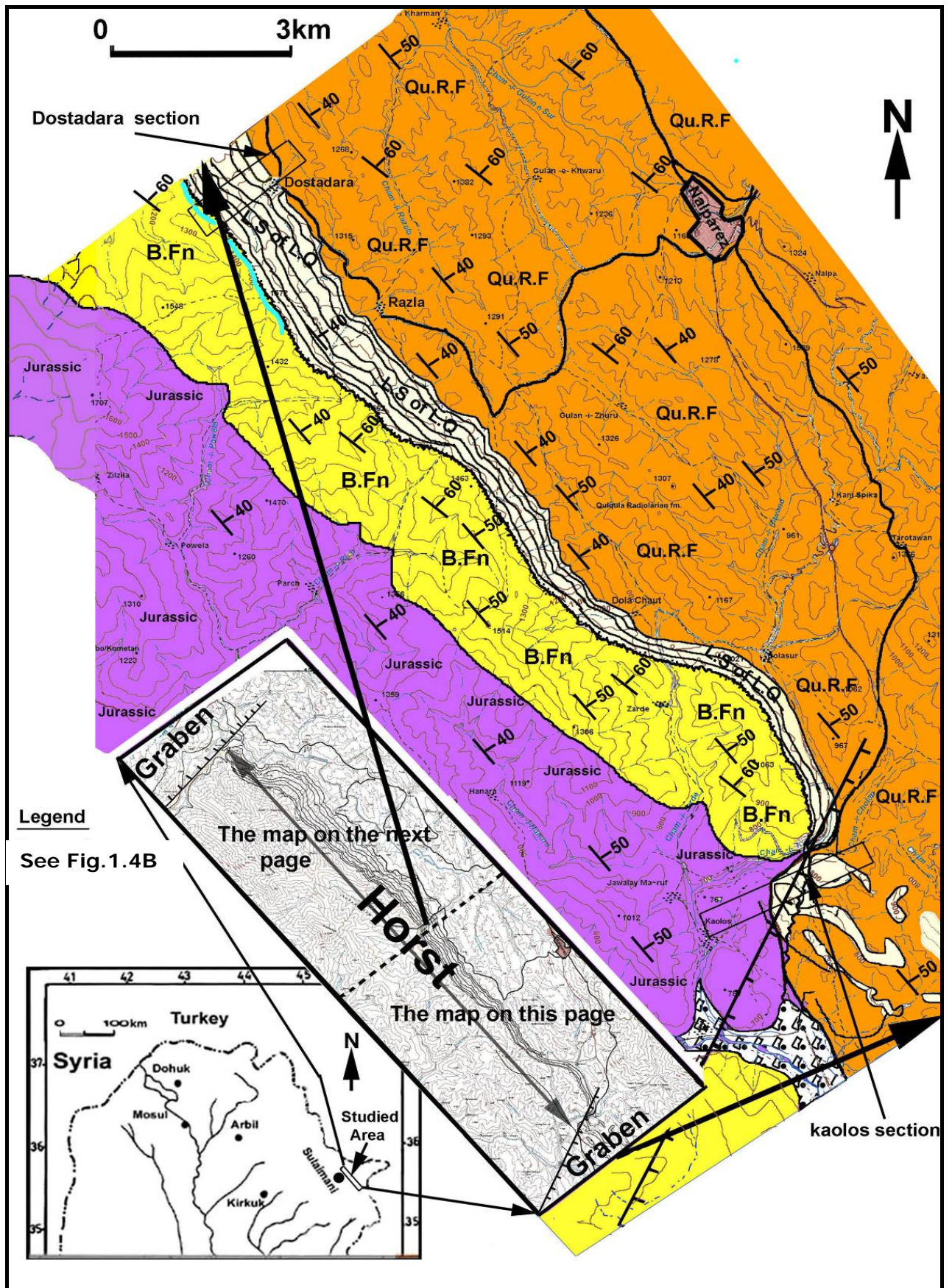


Fig. 1.4 A: Location and geological map of central part of the studied area (the SE part)

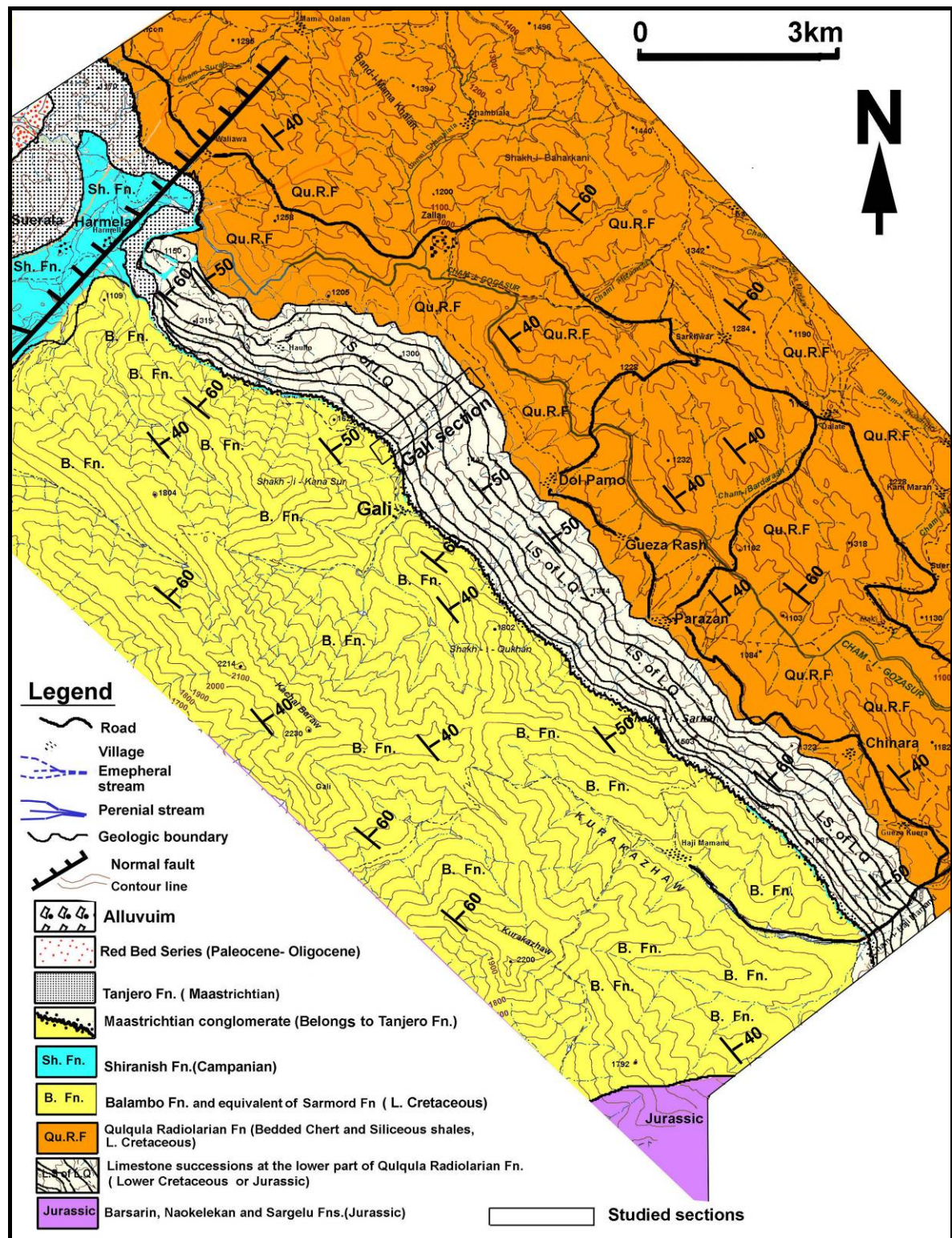




Fig.1.5: Geological map of the northeastern part of the studied area showing outcrop of Qulqula Formation and the sampled section (solid black line) modified from Sissakian, (1997) from Karim and Baziany (2007).

CHAPTER TWO

STRATIGRAPHY AND SEDIMENTOLOGY

2-1-Introduction

The present study deals with the lower boundary and Lower Member of the Qulqula Formation. The field study showed that this part of the formation is well exposed throughout the Thrust Zone, usually forming successions, along the northeastern side of Kurra Kazahaw Mountain, southwestern side of both Avroman and Qandil Mountains and north of Chuwarta–Mawat area. In these areas the lower part, as a lower unit of the formation, consists mainly of successions of black (light grey or white weathering) limestone. The number of these successions is more than four (Karim, 2003).

Buday, (1980) mentioned that, in the type area, the formation consists of different members. The lower member consists predominantly of moderately thickly bedded, oolitic and detrital limestones with thick beds of white chert. Both limestone and chert layers are interbedded with grey marly shale. The Middle Member is composed of thinly bedded, red and grey and green shale with intercalation of cherty radiolarian limestones and dark ferruginous shale. Moreover, he added that the upper part is dominated by thick sequence of dark red ferruginous-siliceous shale and ruby mudstone with occasional beds of oolitic and detrital limestones. The author mentioned the presence of contemporaneous synsedimentary effusion rocks, but they are not present in the type locality. Buday, (1980) cited that the extrusive rocks (volcanic rocks) are diabase, but their stratigraphic position is not clear enough. He also mentioned that limestone is very frequent in the Kani Manga – Nal Parez area.

Although these lithological characteristics are generally true but we have observed the following variations:

2-2-Lithology of the Lower Member of the Qulqula Formation

This section is concerned with the lithology of the lower part and contact of the formation which contains two main lithologies:

It composed of Limestone successions as a lower part of Qulqula Formation which intercalated with chert layers and shales and overlain a conglomeratic bed and Slices of Shiranish Formation below Qulqula Formation.

The constituent and stratigraphic position of these lithologies is important for inferring both tectonic and paleogeographic setting of the lower part of the formation.

2-2-1. Conglomeratic Bed at the Base of the Lower Member as Lower Boundary of the Formation

A Conglomeratic bed, exists at the base of Qulqula Formation, has thickness of 0.2–2 m which make up the lower boundary of the formation in the middle part of the studied area (MP). It occurs only in the middle part of the studied area (Fig.1.4A and B). It consists of in-sorted and sub-rounded gravels (with some boulders) of cherts and limestones (Figs.2.1 and 2.2) and extends between Chuwarta in North West and Said Sadiq towns in southeast (Karim, 2003). It seems that the most problematic aspect of the Qulqula Formation is the nature of its boundaries. This is because; there is a clear sedimentary conglomerate in the area of the northeastern side of the Kurra Kazaw Mountain. This conglomerate exists at the base of the formation and extends continuously for about 35 Km in the area between Chuarta and Said Sadiq (Figs 1.4A and B). On the basis of its deposition on the Balambo or Kometan Formations, Karim, (2003) aged its deposition Late Cretaceous. Depending on the stratigraphic position of the conglomerate, he assumed that the overlying Qulqula Formation is autochthonous. In the present study the ideas of the Karim, (2003) are re-studied in detail in the field and the following points were proved

The **first** is that, it is true that the conglomerate is deposited during Late Cretaceous. This is proved by tracing (following) the conglomerate towards the northwest till it combined with a conglomerate that exists in the lower part of the Tanjero Formation, southeast of Harmella Village 8 Km southeast of Chuwarta Town) (Fig.2.3 and 2.4). The lithologies of both conglomerates are the same (variegated chert and oolitic–peloidal limestone). Therefore, the author believe that the conglomerate is belongs to Tanjero Formation. The conglomerates within this formation is studied in detail by Karim, (2004); Karim and Surdashy, (2006) and Karim and Surdashy, (2005), they called it Kato Conglomerate and concluded that this conglomerate consists of chert and limestone gravels and boulders with more than 500m thick.

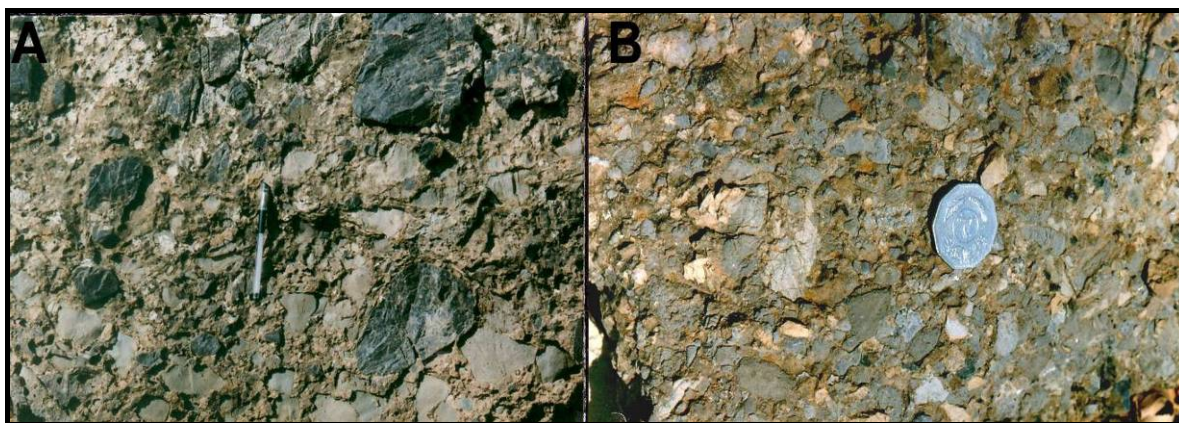


Fig.2.1: Texture (A) and lithology (B) of the conglomerate bed between Balambo and Qulqula Formation, near Kaolos and Dostadara Villages from Karim, (2003). White patches are limestone clasts, grey and black are chert clasts.



Fig.2.2: The conglomerate bed at the base of Qulqula Formation exposed 1 Km north of Kaolos Village, 6 Km north of Said Sadiq Town. The width of the landscape in the photo is 4.5 m.

The **second** is that, the age of Qulqula Formation is still controversial. According to Tahrani, (2006) in Iran, the age ranges from Jurassic to Late Cretaceous. Karim, (2003) suggested Turonian age, while in the present study no evidence of specific age was found, but Early Cretaceous age is preferred.

The **third** is that, the Qulqula Formation is allochthonous and evidences could be seen showing transportation to some extent. According to Aswad, (1999), it is parautochthonous (partially transported) unit and it represents the marine sediments deposited parallel to the Arabian shelf carbonate and slightly dislocated by a reverse fault. The last two points are assumed as slight amendment for the previous idea of Karim, (2003).

The **fourth** is that, at the base of the Qulqula Formation not only conglomerate of Tanjero Formation occurs; there are also slices of Shiranish Formation too. These slices have thickness of 5-30m, located above the conglomerate and have the same

lateral extension such as that of the conglomerate. The evidences for these slices belong to Shiranish Formation are that they combine with the Shiranish Formation at same location of the conglomerate (Fig.2.3 and 2.4). A sample from the Shiranish Formation (in Dokan area) is compared (under stereoscopic microscope) with slices, showed the same appearance and lithologies (clay limestone with small disseminated grains and sparce fossils of multiglobolar chambered foraminifers). The cooking and thin section yield no well preserved microfossils for accurate age determination but according to badly preserved fossils the age of slices is most probably Upper Cretaceous (K. M. Sharbazery, personal communication).

In the northwestern part of the studied area (NP), the lower boundary of the Qulqula Formation is not exposed and there is no conglomerate below the formation, while in the southeastern part (SP), from Kaolos to Tawella Village there is a conglomeratic bed (3-6m thick) in some places. In this area, the conglomerate is located between Avroman Limestone and Qulqula Formation. This bed is located close to the Iranian border and near the Peak of Avroman Mountain. Therefore, it can not be studied properly and the origin of this conglomerate is not certain.

The lower boundary of the Qulqula Conglomerate Formation can be seen in this area with Avroman Limestone. The contact seems sharp and tectonic, which coincides with the literature citation by Buday, (1980), Jassim and Goff, (2006) who inferred the age of Lower Cretaceous and Triassic respectively. In this area the relation between these two formations is illustrated by diagrams by Ali and Ameen, (2005), Baziany, (2006) and Karim and Baziany, (2007) (Fig. 2.5).

It is worth to mention that according to Bolton, (1955), Buday, (1980), Jassim and Goff, (2006), there is another thick conglomerate (about 1200 m thick) at the top of the Qulqula Formation, which is called, by same authors, Qulqula Conglomerate Formation. This conglomerate is studied by Baziany, (2006), Karim and Baziany, (2007).

2-2-2-Limestone Successions at the Lower Member of the Qulqula Formation

For the first time the exposed limestone successions of Qulqula Formation are studied for the first time in detail in term of sedimentology and stratigraphy. This is executed in order to simplify the later study of geochemistry of the Formation in different selected sections. This aim to deduce whether the limestone successions are overturned or have normal stratigraphic position that obeys the law of

superposition. As the formation is exposed in the Thrust Zone, so the overturning and even tectonic dislocation of different strata and rocks of different ages could be expected.

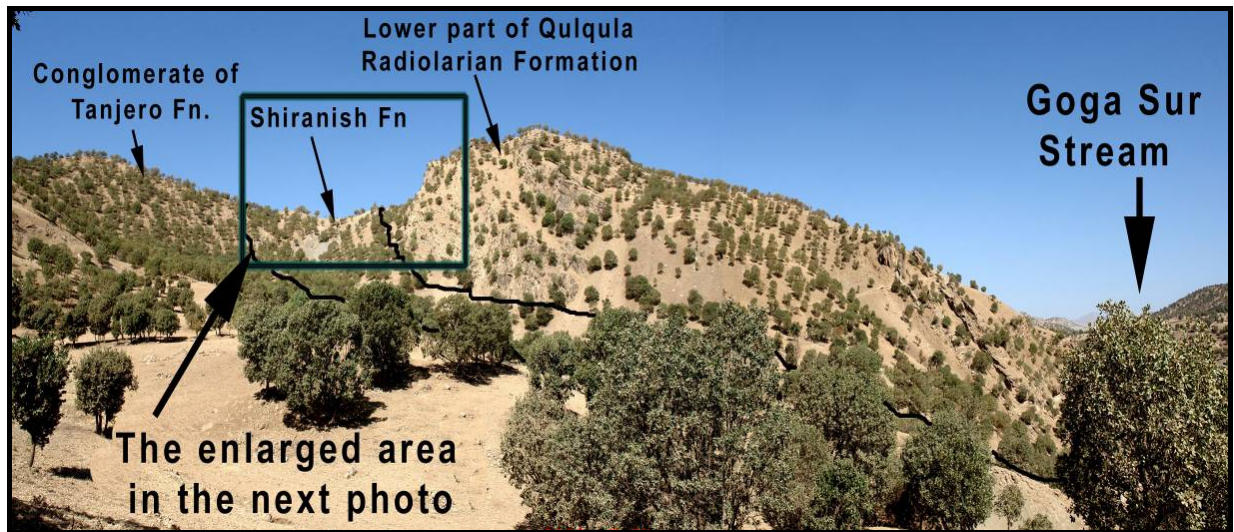


Fig.2.3: Qulqula Formation (L. Cretaceous) is overlying both Shiranish Formation and Tanjero Formation (U. Cretaceous) due to thrusting (reverse faulting), at 1km west of Harmella Village (8km west of Chwarta Town).

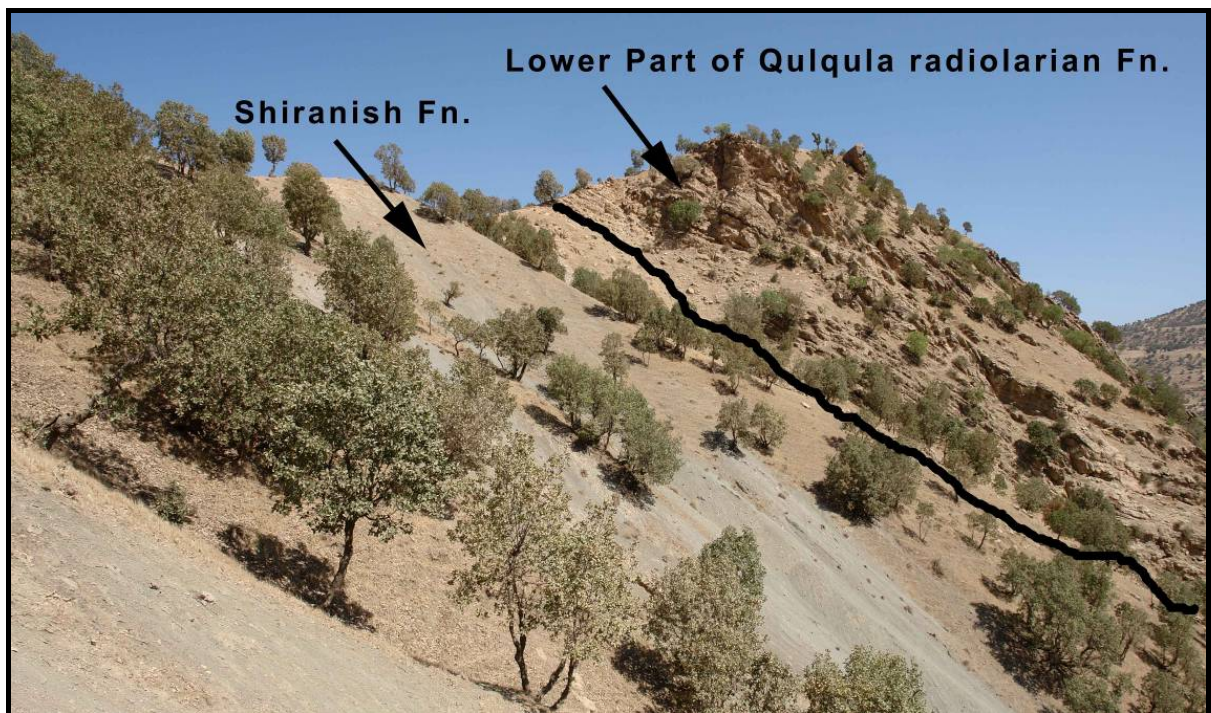


Fig.2.4: The enlarged area in the black parallelogram in the previous photo shows Qulqula Formation overlying Shiranish Formation due to thrusting (reverse faulting), at 1km west of Harmella Village (8km west of Chwarta Town).

In the studied areas, the lower part of the formation consists of more than four limestone successions, which are located above either the Conglomerate Bed or Balambo and/ or Kometan formations. These successions (Lower Member of Bolton,

(1958) are separated by thick interval of alternations of bedded cherts and marls (Figs. 2.6, 2.8, 2.9 and 2.10).

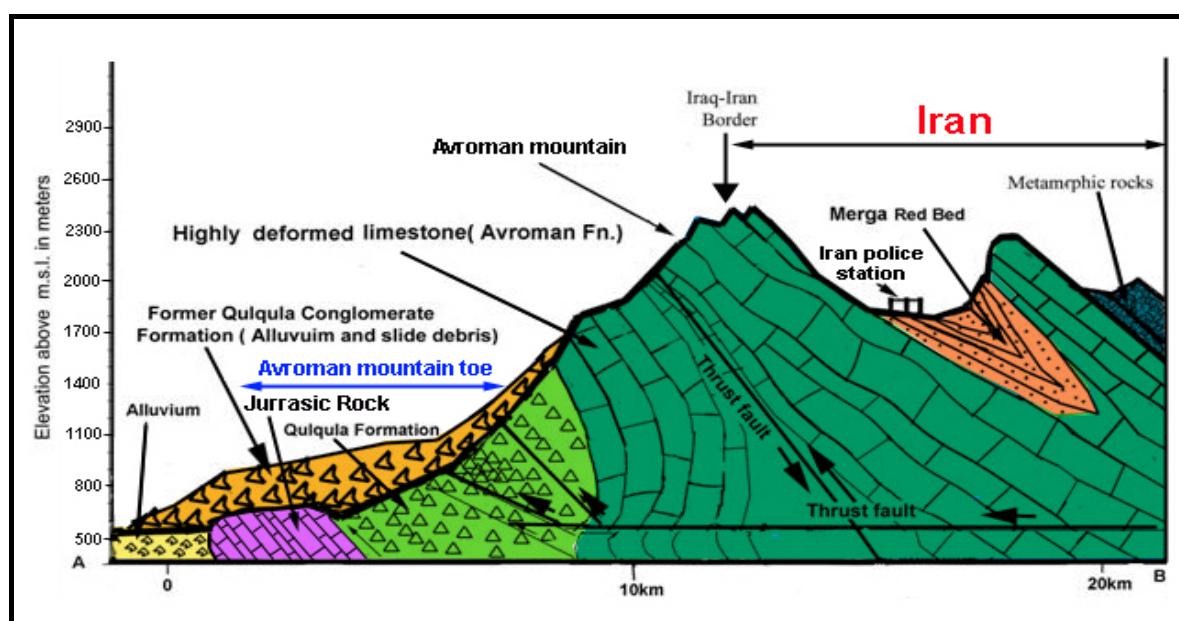


Fig. 2.5: Relation between Qulqula Conglomerate and Avroman Formation at the area between Kaolos Village and Tawella Town (Karim and Baziany, 2007).

These limestone successions are well developed in the area between Chuwarta town and Razila Village, where each succession has a thickness of more than 25 m. They crop out 3 Km to the south of Harmela Village near Chuwarta Town, and extend to Kaolos Village, passing near by (to the south of) Dolpamo, Goezarash, Parazan, Chinara, Piraziz, Dostadara and Razila Villages (Figs. 1.4A and B). In the area between Chuarta and Kaolos, each succession consists of more than 50 beds (20–130cm) thick of black and fine to coarse grain limestone which has light grey weathering colour. Occasionally, the limestone beds contain nodules and strings of chert (these nodules will be discussed later).

From Razlla Village to about 800 m of Kaolos Village, the number and thickness of the limestone successions decrease to about 8 m and 2 successions (near Dolpamu Village) respectively. Near Kaolos village, the limestone successions disappear. Before disappearing, they become highly deformed and Sargelu Formation appears below them. In this locality, the Sargelu Formation consists of thick sequence of black limestone containing *Posidonia* shell and their bioclasts.

From Kaolos Village to Khurmal Town, the Qulqula Formation is covered partially by Quaternary sediments (Baziany, 2006; Baziany and Karim 2007) and there is no

limestone that can be seen clearly, which belongs to the formation. But, there are black limestones under Qulqula Formation that are not associated with chert and they are not known if they belong to Qulqula or Sargelu Formation.

From Khurmali to the Iraqi-Iranian borders through Biara and Tawella towns, the limestone members are more cherty and thinner. They are located above Avroman Limestone and the limestone successions can not easily be separated from the later formation. To the south of these two towns, very thick and nearly pure chert succession is located on the Balambo Formation. The contact between these two formations is not known exactly, because of intense deformation, but at 2km to the east of Tawella Village, it looks like tectonic. At the Qandil Mountain toe especially at type locality, the limestone member is less in thickness and numbers than other areas



Fig. 2.6: Part of the P1 (succession number one) showing distinctive characteristics of bedding and white weathering colour (fresh black or dark grey). Chert nodules (ch), at 2km to the north of Dostadara Village, on the Peak of Qalay Kurre Mountain.

Age	Fn.	Thic. in m.	S.NO.	Limestone Packages	Lithologic Symbols	Description
Cretaceous	Qulqula Radiolarian Formation	12	4DS12 4DS1	P4		Very thick succession of varicoloured, bedded chert and light yellow and brown marl
		15	3DS15 3DS1	P3		Dark grey to black fine grain limestone. In thin section consists of medium grain moderately sorted peloidal, bioclastic and oolitic limestone.
		20	2DS17 2DS1	P2		Thick succession of varicoloured, bedded chert and light yellow and brown marl
		25	1DS22 1DS1	P1		Dark grey to black coarse grain limestone. In thin section consists of coarse grain moderately sorted, peloidal, bioclastic and oolitic limestone. The lower boundary is most possibly tectonic
Late Cret.	Shiranish Fn.	10m				Highly deformed bluish white marl (Most possibly belong to Shiranish Fn)
	Tanjero Fn.	0.5m				Conglomerate composed of angular to subangular and badly sorted chert and limestone pebbles with very rare graded sandstone beds.
Early Cretaceous	Balambo					
Late Jurassic	Possibly Barsarin					

LEGEND

Bedded chert



Peloidal and oolitic limestone



Marl



Conglomerate



Limestone (Upper part of Balambo Fn.)



Marly limestone (Lower part of Balambo Fn.)



Dolomitic limestone (possibly Barsarin Fn.)

P= limestone package

Fig.2.7: Cross Section of the lower part of Qulqula Formation in Dostadara Village sections.

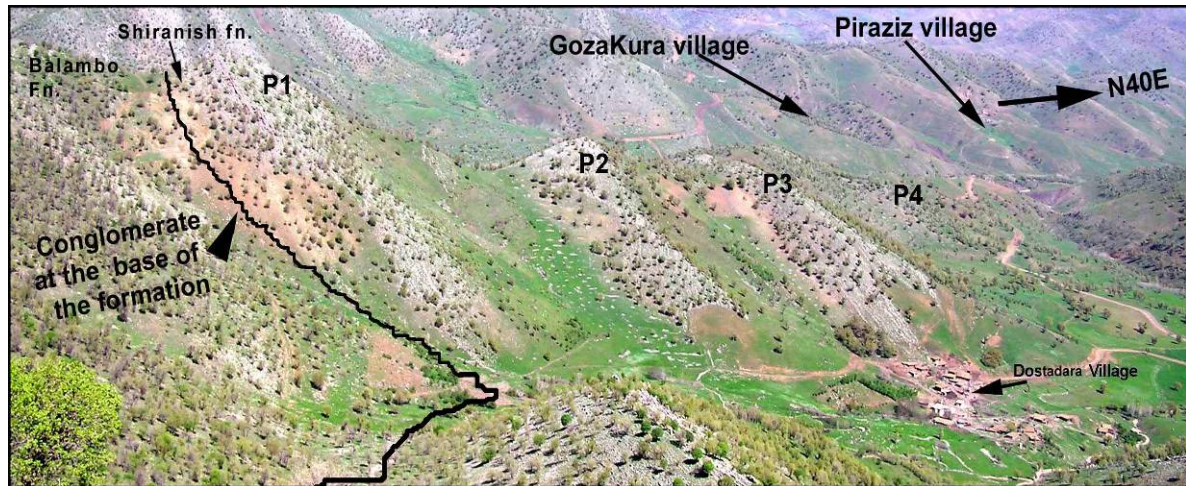


Fig.2.8: Four limestone successions at the lower part of Qulqula Formation, west of Dostadara Village, N latitude $35^{\circ} 34' 47.33''$ and E longitude $45^{\circ} 46' 45.63''$ (P1, P2, P3 and P4 are limestone successions).

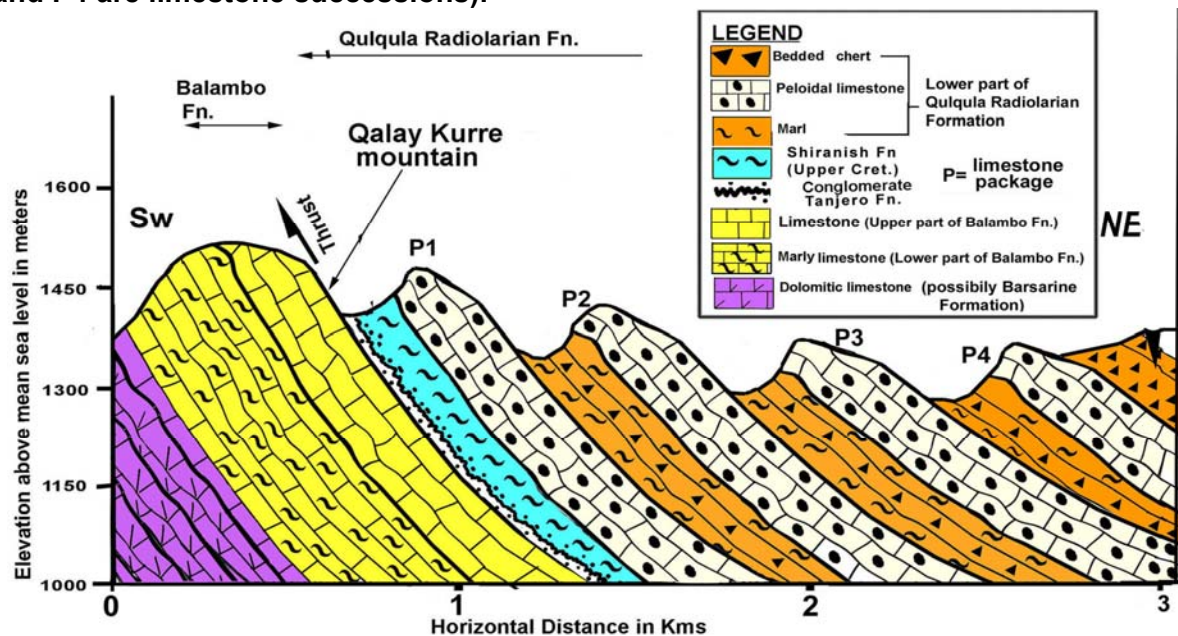


Fig.2.9: Geological cross section near Dostadara Village, passing directly by the west of Village sections.

2-3.Criterion for Finding the Top and Bottom (Way Up) of the Limestone Members

One of the difficulties that stand against this study is indicating whether these limestone successions are overturned or not. As the studied area is located in the Thrust Zone, the overturning is not excluded, due to imbrication and subsequent possible thrusting. To achieve these data, the field study was conducted to indicate the top and bottom of the successions by using sedimentary structures. Most outcrops are almost devoid sedimentary structures. The useful structures are:

2.3.1- Rip-up Clasts

The lithology and stratigraphic position of the clasts show that these clasts are intraformational and grains, which are removed from semi lithified substrata by current or wave. After removal, they are transported for short distance and then deposited with other sediments. The light grey sub-rounded clasts of the lower limestone bed can be seen in the upper layer of limestone of darker colour (Fig.2.10). These clasts were used for indicating the top and bottom of the beds. The clasts occur on the top of the bed (not at the top) therefore, the bed that is shown in the Figs. (2.10) is in the right depositional condition and not overturned.



Fig.2.10: Rip up Clast found in the limestone member of Dostadara section, at 1km to the south of Razila Village at 30km to the north of Said Sadiq Town.

2.3.2- Cross Lamination

Several small scale cross laminations are observed in medium and coarse grain limestone (Fig.2.12). According to Pamela, (1998), cross bedding exists in several environments; they are more common in river point bars, tidal channels, and delta and shelf environments. The acute angle between the underlying bed and tangential lamina is pointing towards the paleo-direction flow or sediment direction transport. The tangential laminas with the flat underlying laminas indicate the top of the strata (Fig.2.13 and 2.15A).

2.3.3- Graded Bedding

In the Qulqula Formation small scale and rare graded beddings are found in two different lithologies. They are found inside the limestone members (graded pebbly limestone) and directly below the conglomerates. Those that are associated with

conglomerate, include ripple marks (Fig.2.12). In both lithologies, the graded bedding have erosional base and grading is normal type in which the grain size decreases upwards. These beds are deposited by either turbidity current or by storm generated geostrophic current. It occurs in both sandstone and pebbly sandstone as normal grading (fining upward), which might be classified as Hummoke Cross Stratification. This structure is a part of ideal cycle called the Bouma cycle (Pettijohn, 1975).

According to Bates and Jackson, (1980) graded bedding is defined as a type of bedding in which each layer displays a gradual and progressive change in particle size, from coarse at the base of the bed to fine at the top. They added that it may form under conditions under which the velocity of the prevailing current declined in gradual manner, as deposition from single short-lived turbidity current. According to Pettijohn, (1975) gadded beds are deposited from waning turbulent flow and may range in thickness from a centimeter to one or more meters.



Fig. 2.11: Cross lamination in the limestone of the P1 (limestone succession one) near Harmela Village, 12km east of Chuwarta Town.



Fig. 2.12: Graded Bedding and Cross Lamination in the conglomerate at the base of Qulqula Formation at the area between Kaolos and Chuarta area 2km to the southwest of Dostadara Village.

2.3.4- Channel Gutter (Small Channels)

This structure consist of small depressions with depth of few centimeters and width more than 5 cm. They are scoured on the top of the limestone beds and filled with coarse sand sized to conglomeratic clastic limestone that show normal graded bedding and lamination (Fig.2.13). The granules rest at the lowest portion of the gutter. They are found in the limestone successions to the north of Said Sadiq, exactly at 2 Km south of Razilla Village at N latitude $35^{\circ} 33' 23.23''$ and E longitude $45^{\circ} 36' 55.05''$. These structures also indicate normal stratigraphic position (not overturned) for the limestone successions. The channel gutters are most possibly formed on the erosional surface as the environment was of fairly high energy. This surface is observed in three thin sections in three different beds, as represented by samples 2Dos-1a and 3Dos-4b of the Dostadara section. In thin sections, the two different lithologies are separated by sharp boundary, the peloidal or lithoclastic grainstones are at the top, while the mudstone are at the bottom of the oriented slide (Fig.2.14, A and B). The aforementioned four structures show that most limestone successions (especially P1 and P3) are not overturned. The condition of P2 and P4 is not known since useful sedimentary structures are not found to indicate their top and bottom.

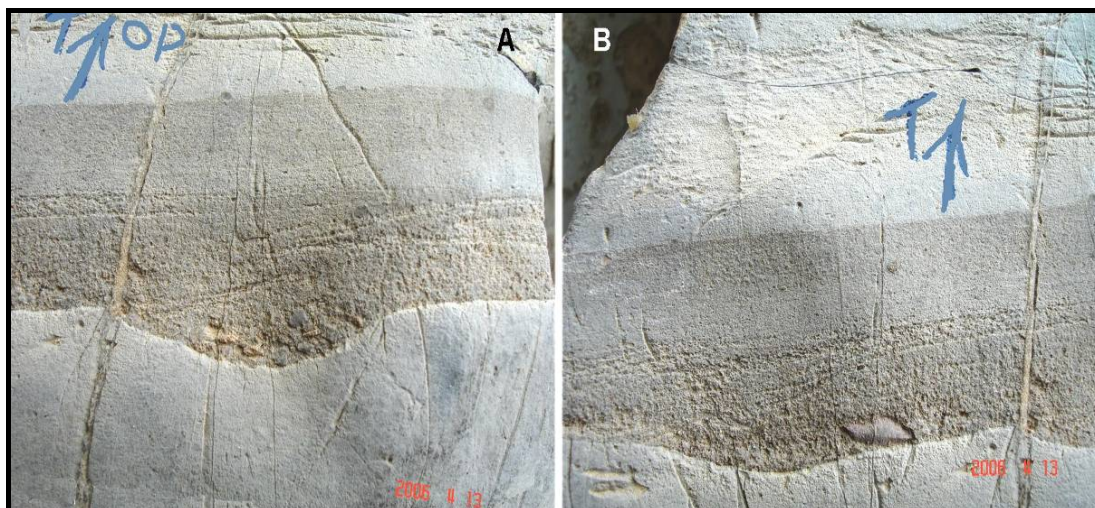


Fig.2.13: Gutter Cast Graded Bedding and Cross Lamination in the studied limestone succession at the lower part of Qulqula Formation at the area between Kaolos and Chuarta area 2km to the southwest of Dostadara Village (The width of photo is 8 cm).

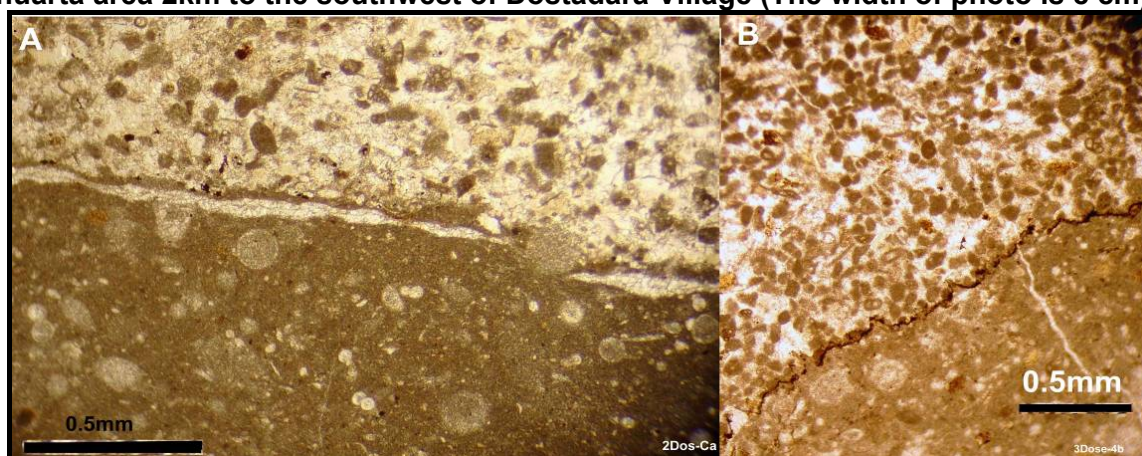


Fig.2.14: Thin section photos of the sharp contact between bottom and top (wackestone and peloidal grainstone respectively) of two limestone layer of the Dostadara sample, 2Dos-1a-P2 (A) and 3Dos- 4b-P3 (B).

2-4- Upper Boundaries of the Qulqula Formation

The most problematic concern of the Qulqula Formation is the nature of its boundaries. This is because there is doubt about the depositional position of the formation yet. This doubt includes whether the formation is deposited inside Iran and thrust to Iraq or it is deposited in the present position inside Iraq. In this concern, Heron and Less, (1943) mentioned that Qulqula Formation is allochthonous rock unit and transported from the east to the present location.

But Bolton, (1958) and Smirnov and Nelidov, (1962) considered the formation as autochthonous rock unit and have not undergone any change in position except faulting. Buday and Jassim, (1987) reported thrusting of Qulqula Formation on the Balambo Formation for about 15 km. They also mentioned that Penjween metamorphic Group (Aptian-Albian) is laterally equivalent to Qulqula Group. Recently, Numan, (1997) established a plate tectonic scenario for Iraq and discussed

historical development of the depositional basins during Phanerozoic. Depending on allochthony, he considered Balambo and Qulqula Formations to be on trench-like basins, at both sides of spreading mid-oceanic ridges (Fig.2.15). Jassim and Goff, (2006) referred to allochthonous nature of Qulqula Formation which cropping out in the Qulqula-Khwakurk Zone.

The most acceptable model is that drawn by Ameen (2008) who considered the formation in foredeep basin between forebulge and accretionary prism. In the model the formation is assumed as lateral facies change of Balambo Formation. Later on Taha, (2008) expanded the model to include the Late Cretaceous formations (Fig.2.16). It is clear from the above citation that most authors referred to Qulqula Formation as thrust and transported rocks. Due to this nature of the formation, the study of the boundaries is extremely difficult.

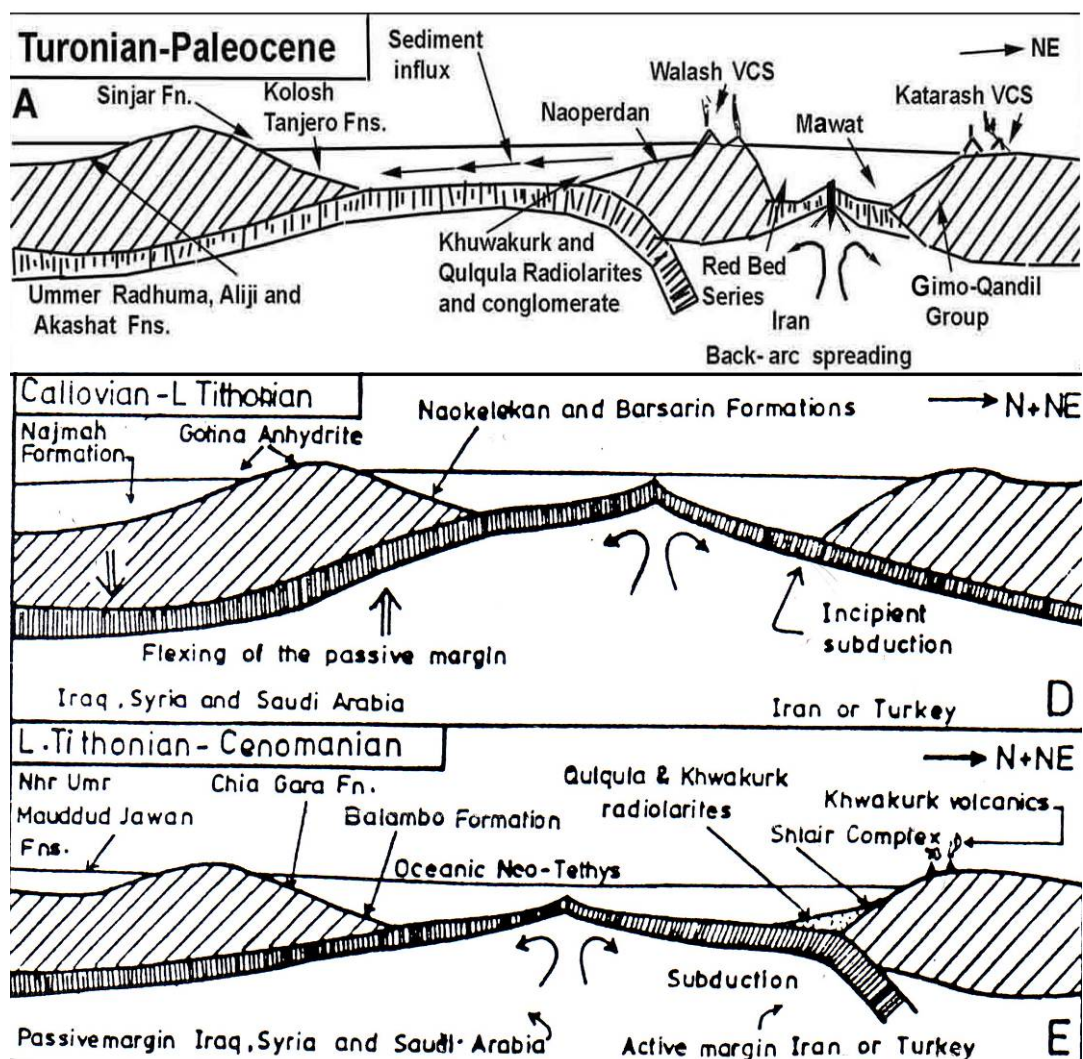


Fig. 2.15: Position of the Qulqula and Conglomerate Formations within Tectonic Scenario of Northeastern Iraq, (Numan, 1997).

2.4.1- Upper Boundary at the Northwestern Part of the Studied Area (NP)

The northwestern part of the studied area is located 20 km to the north of Qaladiza Town. In this area, the lower boundary of the formation is not exposed while the upper boundary forms tectonic contact with the Red Bed Series. In this area Baziany, (2006) recorded and described angular unconformity between the Red Bed Series and the underlying Qulqula Formation in Qulqula gorge, Qandil Mountain toe and north of Basne Town (Figs.2.16 and 2.17). In these two areas, the Red Bed Series overlies the Qulqula Formation in angular unconformable condition. The dip angle (dip angle of the plane of angular unconformity) is equal to 17° and 21° respectively. Above the unconformity, the Late Cretaceous rocks are missing from stratigraphic section of Cenozoic.

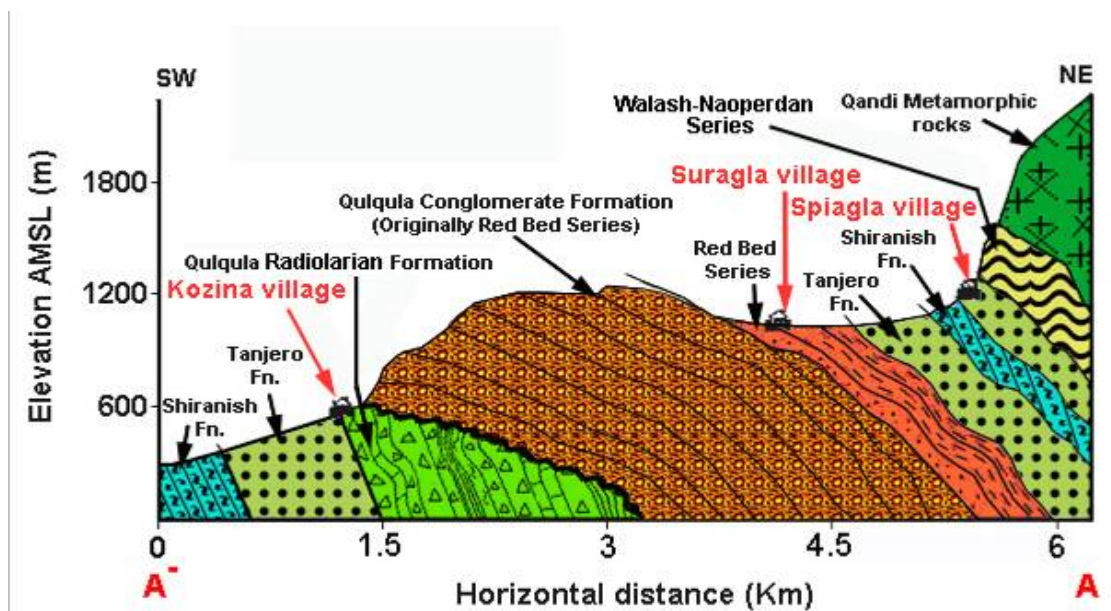


Fig. 2.16: Angular unconformity between Red Bed Series and Qulqula Formation at Northwest of Qaladiza Town (Baziany, 2006).

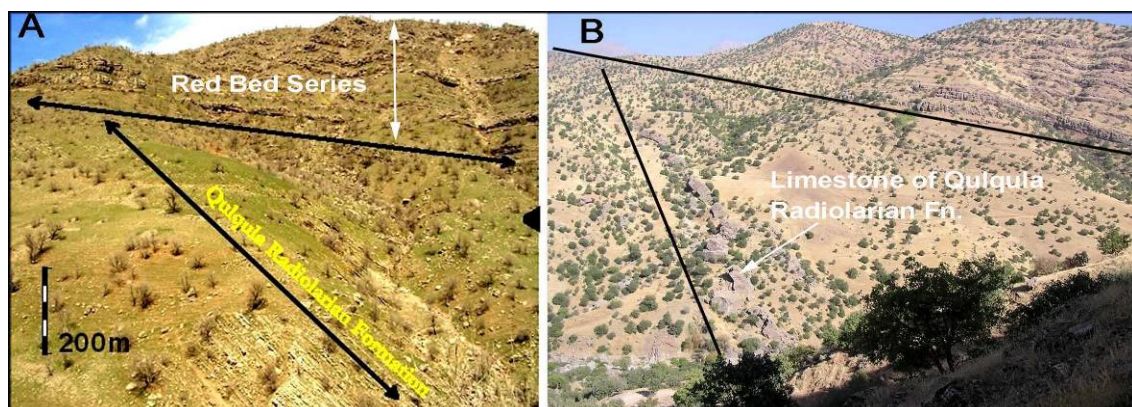


Fig.2.17: Angular unconformity between Red Bed Series and Qulqula Formation at Northwest of Qaladiza Town (Baziany, 2006).

2.4.2. In the Area between Nalparez and Tawella Towns

According to Baziany, (2006), in this area, the Qulqula Formation is covered by different Quaternary sediments (Fig.2.18) and rocks as following:

2.4.2.1. Thickly Bedded Conglomerate

This type of Quaternary sediments is most common and found as thick beds, which have lateral extend for several Kms. It is exposed along the lower slope of southwestern side of Suren and Avroman mountains, north of Khurmal and Said Sadiq towns. At these localities, in some cases, the conglomerate appears as a thick massive limestone and shows rare granularity.

2.4.2.2. Separate Block of Conglomerate

The second type is found as relatively small and isolated blocks. These blocks can be seen along the two paved roads to Nalparez from Shanadari and Kaolos especially between Tarratawan and Dolla Chawt villages. These blocks rest on outcrops of the Qulqula Formation and they consist of gravels of alluvial origin as they show sign of transportation. These blocks are most possibly derived from bedded conglomerate (type one) by sliding from Suren Mountain.

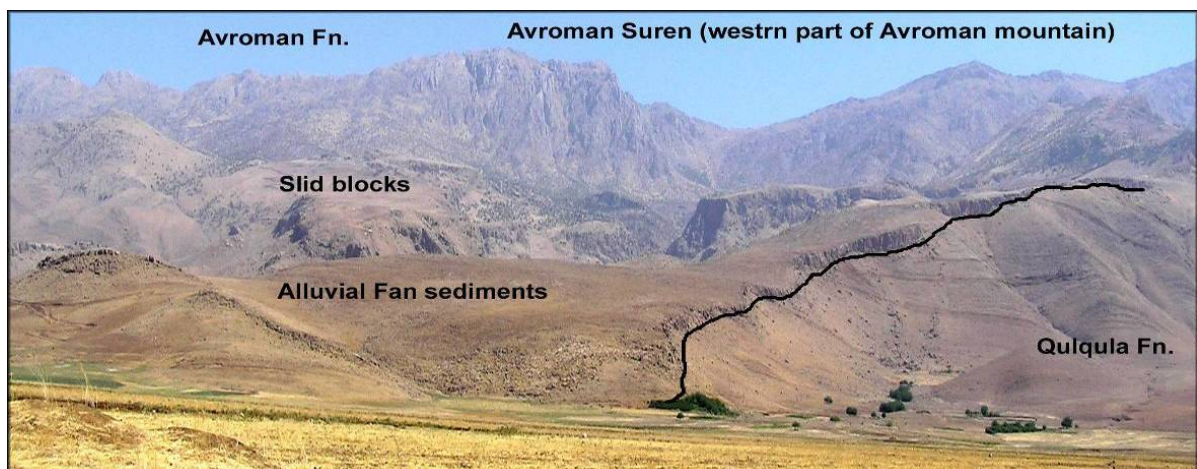


Fig.2.18: Resting of alluvium fan sediment (Quaternary) on Qulqula Formation at northern boundary of Sharazoor plain.

2.4.2.3. Sliding Bedded Bocks

In the area of northern boundary of Sharazoor plain near the western part of Avroman Mountain, many very thick and massive beds can be seen over Qulqula Formation. The thickness of some of these bed reach more than 500m of limestone. These beds rarely show granularity and laterally change to type one or type two. According to Baziany, (2006) due to huge thickness, massiveness and gray colour represents Qamchuqa Formation (Jovanovic and Gabre, 1979) and (Ali and Ameen,

2005). Baziany, (2006) interpreted these beds as large blocks of Avroman Limestone which have slipped (slid) from high elevation and rested on Qulqula Conglomerate Formation at lower elevation.

2-4-2-4. In the Penjween Area

According to Jassim and Goff, (2006), Merga Red Beds Group overlies unconformably Qulqula Formation. They mentioned that the former consist of red silty calcareous shale and pebbly sandstone which laterally pass into conglomerate.

2-4-2-5. In the Area at the Northwest of Halabja Town

The upper boundary of the Qulqula Formation is also inspected at Halabja area, which shows a tectonic looks like contact with Balambo Formation. In this area, especially at northeastern limb of Shinarwe anticline (or mountain) exactly at 8 km northeast of Halabja Town the contact is exposed. At this area the Qulqula Formation changes from bedded chert to limestone passing through marl and marly limestone as intermediate lithology.

2-5- Cyclicity Indicators in Qulqula Formation

2-5-1- Signals of Cyclicity

The signals of cyclicity are very impressive and clear in all parts and in the whole exposed areas of the formation. This cyclicity does not change neither laterally nor vertically. The sign of cyclicity is well demonstrated by several cycles of lithologies. Each lithology of the cycle's constituent beds and laminations, the beds are of few centimeters to one meter in thickness while those of the lamination have thickness of one millimeter to few centimeters (Fig. 2.19). The cycles consist of the following lithologies:

A- limestone-Marl (limestone is background and interbedded with lamiane of marl) at the lower part and upper part of the formation (Fig. 2.19A).

B-Shale-chert (Chert is background), at the middle part

C-Marl-Chert (Chert is background) at the middle part.

D-Marl- siliceous shale (at the middle part) Fig. (2.19B).

E-jasper-Shale (at the middle part).

F-Jasper -marl (at the middle part).

Each cycle alternating as very thick succession, forming long duration and constant repetition of cyclicity in the basin of the formation.



Fig.2.19: (A) Alternation of marl laminas and limestone beds, (B) Alternation of marl and siliceous shale at the middle part of the formation.

2-5-2-Reason of Cyclicity and Time Relation between Lithologies

The clear and impressive signals of cyclicity could be attributed to the Milankovitch astronomical theory (or Milankovitch band) for interpreting and classification of layering of sedimentary rocks. In this study, the cyclicity of the formations is estimated to be resulted from earth orbital cyclicity (orbital signals). Orbital cyclicity, in turn, generates alternated warm and cold long and short durations (repeated climatic fluctuations) which reflected by rocks by deposition of different lithologies in the sedimentary basins. The climatic variations affect ice accumulation in the poles and sea level change (rise and fall). Milankovitch band consist of three types of wave lengths which have the duration of 106, 41, 19 Ka. (Doyle and Bennett, 1998). These wave lengths (earth orbits) are called eccentricity obliquity and precession cycles respectively which are resulted from different orbital of earth around itself and sun. For more detail see (Haq, 1991), (De Boer, 1991) and (Gale, 1995), and (Holland, 1998).

The cyclicity of the Qulqula Formation is from most possibly attributed in the Milankovitch band especially the wave length (sea level change duration) of obliquity (40 ka), which modulated by eccentricity (100 ka) and precession (20 k). This is because the total number of cycles, is very high, which exceeds 1000 cycles. When the total numbers of the cycles are multiplied by 40000 years, the duration of the deposition of the formation is equal to forty m.y. This age estimation of one couplet is rough estimation only, because the time space of the formation is not precisely known. Moreover, the formation might be suffered from imbrications and repetition, several times so that the actual number of the couplet can not be calculated.

During the sea level rise, as formed by high obliquity and precession with low eccentricity, the chert is deposited during warm duration, when the studied area had become caloric equatorial zone. This leads to the ice cap thawing on the northern

hemisphere of the earth and consequently sea level rise. The deposition of limestone started in the opposite situation to that of chert. The marl or shale is deposited at the intermediated distance. Hori et al., (1993) ascribed the occurrence of chert/shale pairs (couplet) in Franciscan Formation to Milankovitch climatic cycle (~100,000 years cycles of warm and cold periods). During the warm periods, the radiolarians bloomed and their skeletons rained into the ocean floor. In colder periods, the radiolarians were scarces and clays transported by ocean currents or winds were deposited.

2-6-Origin of the Chert in the Qulqula Formation

2-6-1-Origin of Chert Nodules

Qulqula Formation is characterized by its bedded chert content and even the limestone beds contain different types of chert nodules and strings (Fig.2.20). These nodules are random and have not any observable cyclicity. The chert nodules show displasive habit and diagenetic origins, which manifested by four points:

The first one is that some nodules are found in cross laminated sandy limestone (lithoclastic or peloidal grainstone). The nodules cut the laminae of limestone bed (Fig.2.21). Therefore, when the principle of “cutter is younger than the cut” is used the nodules become younger than limestone. In the other samples, strings (discontinuous narrow belt) of the black chert are found in the sandy limestone of the limestone succession of the lower part of the formation.

The second point is that the nodules are found also in limestone with trace fossils (Fig.2.22).

The third point is that under stereoscope microscopes, the nodules show displasive habits, which pull apart the limestone material away from the boundary of the nodules.

The fourth point is that under stereoscope microscopes the transitional stage of silicification (partial silicification) of peloidal and bioclastic limestone can be seen. In these partially silicified rocks, the original constituent can be found such as crinoidal fragment, which has net texture of the crinoids, but it loss its famous syntax extinction. These features of relations between chert nodules and host limestone prove that they formed after deposition of the limestone by diagenesis. Most possibly they formed after or during burial of the sediments.

Replacement and displaced growth of chert nodules in Qulqula Formation require concentration of silica ions in certain locus within the limestone. The diffusion and

movement of watery solutions are the most important dynamic factors for transferring silica from direct or roundabout neighbouring areas. This occurs mostly during burial in which the pressure increases and the silica rich migrate by diffusion in basic solution and metasomatism, which consist of movement of silica ions in stationary solutions and ion replacement in materials, (Blatt, et al., 1980).

During the burial, the pressure and temperature increase and both factors are increasing. The sites of high silica concentration are supplying silica for diffusion and metasomatism. The main source for diagenetic growth of the nodules in the limestone successions is attributed to two sources. The first source is the silica super saturated deep water that existed during deposition of the bedded chert that overlies the limestone successions. This source is responsible for early diagenetic silicification of limestone beds.

The second source is from the bedded chert by which silica-rich watery solution had moved downward and passes through the porous limestone successions (grainstone) and converts part of the chert nodules. This source is responsible for the late diagenetic nodules development.



Fig.2.20: Cutting of the laminae of a Cross Lamination by Chert Nodules in the limestone succession of Qulqula Formation at 2 km east of Zallan Village on the road between Chuarta Town and Nalparez Village.



Fig.2.21: Cutting of the Laminas of a Cross Lamination by Chert Nodules in the limestone succession of Qulqula Formation.



Fig.2.22: Occurrence of Chert Nodules in sandy limestone (lime sandstone) in the limestone succession of Qulqula Formation at the west of Dostadara Village.

2-6-2- Origin of Bedded Cherts

As mentioned before, the most important characteristics of Qulqula Formation is its bedded cherts, which occur as (5-30) m thick successions of thin bedded (3-10) cm cherts. The numbers of these beds reach thousands and each bed is laterally traceable for more than several kilometers. According to (Reading, 1986), the origin of the bedded cherts can be attributed to the deep environment, where the depth is below calcite compensation depth. In this depth the calcite does not deposited on the sea floor.

Bedded radiolarian cherts range in age from at least Cambrian to Eocene. Siliceous deposits formed in modern seas are not the same and diatoms have become the dominant siliceous contributing organism since the Oligocene. Reading,

(1986), added that papery thin and thicker argillaceous layers, rich in alumina, are the commonest sediments interbedded with the radiolarian cherts. Possible origins are (1) rapid accumulation of radiolarian (blooms) with slow accumulation of argillaceous material, (2) rapid accumulation of radiolarian turbidites with slow accumulation of argillaceous material, (3) slow accumulation of radiolaria with rapid accumulation of argillaceous turbidites, Table (2.1). It is though that all three origins occur but number (1) seems more common. In Cyprus, radiolarian chert beds are found in chalk. In these environments the chert appears to form more rapidly than the other rock types but in one sequence of alternating limestone and chert the depositional rate may be similar. Late Paleozoic and Triassic chert sequences in western North America have formed mostly in more shallow waters than those of the Jurassic and younger. Many chert sequences sit on greenstones and are overlain and interfinger upward with greywacke indicating origin in Open Ocean and transported by sea floor spreading toward sites of turbidite clastic deposition. Other sequences show reappearance of chert upward at several intervals (Danner, 1985).

Table (2.1): seven hypotheses proposed for the origin of bedded radiolarian cherts(Hori, et al., 1993).

Diagenetic Process	Deposition of clay-radiolarian mixture with (see the right cell)	1. Post depositional separation of clay and silica of radiolarians.
Depositional Processes	Deposition of clay-radiolarian mixture with	2. Silica compensation depth (SCD) perturbation removes radiolarians through dissolving.
	Deposition of clay-radiolarian mixture with	3. Turbidites of clay-radiolaria mixture and consequent sorting.
	Constant deposition of Clay with	4. Episodic and rapid deposition of radiolaria.
	Constant deposition of Clay with	5. Turbidites of Radiolaria.
	Constant deposition of radiolaria with	6. Episodic and rapid deposition of clay.
	Constant deposition of radiolaria with	7. Turbidites of clay

Hori, et al., (1993) mentioned that the absence of CaCO_3 in the Franciscan cherts suggests that they were formed below the carbonate compensation depth (CCD). They added that fourth hypothesis may be supported by sediment accumulation rates for the Franciscan chert/shale pairs suggesting that the Milankovitch climatic cycle (~100,000 years cycles of warm and cold periods) could explain the pairings. In this hypothesis and during the warm periods, the radiolarians thrived and their skeletons rained onto the ocean floor. In colder periods, the radiolarians were scarce and clays transported by ocean currents or winds were deposited.

Cecil, (2004) ascribed the origin of sedimentary chert to eolian dust in warm-arid environments as shown in the next paragraph. Dust as a precursor for chert is likely restricted to aerosols derived from warm-arid deserts where fine-grained quartz is the predominant mineral component. Significant quantities of quartzose eolian dust are exported from modern terrestrial warm-arid environments. For example, 130 to 760 million tones of dust are blown from the Sahara Desert each year (Wright, 2001).

The Saharan dust is composed predominantly of fine-grained quartz with minor amounts of carbonates, feldspars, and clay minerals, unlike the heterogeneous composition of dust in cold-climate deserts. Rates of dust deposition in modern warm deserts range from 50 to 200 tones $\text{km}^{-2} \text{ yr}^{-1}$, summarized in Pye and Tsoar, (1987), which could result in accumulation rates that range from 2 to 7.5 10^{-3} cm/yr (2 to 7.5 m/100 Ka). Such accumulation which rates in marine environments would equal to or exceed the interpreted rates of chert accumulation. Furthermore, dust deposition rates during the Pleistocene were at least two orders of magnitude greater than the present rates, (Pye and Tsoar, 1987). Such temporal variations in dust deposition in marine environments can account for the stratigraphy of bedded cherts where chert may form during periods of high dust input, but other lithologies (for example, shale, evaporites, or impure limestone) are deposited during periods of relatively low input of siliceous dust.

The origin of silica in the Qulqula Formation can be attributed to the following sources:

- 1- It can be attributed to the deposition of planktonic radiolarians, which can be seen in the thin section and under binocular stereoscopic in the cooked marl samples of marls of the Qulqula Formation. The deposition of these fossils below CCD and above SCD concentrate sufficient amount of silica to form beds on the expense of

limestone. While slight perturbation of both calcium and silica compensation leads to deposition of mixture of siliceous limestone or limy chert.

2- Another source of silica in Qulqula Formation is that it might be derived possibly from eolian dust, which consists mainly of quartz grain and suggested by Cecil, (2004) for silica source in marine environment in the warm and arid climate. This is because it is possible that the basin of the Qulqula Formation was surrounded by warm and arid deserts during lower Cretaceous. These deserts most possibly located at present position of southwestern Iraq, Jordan and Saudi Arabia. In the Paleocene rocks of Iraqi Western Desert, Al-Rawi, (1988), showed clear photos of polished slab of chert nodules in which distinctive nummulites can be seen in silica matrix. The central Asia is not excluded from the source of silica as it was a shield during most geological time.

CHAPTER THREE

MICROFACIES ANALYSES

3.1. Introduction

The present study has utilized the classification of Dunham, (1962) and its modified version by Embry and Klovan, (1971) for studying the carbonate rocks of the formation and its facies analyses. This is because this classification gives good indications on genetic of the rocks than other classifications (Fig.3.1).The derived name from this classification, gives information on the depositional texture and energy of the environment. Dunham classification has presented different types of carbonate that can be used as facies.




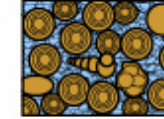
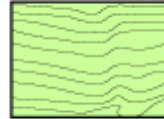
Original components not bound together at deposition				Original components bound together at deposition. Intergrown skeletal material, lamination contrary to gravity, or cavities floored by sediment, roofed over by organic material but too large to be interstices
Contains mud (particles of clay and fine silt size)		Lacks Mud		
Mud-supported		Grain-supported		
Less than 10% Grains Mudstone	More than 10% Grains Wackestone	Packstone	Grainstone	
				

Fig 3.1: Classification of Dunham, (1962) for carbonate rocks

3.2. Lithofacies Variation

The limestone successions in single section and even in the five different sections imply different types of facies, but generally the successions show low diversity of the facies. The variations in the facies could be used to infer the environmental conditions during the deposition of lower part of the Qulqula Formation. The changes

in the environmental conditions are reflected by different types of lithofacies which could be controlled by the tectonic instability of northern Iraq and Iran during Late Jurassic and Early Cretaceous times (as assumed depositional ages of the Qulqula Formation).

3.3. The Microfacies of the Limestone Successions

The carbonate rocks of Qulqula Formation are composed mainly of coarse grain limestone (sandy limestone). This can be seen in the middle part of the successions while toward the base and top they contain some fine grain limestone (mudstone).

The lithoclasts, peloids, ooids and the broken skeletons of invertebrates and calcareous algae are the main allochems and produce sandstone –like carbonate.

In limestones of the Qulqula Formation, the lithofacies or microfacies are rarely consisting of one type of allochems because most facies contain more than two types of grains. Therefore the microfacies are named on the basis of one or two main allochems constituents.

The sand, commonly 0.02 mm and larger, is formed by many processes, as will be seen later. In Qulqula Formation the sand grains are all almost intraformational (intraclast) and derived from near the site of deposition. In ancient rocks, these grains usually can be easily recognized by microscopic examination either in reflected light or in thin section.

The lithofacies (microfacies) of the formation are as follows according to their frequency in the successions, Table (3-1):-

3.3.1. Grainstone Microfacies:

This facies consists of non-skeletal grains (intraclasts) such as lithoclast, peloids and ooids in addition to broken skeleton fragments (bioclasts) in Dostadara (1st, 2nd, 3rd Ridges) and Type sections. This grain, when compared with the literature, they imply that they are deposited in high energy normal marine environments, (Tucker, 1991). All the above allochems are suffered of different degrees of micritization, Figs (3.4., 3.10. 3.13. and 3.18.) respectively.

3.3.1.1. Lithoclasts Grainstone

Lithoclasts are equivalent to extraclasts, which their size varies from 0.3mm to several centimeters. According to Blatt et al, (1980), Lithoclast (or mudclasts) is used to imply a rock fragment derived from outside the basin of carbonate deposition by

erosion and transportation. They added that, in terms of the hydraulics of transport and history, there is significant genetic difference between a mud crack flake or an eroded fragment of contemporary beach rock (both are intraclasts) and an older limestone pebble (lithoclasts).

Table(3-1): Lithofacies variation of the Qulqula Formation according to their frequency in the successions

Grainstone Microfacies consists of non-skeletal grains (intraclasts) such as lithoclast, peloids and ooids in addition to broken skeleton fragments (bioclasts) in Dostadara(1st , 2nd, 3rd Ridges) and Type sections.	Lithoclasts Grainstone , both sign of lithoclasts and intraclasts can be seen in Dostadara limestone successions, generally badly sorted and occasionally contain whole skeletal grains such as algae and planktonic forams.
	Bioclastic Grainstone , the most common bioclasts are pelecypod, green algae, fragment and forams (Tetrataxis).
	Peloidal Grainstone , different in size, shape and roundness (Figs. 3.10, 3.11 and 3.12). The most possibly developed that from micrization of different lithoclast and bioclast and even from skeleton.
	Oo-Peloidal Grainstone , In Dostadara section, south of Razilla and Parazan villages, this section contain cross laminated bed of ooid-peloid grainstones which shows, in some case, cross cutting by chert nodules
Rudstone Facies	Consist of self-supporting large allochems (more than 2 mm in diameter) which are bounded by mudstone, only found in two places, east of Gali village and south of Razla Village.
Bindstone Lithofacies	Present in Dostadara (2nd Ridge) and Type Locality sections, contains green algae which consists of irregular clotted bodies which enclosed by encrusted thin lamina.
Floatstone Facies	This facies is rare and consist of grains larger than sand size which floating or embedded in fine matrix of lime mudstone in Dostadara section
Mudstone Microfacies	This facies restricted to the base of successions of Dostadara section
Diagenetic Chert Bearing Lime Wackestone Submicrofacies	Occurs nearly in all section especially at the base of the sections, such as Dostadara, Kaolos and Gali.
Intraclastic Wackestone	Several places of intraclastic wackestone found in the east of Dostadara and south of Razilla villages.

Fossiliferous sedimentary rock fragments that can be dated as significantly older than the host rock are lithoclasts while the implication of the term intraclast is the lithified particle and its disruption from its original setting and redeposition took place essentially contemporaneously with the sedimentation of the stratigraphic unit in which it is found. According to the Blatt et al., (op. cit), the distinction becomes more difficult; however with limestone fragments are lacking internal evidence for their age. In general, lithoclasts are very uncommon in most carbonate rocks. Where a carbonate platform terminates landward against a sea cliff of older rocks, the eroded products of that cliff may contribute lithoclasts to the new sediment. Both intraclasts

and lithoclasts have been termed limeclasts when the distinction between distant and local derivations cannot be made.

According to Tucker, (1991), intraclasts are fragments of lithified or partly lithified sediments. A common type of intraclast in carbonate sediments is a micritic flake or chip derived from desiccation of tidal-flat muds or disruption by storms of partially lithified or cemented subtidal lime muds (Fig. 3.6).

In Qulqula Formation, both sign of lithoclasts and intraclasts can be seen in Dostadara limestone successions. The lithoclasts mostly contain some fossil structures and show more angularities than intraclasts, while intraclast are mostly rounded structures.(Fig. 3.2 A). They have darker colour tone as compared to the lithoclasts. This facies is generally badly sorted and occasionally contain whole skeletal grains such as algae and planktonic forams (Figs. 3.3, 3.4, 3.5 and 3.6).

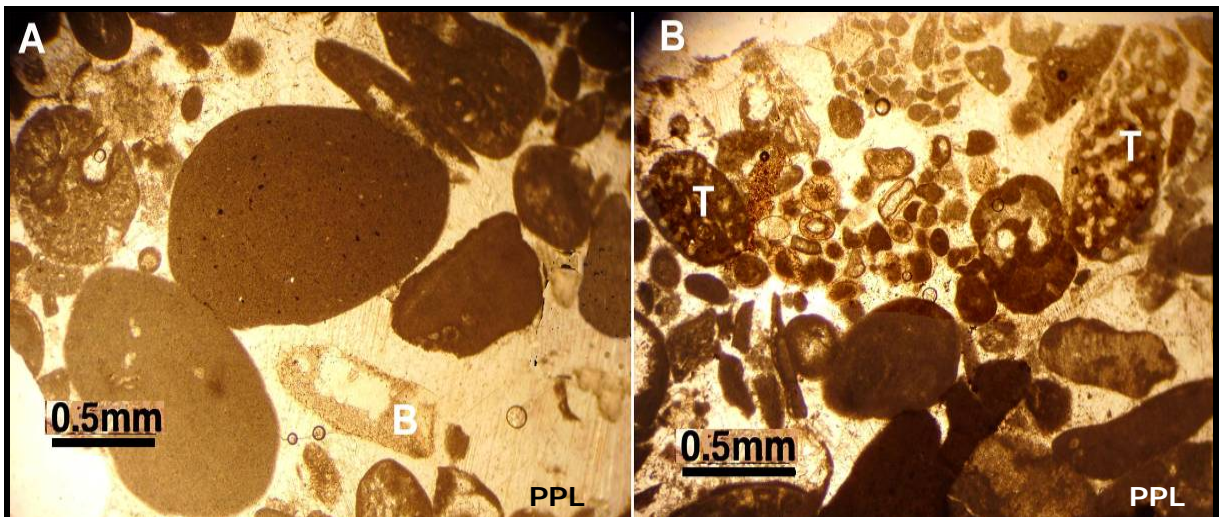


Fig.3.2: A) Well rounded different lithoclast (dark colour) with bioclasts. B) Different lithoclast (dark colour) with bioclasts (T). Sample: 1Dos-20b and 20d.

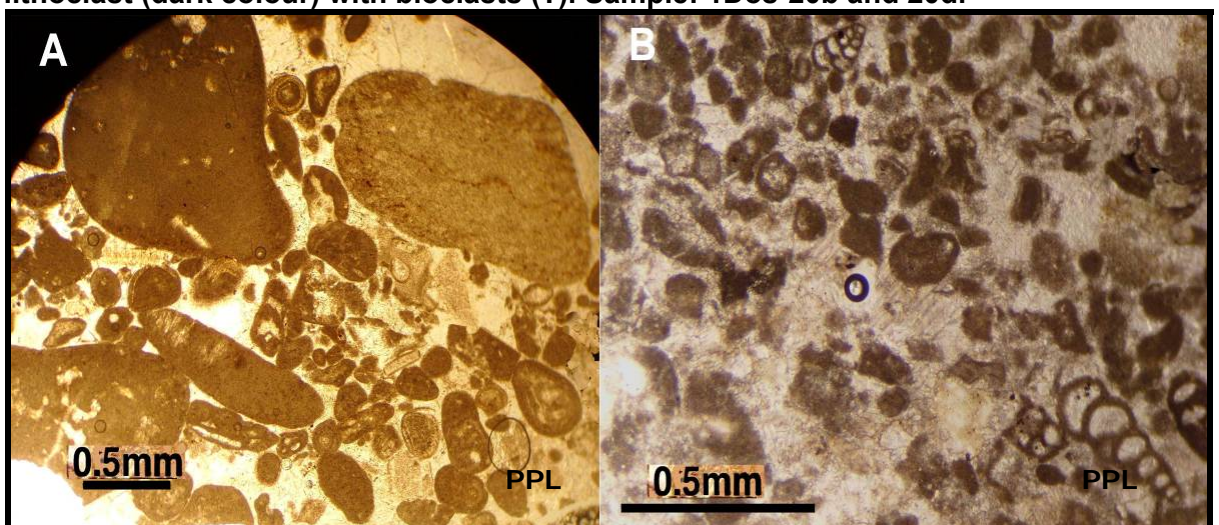


Fig.3.3: A) Badly sorted different lithoclast. B) Subangular lithoclasts with foramoniferas whole skeletons. Sample: 1Dos-20b and 20d.

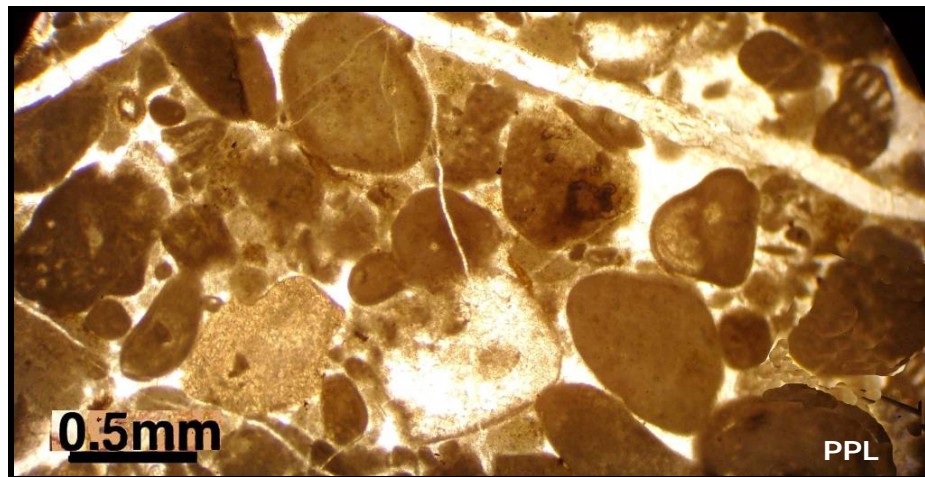


Fig. 3.4: well rounded different lithoclast and few bioclasts showing different degrees of micritization with two sparite filled cracks at the top left and right. Sample: 2Dos-15a.



Fig. 3.5: Well rounded different lithoclast showing different degrees of micritization. Sample: 2Dos-15a.

3.3.1.2. Bioclastic Grainstone

According to Blatt et al., (1980), the whole and broken skeletons of invertebrates and calcareous algae may produce carbonate sand. The type of grain and its mineralogy naturally depend on the available organisms. Therefore the age of the rock as well as the specific environment of formation determine the types of grains found. They added that the skeletal particles may be broken into smaller grains by several mechanisms such as waves, currents and organism. They added that organisms like the boring sponges and algae may perforate a larger particle.

In the Qulqula Formation, the most common bioclasts are pelecypod, green algae, fragment and forams (Figs. 3.6, 3.7 and 3.8). In most cases the pelecypod clasts show well roundness and different degrees of micritization by algae (Fig.3.6). These green algaes are large fragment and subangular which consist of colony of cross section while in longitudinal section it resemble finger (Fig.3.6). Its size of the individual is very small (0.05mm in diameter).

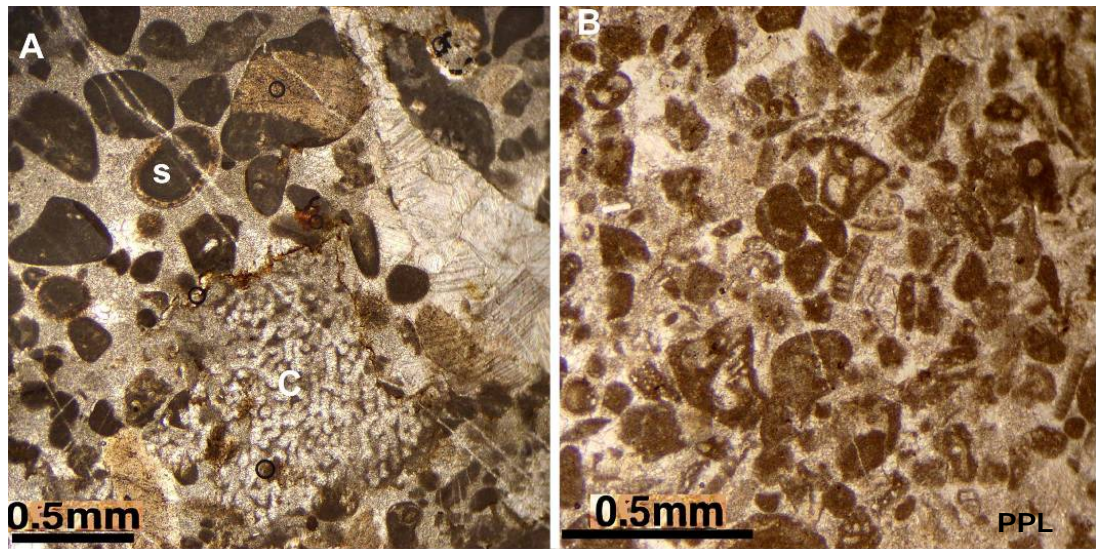


Fig.3.6: A: Intensely micritized lithoclasts with one longitudinal section of green algae(c) and superficial ooids(s). B: Badly sorted bioclasts (possibly pelecypods) with lithoclasts. Sample: 1Dos-9b and 10b.

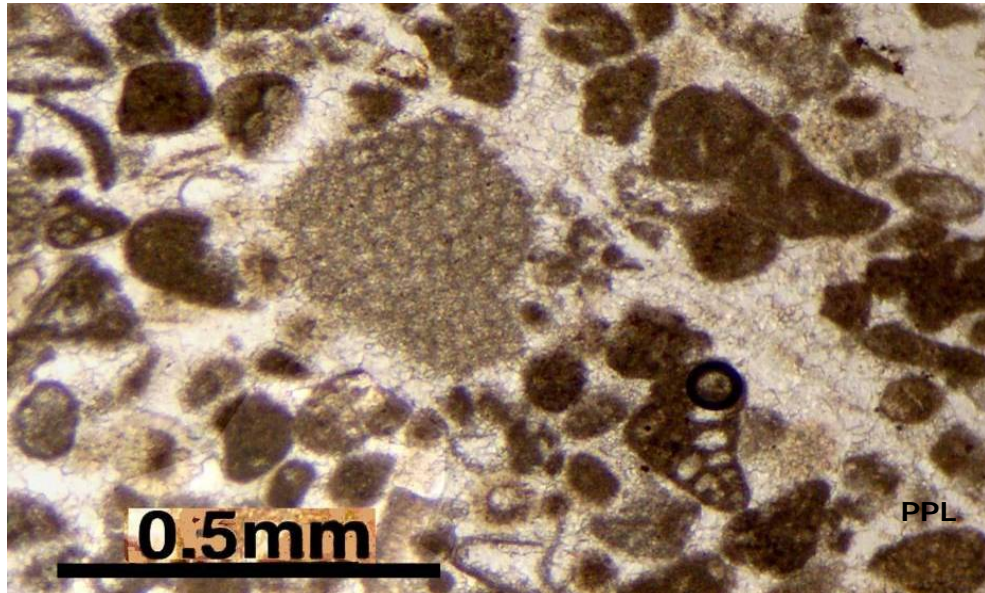


Fig. 3.7 Longitudinal section of *Tetrataxis inflata* (Bottom Right) and some other foraminiferal clasts and lithoclasts. Sample: 1Dos-11a.

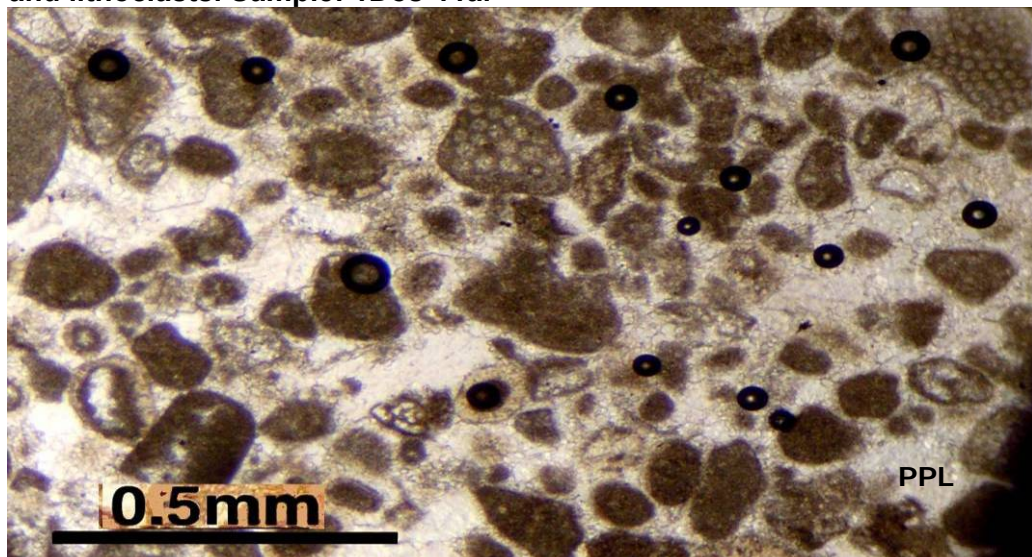


Fig. 3.8: Some foraminiferal clasts (as a colony), lithoclasts and superficial ooids. Sample: 1Dos-11b.

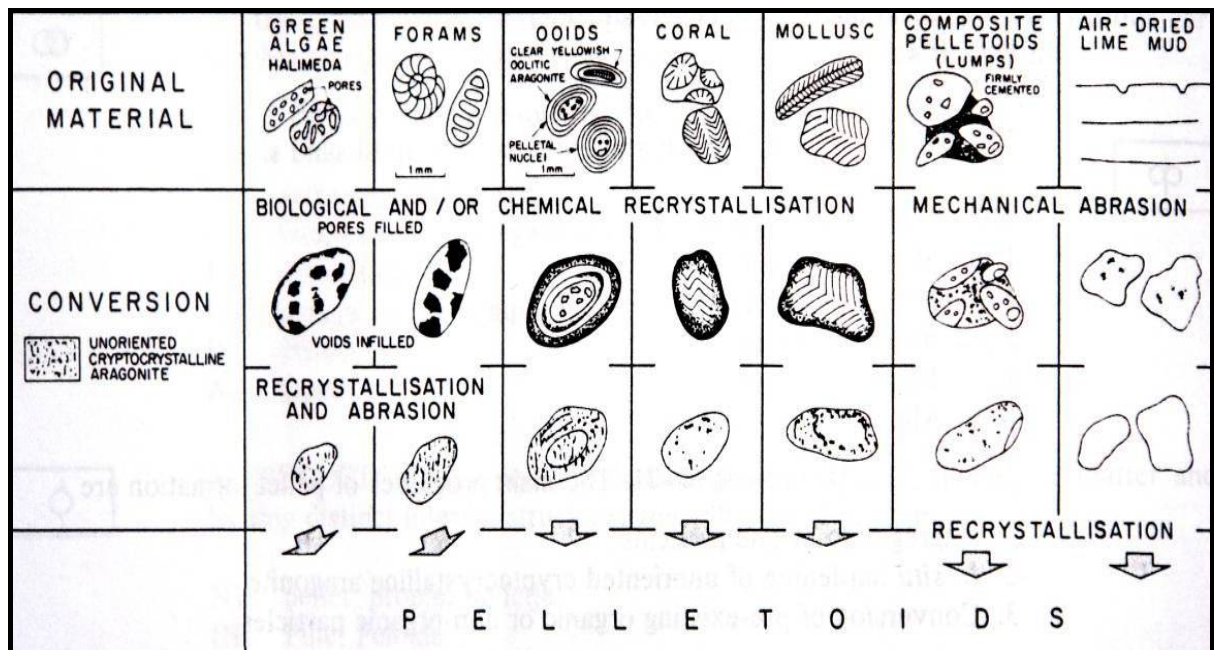
3.3.1.3. Peloidal Grainstone

Peloids are circular to elliptical grains composed of micrite and lacking the internal structure with dark colour. They are relatively well rounded and sorted particles, with different sizes. In general, the name of peloid was applied to all particles of various origins, which consist of cryptocrystalline carbonate (Mc Kee and Gutschick, 1969 in Flugel, 1982). Peloids (including pellets) can be developed and created by progressive micritization of bioclasts and/or due to reworking of their particles in agitated water (Reijers and Hsu, 1985 and Tucker, 1991). Peloids, with some bioclast, are the major components of this facies, which are (0.07- 0.2) mm in diameter (Figs. 3.9 and 11). They are most probably formed by algal mercerization of the bioclasts, whole skeletons and lithoclasts. This is due to the presence of different degrees of micritization can be seen. This facies is found in shallow water with moderate circulation (Wilson, 1975).

According to Tucker, (1991) Organisms such as gastropods, crustaceans and polychaetes produce fecal pellets in vast quantities. Fecal pellets have a regular shape and they are rich in organic matter. The definition of pellets is commonly lost as a result of diagenetic processes and the limestones may show a flocculent or clotted texture, which referred to grumeleuse structure.

According to Blatt, *et al*, (1980), the most common carbonate particle in modern sediments and ancient carbonate rocks are peloids which have round and oval shape. Generally they are 30 to 100 μ in diameter and have a smooth outer surface, and are composed predominantly of microcrystalline carbonate. They are devoid of internal structure but may contain very small fragments of skeletal material. Ben Ismail and Mrabet, (1990) found peloid and ooid grainstones in the Jurassic Carbonate rocks of Tunsia that highly resemble those of Qulqula Formation. They cited that they were deposited in shallow carbonate platform that are bounded by graben.

In Qulqula Formation, the peloid allochems are the most common after lithoclasts which are different in size, shape and roundness (Figs. 3.10, 3.11 and 3.12). The most possibly developed that from micritization of different lithoclast and bioclast and even from skeleton. In thin section many evidence and transition of peloids exist that the application of the diagram of Reijers and Hsu, (1985) to generation of peloidal in limestone successions of the lower part of Qulqula Formation. Among these evidences we can mention, the slight and partial micritization of both lithoclasts and bioclasts (Fig.3.11).



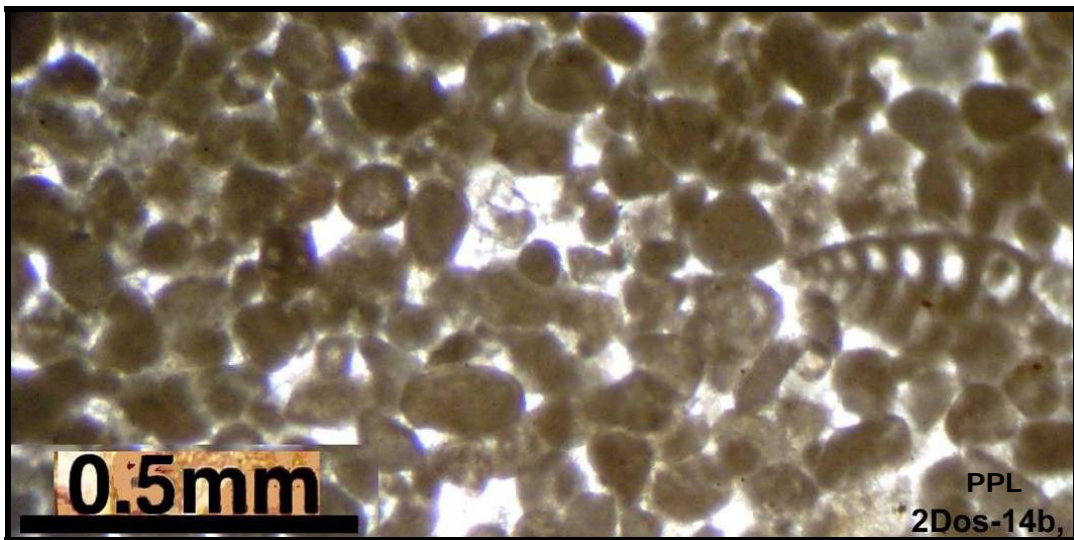


Fig. 3.12: Peloid Grainstone contains biserial foram at the right side with sparry calcite cement (white). Sample: 2Dos-14b.

3.3.1.4. Oo–Peloidal Grainstone

This microfacies mainly consists of moderately ooids and peloids which are bounded by coarse grain sparry calcite. According to Tucker, (2000) modern ooids are spherical-sub-spherical grains which consist of one or more regular concentric lamellae in which they are deposited around a nucleus, usually of carbonate particle or quartz grain. Sediment composed of ooids is referred to as an oolite. The term ooid (formerly oolith) has been restricted to grains less than 2mm in diameter and the term pisoid (formerly pisolith) is used for similar grains of a larger diameter. He added that, If only one lamella is developed around a nucleus, then the term superficial ooid is applied. Composite ooids consist of several small ooids enveloped by concentric lamellae. Coated grain is a general term frequently used for ooids and pisoids, and includes oncoids, grains with an algal- cyanobacterial–microbial coating.

According to Pettijhon, (1975) ooids are small spherical or subspherical bodies of diverse mineral composition and various internal organizations. He added that they are accretionary bodies, although spherical form is the rule, some ooids are oblate ellipsoidal, (0.25 to 2.00)mm in diameter; most commonly they are (0.5 to 1.0)mm in diameter. He used the term oolites for those rocks that are composed of ooids. Carozzi, (1957) distinguishes between ooids and superficial oolids (a mineral or skeletal grain surrounded by one concentric layer). If two or more layers are present, the object is a true ooids moreover he further added that superficial oolites may be confused with those calcareous grains which display a dense micritic rim, a product in some cases of peripheral micritization of the original grain and not an added precipitated layer.

According to Blatt et al. (1972), present day oolitic coatings commonly show a series of concentric shells usually a few microns thick. These individual coatings may be interrupted by discontinuous patches, crescents, or continuous rings of cryptocrystalline aragonite. Such breaks in the concentric oolitic rings or sheaths are normally produced by blue green algal accretions or the diagenetic effect of small boring organisms. He added that these interruptions represent micro unconformities in the deposition of the oolitic coatings. In the ancient rocks, the structure of the oolith may be changed by diagenesis to destroy the simple original concentric arrangement and substitute for it a radial or mosaic crystal fabric.

According to Pettijohn, (1975), the majority of modern ooids range from (0.2 to 0.5)mm in diameter. They typically form in agitated waters where they are frequently moved as sand by waves, dunes and ripples by tidal and storm currents, and wave action. On the Bahama platform, the ooids form shoals close to the edge of the platform, while in the Arabian Gulf, the ooids form in tidal deltas at the mouth of tidal inlets between barrier islands along the crucial coast (Loreau & Purser. 1973). Along the Yucatan shoreline (NE Mexico), ooids are being precipitated in the shoreface and foreshore zones.

According to Blatt et al., (1980), it seems that there is little doubt that the marine oolitic coatings represent a direct inorganic precipitate of aragonite deposited with brief interruptions on moving particles. Independent evidence that the particles were moving during formation of the coating is that the oolitic rings are continuous around the grain. The reason for the formation of oolitic coatings has long been studied. Earlier workers emphasized the proximity of modern ooliths to upwelling currents, the role of organisms, and the accretion of sedimentary aragonite.

In the limestone successions of the Qulqula Formation, ooids are the major components of this facies which exist as beds have thickness of (10-90)cm in the P1, P2, P3 and P4 of the Dostadara and Gali sections. In many areas, such as Dostadara section, south of Razilla and Parazan villages, this section contain cross laminated bed of ooid-peloid grainstones which shows, in some case, cross cutting by chert nodules (Figs. 2.22 and 2.25). The ooids in this study are characterized by the presence of one or very few thin laminas around a large nucleus, which belong to superficial types (Figs.3.13, 3.14, 3.17 and 3.18). The bacterial and algal origins of the present ooids are not excluded, since, the peloid and micritization are very common in the limestone successions. Therefore, it is possible to call the studied

oids “micro oncoids” as it used by Blomeier, and Reijmer, (1999) for zoogenic oolite in which their diameters are less than 2mm.

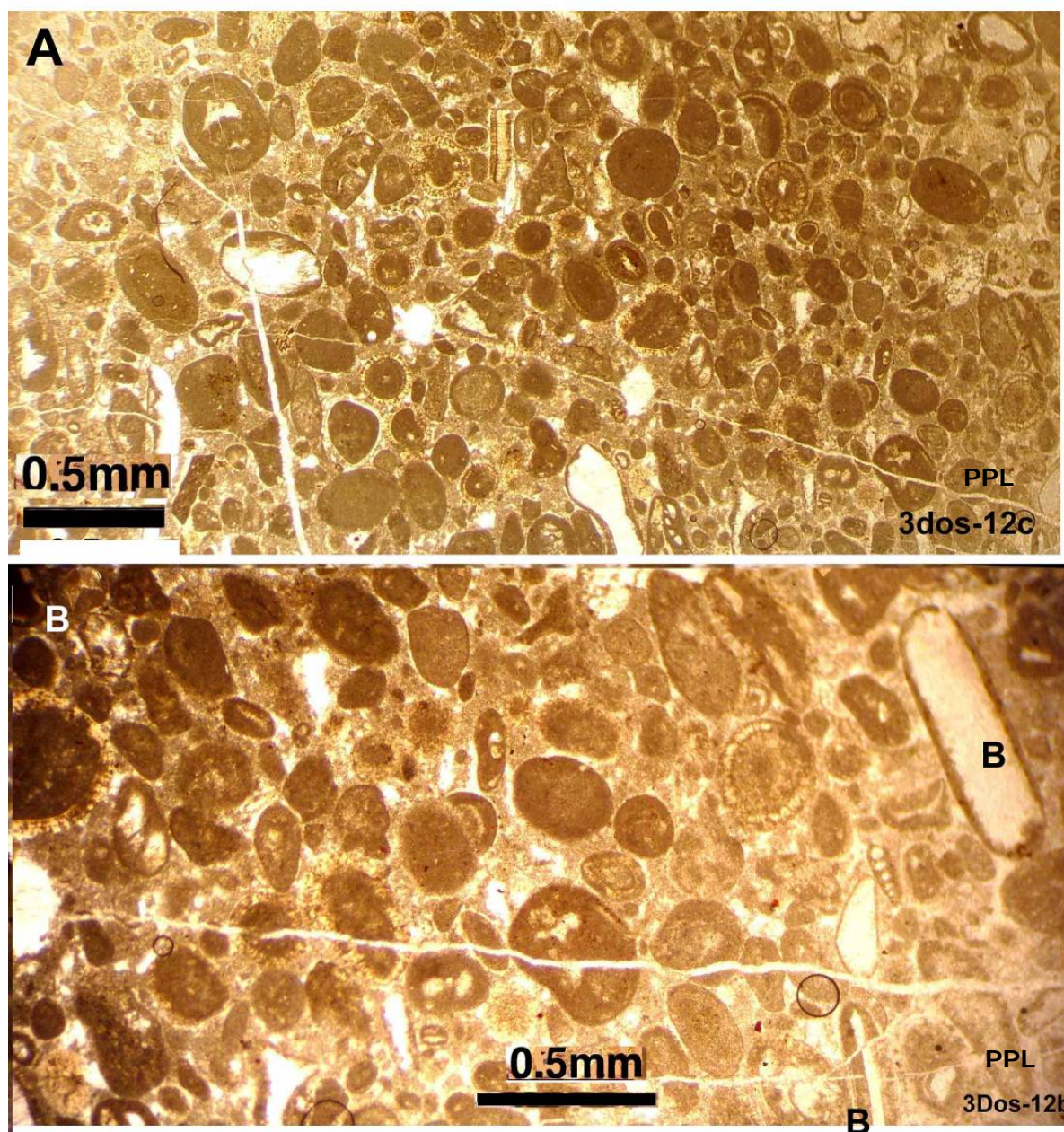


Fig. 3.13: Ooids-peloids grainstone which composed of spherical and oblate (B) superficial ooids. The oblate ooids are formed around bioclasts. Some unknown origin peloids can be seen. Samples: A: 3Dos-12c, B: 3Dose-12b b.

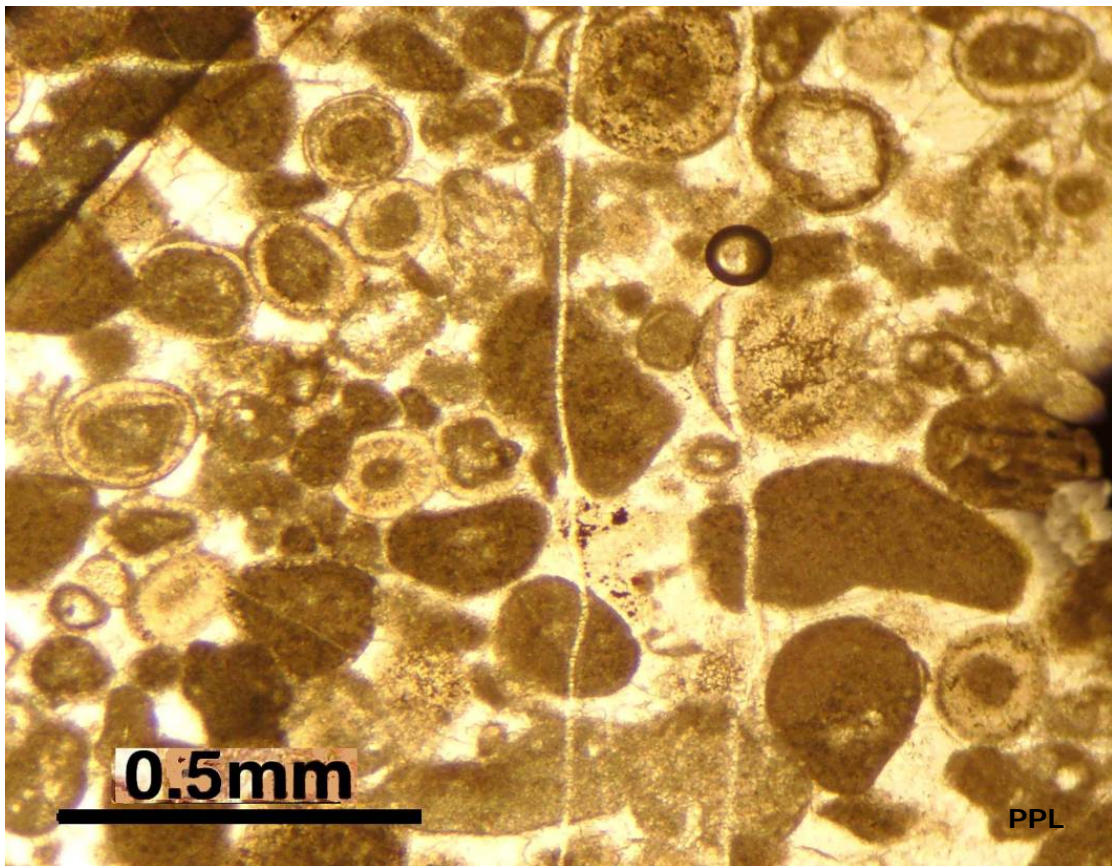


Fig.3.14: Ooids- Peloids grainstone which is composed of spherical superficial ooids with partially micritized lithoclasts. Sample:1Dos-14c

3.3.2. Rudstone Facies

This facies are introduced to Dunham's classification by Embry and Klovan, (1971) which consist of self-supporting large allochems (more than 2 mm in diameter) which are bounded by mudstone (micrite) (Fig. 3.15).

According to Wilson, (1975), this facies is deposited in forereef environment where the strong wave and current action are prevalent. According to above authors, the allochems of this facies must be derived from the reef but many authors has included the non-reefal allochems in this facies such as Sadooni and Alsharhan, (2003) where they assigned the orbitolina bearing limestone as orbitolina rudstone. Kenter et al, (2005) found boundstone breccia in the forereef area which is formed by gravity.

This facies is rare in the formation and only found in two places. These places are east of Gali village (15 km southeast of Chuarta town) and south of Razla Village. In these places, the large self-supported lithoclasts are binded by fine grain matrix. These facies underlined by erosional surface which are generated by strong wave and currents. The clast of this facies not derived from reef but most possibly derived from intertidal area by very strong wave during storm.



Fig. 3.15: Conglomeratic limestone (rudstone) of the P1 at 2 km southeast of Harmella Village.

3.3.3. Bindstone Lithofacies

This type of facies is present in Dostadara (2nd Ridge) and Type Locality sections, contains green algae which consists of irregular clotted bodies which enclosed by encrusted thin lamina. The bodies contain fenestrate and internal sedimentation as a graded bedding as shown by arrow in the fig (3.16). These bindstones are probably resembling thrombolite. According to Aitken, (1967) and Shapiro, (2000), the laminations in stromatolite are disturbed and hard to be identified, but they contain a network of small-coated fenestrate and coated grains.

They added that stromatolite products of trapping and binding of grains by filamentous cyanobacteria or they were an extensively burrowed form of stromatolite. Feldmann, (1998) mentioned that the thrombolites formed by microbes, algae and metazoans, and also mentioned Phanerozoic thrombolites have been interpreted as unlaminated stromatolites constructed by cyanobacteria.

Environmental conditions must favour growth of thrombolite to accumulate thickly enough, to be recognized in the fossil record. Such conditions may include a super saturation of calcium carbonate in the water, slow rates of sediment accumulation, or elevated salinity and temperature conditions. Modern thrombolites are found in a variety of environments including hypersaline lagoons, tidal channels and fresh water lakes.

Oliver et al. (2002) mentioned that the microbial crusts played an important role in the stabilization and growth of the reef body, which developed on various substrates such as corals, bivalves or bioclasts. Grotzinger, et al., (1998), Johnson and Grotzinger, et al., (2000) studied the thrombolitic microbiolite growth and morphology in Nama Group at Namibia.

Leherman, et al, (1998) found that the clasts of boundstone contain scleractinian corals, Tubiphytes, sphinctozoan sponges, rhyzozoans, *Ladinella porota*, solenoporacean algae, and inozoan sponges. These boundstone clasts could have been derived from diverse platform-margin reefs that were completely eroded from the margin. The breccias also contain clasts of skeletal-peloid packstones to grainstones similar to the strata presently exposed along the escarpment.

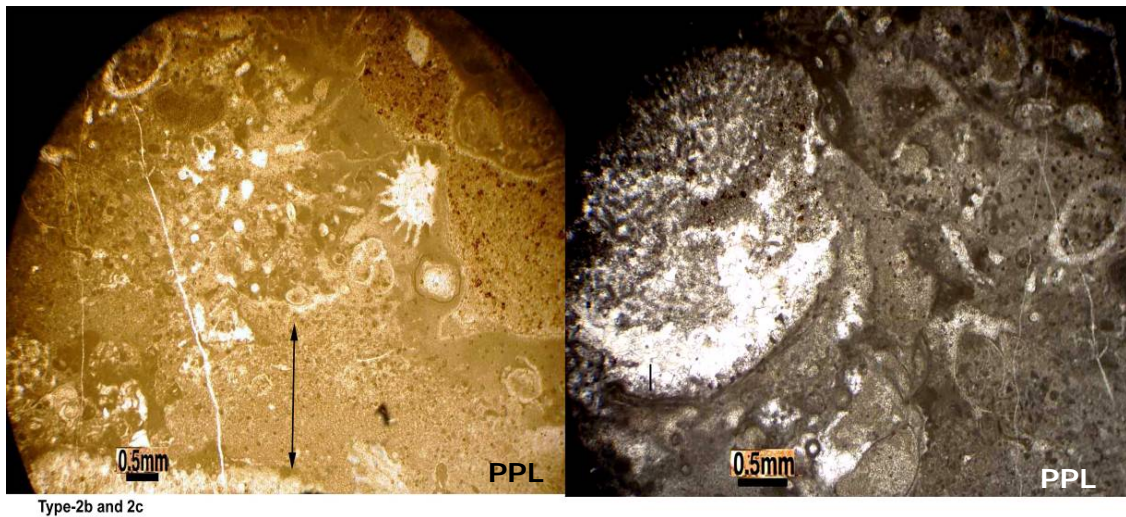


Fig. 3.16: Green algal encrustation as bindstone facies. Sample: Left: type-2b, right: type-2c.

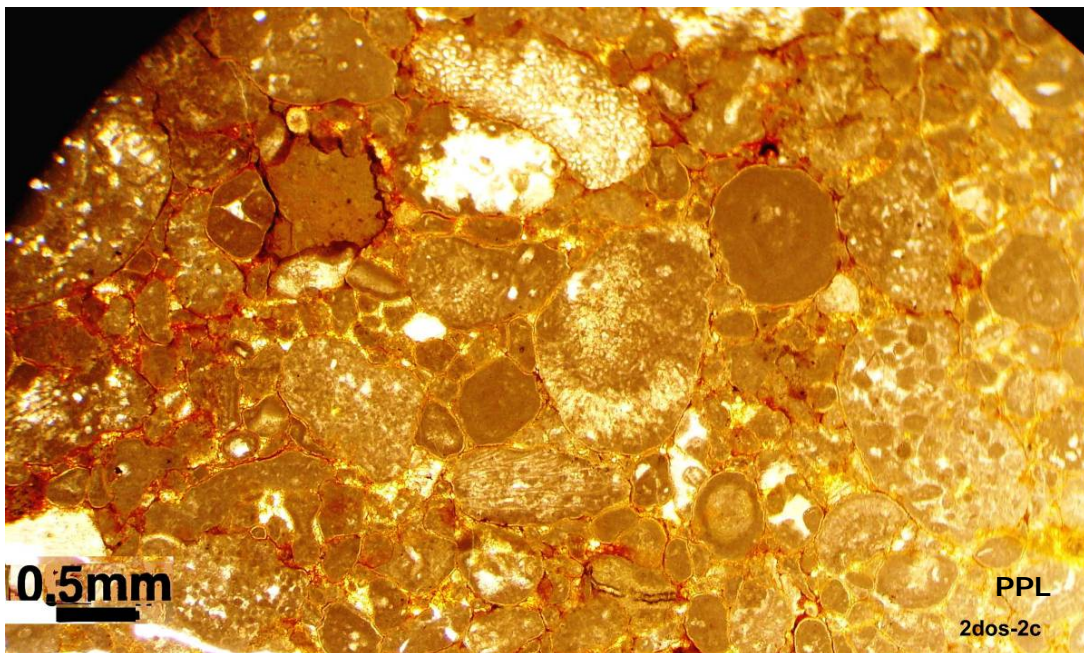


Fig. 3.17: Oncoids and green algal by separate encrustation, sample: 2dos-2c

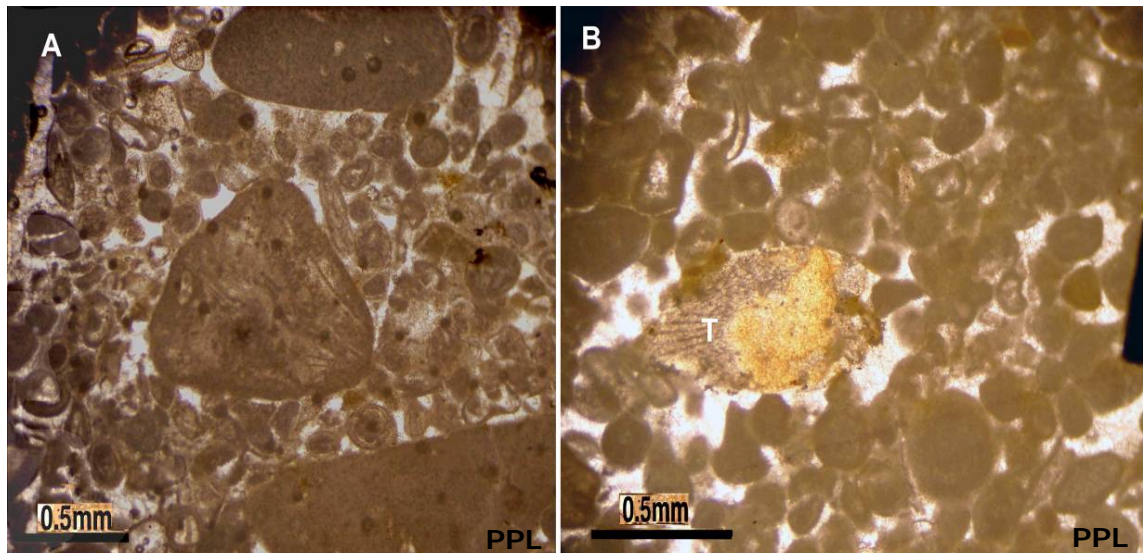


Fig. 3.18: A) Lithoclastic-peloidal Grainstone in which the peloidal show some trace of superficial ooids, (Type Section, No.7a). Peloidal with phosphatic grain (T) (sample, No.7b).

3.3.4. Floatstone Facies

This facies is rare and consist of grains larger than sand size which floating or embedded in fine matrix of lime mudstone. In all sections there are few beds rich in large bioclasts or lithoclast of the size of gravels and granule, if one put these rocks in a floatstone facies, it become common, but the problem is that it is not known if they derived from the reef or from fossiliferous beds (biolithosome). Example for this facies is shown in Fig (3.21.) in Dostadara (1st ridge) section.

3.3.5. Mudstone Microfacies

According to Dunham, (1962), this facies composed of more than 90% micrite and deposited in low energy environment either in protected seas or below fair weather base. This facies contains some sand size litho-and bioclasts. This facies restricted to the base of successions of Dostadara section (Fig.3.19).

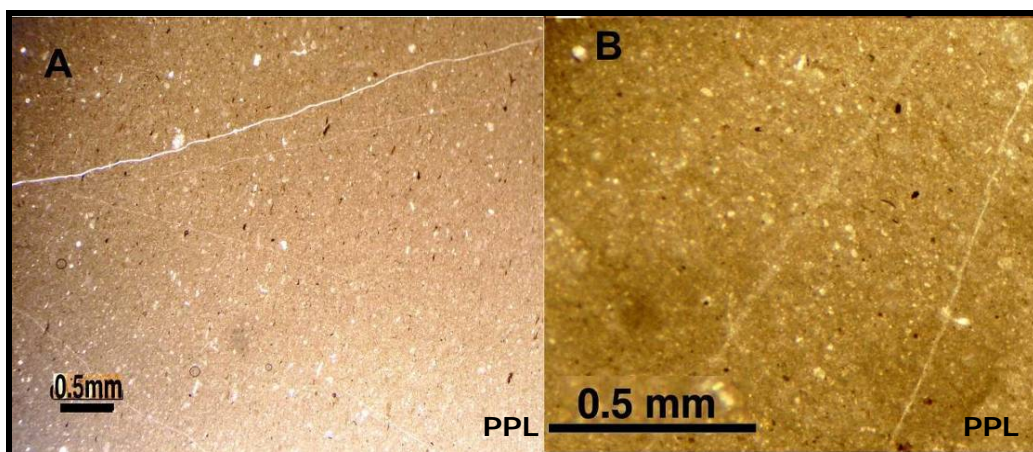


Fig. 3.19: Mudstone Lithofacies at the base of Dostadara Section, sample: A: 2Dos-1, B: 1Dos-3b

3.3.6. Diagenetic Chert Bearing Lime Wackestone Submicrofacies

The cherty facies consists of decimeter-scale beds and the chert normally follows the bedding planes and occurs either as isolated nodules or continuous string only for few meters laterally. This facies occurs nearly in all section especially at the base of the sections, such as Dostadara, Kaolos and Gali (Fig.2.21 and 2.22).

3.3.7. Intraclastic Wackestone

According to Blatt *et al*, (1980), these particles are fragments of partially lithified carbonate sediment that was eroded from the sea bottom or adjacent tidal flats.

They may be of any size or shape and become incorporated within new sediment. They added that, the prefix “intra” indicates that they formed as particles within the general area of deposition of the host sediment. They gave several mechanisms serve to produce these grains. The main of which are cited below:

1. Fine carbonate sediment exposed to the air either by a drop in sea level or on high intertidal or supratidal flats will develop mud cracks and mud curls. These dried-out wafers of carbonate sediment may receive some small amounts of carbonate cement in the subaerial environment, thus ensuring their existence as particles. They range in size from a fraction of a centimeter to over a meter across and commonly are covered by later sediment or washed into the nearby shallow-marine environment. Most flat pebble conglomerates common in the ancient record originated in this way.

2. Carbonate sand on beaches within the intertidal zone is easily cemented by fine fibrous aragonite into “beach rock.” In addition, carbonate sediment may be cemented locally in a submarine environment. Eroded fragments of these materials will produce intraclasts. The origin of grapestone lumps that are intraclasts composed of loosely cemented carbonate sand grains is imperfectly known. These grains are common in most modern carbonate deposits, and the cement may be finely fibrous aragonite. Many may have originated as eroded beach rock. Some may have been cemented while still within the marine environment.

According to Pettijhon, (1975), the term intraclast was introduced by Folk, (1974) to designate fragments of penecontemporaneous, generally weakly cemented carbonate sediment that has been broken up and redeposited as a clast in a new framework. He added that carbonate intraclasts, most of which seem to have been produced by erosion of a layer of semi-consolidated carbonate sediment. Hence

many of them are flat; the largest are slab-like and elongated parallel to their bedding. They may show internal laminations parallel to their flat sides. They have been some what abraded and rounded. They range from fine-sand size to the larger slab-like pieces of intraformational limestone conglomerates. Most are composed of microcrystalline carbonate. If these are small and well rounded, they are difficult to distinguish from pellet.

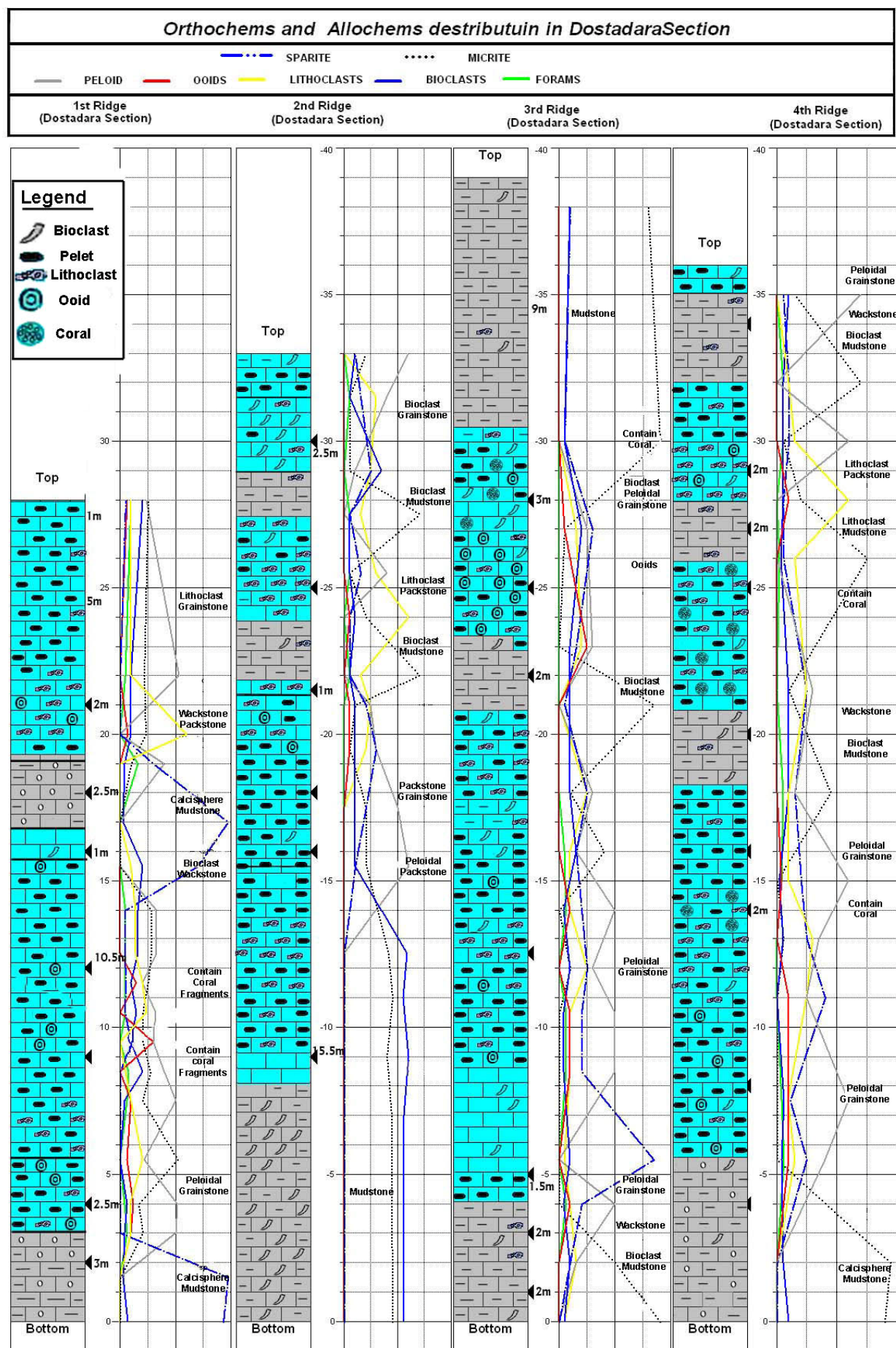
In the present study, several places of intraclastic wackstone found in the east of Dostadara and south of Razlla Villages. In these two places the intraclasts consist of white colour gravel and granule grains that have the colour and lithology different from the matrix, but similar to the underlying bed. The clasts are edgeless which show ripping up of semi-lithified from the underlying bed by wave and currents (Figs.3.20 and 3.21).



Fig. 3.20: Rip-up Clasts (Conglomerate) in the P1 2 km Southwest of Dostadara Village.



Fig. 3.21: Rip-up Clasts (as a Floatstone Facies) in the P1 4 km Northeast of Haji Mamand Village.



Fig(3.22A) Distribution of the Lithofacies and microfacies in the limestone successions of the Dostadara section.

Orthochems and Allochems distribution in Type-Locality, Kaolos, Kaolosz, Tawella and Gali sections

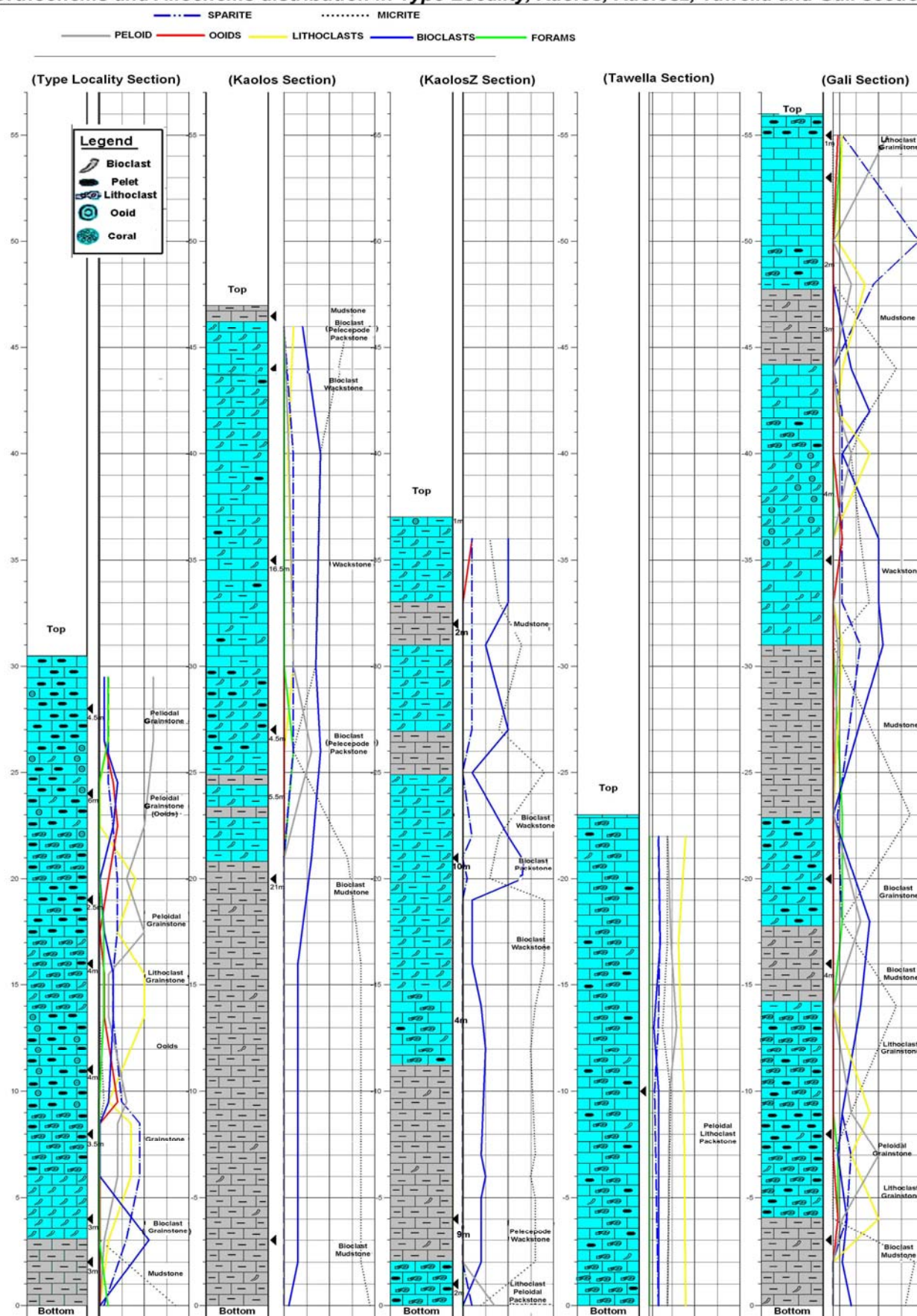


Fig. (3.22B) Distribution of the Lithofacies and microfacies in of the limestone successions of the Gali, Kaolos Tawella and Type Locality sections (only the digested samples are indicated).

3.4. Environment of Deposition

Depths of water where ooids precipitate are usually less than 5m, but they may reach 10-15m. Benthic foraminifera are common in warm, shallow seas, living within and on the sediment, and encrusting hard substrates (Tucker, 1991).

The peloidal grainstone microfacies may deposit at shallow warm waters with moderate circulation (Wilson, 1975). According to Blatt et al.(1980), modern oolites are found only where strong bottom currents exist typically in areas of tidal bar accumulation or within tidal deltas. In ancient rocks, the oolids commonly shows abundant evidence for current transport, such as large-scale cross bedding. According to Lehman, et al., (1998) the boundstone could have been derived from diverse platform-margin reefs that were completely eroded from the margin.

From the association of the organisms (as observed in the thin section) the temperature and salinity can be approximately known. The intraclasts contain tetrataxid forams, green algae and some benthonic forams (Fig. 3.6, 3.7, 3.8, 3.16 and 3.17). Therefore, this assemblage is according to Nichols, (1999) and Einsele, (2000) belong to normal salinity and intermediate temperature between low latitude (warm water) and cooler water of high latitude. This is because the existed assemblage can be regarded as mixture of Chlorozoan and foramol assemblages.

Blomeier and Reijmer, (1999) found tetrataxid forams in the sediment of pre-drowning phase of the Jurassic carbonate platform in Morocco. They mentioned that they survived as frambuilder organism in the platform margin as a small patch reef. After erosion, the fragment of these forams are transported and deposited on the platform slope.

According to Tucker, (1991), the skeletal components of a limestone are a reflection of the distribution of carbonate-secreting invertebrates through time and space. Environmental factors, such as depth, temperature, salinity, substrate and turbulence, control the distribution and development of the organisms in the various carbonate subenvironments. Throughout the Phanerozoic, various groups expanded and evolved to occupy the niches left by others on the decline or by becoming extinct.

According to the above facts that are closely related to the limestone succession of Qulqula Formation are deposited in high energy normal marine environment. This is because it contains mainly grainstone of lithoclasts, peloids, ooids and bioclasts of tetrataxid forams and green algae (Fig. 3.6, 3.7 and 3.8). The occurrence of ooids

grainstone (Fig.3.13 and 3.14) indicate shallow agitating water with local bioherm and carbonate sand banks. The occurrence of the mudstone and wackstone (Fig. 3.19) indicate the occurrence of small protected lagoon and tidal flats behind the bioherm and banks (Fig. 3.23). The recorded rip-up clasts and cross stratification (Fig. 3.21 and 2.22) shows that most of the carbonates are deposited above fair weather base, while the fine grain pelletal limestones inside the bedded radiolarian chert are deposited below fair weather base.

3-4-1- Rimmed Versus Ramp Platform

According to Tucker (1991), Nichols, (1999) and Einsele, (2000), ramp is gently slopping sea bottom (less than 2 degrees) with generally high energy inner-ramp near shoreline which passes off-shore to quiet and deep-water outer ramp. They added that large reefs are generally not present on ramp. When one looks at the lateral and vertical distribution of carbonate facies and grain size he realizes that the platform topography that fit the carbonate successions of Qulqula Formation is ramp. In these successions the grains size and facies are changing gradually which change from coarse intraclastic and oolitic, at the middle to fine peloidal limestone toward the top and bottom. The occurrence of about 10% of algae as intraclasts reveals that the ramp contained some small patch reef (bank) near the coastal area and the erosion of which supplied the with the reefal limestone bioclasts (Fig.3.23 and 3.24). Another evidence for ramp setting is the mixing of different allochems in the facies which imply that the platform has not high contrast topography. Behind the banks of the ramp, mudstone facies are deposited in the protected low energy pond or lagoons. This facies can be observed at the base and top of the P1, P2 and p3. In contrast to the ramp any evidence of rimmed shelf can not be seen. The floatstone and coarse grainstones are deposited on the middle ramp near to the shore line while the medium grain cross- stratified grainstones are deposited on mid-ramp above fair-weather base (Fig. 2.22). The thin bedded limestone with fine pelletal allochems is deposited in the outer ramp (Fig. 2.21).

It is possible that the ramp is developed during final stage of the extensional phase of southern Neo-Tethys in Upper Jurassic. During this phase, the ramp covered a part of gently dipping near shore topography that was formed by half grabens or lithric fault on the northeastern margin of Arabian Plate (Fig. 3.23 and 3.24). After final phase of extensional phase, the basin suffered from convergence due to descending of the Arabian Plate under the Iranian one. During this phase of the

convergence the radiolarian parts of the Qulqula Formation are deposited during Early Cretaceous as Equivalent of Sarmord and Balambo Formations (Fig.3.25).

3-3-2- Source Area

For knowing the type of source area, two facts must be mentioned. The first is that, as mentioned in the facies analyses, the studied limestone successions contain bioclasts of tetrataxid forams and green algae in addition to lithoclasts of pelletal and fine grain limestone. The second is that the limestone successions are devoid of any silicilastics. Therefore, the source area, if any, is mainly consisted of intermittently emerged and recently lithified intraformational (intrabasinal) reefal limestones. The existence of limestone positive low land source area is not excluded in the coastal area which was eroded by wave and current and transportation to the basin (Fig. 3.23). This source area, according to the recorded lithology and grains size of the allochems, was carbonate reef limestone which located to the southwest of the studied area.

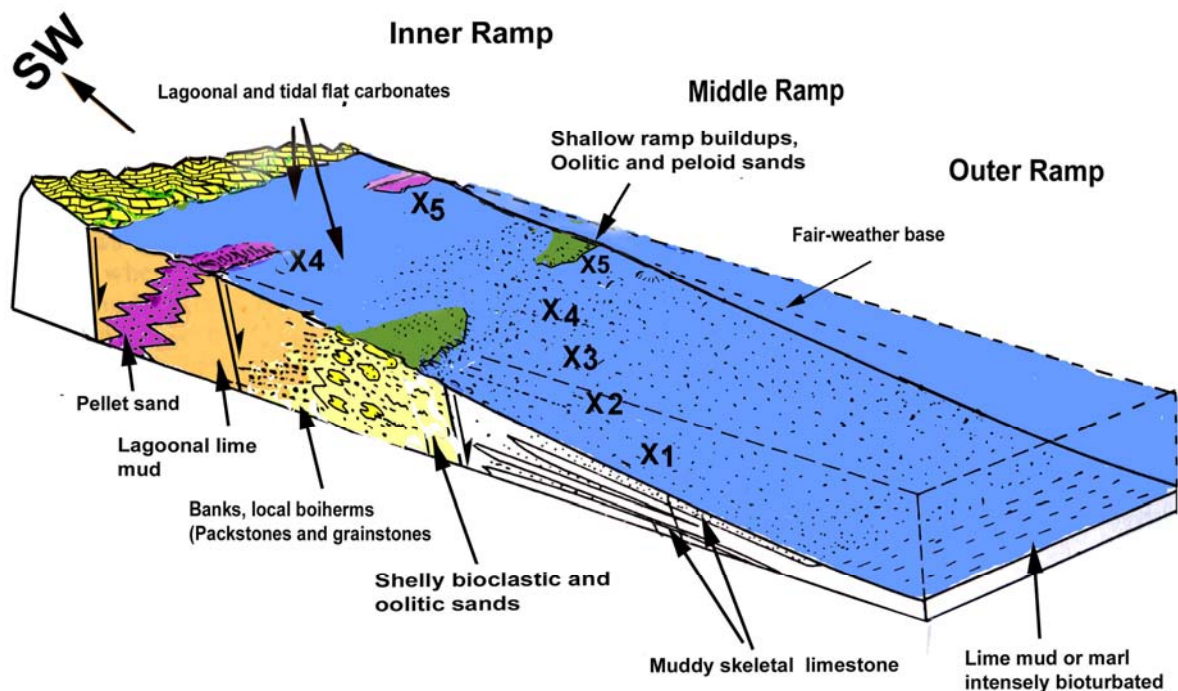


Fig. 3.23A: Depositional environment of the limestone successions of the Qulqula Formation as a ramp on the Jurassic extension platform (on the half graben). X1, X2, X3, X4, and X5: are representing the locations of Tawella, Kaolos Dotadara, Gali and Type section respectively.

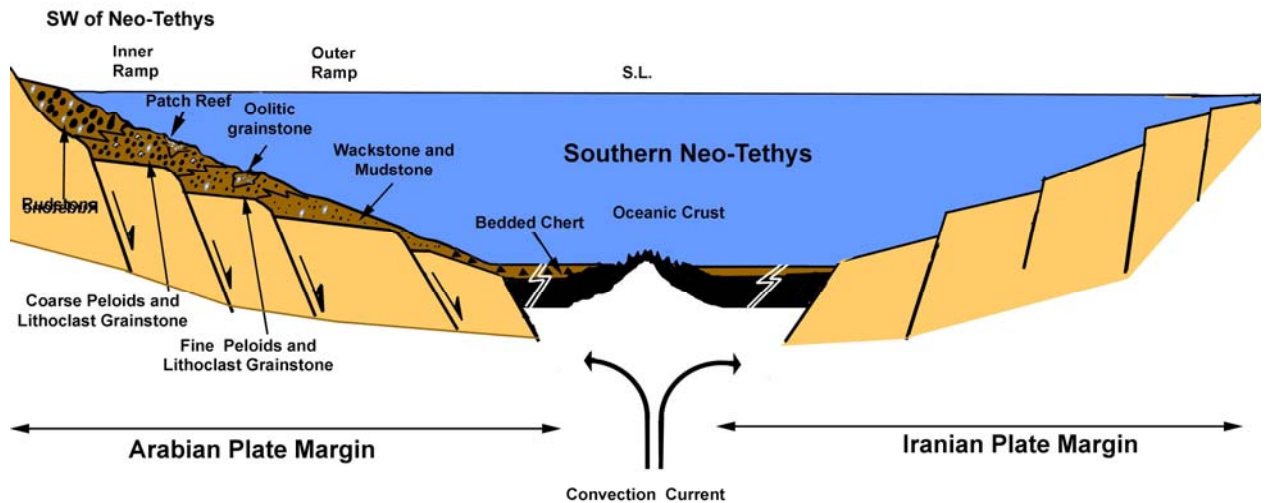


Fig.(3.23B): Possible tectonic setting (extension platform margin) of the upper Jurassic showing ramp platform on the southwestern side of the Neo-Tethys on which the limestone successions of Qulqula Formation are deposited.

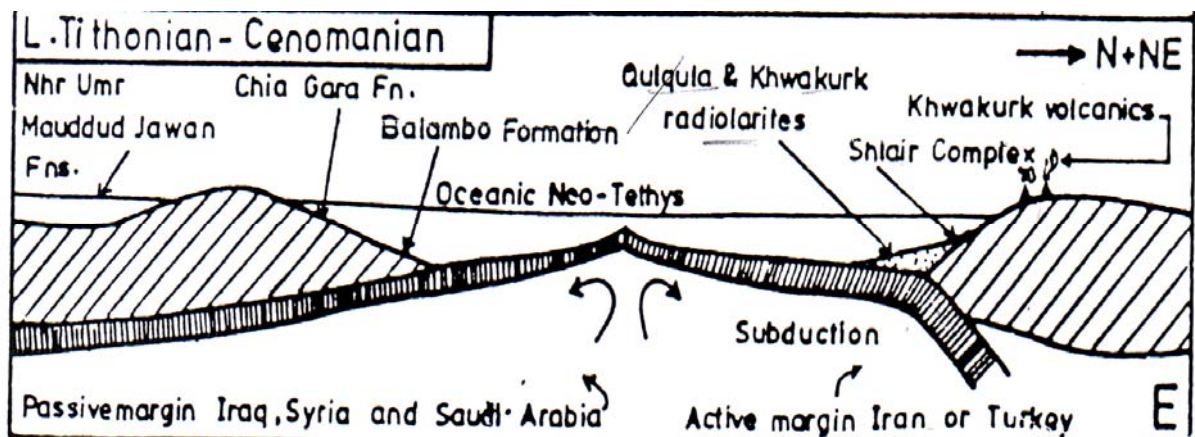


Fig.(3.24): Tectonic and environment of Qulqula Formation with in the tectonic Senario of Phanerozoic by Numan, (1997).

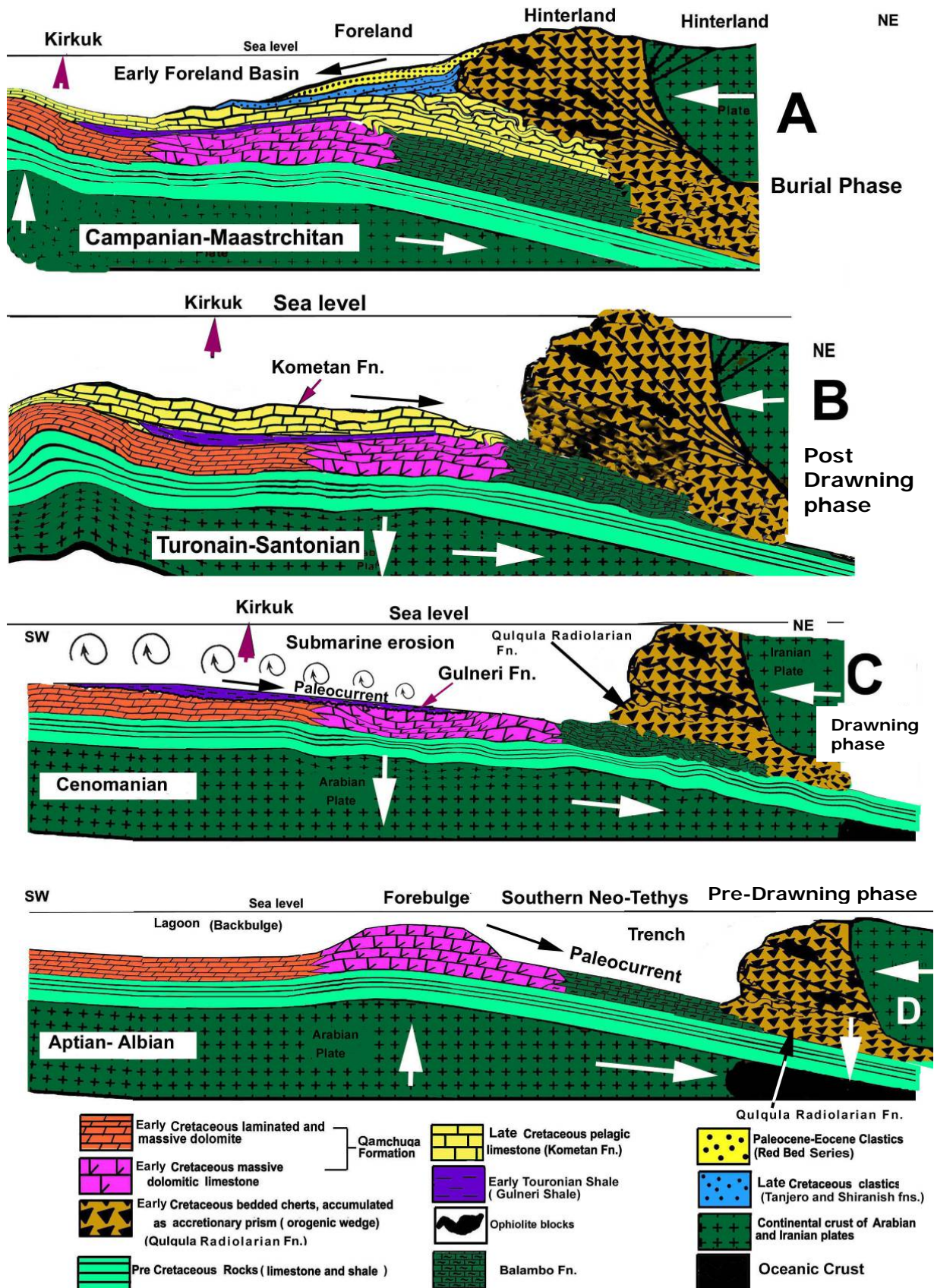


Fig.3.25: Basinal and tectonic setting of Cretaceous formations in which position of the Qulqula Formation is indicated as equivalent of Balambo Formation. A) (Karim, 2004), B and C) (Taha, 2008), D) (Ameen, 2008).

Chapter Four

GEOCHEMISTRY

4.1. Introduction

The study of limestone or carbonate rocks in general, has attracted the attention of many geologists since long time. This is perhaps partly due to their economic importance and partly due to their academic interest.

Carbonate rocks are composed of two main parts; a soluble carbonate by weak acid and non carbonate insoluble or insoluble residue part which differs in percentage according to different sedimentary environments and also affected by physiochemical and biochemical agents.

The most abundant minerals existing in insoluble residue in carbonate rocks are (Clay, pyrite, quartz, anhydrite and organic matter), and the suitable hosts for the trace elements are clay minerals which have an environmental importance. Trace elements increase by increasing insoluble residue in the total rock analyses especially (Fe, Cr and Ni) but the later is less affected on Sr due to its low content. So the total analyses of a bulk sample are not alone useful without special insoluble residue analyses or soluble carbonate part.

The goals of this chapter are many, which include understanding of the chemical compositions of the four successions and using them for correlation if anomalies are obtained. The strong and weak chemical variation, between successions and sections can aid or oppose the conclusions of the facies analyses in chapter three.

In this chapter, the distribution of major and trace elements are discussed in the samples of the five studied sections of Qulqula Formation. Many statistical parameters were employed in order to give a clear picture for the abundance and the sites of enrichment of each element.

These parameters include range, mean, and standard deviation for each element in the bulk samples, the precision, accuracy and correlation coefficient for the concentrations of each element was calculated to provide a scale for the variability of the obtained data.

4.2. Analytical Procedure.

4.2.1. Determination of Major and Trace Elements

Sixty carbonate bulk samples from the five localities have been analysed by Carbonate Detection software in China by *Fa Tai* Co. for Petroleum Technology Equipment. The analysis is to determine the percentage of CaCO_3 and MgCO_3 .

Chemical analyses were carried out by a wet chemical method for their major, as well as, some trace elements in Baghdad University. The major oxides are CO_2 , MgO , and CaO , and for (Al and Si by UV Spectrophotometer, while Fe, Na, K and Mn by Atomic Absorption Spectrophotometer. The same samples were selected for trace elements analyses for Co, Ni, Cu, Pb, Zn, Sr, and Cr by Atomic Absorption Spectrophotometer– Perkin-Elmer/USA, model 5000). The PO_4 concentration is done by UV Spectrophotometer. The insoluble residue content in 20 selected samples are determined by the method of weight loss after treatment with dilute acetic acid 15%.

4.2.2. Separation of Insoluble Residue Contents

Many methods were previously applied by many workers to separate the noncarbonated materials (clay minerals, silica and some resistant heavy minerals) from carbonate rocks using different acids with different concentrations. In the present work, the insoluble residue was separated by the treatment of samples with 15% acetic acid for 24 hours. The use of the weak acetic acid instead of the stronger acids minimizes the distortion and possible dissolution of the clay fraction, nevertheless some elements particularly the alkalies suffer slight leaching during the reaction with the acid. When the reaction had come to its end, the insoluble residue was then filtered and washed with distilled water to remove excess acid present (Haddad, 1980).

4.2.3. The Loss On Ignition

The approximate carbon dioxide content of the same portion of the sample may be determined by the weight loss on ignition at $(1000-1100)^\circ\text{C}$ for one hour. Samples that are very impure will lose water of hydration in addition to carbon dioxide. The loss on ignition will be the combined loss of carbon dioxide plus any other constituents present and evolved at temperature above 1050°C . In this temperature hydrocarbon compounds and organic materials will be lost, whereas in high-carbonate samples (which is the characteristic of all analysed samples in this study), the carbon dioxide will be the loss of ignition only. This was then calculated as percentage of the sample weight. This determination is made by using a

temperature-controlled muffle furnace by weighing the sample before and after ignition by which the difference between the two weights yield the loss on ignition.

4.2.4. Micro Probe Analyses (MPA):-

Based on careful petrographic microscopic study, three samples were selected for electron microprobe analyses. Mineral compositions of carbonate and phosphate minerals were made with JEOL-840A scanning electron microscope, which is equipped with an Oxford energy dispersive (EDX) analytical system (Link ISIS series L200I-S) at Osaka Prefecture University in Japan. Operating at 15Kv and 0.5nA. Raw data were ZAF corrected. Chemical analyses of analysed mineral are given in table (4-1), and the analysed phosphate mineral is typical Apatite.

Table (4-1): MPA of Type-8 sample in Type locality section shows the typical Apatite.

Mineral	1 ap	2 ap	3 ap	4 ap	5 ap	6 ap	7 ap
SiO ₂	0.06	0.05	0.09	0.09	0.09	0.04	0.00
Al ₂ O ₃	0.06	0.06	0.09	0.07	0.08	0.08	0.06
FeO	0.23	0.02	0.04	0.07	0.03	0.36	0.33
MgO	0.00	0.10	0.14	0.12	0.11	0.15	0.12
CaO	54.05	53.46	53.41	53.44	53.61	53.96	53.74
K ₂ O	0.04	0.11	0.08	0.08	0.09	0.27	0.17
P ₂ O ₅	47.56	47.60	47.68	47.72	47.75	46.51	46.72
Total	102	101.4	101.53	101.59	101.76	101.37	101.14
O ⁼	4.000	4.000	4.000	4.000	4.000	4.000	4.000
Si	0.002	0.001	0.002	0.002	0.002	0.001	0.000
Al	0.002	0.002	0.003	0.002	0.002	0.002	0.002
Fe ²⁺	0.005	0.000	0.001	0.001	0.001	0.008	0.007
Mg	0.000	0.004	0.005	0.005	0.004	0.006	0.005
Ca	1.457	1.446	1.442	1.442	1.444	1.471	1.466
K	0.001	0.004	0.003	0.003	0.003	0.009	0.006
P	1.013	1.017	1.017	1.017	1.017	1.002	1.007
Total	2.479	2.474	2.472	2.472	2.473	2.499	2.492

4.3. X-Ray Diffraction Analyses

The bulk carbonate samples and their insoluble residues are analysed using X-Ray Diffraction technique to determine the mineral content which showed that the mineral consist mainly of calcite, quartz and kaolinite.

Twenty selected bulk and IR samples (1Dos-5,17 and 21 of the 1st Ridge, 2Dos-1 and 17 of the 2nd Ridge, 3Dos-3,7 and 11 of the 3rd Ridge, Type-1 and 7 of the type locality section, Kol-1 and 3 of the Kaolos section) were selected for X-Ray analyses.

The insoluble residue samples are (3Dos-3,7 and 11, Type-1, and Kol-1 and 3), two of them (Kol-1 and 3Dos-3) were heated to 550°C, Appendix (B)-Fig (B-8 and B-18). All of these samples were investigated by X-Ray Diffraction in Sulaimani Univ. Dept. of Geology. Each sample was irradiated with X-Ray using PANanalytical, Goniometer PW3050/60, Sample stage PW3071/xx Brachket, Diffractometer system XPERT-PRO, and Cu, K-alpha radiation and Ni filter, at setting of 45kv and 40mA. Scanning rate was 2θ per minute, in the range of 2 to 65 degrees.

4.3.1. Bulk Sample Mineral Content

The X-Ray Diffractograms for all bulk samples almost show similar patterns which show clearly calcite as a main constituent mineral. There was a noticeable variation in the intensity of kaolinite and quartz peaks generally, which is directly proportional to the amount of the insoluble residue, Appendix (B)-Fig (B-4). . Calcite is the main constituent of all samples which can be easily seen with the petrographic microscope. The quartz and kaolinite are the secondary constituents which can be seen as notable percentages from the selected samples.

The maximum intensities of the first- order diffraction peaks of calcite, 3.01, and 3.00. 3.02 angstroms, quartz 3.32 Å and kaolinite are at; 7.11, 7.09, 7.08, 7.02, 7.06, 7.12, 7.07, 7.1, 7.03 angstroms respectively, Appendix (B)-Fig (B-1, B-2, B-3, B-4, B-5, B-6, B-9, B-11, B-13, B-15, B-16 and B-19) are the X-Ray Diffraction patterns showing the peaks of calcite, quartz and kaolinite minerals.

4.3.2. Mineral Content of the Insoluble Residue

X -Ray Diffraction analyses was also used as a supplementary method for the study of the insoluble residues of the eight selected samples, the patterns show that the quartz is the main insoluble residue constituent with little kaolinite except (Kol-1 and 3) samples of the Kaolos section and (3Dos-11) from the 3rd Ridge which are mainly kaolinite and little quartz, Appendix (B)-Fig (B-7, B-10, B-12, B-14, B-17, B-

18 and B-20). Two samples Kol-1 and 3Dos-3 were heated to 600°C to confirm the presence of Kaolinite, Appendix (B)-Fig (B-8 and B-18) shows the disappearance of Kaolinite peaks. The mineralogical content of the separated insoluble residues fraction as revealed by X-Ray Diffractograms are variable within the six selected samples; the variation is reflected by different peak positions and intensities.

Common to all X-Ray Diffractograms are the sharp and intense quartz peaks. Also on a visual basis, the relative peak intensity indicates that silica is one of the dominate constituents of the insoluble residues. However the well crystalline nature of quartz could partly be responsible for the intense and sharp peaks. X-Ray Diffractograms also showed that the clay mineral content only kaolinite, The Kaolinite peaks especially those related broad indicating their poorly crystalline nature (Haddad, 1980). The quartz could not be seen in the thin sections as extracrust and intracrust in the related samples, therefore it is introduced to the sample by metasomatism and replacement of calcite (which means diagenetic origin).

Kaolinite is the only dominant clay minerals in the insoluble residues of selected samples, Appendix (B)-Fig (B-7, B-10, B-12, B-14, B-17, B-18 and B-20). It occurs in variable proportions, however kaolinite content is found to increase in Kaolos section and 3rd Ridge (towards the younger beds). The maximum intensities of the first- order diffraction peaks of Quartz 3.318, 3.32, 3.34 Å and kaolinite 7.06, 7.033, 7.09, 7.07, 7.04 angstroms Fig.(4.2 to 4.15) are the X-Ray Diffraction patterns showing the peaks of quartz and kaolinite minerals. The presence of kaolinite agrees with the conclusion of petrographic and facies analysis studies which showed shallow marine (platform) environment , Fig.(4-1).

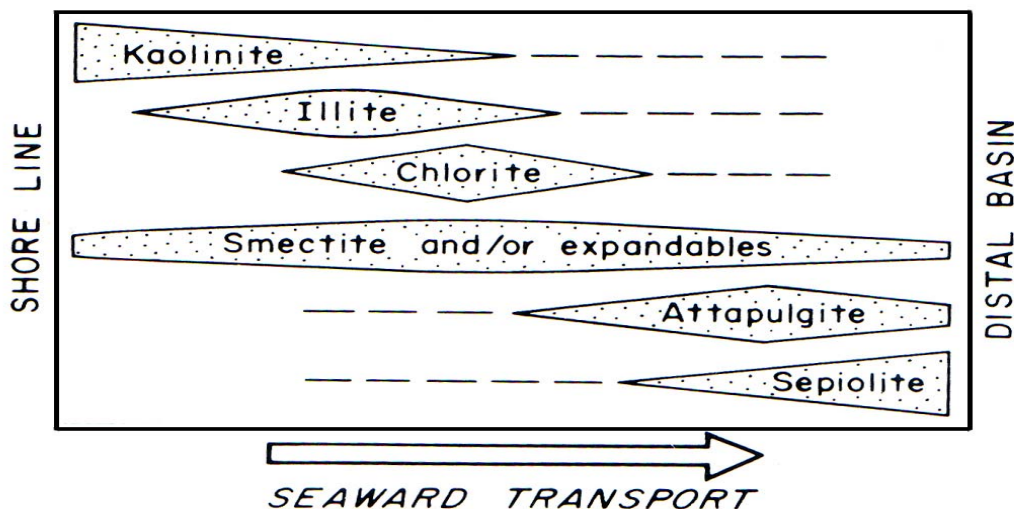


Fig.(4-1) Distribution of clay minerals in marine environment (Potter, et al.,1980) which show that Kaolinite (the only clay mineral in the present study) is deposited in shallow water environments.

4.4. Major Oxides Geochemistry

The analyses were done for principle components of about 60 bulk samples for indication of the geochemistry of major elements. The result of this analyses will be interpreted depending on the mineralogy and element constituent of these minerals. Mineral variation is very little in limestones especially in the studied sections, which are generally composed of pure limestones, Appedix (A)-Tables (A-1a, A-2a, A-3a, A-4a, A-5a, A-6a, A-7a, A-8a and A-9a).

CaO

CaO is a good indicator of carbonate rocks and calcareous cementing material. CaO and MgO profiles form to some extent mirror images of one another Fig(4-3). The former shows a decrease with increasing MgO content, calcium increases when there is MgO depletion zone (Al-Gailani, 1980).

The distribution of CaO was shown in Figs (4-2 and 4-3 UL & UR) which is unimodal. The highest peak is in the class interval (40-45)% and (45-50)% which suggest that the majority of the Qulqula limestones are of the low Mg-limestone and argillaceous limestone type.

CaO concentrations in the studied samples are on average range between (37.81 and 52.05)%. The mean CaO contents are (42.18, 48.21, 44.52 and 44.07)% in limestone successions (P1, P2, P3 and P4) of Dostadara section respectively, and (44.75, 40.32, 44.58, 43.6, 33.77 and 42.18)% for sections (Dostadara, Type Locality, Kaolos, Kaolos-Z and Gali sections) respectively, tables (4-2 and 4-3). So the majority of samples are almost pure carbonate.

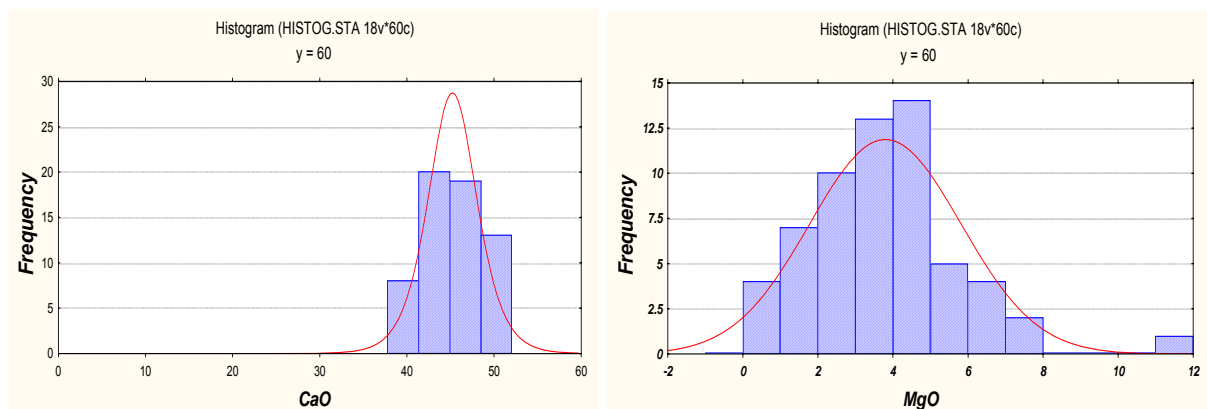


Fig (4-2): Frequency diagrams of CaO and MgO content in limestones of the studied sections.

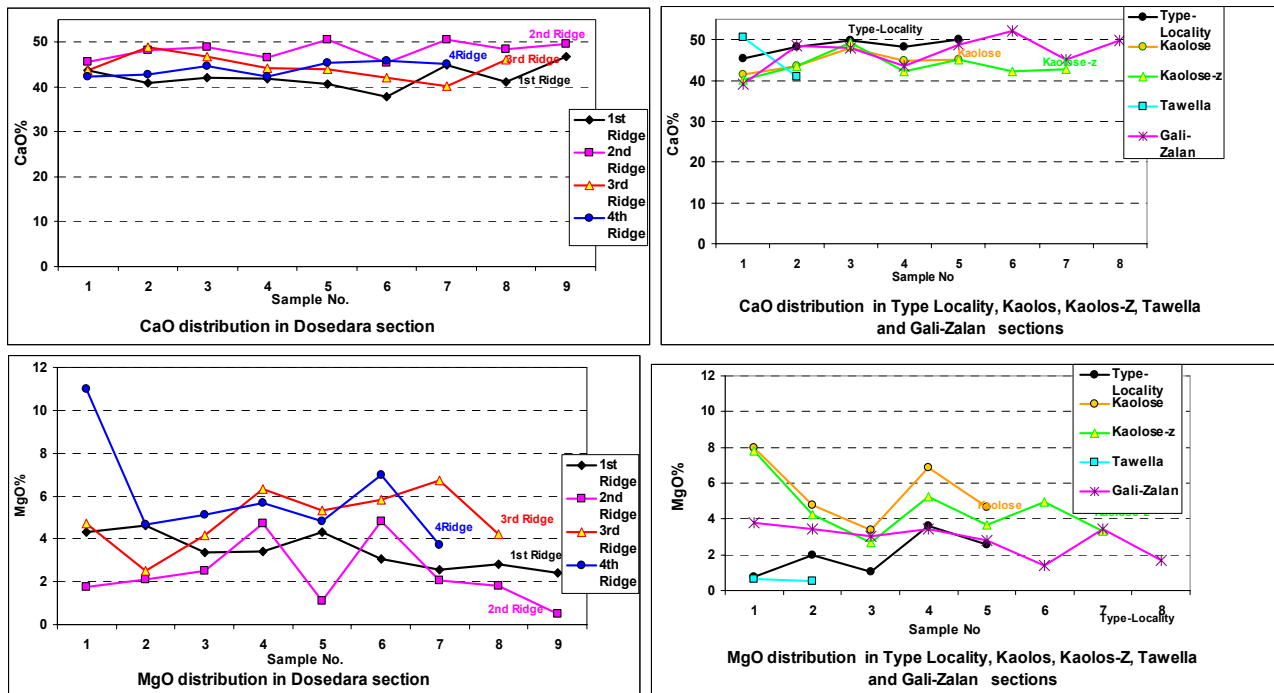


Fig (4-3): In all sections the CaO content is a mirror of MgO content as it shown in these four graphs. (UL) is CaO% in limestone successions; (UR) is CaO% in other sections; (BL) is MgO% in limestone successions and (BR) is MgO% in other sections.

The Coefficient of Variation, Range, Mean content and Standard Deviation of CaO, MgO, Al_2O_3 , SiO_2 , Fe_2O_3 , Na_2O , K_2O and MnO in samples from the five studied sections are shown in tables (4-2 and 4-3)

The variations in CaO content between all sections are considerably lower coefficient of variation which suggests that these sections are considerably of chemically homogeneous limestones. It is clear from the tables mentioned before that the CaO content and hence the acid soluble carbonate fractions are generally the highest in all sections.

CaO is largely derived from carbonates; therefore it shows significant positive correlation with CO_2 in all sections, table (4-4).

The average CaO content in limestone successions of Dostadara section are close to each other. Impurities detected by XRD and petrography are mainly silicate and kaolinite mineral. Moreover MgO, SiO_2 , Al_2O_3 and Cr have negative relations for all limestone successions which indicate that CaO is controlled mainly by carbonate phases. The close correlation between CaO and CO_2 indicated that most CaO is hosted by carbonates of either biogenic or authigenic origin (Hailong et al, .2000), and calcite is the only major carbonate mineral present in these rocks.

The negatively CaO correlation with MgO in all sections which are, indicating the occurrence of Mg in non-carbonate minerals, experimental and thermodynamic

considerations led Fuchtbauer and Hardie, (1976) to suggest that the MgO content of calcite decreases almost linearly with temperature (Rao, 1985).

The negatively correlation with Al_2O_3 SiO_2 in all sections related to deficiency of CaO in clay and insoluble residue, and the difference between ionic radius of K and Ca causes generally weak relation.

Cr content has negatively correlation with CaO; this may indicate the relative enrichment of chromium in the no-carbonate fraction which is due to the presence of this element in clay minerals (Kas-Yonan, 1989), table (4-4).

MgO:

Two sources are the main supplier of the magnesium in these rocks. MgO in the carbonate fraction is present as replacement for Ca in calcite (isomorphous substitution) on the other hand; the Mg content in the insoluble fraction would mainly be related to the clay minerals since it is one of the major constituents of this fraction.

The enrichment of Mg in the clay minerals could be attributed to the reducing environment. This could be explained according to the findings of Derver, (1971) who stated “the clays from strongly reducing environment, from separate groups, characterized by higher Mg content than clays with similar mineralogy from oxidizing environment (Haddad, 1980). Moreover, the detrital magnesium bearing minerals could also be responsible for the enrichment of MgO in the insoluble fraction.

Generally, the MgO content in all samples is distributed between the carbonate fraction and the insoluble fraction. When MgO content in most samples increases, residue content increases. This is clearly illustrated in the Fig(4-4A) which shows that the distribution coefficient trends of MgO are obviously following the insoluble residue trend similarly, the MgO content is high in carbonate enriched samples.

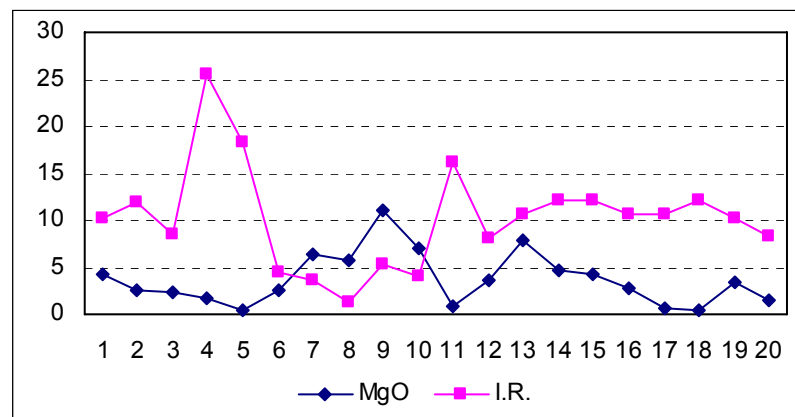


Fig (4-4A): MgO and I.R. content in limestones of the studied sections

Table (4-2); Showing Coefficient of Variation, Ranges, Mean content and Standard Deviation of geochemical analyses in bulk samples of the **Dostadara Ridges**.**Coefficient of Variation, Ranges, Mean content and Standard Deviation of geochemical analyses in bulk samples of the Dostadara 1st Ridge.**

S.No.	CaO	MgO	Al ₂ O ₃	SiO ₂	SiO ₂ / Al ₂ O ₃	Fe ₂ O ₃	Na ₂ O	K ₂ O	MnO	P ₂ O ₅	Co	Cu	Ni	Pb	Zn	Sr	Cr	CO ₂	LOI
C.V.	6.23	28.25	30.04	20.73	26.67	36.45	105.99	79.07	24.38	12.75	68.67	19.84	22.07	10.78	32.79	20.32	35.09	3.17	5.45
S.D.	2.63	2.067	1.257	1.12	0.364	0.0496	0.0405	0.0168	0.002	0.005	44.407	1.7638	10.398	3.1623	8.3066	79.9611	22.23	1.3025	2.383
Mean	42.18	7.32	4.18	5.41	1.36	0.14	0.04	0.02	0.01	0.04	64.667	8.8889	47.111	29.333	25.333	393.556	63.33	41.08	43.76
Range	37.81	2.42	2.04	4.49	1.09	0.08	0.01	0.01	0.01	0.03	20	6	30	26	16	270	30	39.376	42.54
	46.82	9.31	6.24	7.06	2.21	0.23	0.12	0.05	0.01	0.05	130	12	64	34	44	532	100	42.315	50.04

Coefficient of Variation, Ranges, Mean content and Standard Deviation of geochemical analyses in bulk samples of the Dostadara 2nd Ridge.

S.No.	CaO	MgO	Al ₂ O ₃	SiO ₂	SiO ₂ / Al ₂ O ₃	Fe ₂ O ₃	Na ₂ O	K ₂ O	MnO	P ₂ O ₅	Co	Cu	Ni	Pb	Zn	Sr	Cr	CO ₂	LOI
C.V.	4.208	62.51	35.56	41.2	31.46	22.007	88.275	50.439	24.439	8.33	7.0445	21.429	20.776	32.751	34.302	18.5868	11.45	3.2273	1.452
S.D.	2.029	1.485	1.664	1.9	0.329	0.0426	0.0476	0.0114	0.0027	0.0028	6.888	2	9.6954	10.99	6.4031	59.0235	3.742	1.3044	0.614
Mean	48.21	2.38	4.68	4.61	1.05	0.19	0.05	0.02	0.01	0.03	97.778	9.3333	46.667	33.556	18.667	317.556	32.67	40.417	42.26
Range	45.33	0.50	3.06	1.72	0.22	0.12	0.01	0.01	0.01	0.03	84	6	34	24	14	220	28	37.668	41.44
	50.65	4.83	7.63	8.38	1.35	0.26	0.13	0.04	0.02	0.04	108	12	60	60	34	440	40	41.986	43.28

Coefficient of Variation, Ranges, Mean content and Standard Deviation of geochemical analyses in bulk samples of the Dostadara 3rd Ridge.

S.No.	CaO	MgO	Al ₂ O ₃	SiO ₂	SiO ₂ / Al ₂ O ₃	Fe ₂ O ₃	Na ₂ O	K ₂ O	MnO	P ₂ O ₅	Co	Cu	Ni	Pb	Zn	Sr	Cr	CO ₂	LOI
C.V.	6.136	27.41	30.22	30	7.375	178.23	108.52	66.654	18.06	10.092	11.559	29.156	25.834	12.169	40.786	20.2778	19.6	2.4933	3.482
S.D.	2.732	1.364	1.239	1.46	0.088	2.0277	0.107	0.0227	0.0026	0.0034	11.212	3.2071	9.8814	3.0119	9.3808	77.8162	6.714	1.0063	1.44
Mean	44.52	4.98	4.10	4.88	1.19	1.14	0.10	0.03	0.01	0.03	97	11	38.25	24.75	23	383.75	34.25	40.361	41.35
Range	40.21	2.52	2.76	3.21	1.09	0.09	0.01	0.00	0.01	0.03	82	6	30	22	16	300	26	38.902	39.59
	48.83	6.73	6.20	7.50	1.37	5.98	0.34	0.07	0.02	0.04	110	16	60	30	44	520	44	41.571	43.51

Coefficient of Variation, Ranges, Mean content and Standard Deviation of geochemical analyses in bulk samples of the Dostadara 4th Ridge.

S.No.	CaO	MgO	Al ₂ O ₃	SiO ₂	SiO ₂ / Al ₂ O ₃	Fe ₂ O ₃	Na ₂ O	K ₂ O	MnO	P ₂ O ₅	Co	Cu	Ni	Pb	Zn	Sr	Cr	CO ₂	LOI
C.V.	3.58	40.34	56.32	48.70	22.09	138.95	88.09	93.01	20.33	10.45	27.94	37.59	27.69	15.83	43.00	26.72	21.05	5.30	6.78
S.D.	1.58	2.42	2.23	2.31	0.29	0.54	0.083	0.038	0.003	0.003	24.028	3.4365	11.075	4.0708	10.565	102.207	7.819	2.16	3.01
Mean	44.07	6.00	3.97	4.74	1.30	0.39	0.09	0.04	0.01	0.03	86	9.1429	40	25.714	24.571	382.571	37.14	40.82	44.43
Range	42.26	3.72	0.72	1.29	1.05	0.06	0.01	0.00	0.01	0.03	50	4	26	22	16	240	28	38.70	41.28
	45.89	11.01	6.69	7.46	1.80	1.60	0.23	0.10	0.02	0.04	120	14	60	34	46	540	48	45.18	49.11

Table (4-3); Showing Coefficient of Variation, Ranges, Mean content and Standard Deviation of geochemical analyses in bulk samples of the Type Locality, Kaolos. Kaols-Z and Gali sections

Coefficient of Variation, Ranges, Mean content and Standard Deviation of geochemical analyses in bulk samples of the Type Locality																			
S.No	CaO	MgO	Al ₂ O ₃	SiO ₂	SiO ₂ /Al ₂ O ₃	Fe ₂ O ₃	Na ₂ O	K ₂ O	MnO	P ₂ O ₅	Co	Cu	Ni	Pb	Zn	Sr	Cr	CO ₂	LOI
C.V.	3.914	58	49.44	57.7	81.8	109.8	211.4	187.6	75.32	199.7	23.8	41.7	27.0	18.2	39.9	30.8	21.6	5.665	6.707
S.D.	1.892	1.16	0.934	4.2	4.57	0.17	0.434	0.123	0.022	0.849	18.5	4.3	6.5	4.1	15.2	93.7	6.4	2.271	2.799
Mean	48.33	2.00	1.89	7.28	5.59	0.15	0.21	0.07	0.03	0.43	77.6	10.4	24.0	22.8	38.0	304.0	29.6	40.1	41.74
Range	45.33	0.76	0.83	3.16	1.10	0.07	0.01	0.01	0.01	0.03	64	8	18	18	20	190	22	36.4	36.76
	50.09	3.63	2.91	13.10	10.55	0.46	0.98	0.29	0.07	1.94	110	18	32	28	62	450	38	42.07	43.33
Coefficient of Variation, Ranges, Mean content and Standard Deviation of geochemical analyses in bulk samples of the Kaolos section																			
S.No	CaO	MgO	Al ₂ O ₃	SiO ₂	SiO ₂ /Al ₂ O ₃	Fe ₂ O ₃	Na ₂ O	K ₂ O	MnO	P ₂ O ₅	Co	Cu	Ni	Pb	Zn	Sr	Cr	CO ₂	LOI
C.V.	5.136	33.4	23.8	18.5	23.3	97.89	33.26	103.8	29.9	69.97	6.3689	38.401	70.748	13.925	25.5	39.47	16.276	2.878	2.27
S.D.	2.29	1.85	0.87	0.92	0.33	0.694	0.005	0.15	0.009	0.059	5.5	4.1	28.9	3.3	5.1	113.7	5.4	1.181	0.958
Mean	44.58	5.54	3.65	4.95	1.41	0.71	0.02	0.14	0.03	0.08	86.0	10.8	40.8	23.6	20.0	288.0	33.2	41.02	42.19
Range	41.56	3.38	2.31	4.12	0.98	0.06	0.01	0.01	0.02	0.04	80	6	20	20	14	220	28	39.47	41.08
	47.85	7.96	4.35	6.38	1.84	1.65	0.02	0.40	0.04	0.17	94	16	90	28	26	490	42	42.66	43.58
Coefficient of Variation, Ranges, Mean content and Standard Deviation of geochemical analyses in bulk samples of the Kaolos-Z section.																			
S.No	CaO	MgO	Al ₂ O ₃	SiO ₂	SiO ₂ /Al ₂ O ₃	Fe ₂ O ₃	Na ₂ O	K ₂ O	MnO	P ₂ O ₅	Co	Cu	Ni	Pb	Zn	Sr	Cr	CO ₂	LOI
C.V.	6.647	36.8	30.62	26	24.5	88.96	26.24	92.36	47.07	50.26	145.99	48.038	56.682	69.636	62.67	48.84	29.304	3.518	3.782
S.D.	2.898	1.68	1.418	1.9	0.41	0.555	0.004	0.125	0.016	0.042	273.01	6.2	33.6	25.0	21.0	184.4	11.1	1.379	1.568
Mean	43.6	4.57	4.63	7.31	1.66	0.62	0.01	0.14	0.03	0.08	187	13.0	59.3	35.9	33.6	377.6	38.0	39.19	41.45
Range	40.16	2.70	2.10	4.46	1.12	0.07	0.01	0.01	0.01	0.04	77	8	22	20	10	200	22	37.12	40
	49.25	7.79	6.05	10.34	2.19	1.48	0.02	0.40	0.06	0.13	806	24	99	88	75	660	52	41.59	44.3
Coefficient of Variation, Ranges, Mean content and Standard Deviation of geochemical analyses in bulk samples of the Gali-Zalan section.																			
S.No	CaO	MgO	Al ₂ O ₃	SiO ₂	SiO ₂ /Al ₂ O ₃	Fe ₂ O ₃	Na ₂ O	K ₂ O	MnO	P ₂ O ₅	Co	Cu	Ni	Pb	Zn	Sr	Cr	CO ₂	LOI
C.V.	8.638	30.7	48.97	70.6	36.8	101.1	49.74	71.33	52.81	58.52	144.57	28.803	55.552	57.457	45.75	54.66	36.237	6.205	4.419
S.D.	4.046	0.88	1.706	4.7	0.69	0.542	0.008	0.09	0.018	0.05	223	3.2404	38.747	20.254	15.9	234.6	13.453	2.475	1.872
Mean	46.84	2.88	3.48	6.67	1.87	0.54	0.02	0.13	0.03	0.09	154.25	11.25	69.75	35.25	34.75	429.3	37.125	39.89	42.35
Range	39.18	1.39	1.51	1.83	1.17	0.11	0.01	0.01	0.01	0.04	67	8	20	20	15	100	20	34.87	39.9
	52.05	3.78	5.48	16.74	3.27	1.44	0.03	0.28	0.07	0.18	706	16	120	80	70	700	55	42.36	44.4

Table(4-4):Correlation coefficient between the geochemical variables of all rock samples

	CaO	MgO	Al ₂ O ₃	SiO ₂	Fe ₂ O ₃	Na ₂ O	K ₂ O	MnO	Co	Cu	Ni	Pb	Zn	Sr	Cr	P ₂ O ₅	CO ₂	LOI
CaO	1																	
MgO	-0.54	1																
Al ₂ O ₃	-0.47		1															
SiO ₂	-0.42	-0.26	0.37	1														
Fe ₂ O ₃	-0.27	0.30			1													
Na ₂ O				0.34		1												
K ₂ O	-0.27	0.25		0.29	0.35		1											
MnO				0.24			0.32	1										
Co				0.21					1									
Cu		-0.22		0.22		0.27	0.24	0.45		1								
Ni		-0.20						0.44		0.37	1							
Pb	-0.32			0.43			0.45		0.20			1						
Zn	-0.22			0.37	0.30	0.22	0.55	0.27				0.46	1					
Sr									-0.20		0.62		0.21	1				
Cr	-0.35								-0.28					0.21	1			
P ₂ O ₅		-0.20	-0.21	0.32		0.85	0.36			0.25			0.36			1		
CO ₂	0.35	0.31	-0.57	-0.90		-0.30	-0.28	-0.23	-0.21	-0.31		-0.34	-0.28			-0.27	1	
LOI			-0.31	-0.40	-0.29	-0.32	-0.38		-0.24	-0.33			-0.25		0.38	-0.37	0.53	1

Note: Less than 0.2 is omitted

It is obvious, therefore, that any variation in the MgO content in the formation is shared between calcium carbonate and clay minerals which is mainly controlled by the content and the mineralogical composition of the insoluble fraction. Consequently, the different types of lithofacies show different ways of MgO distribution.

Experimental and thermodynamic considerations explain that the MgO content of calcite decreases almost linearly with temperature (Rao, 1986). It reflects also that the increase in CaO decreases MgO content as well as clay minerals (Al-Hazza'a, 1996). Magnesium content also increases in shallow marine and decreases in deep basins (Abdul-Hamid, 1980).

The distribution of MgO was shown in Fig (4-2 and 4-3 LL & LR) is normal and unimodal due to the enrichment of MgO in one phase which is the insoluble fraction only with a very small phase of secondary Mg including one sample separated by a break . This major MgO population is the constituents of the most of the studied rocks ranged between (0.31 to 11)%.

The MgO concentrations in the studied samples are nearly identical and on average range between (1.43 and 7.31)% , the mean MgO contents are (7.31, 2.37, 4.97 and 6.01)% in limestone of the four successions in Dostadara section respectively, and (4.06, 1.71, 5.54, 4.56, 1.43 and 2.66)% in Dostadara, Type- Locality, Kaolos, Kaolos-Z, Tawella and Gali sections respectively, table (4-2) and (4-3). It is possible that the Mg is introduced from the overlying or underlying

formations or it is indigenous and attributed to shallower environment in the bottoms of the successions and the idea of Abdul-Hamid, (1980) can be applied for increase of Mg with shallowness.

The correlation coefficient is negative with CaO in all sections indicating to its enrichment in the insoluble residue.

SiO₂

As mentioned in the chapter three, that some intervals of the successions contain chert nodules and bands which have diagenetic origin. Therefore studied samples were barren from nodules and silica replacements. It is possible that samples may contain some foreign (diagenetic) silica which appears in some samples as abnormal peaks.

The variation in SiO₂ contents in samples of the studied sections are obviously related to the variation in the mineralogical composition of the insoluble residues, so the existence of carbonate and ferruginous weathering horizons causes depletion in SiO₂ values. It is also expected that SiO₂ decreases with depth (Al-Gailani, 1980).

The SiO₂ content is partitioned mainly between two phases as free silica (quartz) and in clay minerals which derived mainly from clay minerals and subordinately from quartz and feldspar grains which may present within the mudstones (Sinjary, 2006). Figs (4.4B) show that the frequency distribution of SiO₂ is normal unimodal which supports the main population of low SiO₂ content.

The studied samples in all sections show low SiO₂ concentrations ranged from (1.29 to 18.025)%. The average SiO₂ content in limestone successions of Dostadara section are close to each other (5.41, 4.61, 4.88 and 4.74)% and (4.92, 20.9, 4.95, 7.31, 23.8 and 12.06)% in Dostadara, Type-Locality, Kaolos, Kaolos-Z, Tawella and Gali-Zalan sections respectively, tables (4-2) and (4-3).

Fig. (4.5 UL & UR) show significant correlations of SiO₂ content between all of the studied sections. Thus, this leads to inference that the SiO₂ is controlled to some extent by clay minerals and also by quartz grains which are present as detrital clay size grains within mudstones or limestones.

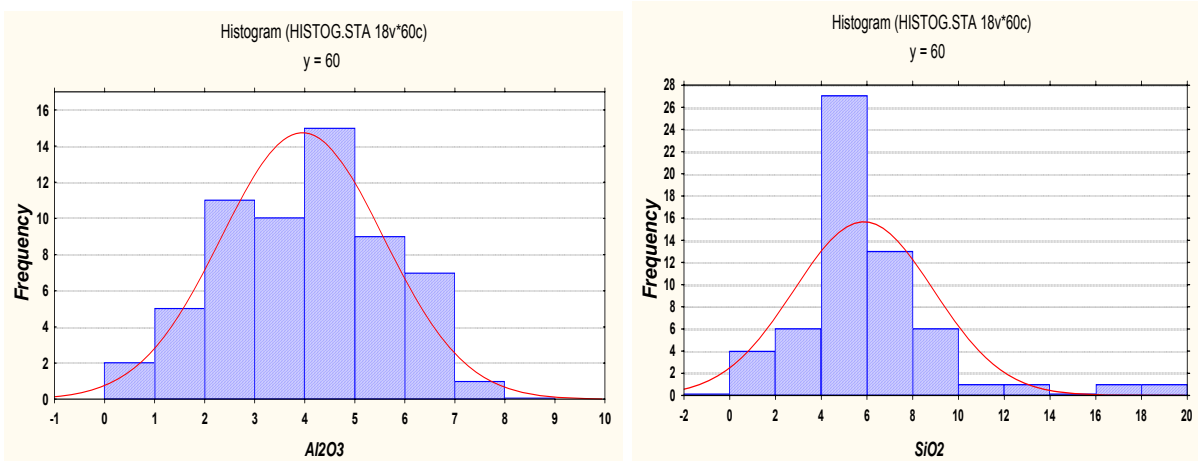


Fig (4.4B): Frequency diagrams of Al_2O_3 and SiO_2 content in limestones of the studied sections.

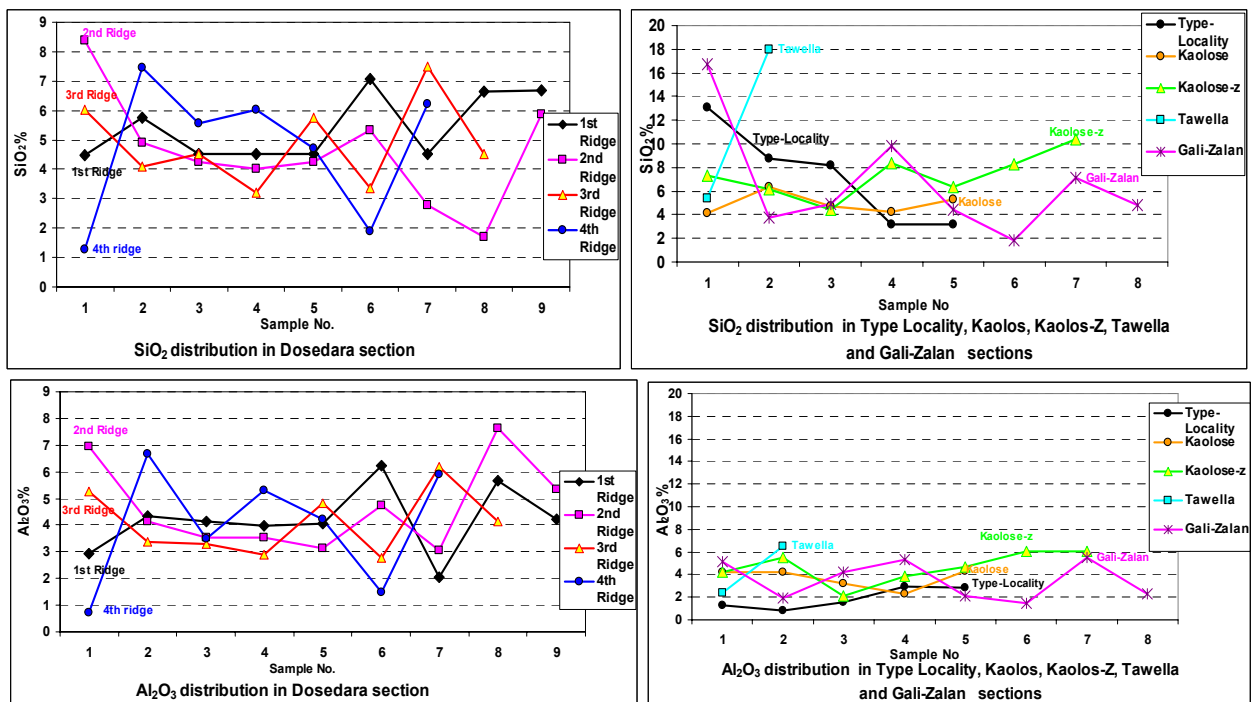


Fig (4.5) SiO_2 and Al_2O_3 contents distribution in all studied sections. (UL) is $\text{SiO}_2\%$ in limestone successions; (UR) is $\text{SiO}_2\%$ in other sections; (BL) is $\text{Al}_2\text{O}_3\%$ in limestone successions and (BR) is $\text{Al}_2\text{O}_3\%$ in other sections.

Table (4-4) show that SiO_2 concentrations are strong negatively correlated with CaO , CO_2 and L.O.I. Moreover, the relation is positive relations with Al_2O_3 and Na_2O in all sections which is due to the presence of these elements and most of silica in the insoluble residue and/or clay minerals.

Positive relations with trace elements Pb and Zn is due to the adsorption of these elements in clay layers (Kas-Yonan, 1989).

Al₂O₃

The content of aluminum in carbonate rocks is mainly controlled by the amount of the non-carbonated constituents. The variation in Al₂O₃ contents is related to the variation in the insoluble residue contents. It is logical to state that all the Al₂O₃ content is related to clay minerals and the very little other insoluble silicate minerals. However little aluminum could be leached from the clay minerals during the separation of the insoluble residue.

The availability of Al₂O₃ (which forms a major part of clay minerals), controls the stability of kaolinite under high temperature transformations (Al-Sadooni, 1980).

The distribution of Al₂O₃ is shown in the Fig (4.4B) which is normal unimodal, it supports the main population of low Al₂O₃ content ranged from (0.72 to 7.63)%.

The presence of aluminum is derived mainly from clay minerals or insoluble residues on the depletion of carbonate. This also represents the lagoonal, landward part of the shelf.

In order to verify the assumption that most of aluminum in this formation is derived from clay minerals, the relation of aluminum with potassium will be discussed. In this study no relation is detected with potassium, this confirms the presence of kaolinite clay mineral only. A second approach will be to discuss the behaviour of aluminum in relation to diagenesis which represented by the MgO content (Al-Sadooni, 1980 and Sinjary, 2006). Al₂O₃ percentages will be very low in the presence of carbonates as well as with extensive dolomitization (Al-Gailani, 1980). In the studied rocks notable relation with MgO is not detected also, table (4-4).

The concentrations ranged from (0.72 to 7.63) % in all sections. The mean Al₂O₃ contents are (4.18, 4.68, 4.1 and 3.97) % in limestone successions of Dostadara section respectively, and (4.2, 2.52, 3.65, 4.63, 10.62 and 6.9)% for sections (Dostadara, Type Locality, Kaolos, Kaolos-Z, Taw and Gali) respectively, table (4-2) and (4-3).

Table (4-5) shows the SiO₂ / Al₂O₃ ratio in the bulk samples from the four successions ranged from (0.22 to 2.21)% in Dostadara section and from (1.1 to 10.554)% in the rest sections. Generally, these sections are composed of high Al₂O₃ percentages which means the presence of free quartz in the insoluble residues such as (Type-1, 3 and 5) in Type Locality section , (Kol-Z 5 and 7) In Kaolos-Z section , (all samples) in Tawella section and (G-1, 3, 9, and 17) in Gali-Zalan section. This variation in this ratio reflects variation in clay minerals to free silica proportions and it may be attributed to either change in rate of sedimentation or difference in grain size

and/or diagenetic activities that lead to the formation of quartz (Hirst, 1962 and Amin, 1979).

High coefficient of variations of Al_2O_3 contents in all sections are due to variations in clay content in the rock samples, table (4-4).

Positive relations with SiO_2 in all sections are due to the presence of these elements and silica in the insoluble residue and/or clay minerals.

Negatively relation with CaO and CO_2 means that this oxide is not related to calcium mineral but related to the clay portion.

Table (4-5): Shows the $\text{SiO}_2 / \text{Al}_2\text{O}_3$ ratio in the bulk samples from the five traverses

Section	Al_2O_3	SiO_2	$\text{SiO}_2/\text{Al}_2\text{O}_3$	Section	Al_2O_3	SiO_2	$\text{SiO}_2/\text{Al}_2\text{O}_3$
Dostadara section	2.948	4.49 ₂	1.524	Type-Locality	1.323	13.1	9.902
	4.346	5.754	1.324		0.8314	8.775	10.554
	4.157	4.514	1.086				
	3.968	4.518	1.139		1.549	8.172	5.276
	4.044	4.522	1.118		2.91	3.205	1.101
	6.236	7.055	1.131		2.834	3.157	1.114
	2.041	4.501	2.205				
	5.669	6.661	1.175	Kaolos	4.195	4.116	0.981
	4.233	6.683	1.579		4.176	6.379	1.528
	6.954	8.381	1.205		3.25	4.758	1.464
	4.157	4.89	1.176		2.305	4.251	1.844
	3.552	4.236	1.193		4.346	5.256	1.209
	3.552	4.026	1.133	Kaolos-Z	4.176	7.325	1.754
	3.137	4.231	1.349		5.499	6.146	1.118
	4.724	5.335	1.129		2.097	4.458	2.126
	3.061	2.777	0.907		3.817	8.341	2.185
	7.634	1.716	0.225		4.724	6.311	1.336
	5.347	5.874	1.099		6.046553	8.250877	1.365
	5.272	6.037	1.145		6.047	10.34	1.710
	3.363	4.077	1.212	Tawella	2.419	5.391	2.229
	3.288	4.514	1.373		6.538	18.02	2.756
	2.91	3.213	1.104	Gali-Zalan	5.121	16.74	3.269
	4.837	5.772	1.193		1.908	3.793	1.988
	2.759	3.359	1.217		4.176	4.886	1.170
	6.198	7.5	1.210		5.329	9.774	1.834
	4.157	4.535	1.091		2.079	4.385	2.109
	0.718	1.292	1.799		1.512	1.833	1.212
	6.689	7.457	1.115		5.48	7.138	1.303
	3.477	5.562	1.600		2.267	4.777	2.107
	5.291	6.041	1.142				
	4.233	4.715	1.114				
	1.474	1.887	1.280				
	5.895	6.204	1.052				

Fe₂O₃ :

Fe₂O₃ concentrations in the studied limestone samples represent the total iron. The Fe₂O₃ content shows a wide range of variation which may reflect different contents of little pyrite, iron oxides. High contents were detected in rock samples 3Dos (7 and 11), 4Dos-7 in Dostadara section and Type-1, Kol (1, 3 and 9), Kol-z (1, 3 and 17), Taw-5 and G (1, 3 and 17) in (Type Locality, Kaolos, Kaolos-Z, Taw and Gali-Zalan) respectively, Appedix (A)-Tables (A-1a, A-2a, A-3a, A-4a, A-5a, A-6a, A-7a, A-8a and a-9a).

The distribution of Fe₂O₃ was shown in Fig (4.6) and Figs (4.7 UL & UR) which is lognormal bimodal and it supports the main population of low Fe₂O₃ content with only two samples 3Dos (7 and 11) of high percentages, which are equal to (1.75, 5.98)% respectively, attributed to the presence of some pyrite viens and iron oxide in some rock samples of the mentioned section.

Generally, Fe₂O₃ concentrations in the studied samples ranged from (0.05 to 1.65) % except in the previous mentioned samples of Dostadara sections. The mean Fe₂O₃ contents are (0.14, 0.19, 1.14 and 0.39)% in limestone succession of Dostadara section, and (0.47, 0.94, 0.71, 0.62, 0.32 and 0.5)% for sections (Dostadara, Type Locality, Kaolos, Kaolos-Z, Tawella and Gali-Zalan) respectively, tables (4-2 and 4-3).

The high coefficient of variations in all sections is due to the different effects of diagenesis on the component limestones, tables (4-2 and 4-3).

Table (4- 4) shows positive relations of Fe₂O₃ with K₂O and Na₂O are due to their association with Fe₂O₃ in kaolinite mineral Weaver and Pollard (op. cit) which is present in the studied limestones and shown previously in XRD analyses.

The study also shows that Zn has positive relations which may indicate possible replacement of iron by Zn in the detrital heavy fraction.

Hem, (1985) mentioned that the adsorption of Zn by iron hydroxides is assumed as an important agent of sedimentation. Generally, this possible replacement of iron by Zn was due to the remobilization during the process of diagenesis and/or their ionic radii similarity (Goldschmidt, 1962).

Na₂O

The association of sodium with carbonate rocks is commonly related to the non-carbonate constituents. Clay minerals and plagioclase, Na salts are the main holders of sodium in carbonate rocks. Sodium is mainly concentrated in the insoluble fraction.

Clay minerals seem to be the chief hosts of Na and could generally be associated with clay minerals either adsorbed or incorporated within their structural lattices. Boggs in Sinjary, (2006) suggests that the Na_2O abundance in the mudstone is related to the presence of clay mineral and plagioclase grains.

In the present work, the average Na_2O content in limestone successions of Dostadara section are (0.04, 0.05, 0.1 and 0.09)% in limestone successions of Dostadara section respectively, table (4-2). However the mean Na_2O content of the studied samples are (0.07, 0.21, 0.02, 0.02, 0.15 and 0.02)% for sections (Dostadara, Type Locality, Kaolos, Kaolos-Z, Taw and Gali) respectively. The Coefficient of Variation, Ranges, Mean content and Standard Deviation of Na_2O in samples from the five studied sections are shown in tables (4-2 and 4-3).

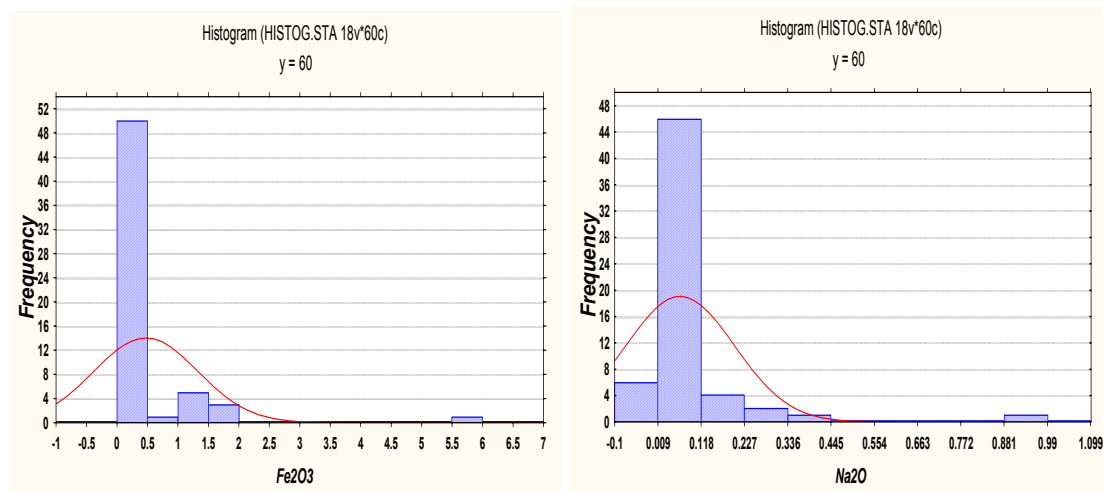
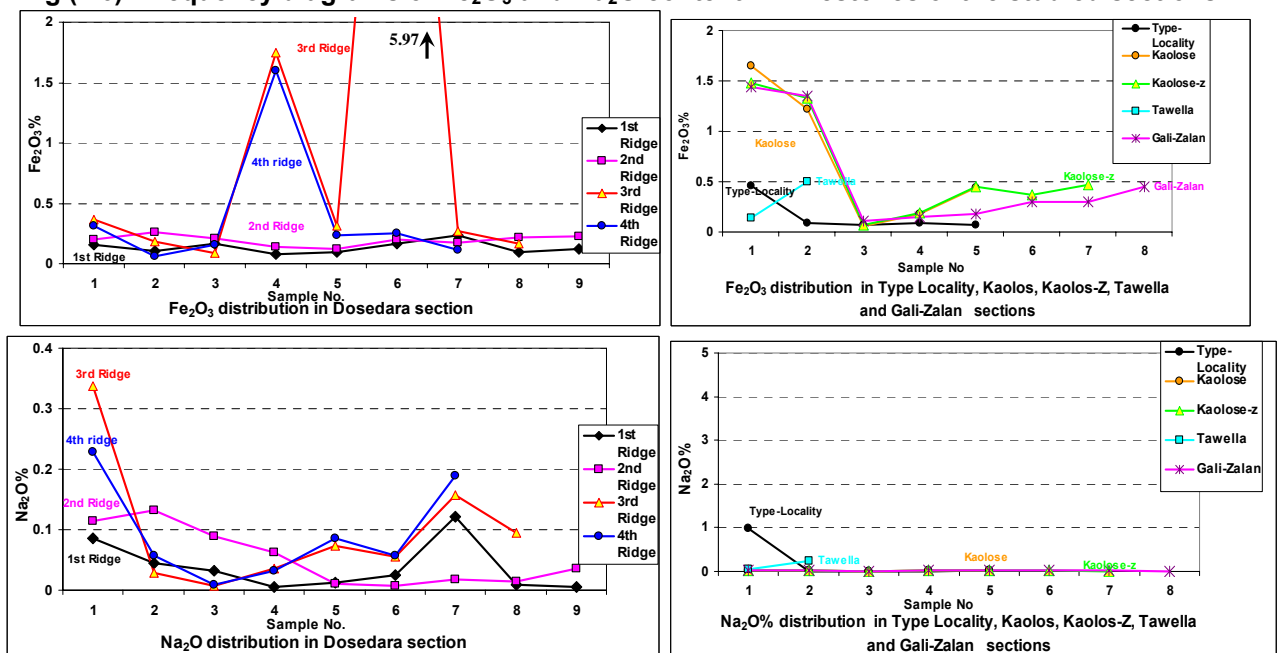


Fig (4.6): Frequency diagrams of Fe_2O_3 and Na_2O content in limestones of the studied sections.



Fig(4.7): Fe_2O_3 and Na_2O contents shows the distribution in all studied sections. (UL) is $\text{Fe}_2\text{O}_3\%$ in limestone successions; (UR) is $\text{Fe}_2\text{O}_3\%$ in other sections; (BL) is $\text{Na}_2\text{O}\%$ in limestone successions and (BR) is $\text{Na}_2\text{O}\%$ in other sections.

The distribution of Na_2O was shown in Fig(4.6) and Figs (4.7 LL & LR) which is lognormal bimodal and it supports the main population of low Na_2O content with only one samples of high percentage (Type-1) in Type Locality section, which is equal to (0.98)%, representing the presence of sodium salt .within the insoluble residue or adsorbed by the clay.

High coefficients of variations in all sections are due to the big difference between Na_2O content in each section. They show much higher mean Na_2O content (1.79 and 1.80)% in Type Locality and Tawella sections respectively as compared with those of the rest sections.

Positive relations with SiO_2 content in the bulk samples indicate its enrichment in the I.R. inside the clay minerals as an adsorbate.

Positive relations with P_2O_5 are due to their associations inside the clay mineral containing apatite.

K_2O

K-salts and clay minerals should be the main holders of potassium in carbonate rocks. So, it is mainly concentrated in the insoluble fraction. Concentration of K_2O in the rock is a reflection of increased alteration of feldspars and the subsequent formation of kaolinites (Al-Gailani, 1980). K_2O in the studied rocks could generally be associated with clay minerals either adsorbed or incorporated within their structural lattices. The negatively relation with insoluble residue confirms that, table (4-4).

The distribution of K_2O is shown in Fig. (4.8) which is lognormal unimodal supports the main population of low K_2O content with only one phase which is clay mineral or insoluble residue.

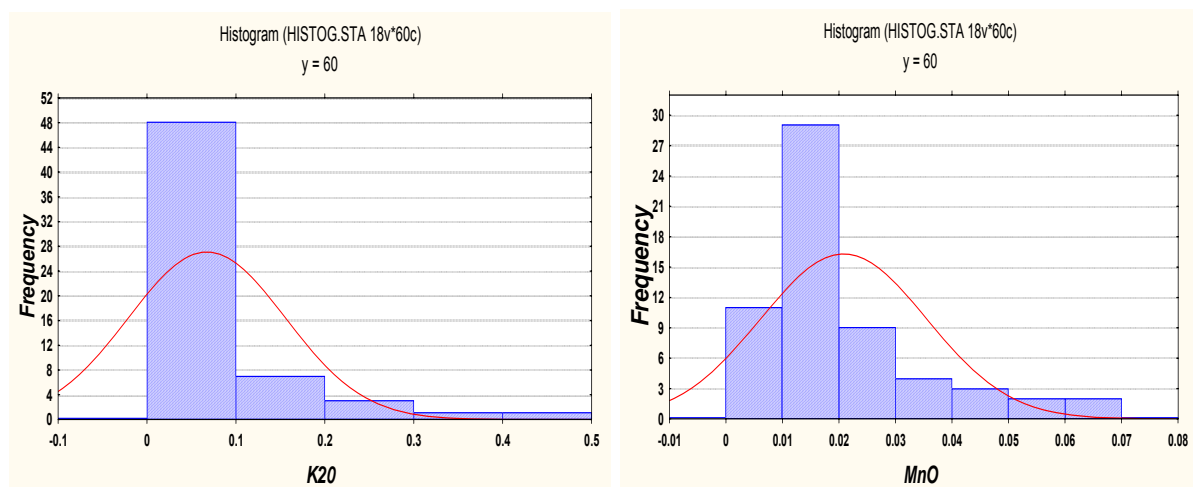


Fig (4.8): Frequency diagrams of K_2O and MnO content in limestones of the studied sections.

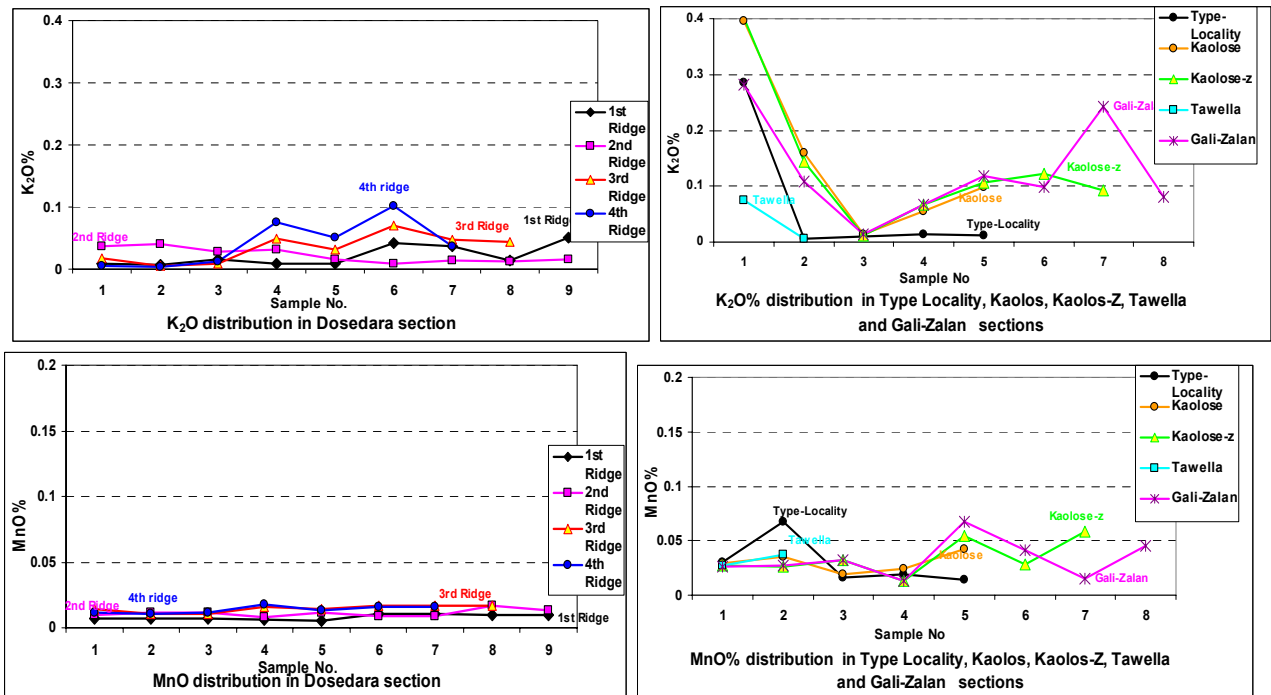


Fig (4.9) K₂O and MnO contents show the distribution in all studied sections. (UL) is K₂O% in limestone successions; (UR) is K₂O% in other sections; (LL) is MnO% in limestone successions and (LR) is MnO% in other sections.

Generally, the mean K₂O content shows rather similar variation Fig (4.9 UL & UR). However the mean K₂O contents of Dostadara section successions are similar and much lower than samples from the other sections. In Dostadara, Limestone successions are ranged from (0.02 to 0.04)%, tables (4-2 and 4-3). The mean K₂O content of the studied samples are (0.02, 0.07, 0.01, 0.14, 0.04 and 0.15)% for sections (Dostadara, Type, Kaolos, Kaolos-Z, Tawella and Gali sections) respectively. These contents are much less than that of the previous studies such as; Graf, (1960), 2.11% in globigerina ooze; Al-Sadooni, (1978), 0.92% in the globigerina ooze of Balambo Formation the basinal equivalent of Qamchuqa Formation).

The high coefficient of variation in all sections is due to the big difference between K₂O content in each section.

Positive relations with P₂O₅ are due to their associations inside the insoluble residue containing apatite, and may replace by Na.

The Positive relations with Pb and Zn indicate that K₂O is enriched in the clay mineral and/or I.R.

MnO

Manganese geochemically is a strong lithophile metal, redox sensitive and the high contents of this element in the rock which probably indicates

reduction (Wallace, 1990). Manganese in carbonate rocks may occur either in the carbonate fraction or in the insoluble fraction. However Hirst, (1962) have mentioned that most of the manganese contribution in carbonate rocks is related to the carbonate fraction rather than the insoluble fraction. Mn in carbonate rocks could replace Ca and Mg in calcite and dolomite lattices. Moreover, foraminifera calcareous shells could also be enriched by manganese.

The Mn concentration, present in the insoluble residue, could be associated with pyrite and/or other iron bearing minerals. Clay minerals could also hold some Mn either adsorbed (especially MnO (OH)) or replacing other elements e.g. Al^{3+} , Fe^{2+} , Fe^{3+} and possibly Mg^{2+} . Amin, (1979) has suggested a possible relationship of Mn to organic matter.

The distribution of MnO in all studied sections which has been shown in Fig.(4.8) is normal and unimodal supports the main population of low MnO content with only one phase which may be the carbonate fraction only.

The MnO concentrations in the studied samples are ranges between (0.01 and 0.07)%. The mean MnO contents are (0.01, 0.01, 0.02 and 0.01)% in limestone of the four successions in Dostadara section respectively, and (0.03, 0.03, 0.03, 0.04, 0.03 and 0.04)% in Dostadara, Type-Locality, Kaolos, Kaolos-Z, Tawella and Gali sections respectively. The high content of MnO reflects marine environment and vice versa for continental (coastal facies) environment (Al-Haza, 1989 and Younis1979).

The low MnO contents in the studied rocks represent a deposition in an arid climate, as reported by Romov Ermishkina-in Moghrabi, (1968), where they found that carbonate which are deposited under such conditions that shows an average MnO content of 320ppm compared to carbonates which are deposited under humid conditions (contain an average content of 810ppm) (Al-Kufaishi,1977).

The coefficient of variation of MnO contents is generally high in all sections and ranged between (18.06 and 87.26)%. It means that the MnO concentration in the studied rocks is variable.

Cu and Ni are related positively with MnO because of its relation to the organic matter and reduced environment (Kas-Yonan, 1989).

P₂O₅

P₂O₅ content is an indicator of reducing environment with organic matter or the presence of phosphate minerals. The distribution of P₂O₅ in the studied rocks is shown in Fig. (4.10) which is normal bimodal explaining two phases of high and low percentages in the insoluble residue. The high percentage is due the presence of apatite mineral which confirmed by MPA, table (4-1). Its content shows the variation on average range between (0.01 and 1.94)%. The mean P₂O₅ contents are (0.04, 0.03, 0.03 and 0.03)% in limestone successions of Dostadara section respectively, and (0.04, 0.43, 0.08, 0.08, 0.05 and 0.09)% in Dostadara, Type-Locality, Kaolos, Kaolos-Z, Tawella and Gali-Zalan sections respectively, tables (4-2 and 4-3).

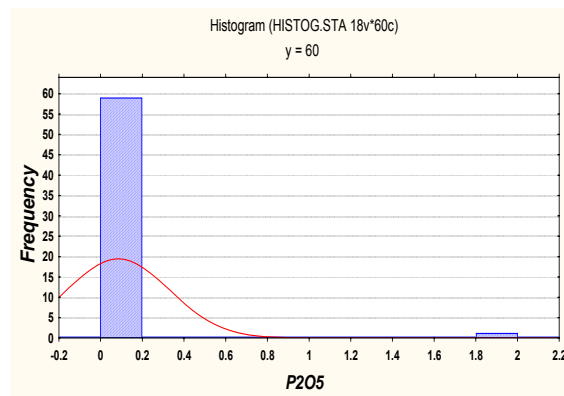


Fig (4.10): Frequency diagrams of P₂O₅ content in limestones of the studied sections.

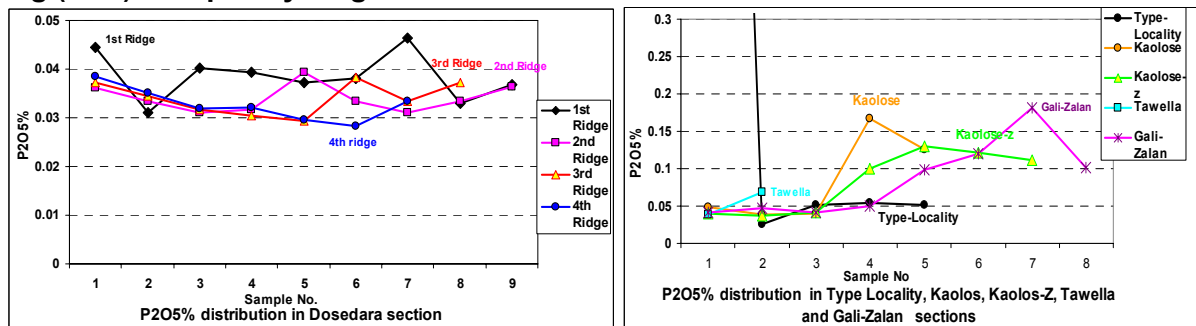


Fig (4.11): P₂O₅ contents show the distribution in all studied sections. (L) is P₂O₅% in limestone successions and (R) is P₂O₅% in other sections.

Positive relations with Na₂O, K₂O and Zn is due to the presence of this elements in reduced environment and precipitation under high saline and organic environment which contains high concentrations of (Na₂O, K₂O) and the negative relation with L.O.I. confirms its presence in the insoluble residue, table (4-4).

4.5. Trace Element Geochemistry

Introduction

The content of the elements: Sr, Co, Ni, Pb, Zn, Cr and Cu in the Qulqula limestone beds discussed in relation to carbonate minerals type, insoluble residue and diagenetic changes in these rocks.

The mean content of each element is also compared with published data on similar rocks elsewhere.

Strontium

A comparison between the strontium content of limestones, with some other published data are shown in table (4-6). In general the mean strontium content in the studied limestone rocks of all sections seems to be similar to the mean strontium contents in other carbonate rocks that have been reported by many authors. Nevertheless, the variation in the mean strontium contents of the studied sections could reflect, relatively, different environmental conditions.

Vlasove, (1966) in Al-Marsumi, (1980) stated that the diagenetic process causes Sr to expel out of the crystal lattice of minerals, so it decreases in older rocks.

Hydrocarbon waters include high Sr content and Ni. Dean and Anderson, (1974) in Al-Marsumi, (1980) explained the effect of low water salinity on the depletion of Sr, so precipitation under high saline environment contain high concentrations of (Sr, K₂O and MgO). Al-Sadooni, (1978) stated that Sr is directly proportional with evaporates and temperature. In cold-water carbonate, Sr is low because of the predominance of calcitic fauna and calcareous cementing material (Rao, 1985).

Wallace, (1990) described a case in which Sr content decreases away from the basin as follows ; Basin (380–1570)ppm, for-reef (150 – 420)ppm, back-reef (60 - 150)ppm and he related to the increase of the rate of recrystallization away from the basin. Kulp et al., in Younis, (1979) shows that Sr content in fossils on the average is twice as much strontium as the surrounding carbonate matrix. Enrichment of molluscs causes high MgO content and low Sr than that of reef coralline algae.

The major part of Sr content in the studied rocks is related to the carbonate fraction (substituting for Ca in the calcite lattice). The very little Sr content found in the insoluble fraction as given in Appedix (A)-Tables (A-1b, A-2b, A-3b, A-4b, A-5b, A-6b, A-7b, A-8b and A-9b).

The distribution of Sr shown in Fig(4.12) and Fig(4.13 UL & UR) is normal unimodal, it supports the main population of low Sr content ranged from (100 to

700)ppm with only two samples which are of high percentages 700ppm in (Kaolose-Z and Gali) sections respectively. The mean Sr contents are (394, 318, 380 and 383)ppm in limestone successions of Dostadara section respectively, and (369, 260, 288, 380, 283 and 440)ppm for (Dostadara, Type Locality, Kaolos, Kaolos-Z, Taw and Gali) sections respectively.

A positive relation with Ni is due to mainly accommodated in the clay minerals.

No significant correlation positive or negative appeared with all of other geochemical constituent which suggests that concentration of Sr may not be controlled by carbonate or clay minerals because of little amount of concentration.

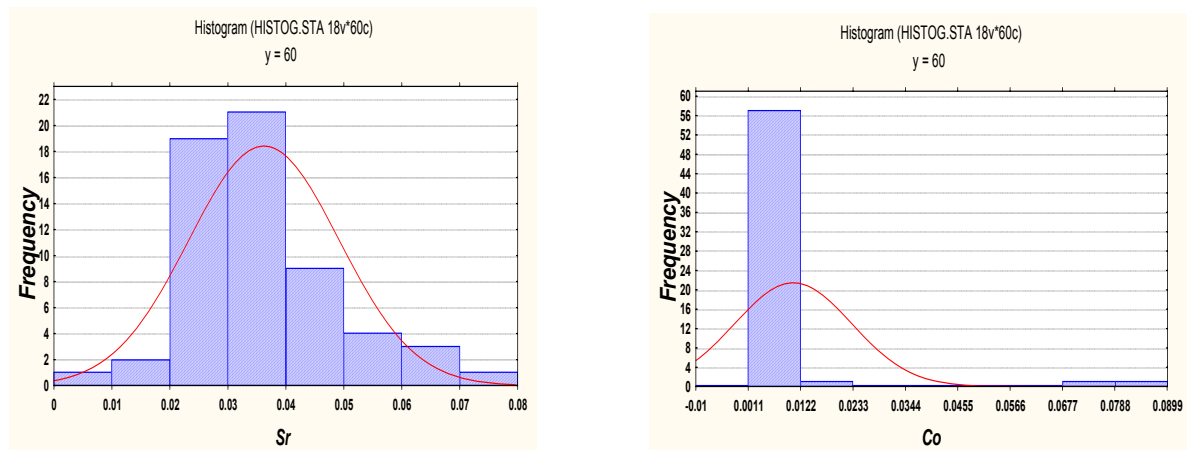


Fig (4.12): Frequency diagrams of Sr and Co content in limestones of the studied sections.

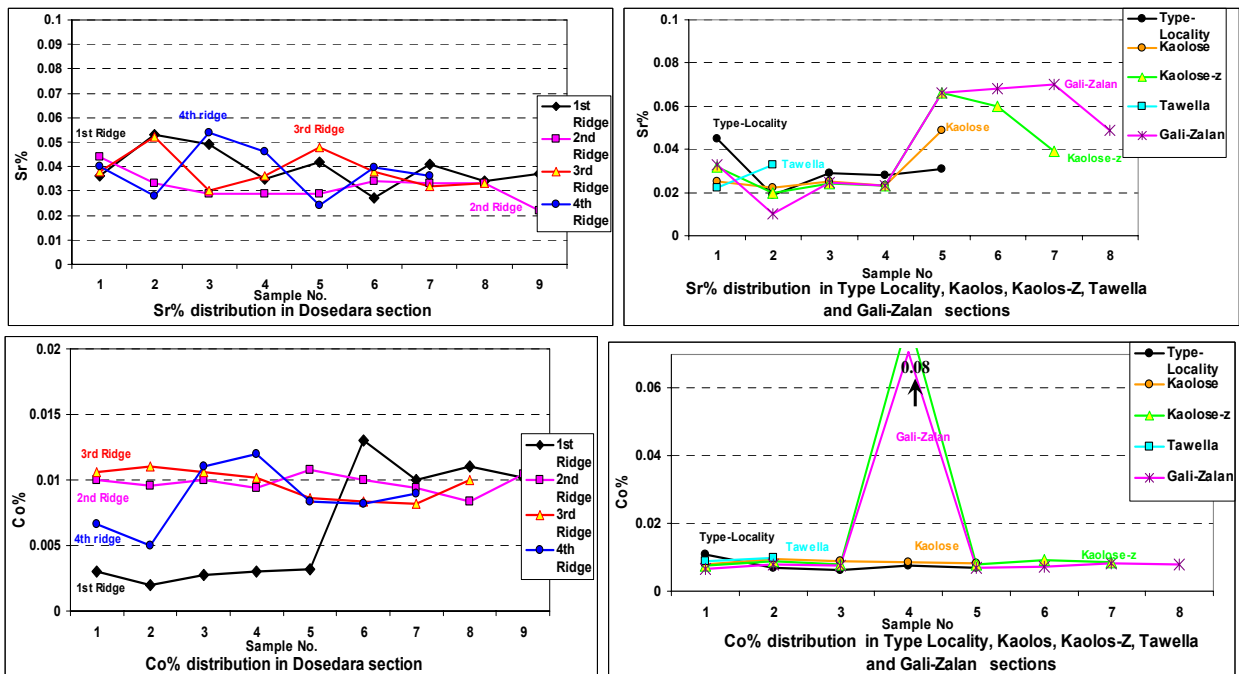


Fig (4.13): Sr and Co contents distribution in all studied sections. (UL) is Sr% in limestone successions; (UR) is Sr% in other sections; (BL) is Co% in limestone successions and (BR) is Co% in other sections.

Table (4-6) shows a comparison between the Fe₂O₃, Mn, Ni, Zn and Sr content of limestone beds of the studied sections, with some other published data.

	Type of rocks or sediment	Fe ₂ O ₃	Mn	Ni	Co	Zn	Sr
Standard	Argill Lst	0.46	193	60		25	250
Dostadara	Black Lst	0.45	116	43.30	86.06	22.78	368
Type Locality	Black Lst	0.81	252	22.14	76.71	34.71	260
Kaolos	Black Lst	0.71	298	40.8	86	20	288
Kaolose-Z	Black Lst	0.62	342	59.29	187	33.57	378
Tawella	Black Lst	0.34	296	45.75	131.5	27	291
Gali	Black Lst	0.50	333	66.67	146	32	436
Rankama & Sahama, 1950	Carbonate rocks	0.45	385		50	490
Ostrom, 1957	Limest	2.46	1400	17	40	595
After Mason, 1960	Limest	22.5	610
Shearman & Shirmoha mad. 1969	Limest.					250
Al-Hashimi, 1972	Limest						618
Al-Sadooni, 1978	Qumchuqa Limest						365.9
Al-Jawadi, 1978	PilaSpi Limest						341
Assafli, 1979	Basinal Limest	0.25	33				389
Younis, 1979	Miocene Carbonate	0.54	49.6	13.58		6.67	868
Al-Haza'a, 1996	limestone (Zahra Fm.)	0.13	84	91	84	12	275

Cobalt

Cobalt is belonging to the mobile elements group and its ionic radius size is (0.83Å^o). The little amount of cobalt present in carbonate rocks is usually related to the non-carbonate fraction. As shown by Nichols and Loring, (1962) in their study of the Bersham rocks, this element has been transported to the basin of deposition with the sediments which either replacing Fe or Mg in the clay minerals or adsorbed to the organic material. Hirst, (1962); Krauskof, (1972) and Kas-Yonan (1989) also mentioned the same. Rankama and Sahama, (1950) indicated that Co concentrated in Insoluble residue.

Amin, (1979) indicated that illite and organic matter could also accommodate some cobalt.

The mean cobalt in the five studied sections is similar to the average contents given by different workers table (4-6). The four successions of Dostadara sections mean samples are also of similar contents of cobalt.

The relatively higher cobalt content in (Kol-z-9 and G-7) samples of (Kaolose-Z, and Gali-Zalan) sections respectively as compared with the rest samples could be attributed to the relatively higher contents of cobalt hosts (organic matter or replacing Fe) in the insoluble residue rocks. Appedix (A)-Tables (A-1b, A-2b, A-3b, A-4b, A-5b, A-6b, A-7b, A-8b and A-9b) show that in some samples, cobalt is distributed in approximately even proportions in the acid soluble fraction and in the insoluble fraction. This may be caused either by leaching of cobalt during the separation of insoluble residue.

Generally the mean Co content shows rather similar variation Fig. (4.12). However the mean Co contents of Dostadara successions are similar. In Dostadara, Limestone successions are (65, 98, 97 and 86)ppm respectively, table (4-2.). The mean Co content of the all studied samples are (86.4, 77.6, 86, 187 and 154.3)ppm for sections (Dostadara, Type Locality, Kaolos, Kaolos-Z and Gali) respectively including two high content abnormal samples (806 and 710)ppm in Kaolose-Z and Gali-Zalan sections respectively.

No significant correlation positive or negative appeared with all of other geochemical constituent which suggests that concentration of Co may not be controlled by carbonate or clay minerals because of little amount of concentration.

Copper

The association of copper with carbonate rocks is very limited and it is generally restricted to the non-carbonate constituents. However Turekian and Imbrie (1966) and Deurer et al., (1978) suggested a possible association of copper with carbonates.

Copper in the studied rocks, is generally related to the non-carbonate constituents, pyrite seems to represent the most important carrier of Cu, since Cu have very strong chalcophile character and its association with pyrite has been widely discussed by many workers. Clay minerals may also accommodate some copper. Hirst, (1962) reported that copper enters the basin of deposition structurally combined in the clay minerals lattice.

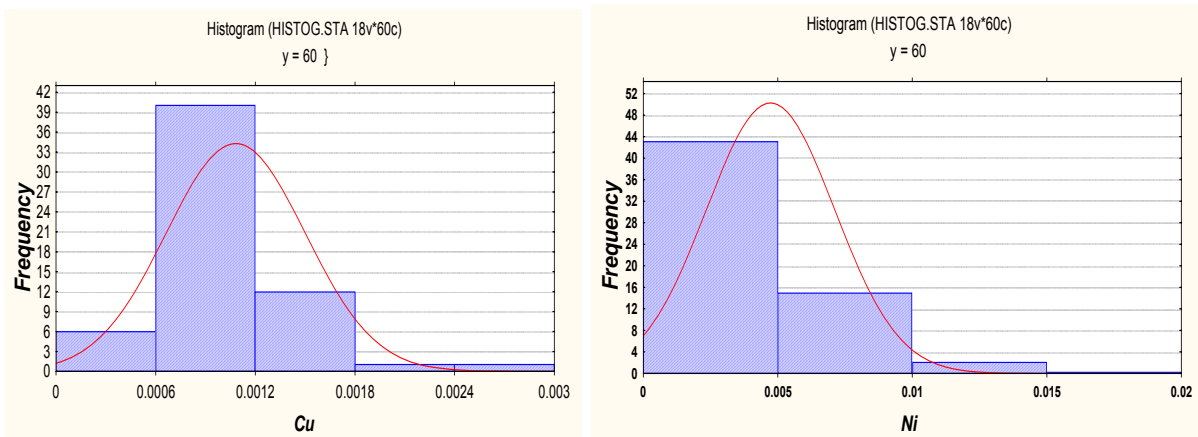


Fig (4.14): Frequency diagrams of Cu and Ni content in limestones of the studied sections.

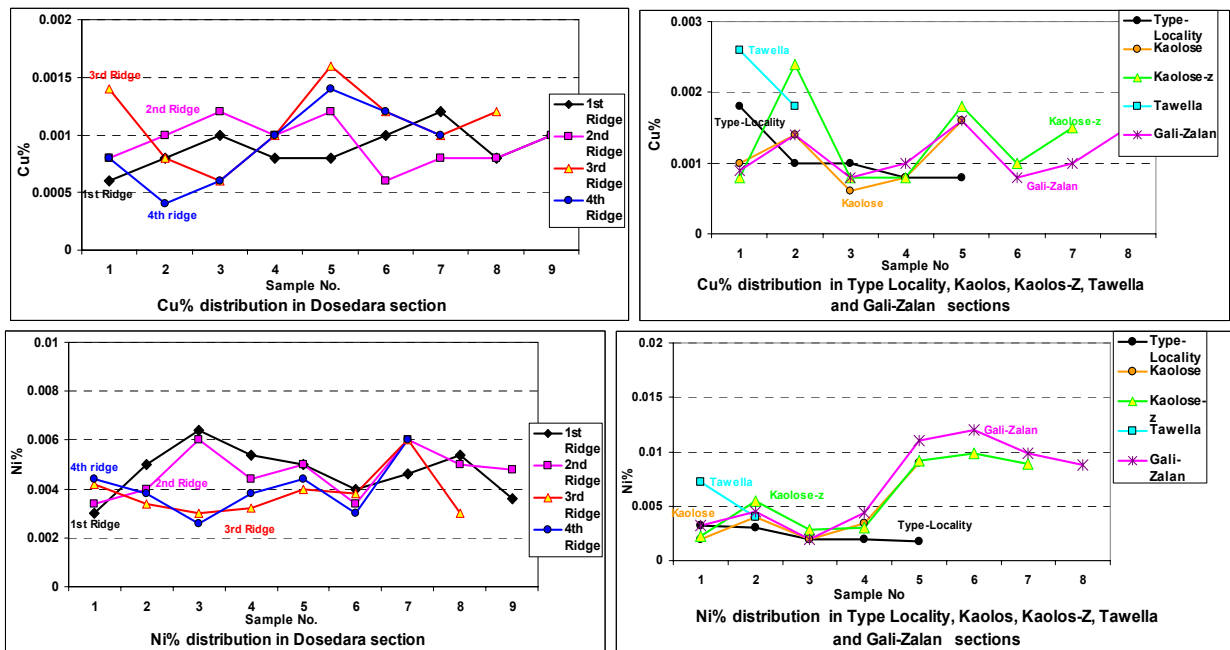


Fig (4.15): Cu and Ni contents show the distribution in all studied sections. (UL) is Cu% in limestone successions; (UR) is Cu% in other sections; (BL) is Ni% in limestone successions and (BR) is Ni% in other sections.

Goldschmidt, (1962) remarked that Cu may possible substituted for iron, lead, zinc and nickel in the hydrolysate sediments. The copper-organic matter association was also reported by Krauskopf, (1959).

Copper could be adsorbed on the hydrated iron oxide (Steele, and Wanger, 1975) and Hem, (1977).

Haddad, (1980) in his study of Shiranish Formation indicated that a large proportion of Cu has been lost during acid treatment. This may be related to the alteration products of pyrite which include the soluble copper phases, like copper sulphate and copper carbonate. Moreover the copper that may be accommodated within the clay minerals and that adsorbed on them, organic matter, quartz and ferric hydroxide could also been leached during acid treatment.

The distribution of Cu in all studied sections was shown in Fig. (4.14) is normal and unimodal due to the enrichment of Cu in one phase which is the non-carbonate fraction only. This major Cu population is the constituents of most of the studied rocks. The Cu concentrations in the studied samples ranges between 6ppm and 26ppm , The mean Cu contents are (8.88, 9.33, 11 and 9.1)ppm in limestone of the four successions in Dostadara section respectively, and (9.57, 10.4, 10.8, 13 and 11.25)ppm in Dostadara, Type-Locality, Kaolos, Kaolos-Z, Tawella and Gali sections respectively.

Positive relations with Ni, MnO and Co are due to the adsorption of these elements and Cu in clay layers, and negatively relation with L.O.I. confirms that.

No significant relations appeared with other major oxides.

Nickel

The nickel content in carbonate rocks is generally low and limited mainly to the non-carbonate materials. Nickel may be found in carbonate rocks as soluble weathering product minerals and mixtures forming the so-called nickel blooms (Read, (1973).

The variation in the nickel content with mineralogical composition of the carbonate rocks may be interpreted that calcitized limestones can accommodate more nickel than dolomite and dedolomite rocks (Haddad, 1980), the positive relation with Sr. confirms that, Table (4-4).

Since, normally Ni is associated mainly with non-carbonate materials; therefore the non-carbonate constituents of the studied rocks (including iron minerals, clay minerals) are considered the main nickel hosts. Clay minerals may also accommodate some Ni as a substitute for Fe and Mg in their crystal structures (Turekian and Carr, 1960).

The large variation in the Ni content in carbonate rocks from different parts of the world can be attributed to differences in the concentration of Ni in the environment from which the carbonate have precipitated, in addition to differences due to mineralogy of the carbonate rocks.

Table (4-6) shows a comparison between the Ni content in all studied sections of limestones and other carbonate rocks of other published data. It shows that the mean Ni content sections are relatively higher than in other carbonate rocks due to the relatively higher clay content in some of the studied rock samples.

The overall mean content of Ni in the samples of Dostadara sections 43ppm is little more than the mean content of 23ppm given by Haddad, (1980) and 20ppm by Turekian and Wedepohl, (1961) for carbonate rocks, and higher than the value of 17ppm given by Ostrom in Graf, (1962) for Pennsylvanian age limestone from Illinois U.S.A. On the other hand, the Ni content in calcareous sediments reported by Rankama and Sahama, (1950) and Goldschmidt, (1962) are exceedingly small (few ppm or less).

The distribution of Ni in all studied sections which is shown in Fig (4.14) is lognormal due to the enrichment of Ni in two phases which are the pure and clay content limestone. The non-carbonate, which is the major Ni population, is the constituents of the most of the studied rocks. The Ni concentrations in the studied samples are on average range between (22 and 67)ppm. The mean Ni contents are (10, 47, 38 and 40)ppm in limestone of the four successions in Dostadara section respectively, and (24, 22, 41, 59, 49 and 67)ppm in Dostadara, Type-Locality, Kaolos, Kaolos-Z, Tawella and Gali sections respectively.

Positive relations with Co and MnO are due to the adsorption of these elements in clay layers. No significant relation appeared with other major oxides.

Lead

The principal minerals of lead are sulphide (galena, PbS) and sulphate (anglesite, PbSO_4) and carbonate (creussite, PbCO_3). Owing to the strong chalcophile character of lead. The lead sulphide minerals are the chief lead minerals formed in reducing environment. Lead sulphate and lead carbonate represent the chief lead minerals developed at the oxidation zone of the sulphide phase (Read, 1973). The association of lead with carbonate rocks is similar to that of copper, cobalt and other heavy trace elements where those elements rarely found in a carbonate phase due to their very low concentration in sea water (Haddad, 1980).

The major hosts of lead are expected to be the non-carbonate constituents.

The black colour of the limestone of the Qulqula Radiolarite Formation is evidence of existence of some organic matter; therefore the Pb may be introduced into the formation by migration of organic matter.

The decomposition of lead sulphide (during late diagenesis and/or during weathering) may lead to a local redistribution of some Pb within other rock constituents. Hydrated iron oxide may adsorb Pb (Hirst, 1962); similarly, it may be

adsorbed on organic matter (Hirst, 1962) or clay minerals. The Pb in such phases will be easily leached away during acid treatment (Haddad, 1980).

The distribution of Pb in all studied sections was shown in Fig (4.16) is normal due to the enrichment of Ni in one phase which is the non-carbonate fraction of the most of the studied rocks.

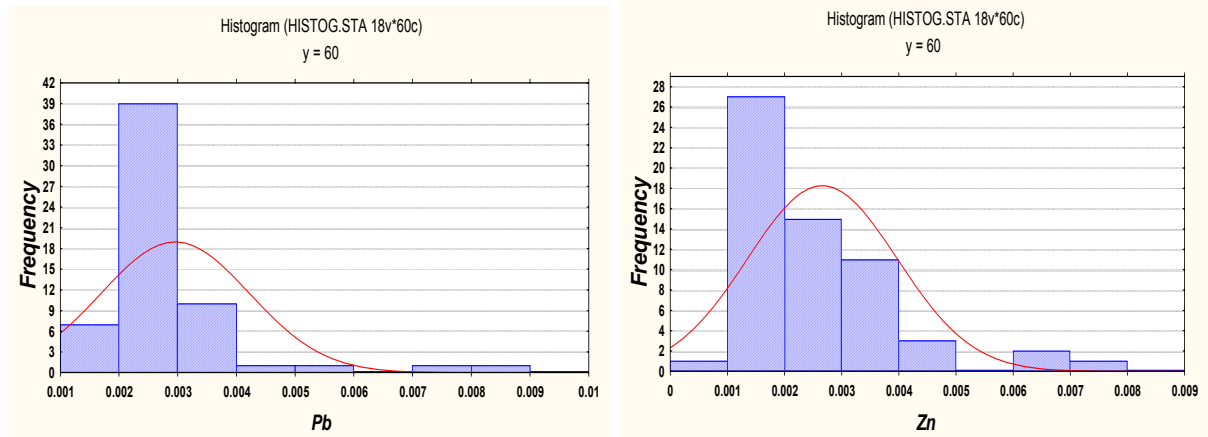


Fig (4.16): Frequency diagrams of Pb and Zn content in limestones of the studied sections.

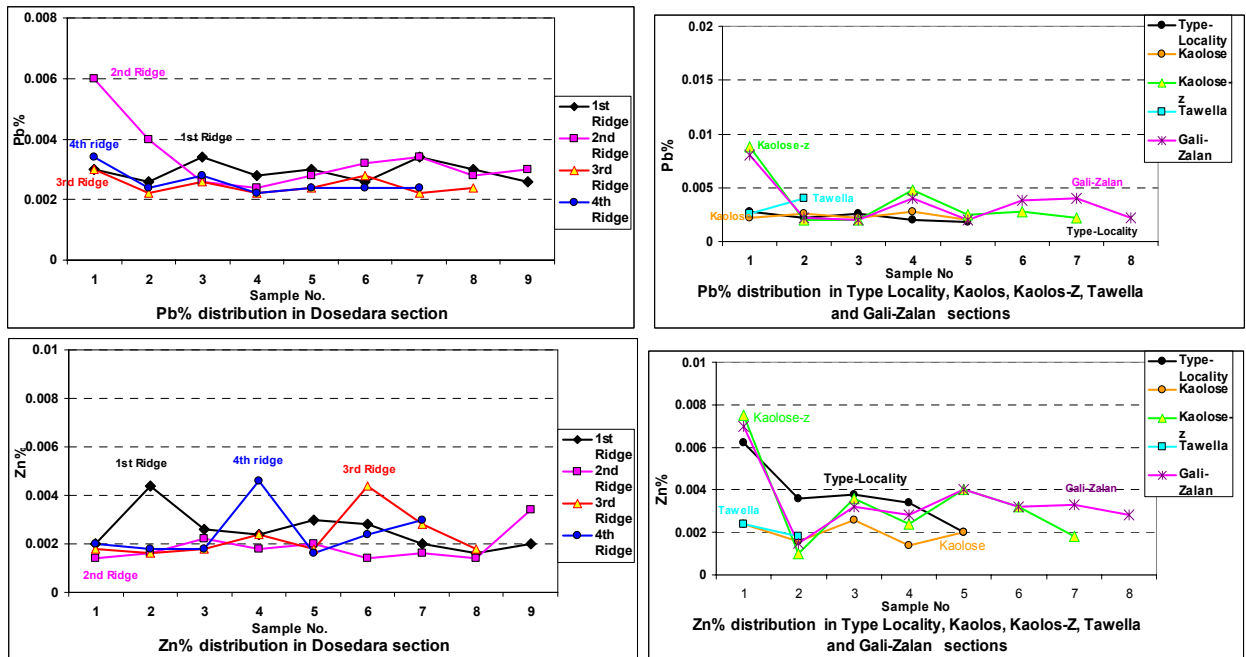


Fig (4.17): Pb and Zn contents show the distribution in all studied sections. (UL) is Pb% in limestone successions; (UR) is Pb% in other sections; (BL) is Zn% in limestone successions and (BR) is Zn% in other sections.

The Pb concentrations in the studied sample ranges between (16 and 88)ppm. The mean Pb contents are (29, 34, 25, and 26)ppm in limestone of the four successions in Dostadara section respectively, and (29, 23, 24, 36, 33 and 35)ppm in Dostadara, Type-Locality, Kaolos, Kaolos-Z, Tawella and Gali sections respectively.

The distribution of Zn in all studied sections was shown in Fig (4.16) is normal due to the enrichment of Zn in one phase which is the non-carbonate fraction of the most of the studied rocks.

Positive relations with SiO_2 , K_2O and Zn are due to the adsorption of these elements in clay layers and negatively relation with CO_2 confirms that.

Zinc

The association of zinc with carbonate rocks is limited and restricted mainly to the non-carbonate constituents (Al-Jawadi, 1978). The geochemical behaviour of zinc in the studied limestone rocks seems similar to that of nickel, cobalt copper and lead.

Kranskopf, (1959) and Stephens *et al.*, (1975) reported the strong association of zinc with the sulphide phase.

Hem, (1977) suggested that the adsorption of zinc by iron hydroxide is very important process that affects zinc immobilization.

The mean zinc content of the samples of Dostadara section 23ppm is more than the mean content of that reported by Haddad, (1980) 10ppm and more than that given by Barnes, (1957). The Zn concentrations in the studied samples are on average range between (10 and 80)ppm. The mean Zn contents are (25.3, 20, 23 and 20)ppm in limestone of the four successions in Dostadara section respectively, and (23, 40, 20, 30, 21 and 35)ppm in Dostadara, Type-Locality, Kaolos, Kaolos-Z, Tawella and Gali sections respectively.

Positive relations with SiO_2 , K_2O , Pb and P_2O_5 are due to the presence of these elements in clay layers and reduced environment.

Chromium

The high charge of Cr^{3+} ion and its small ionic radius (0.59\AA) make it very difficult to substitute for Ca^{2+} and Mg^{2+} in carbonate minerals therefore, the Cr content in carbonate is most probably associated with insoluble residue.

The distribution of Cr shown in Fig (4.18) is normal and bimodal due to the enrichment of Cr in two phases which are the insoluble residue and carbonate fraction. The Cr content in the studied rocks shows a wide variation ranges between (20 and 10)ppm.

The mean Cr contents are (63, 33, 34 and 37)ppm in limestone successions of Dostadara section respectively, and (42, 28, 33, 38, 31 and 35)ppm in Dostadara, Type-Locality, Kaolos, Kaolos-Z, Tawella and Gali-Zalan sections respectively.

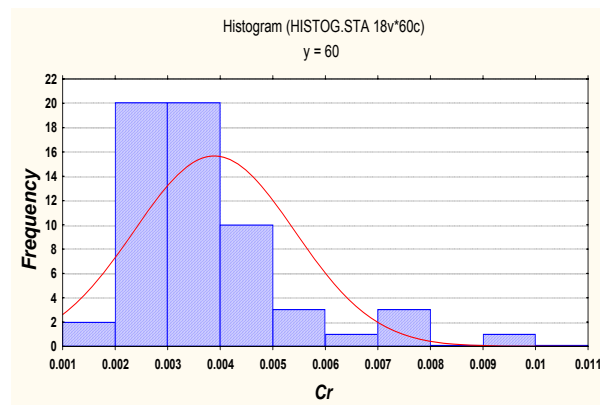


Fig (4.18): Frequency diagrams of Cr content in limestones of the studied sections.

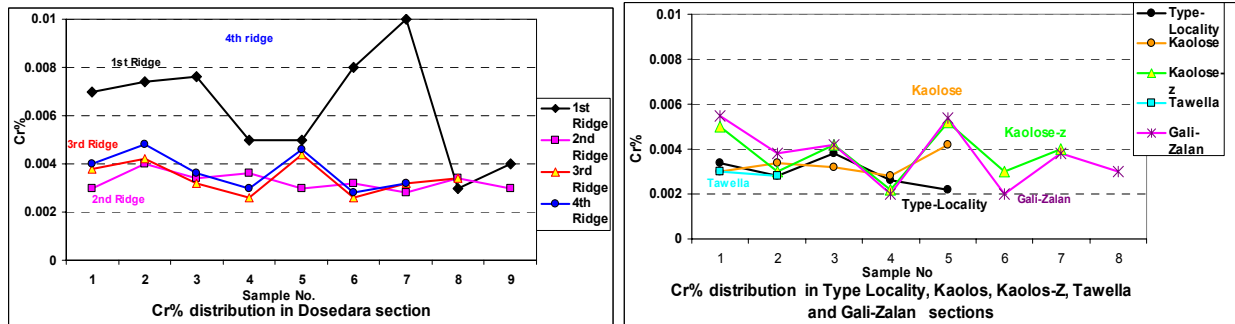


Fig (4.19): Cr contents show the distribution in all studied sections. (L) is Cr% in limestone successions; (R) is Cr% in other sections.

Negative correlations with CaO are due to its adsorption by the clay mineral.

Positive relation with L.O.I indicates that the little Cr content is sometimes could be leached from the clay minerals during the separation of the insoluble residue.

4.6. Statistics and Data Analysis

4.6.1. Preface

Statistical analyses are done for all geochemical analyses to get all useful parameters that related to distribution and mutual relation between the elements. These parameters give more information about the behaviour of the major and trace elements during sedimentation and diagenesis of the mineral components of the limestones in all sections. These analyses give the numerical distribution of different elements and oxides among the limestone successions and sections, to see if the geochemical analyses aid or oppose the result of the lithological and stratigraphical studied of the limestone successions in the chapter two and three. As it is shown, in chapters, two and three, the successions are most possibly have the same origin (originally deposited as one succession) and repeated four times due to faulting (thrusting) and imbrication. For this relation the statistics analyses were used to show

the frequency and cluster analyses, correlation coefficient, coefficient of variation, precision and accuracy, mean, standard deviation and factor analyses.

4.6.2. Precision and Accuracy:-

Determination of accuracy and precision is the most important step in generating high quality data. Without an understanding of these, the data are useless (Kebbekus, *et al*, 1997). The function of the analyses is to obtain a result as near to the true value as possible by the correct application of the analytical procedure employed.

The level of confidence that the analyst may enjoy in his statistical analyse will be very small unless he has knowledge of the accuracy and precision of the method used as well as being aware of the sources of error which may be introduced. The results must then be evaluated to decide on the best value to report (Basset et al, 1979)

Although the final results of the analyses achieved in this work are of considerable accuracy, there are many factors affecting the accuracy of the analyses. The hammering and powdering processes may contaminate the samples by iron. Moreover, sieving process may contaminate the samples by copper, but the overall contamination was of very small effect.

The analytical results obtained are relative determinations against standards, and such determinations may affect the accuracy of the obtained results. The concentrations of the major elements for samples which were analysed by wet chemically were determined relatively against standards...

Precision:-

A precision expresses as a reproducibility of measurement. Precision always accompanies accuracy, but a high degree of precision does not imply accuracy, or it is the agreement between a set of results for the same quantity of an individual and set of samples (Rose et al.1979).

It is defined as the concordance of a series of measurements of the same quantity. The mean deviation or the relative mean deviation is a measure of precision. Stanton, (1966); Maxwell, (1968); Stoody, (1980) defined it as a level of confidence at 63% and the acceptable result ranged between (5-15%). Maxwell (op.cit) assumed the acceptable result of 95% level of confidence from (5-25)%.

This was illustrated by the following formula:-

$$C.V(\text{precision } \%) = \frac{S.D}{X} \times 100 \quad \text{At 63\% level of confidence}$$

$$C.V(\text{precision } \%) = \frac{2S.D}{X} \times 100 \quad \text{at 95\% level of confidence}$$

When:-

CV = Coefficient of Variation

X = Arithmetic Mean calculated by the following formula:-

$$X = \frac{\sum_{i=1}^n xi}{n}$$

When:-

i = Variable

X = Arithmetic Mean

n = Number of Samples

The Standard Deviation (SD) is calculated by the following formula:-

$$S.D = \sqrt{\sum_{i=1}^n \frac{(xi - x)^2}{(n - 1)}}$$

For CaCO₃ results by wet and calcimetry analyses in the samples of Dostadara, Type Locality, Kaolos and Tawella sections, the coefficient of variations has been calculated at 63% and 95% levels of confidence. Table (4-7) shows acceptable coefficient of variations of calcite percent in all samples of the mentioned sections.

Table (4-7):- Standard Deviation and Precision (C.V %) of all samples for CaCO₃ which were analysed by Calcimetry and AAS.

S. No. 1st Ridge	CaCO ₃ % From calcimetry	CaCO ₃ From AAS	S.D CaCO ₃	CV% 63% L.of Conf CaCO ₃	CV% 95% L.of Conf CaCO ₃
5	82.87	78.01	3.44	4.28	8.55
7	73.03	72.96	0.05	0.07	0.13
9	73.6	74.91	0.93	1.25	2.50
11	72.8	74.71	1.35	1.83	3.66
13	71.5	72.56	0.75	1.04	2.09
15	67.4	67.47	0.05	0.07	0.14
17	74.9	79.95	3.57	4.62	9.23
19	74.6	73.31	0.91	1.23	2.46
21	95.7	83.55	8.59	9.59	19.17
2nd Ridge					
1	95.87	81.35	10.27	11.58	23.17
3	88.92	80.98	5.61	6.61	13.21
5	94.54	87.40	5.05	5.55	11.11
7	86.65	82.90	2.65	3.13	6.25
9	93.92	90.39	2.49	2.71	5.41
11	89.15	80.90	5.83	6.86	13.72
13	92.92	90.39	1.79	1.95	3.90
15	89.2	86.40	1.98	2.26	4.52
17	95.79	88.64	5.05	5.48	10.96
3rd Ridge					
1	73.64	77.91	3.02	3.98	7.96
3	75	87.15	8.59	10.59	21.19
5	76.41	78.73	1.64	2.12	4.24
7	73.55	69.99	2.52	3.51	7.02
9	80.79	78.66	1.51	1.89	3.79
11	82.51	75.16	5.20	6.59	13.19
13	72.86	71.76	0.78	1.07	2.14
15	81.73	82.40	0.47	0.58	1.16
4th Ridge					
1	73.18	75.41	1.58	2.12	4.24
3	77	76.41	0.42	0.55	1.09
5	77.41	83.65	4.41	5.48	10.96
7	75.55	78.91	2.37	3.07	6.14
9	82.11	81.15	0.68	0.83	1.66
11	80.54	81.90	0.96	1.19	2.37
13	82.22	80.40	1.28	1.58	3.16
Type Locality					
1	79.17	80.90	1.23	1.53	3.06
3	94.59	85.90	6.15	6.81	13.62
5	94.02	88.89	3.63	3.96	7.93
7	93.7	86.15	5.34	5.94	11.88
9	93.21	89.39	2.70	2.96	5.91
Kolose					
1	71.35	74.16	1.99	2.73	5.46
3	78.44	77.91	0.38	0.48	0.96
5	88.21	85.40	1.99	2.29	4.58
7	77.2	79.90	1.91	2.43	4.87
9	89.53	80.40	6.45	7.60	15.19
Taw					
1	87.67	90.39	1.92	2.16	4.32
5	64.71	72.91	5.80	8.43	16.86

Accuracy:-

Accuracy is the difference between two measurement values and the true value for the quantity which has been determined (Basset *et al.*1979). The accuracy of a

determination may be defined as the concordance between it and the true or most probable value. It is a measure of deviation from the true value (Kebbekus, 1997).

$$RelativeDifference(R.D) = \frac{|C_f - C_s|}{|C_f + C_s|} \times 100, \text{ When:-}$$

C_f = Concentration of 1st analyses of an element or oxide

C_s = Concentration of the true or standard analyses of an element or oxide

Chemical analyses are accepted when the value of Relative difference is (<5%), between (5-10)% is depending on more attentively values (>15) are independent and not accepted for chemical interpretations. The following table is accuracy of Fe₂O₃, MnO, Ni, Zn and Sr content for the limestones of all studied sections. It is clear and acceptable for the most with some errors due to the diagenesis effect which increases the mentioned Fe₂O₃, MnO and decreases Ni contents abnormally.

Table (4-8): Results of analytical accuracy of Fe₂O₃, Mn and Sr contents in limestone of all studied sections.

	Type of rocks or sediment	Fe2O3	Mn	Ni	Zn	Sr	Fe2O3 Accuracy (R.D.)	Mn Accuracy (R.D.)	Ni Accuracy (R.D.)	Zn Accuracy (R.D.)	Sr Accuracy ((R.D.)
Present Work Dosedara	Black Lst	0.4484	116	43.30	22.78	368	1.27	24.92	16.17	4.65	19.09
Present Work Type Locality	Black Lst	0.81	252	22.14	34.7	260	27.84	13.26	46.09	16.26	1.96
Present Work Kaolose	Black Lst	0.71	298	40.8	20	288	21.32	21.38	19.05	11.11	7.06
Present Work Kaolose-7	Black Lst	0.62	342	59.29	33.57	378	15.11	27.85	0.60	14.63	20.38
Present Work Tawella	Black Lst	0.34	296	45.75	27	291	15.27	21.06	13.48	3.85	7.58
Present Work Gali-Zalan	Black Lst	0.50	333	66.67	32	436	3.70	26.62	5.27	12.28	27.11

4.6.3. Cluster and Factor Analyses

Geochemical interpretations and discussions are based completely on cluster and factor analyses as they are most widely used multi-variant statistical methods in recent geochemical studies. Davis, (1973) described cluster analyses as a statistical

method used to place the variables into groups (R-Mode) or the samples (Q-Mode) in a way they have strong interrelations, while factor analyses another statistical method used to find interrelations in a matrix of correlations between variables (R-Mode) or between samples (Q-Mode) (Jamil and Al-Hilaly, 1989).

In this study, both analyses are applied to the geochemical data using program given by Davis, (1973) and using software (STATISTICA) and (SPSS 14) programs.

Cluster Analyses

It is a classification and placing of objects into more or less homogeneous groups, in a manner so that the relation between groups is revealed.

The clusters are groups of observations with similar characteristics. To and from the clusters, the procedure begins with each observation in a separate group. It then combined two observations, which were close to each other, to form a new group. After recomputing the distance between the groups, the two groups when closest together were combined. This process was repeated until only one group remained.

Cluster (R-Mode) analyses are used to conclude contributed geochemical agents to the limestone origin in Qulqula Formation, especially the presence of several geochemical variables due to variability of contributed agents and diagenesis (Ismail, 1996).

The following figure shows the cluster analysis of the 18 geochemical variables for all samples taken from the five sections of the studied area respectively:

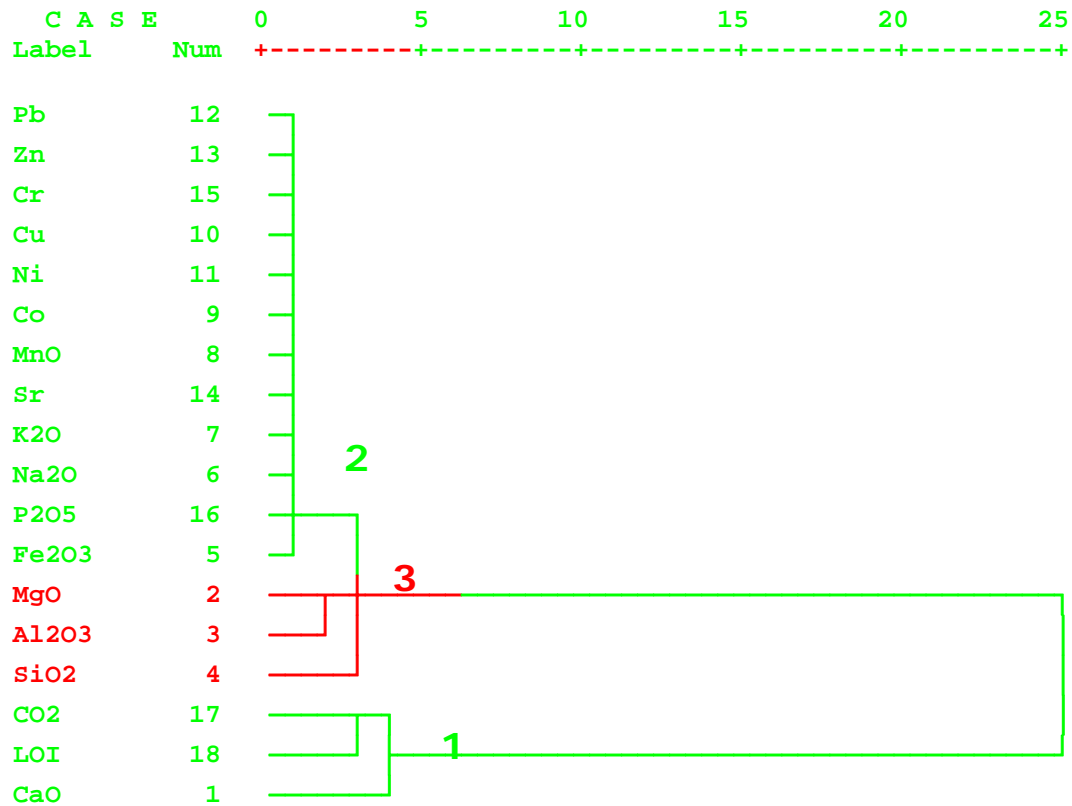
The chemical composition of the limestones in all studied sections were categorized to three major groups when the distance value (4.5) was taken as a minimum linkage distance to measure the strength of correlation between the variables, this was shown in Fig(4.20) as a cluster (R-Mode) diagram :-

* * * * * H I E R A R C H I C A L C L U S T E R A N A L Y S I S *

All Sections (Median Cl, Euclidean dist, cosine)

Dendrogram using Median Method

Rescaled Distance Cluster Combine



Fig(4.20): Cluster Analyses (R-Mode) of geochemical variables of all limestones in the five studied sections.

1st group: Including (CaO, L.O.I and CO₂) indicating high limestone content of these samples.

2nd group: Including (Al₂O₃, SiO₂, MgO) indicating the insoluble residue and its contents of the clay. The Al₂O₃–SiO₂ relation explains the presence of kaolinite under acidic environment.

3rd group: Including (Pb, Zn, Cr, Cu, Ni, Co, MnO, Sr, K₂O, Na₂O, P₂O₅ and Fe₂O₃.) indicating that the only notable relation between them is their low percentages in both clay and carbonate fractions, but the most related ones to the clay portion is Fe₂O₃. and P₂O₅ is also weakly related to this group due to abnormal distribution in the studied limestones.

Q-Mode cluster analyses are used to conclude interrelation between samples to the limestones. Fig (4.21) illustrates the distribution of the samples taken from all sections explaining seven groups of samples:

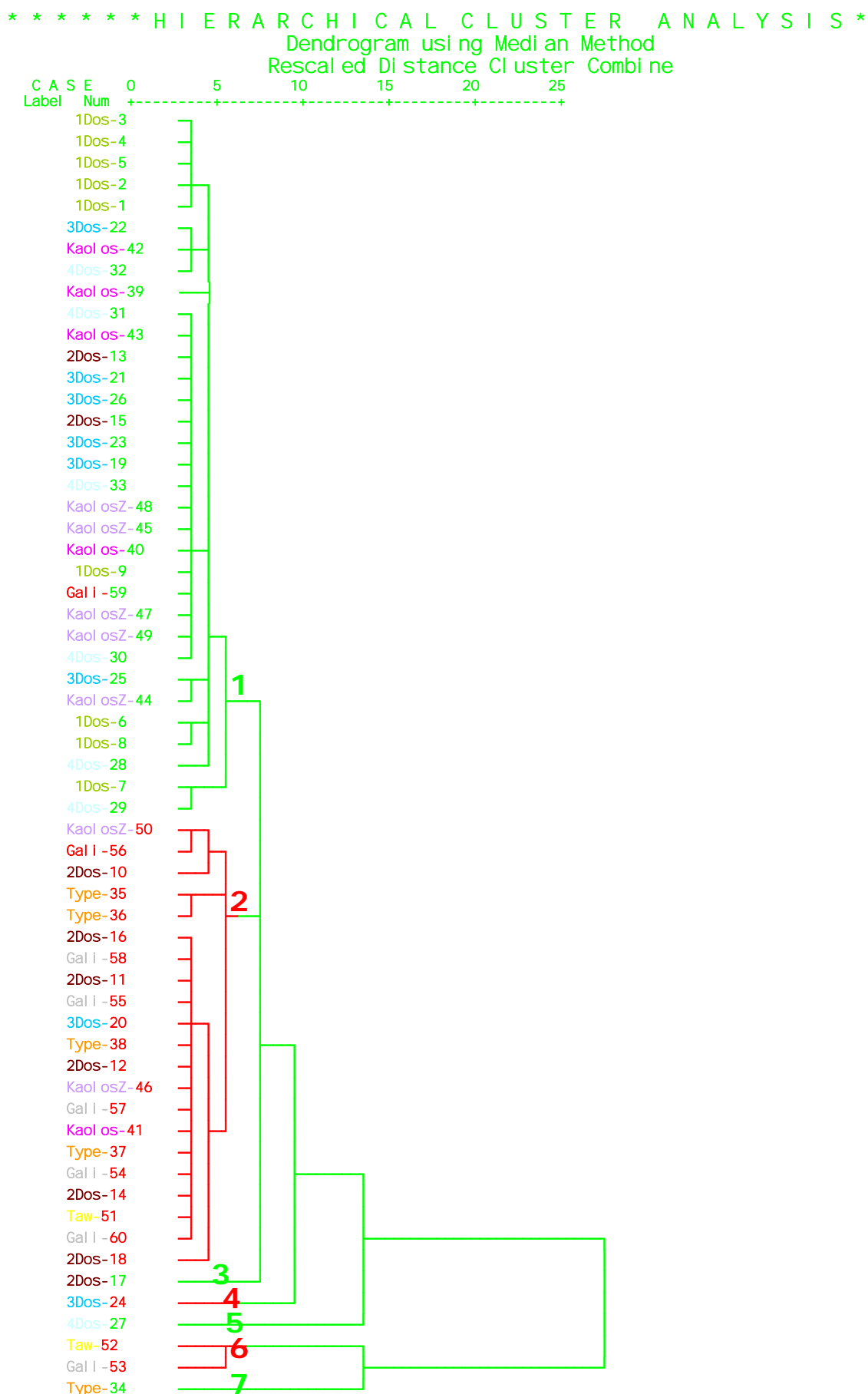


Fig (4.21): Cluster analyses (Q-Mode) of geochemical variables of all Sections.

1st group: Including the most samples of Dostadar (1st, 3rd and 4th Ridges), Kaolos and Kaolos-Z, which are characterized by high MgO, Fe₂O₃ at bottom, K₂O, lower CaO, MnO, medium Sr, Medium to high Cr and higher P₂O₅ on the bottom.

2nd group: Including the most samples of Dostadara (2nd Ridge), Type Locality and Gali section, which are characterized by lower MgO, SiO₂, Fe₂O₃ at bottom, Sr, Cr, very low K₂O, higher CaO, MnO, medium Sr, and higher P₂O₅ on the bottom.

3rd group: Including one sample, 2Dos-17 (2nd Ridge) in Dostadara section which is characterized by high Al₂O₃.

4th group: Including one sample, 3Dos-24 (3rd Ridge) in Dostadara section which is characterized by high Fe₂O₃.

5th group: Including one sample, Dos-27 (4th Ridge) in Dostadara section which is characterized by low MgO and very low Al₂O₃.

6th group: Including two samples, Taw-52 and Gali-1 in Tawella and Gali sections respectively, which are characterized by high silicate limestones.

7th group: Including one sample, Type-34 in Type Locality section, which is characterized by high SiO₂, P₂O₅, Na₂O and very low MgO.

Factor Analyses:-

The purpose of factor analyses is to interpret the structure within the variance – covariance matrix of a multivariate data collection. The technique which it used is extraction of the Eigen values and eigenvectors from the matrix of correlation of covariance. Factor analyses have the ability to reduce a large number of variables and identify a set of dimensions, which can not be easily observed in a large set of variables (Al-Rawi and Shihab, 2003).

The aim of factor analyses (R-Mode) is the study for geochemical variables is to show and evaluate factors explaining the relationship between these variables where there is complex symmetrical relations that cannot be identified (Al-Haza'a, 1996).

Factor analyses divide these complex variables into easily related and identified variables called Assumed Variables or Factor (Babasheikh, 2000). Eighteen geochemical variables for 60 samples of all sections were entered into a computer using software (STATISTICA) and (SPSS-14) programs to evaluate and describe factor analyses.

According to Comery (1973) in Tamish (1988), who suggest the sizes of correlation used in interpretation of factors are as follows:

Loading in excess of (0.71) are considered (Excellent).

From 0.71-0.63 (very good).

From 0.63-0.55 (good),

Form 0.55-0.45 (fair),

Form 0.45-0.32 (poor).

Loadings lower than 0.32 are not suitable for interpretation.

Gathering the data from all localities included in this study revealed seven factors affecting the total number of samples which is 60 samples table (4-9). The significant value (according to the table of Murdoch and Barns (1985) is 0.33.

Factor (1): Affects on 15.09% of the total number of samples and represented by the excellent positive loading of Al_2O_3 and SiO_2 indicating for the kaolinite minerals present in the carbonate rocks which indicated by excellent negative effect of CO_2 , good negative with CaO and poor negative with L.O.I.

Strong negative correlation coefficient between CaO , CO_2 and SiO_2 , Al_2O_3 confirms that, table (4-4).

Factor (2): Affects on 12.61% of the total number of samples and represented by the excellent positive loading of P_2O_5 and Na_2O and the poor negative loading of L.O.I indicating the presence of phosphate grains in the rocks.

Strong correlation coefficient between P_2O_5 negatively with L.O.I. and SiO_2 , positively with Na_2O confirms that.

Factor (3): Affects on 12.54% of the total number of samples and represented by the excellent positive loading of Zn and Pb, fair of SiO_2 and very good of K_2O , indicating the presence of Zn, Pb and K adsorption by the clay with little free quartz.

Strong correlation coefficient positively between Zn and Pb or SiO_2 confirms that.

Table (4.32) Rotated Factor Loading for all Studied Section Samples

Extraction Method: Principal Component Analysis.										SG.V = 0.33 60 samples	
Rotated Component Matrix(a)											
			F 1	F 2	F 3	F 4	F 5	F 6	F 7	Communalities Initial	Extraction
	Al ₂ O ₃		0.858	-0.19	-0.153	-0.13		0.13615		1	0.99
	CO ₂		-0.824	-0.2	-0.285	-0.28	0.136		0.1761	1	0.95
	SiO ₂		0.734	0.25	0.4365	0.179	-0.21	-0.133		1	0.95
	CaO		-0.611		-0.18	0.241	-0.594		-0.252	1	0.95
	Na ₂ O			0.95						1	0.99
	P ₂ O ₅			0.93	0.1921	0.113				1	0.96
	Zn			0.23	0.8316	0.132	0.118			1	0.95
	Pb		0.293		0.7733	-0.27				1	0.97
	K ₂ O			0.21	0.6324	0.292	0.412	0.11323	-0.103	1	0.67
	Cu		0.177	0.25	-0.167	0.774				1	0.95
	MnO				0.2623	0.771	-0.12	0.22385		1	0.92
	MgO		-0.127			-0.29	0.846			1	0.95
	Fe ₂ O ₃				0.2107	0.35	0.674	-0.1799		1	0.99
	Sr			0.11	0.1306			0.88805	0.1699	1	0.99
	Ni			-0.11		0.374	-0.113	0.84585		1	0.95
	Cr		0.117		0.1212	-0.2		0.11023	0.843	1	0.95
	Co		0.195		0.1247	-0.27			-0.681	1	0.95
	LOI		-0.424	-0.38		-0.26	-0.23		0.5294	1	0.98
Total Variance Explained	Factors		1	2	3	4	5	6	7		
	Initial Eigen values	Total	4.08	2.55	2.07	1.88	1.63	1.25	1.04		
		% of Var	22.64	14.18	11.51	10.44	9.03	6.95	5.80		
		Cum %	22.64	36.82	48.34	58.77	67.81	74.76	80.56		
	Rotation Sums of Squared Loadings	Total	2.72	2.27	2.26	2.09	1.87	1.67	1.62		
		% of Var	15.09	12.61	12.54	11.63	10.38	9.30	9.01		
		Cum %	15.09	27.70	40.24	51.87	62.25	71.55	80.56		

Factor (4): Affects on 11.63% of the total number of samples and represented by the excellent positive loading of Cu, MnO and poor of Fe₂O₃ and Ni indicating for recrystallization.

Factor (5): Affects on 10.38% of the total number of samples and represented by the excellent positive loading of MgO, very good of Fe₂O₃, poor of K₂O, and fair negative loading of CaO indicating the Mg-Calcite and diagenesis.

Negative relation between CaO and MgO and positive between Fe₂O₃ and K₂O confirms that.

Factor (6): Affects on 9.3% of the total number of samples and represented by the excellent positive loading of Sr and very good of Ni indicating for the recrystallization process. Positive relation between Sr and Ni confirms that.

Factor (7): Affects on 9% of the total number of samples and represented by the excellent positive loading of Cr and fair of L.O.I with very good negative loading of Co indicating for the Cr enrichment in the insoluble residue.

Positive correlation between Cr and L.O.I confirms that.

Result of the study of geochemistry, sedimentology and stratigraphy as applied on stratigraphic column

From facies and geochemical analysis, it is a certain that the four limestone successions are originally one package, but by thrusting (faulting) or imbrication, and they are now appear as four successions. This can be called tectonic repetition as indicated by curved arrow which has no relation with stratigraphic succession. This tectonic repetition is due to the fact that the studied area is located in the thrust zone. These limestone successions are deposited outside the studied area and transported from the northeast to the present position. Now they can be seen over conglomerate of Tanjero and marl of Shiranish Formations. Fig (4.22 and 4.23).

It is worth to mention the tectonic is not uniform in studied sections as in Kaolos section; the conglomerate of Tanjero Formation is located inside Qulqula Formation, as seen from Fig (4.23). It is possible that the conglomerate of the Tanjero Formation is also repeated by faulting and thrusting, but the lower one at the bottom is not exposed while repeated one indicated in the Fig (4.23).

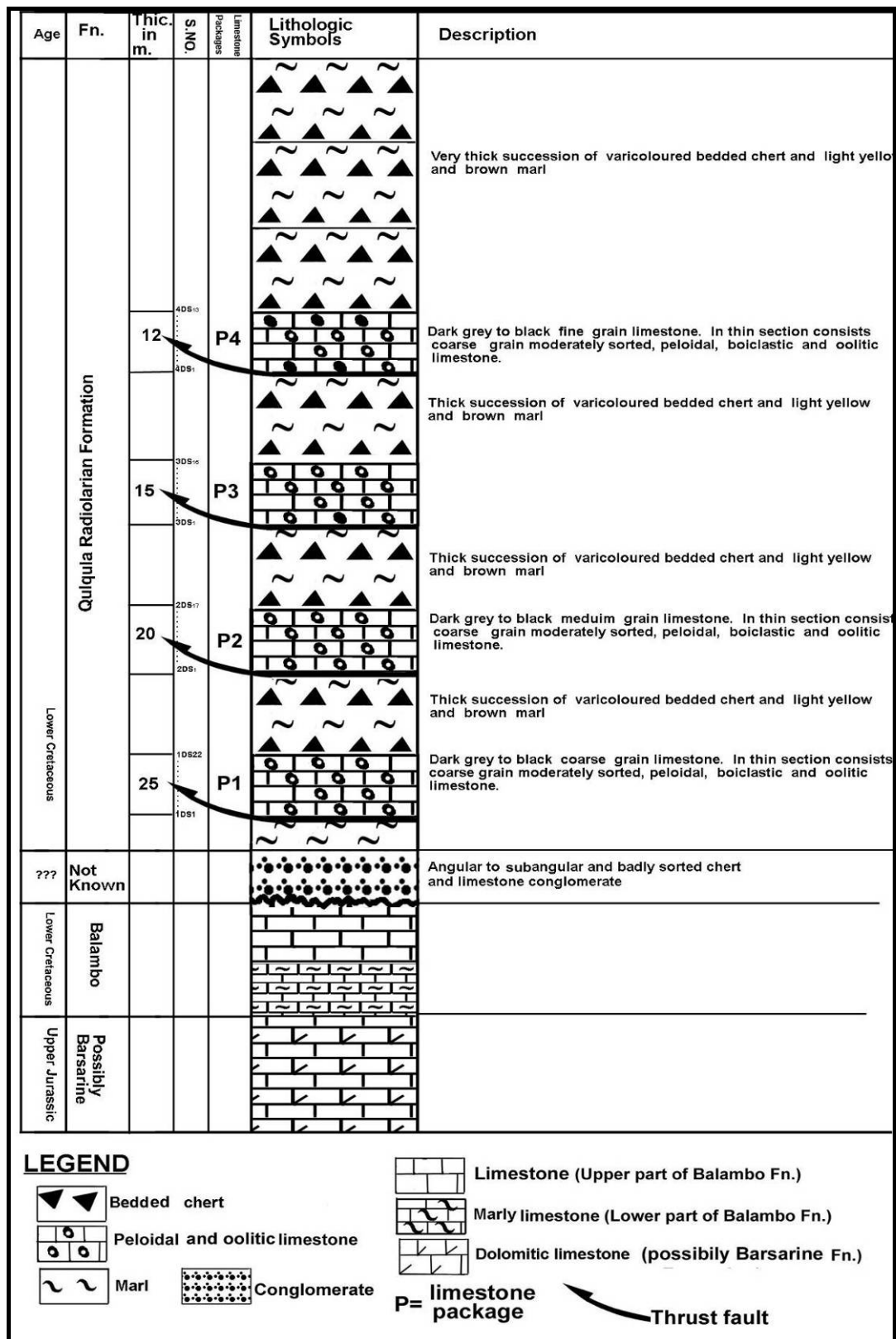


Fig (4.22): Result of the study of geochemistry, sedimentology and stratigraphy as applied on stratigraphic column of the Dostadara and Gali sections which shows that the four successions are derived from one succession due to thrust faulting.

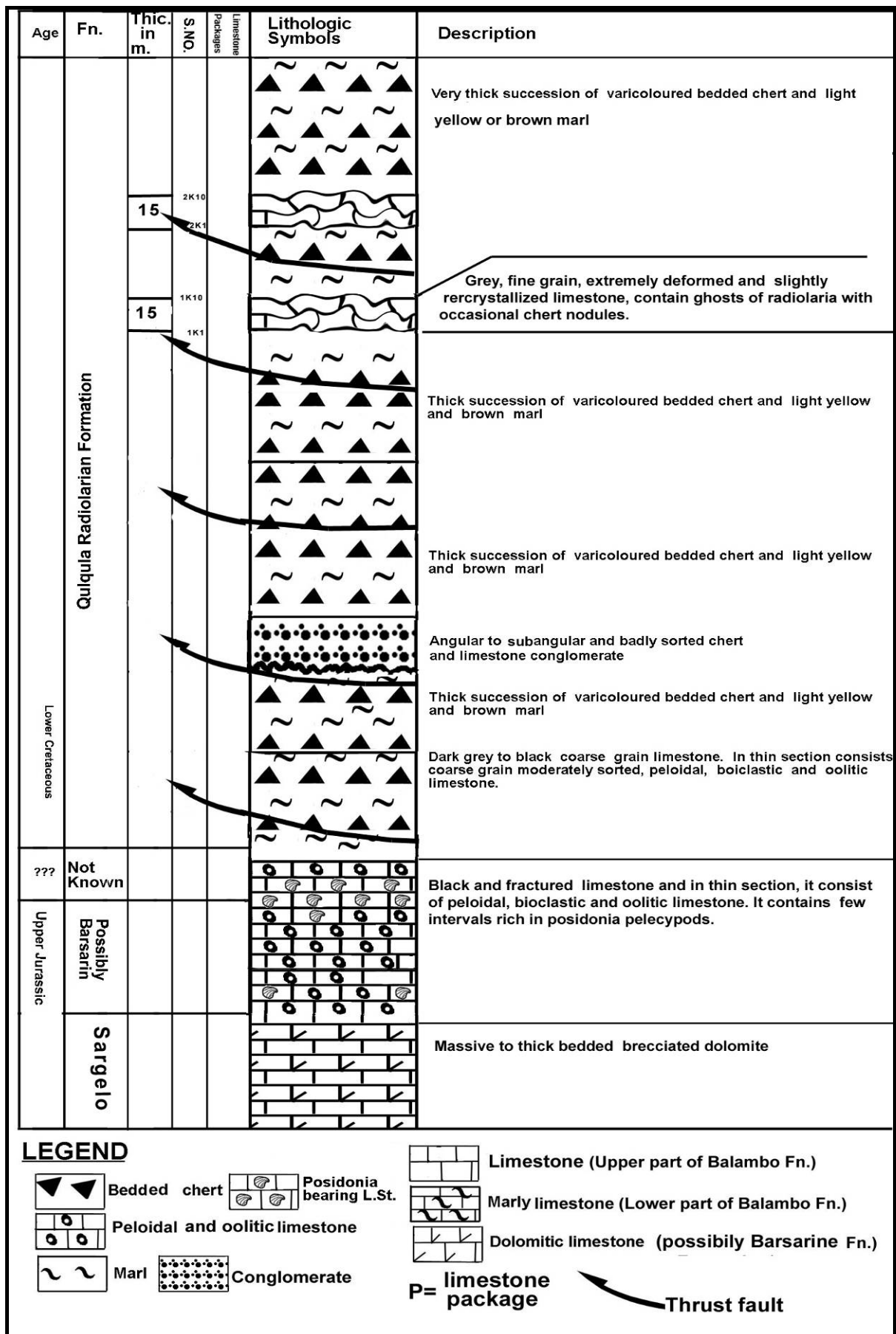


Fig. (4.23) Result of the study of geochemistry, sedimentology and stratigraphy as applied on stratigraphic column of Kaolos section which shows that the two successions are derived from one succession due to thrust faulting.

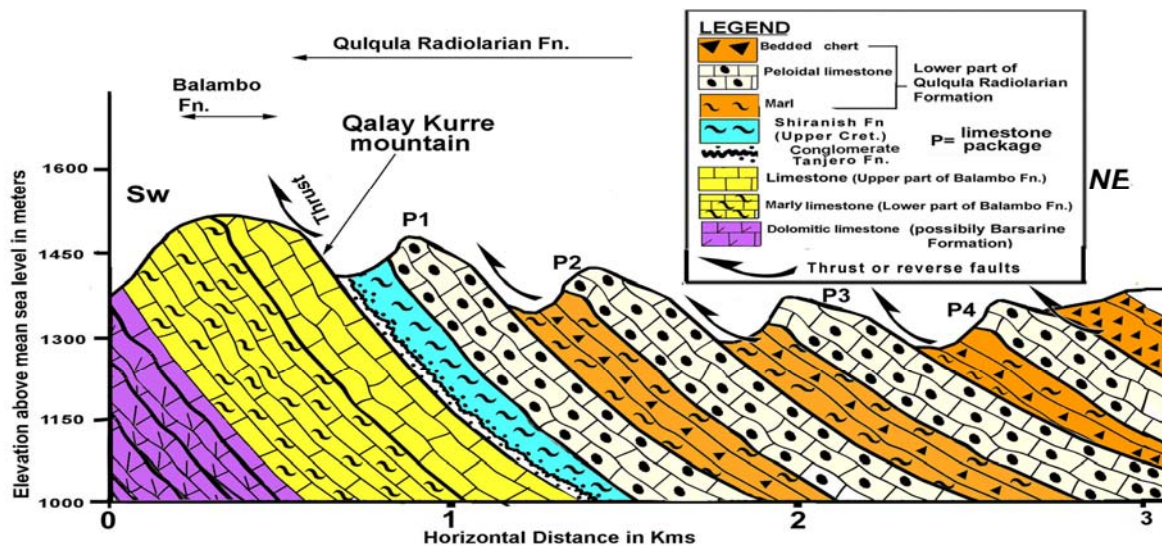


Fig. (4.24) Result of the study of geochemistry, sedimentology and stratigraphy as applied on stratigraphic cross section of the Lower Part of the Qulqula Formation of Dostadara and Gali sections which shows that the four successions are derived from one succession due to thrust or reverse faulting.

The following figures are showing the distribution of the major oxides and minor elements in all sections. Fig (4.25) shows the major and minor constituents of the limestone successions of the Dostadara section, it can be explained as following:

MgO, Na₂O, Sr and K₂O variations are similar to each other in all limestone successions, they are the inverse values of SiO₂ and Al₂O₃. The bottom part in all successions is similar to each other containing high contents of MgO, Na₂O, Sr with relatively low percentages of Fe₂O₃, K₂O, MnO, Co, Ni and Zn. This is clear also in Type-Locality and Gali-Zalan sections, Fig (4.26).

Notable decrease in all major and trace elements can be seen in Type Locality section except that of MgO and MnO which increases toward the upper part of the section, and also Al₂O₃ increases in the upper succession of this section toward the upper part.

In Gali-Zalan section SiO₂, Al₂O₃, MgO and Fe₂O₃ decreases toward the upper part, as well as the trace elements Ni, Sr and P₂O₅ increases.

In Tawella section all of the geochemical constituents are similar except that of CaO which inversely proportional, that is due to the presence of high percentages of silica, Fig (4.26). Major elements are increases toward the upper part generally except K₂O which decreases; Zn, Cr and Ni are also decreases clearly.

In Kaolos section limestones notable decreasing toward the top also can be seen for Fe₂O₃, Na₂O and K₂O, as well as Ni, Sr, P₂O₅ and Mn increases.

Log-Plot of Calcimetry and Chemical Analysis

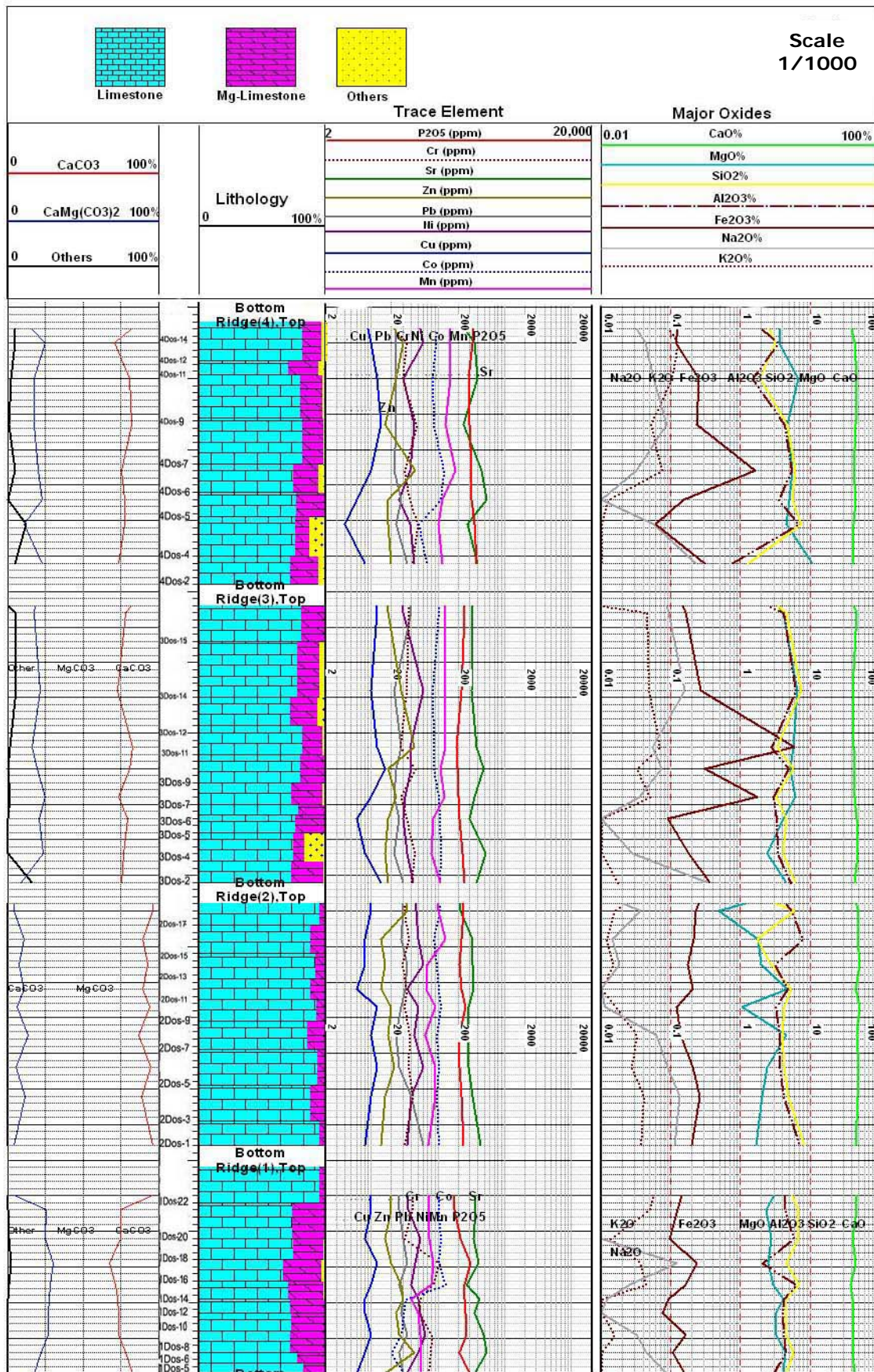


Fig. (4.25) Distribution of the major oxides and miner elements (including traces) of the limestone successions of the Dostadara section.

Log-Plot of Calcimetry and Chemical Analysis

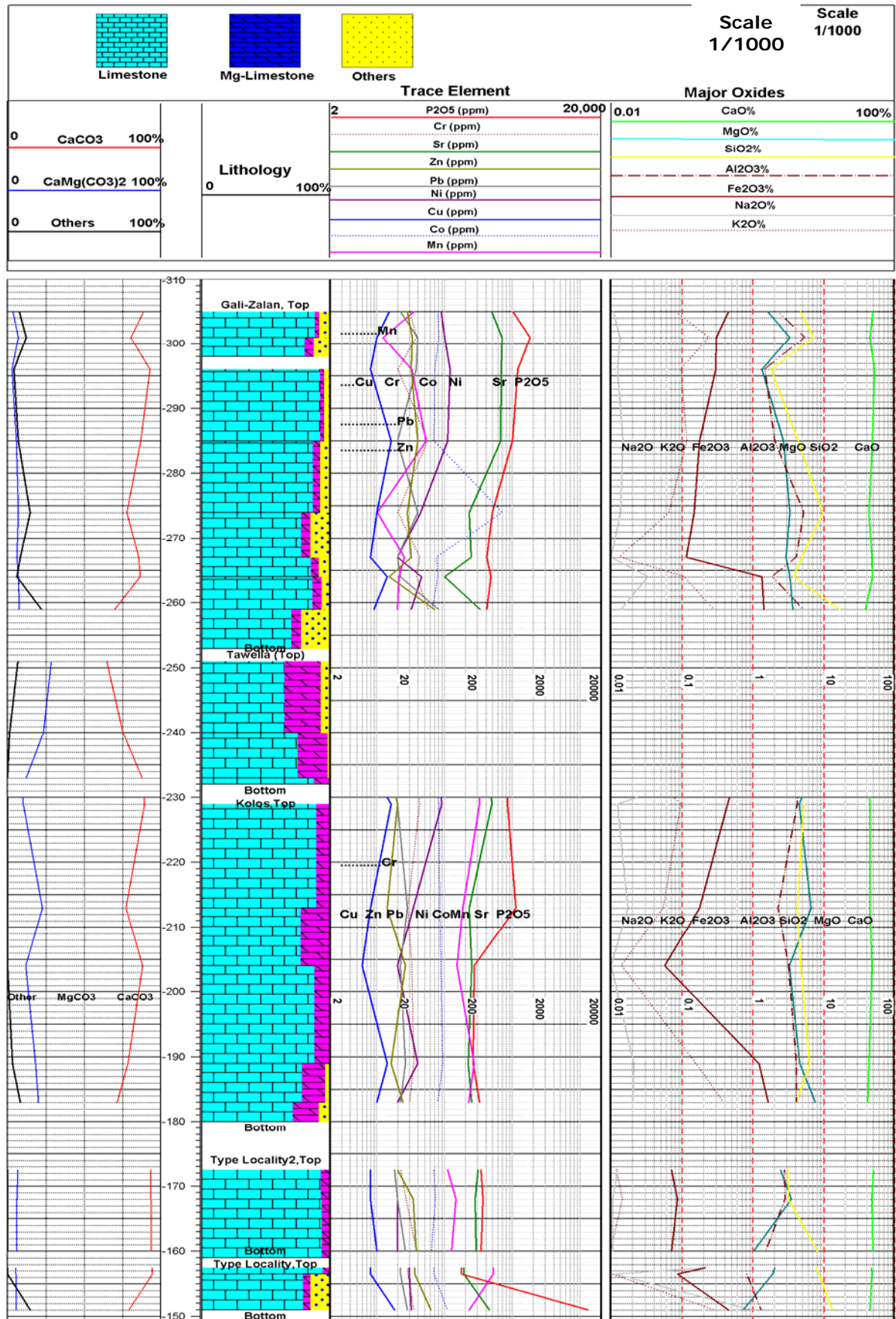


Fig. (4.26) Distribution of the major oxides and miner elements (including traces) of the limestone successions of the Gali, Kaolos Tawella and Type Locality sections (only the digested samples are indicated).

CONCLUSIONS

This research has concluded the followings:

- 1- The Conglomerate bed that is located in the base of Qulqula Formation and in the top of Balambo Formation is aged Late Cretaceous (possibly Early Maastrichtian).
- 2- The Conglomerate is traced for about 30 Km continuously in Said Sadiq and Chuwarta area. There it combines with the conglomerate of the lower part of Tanjero Formation (Early Maastrichtian) near Chuwarta town. Therefore, it belongs to conglomerate of lower part of Tanjero Formation.
- 3-Slice of the Shiranish Formation occurs at the base Qulqula Formation. This is due to thrusting of latter formation over both Tanjero and Shiranish formations in addition to Balambo Formation.
- 4- The Lower part of Qulqula Formation is composed of more than four limestone successions, which have nearly similar lithologies. These lithologies constitute shallow marine limestone which composed of peloid, ooid, lithoclast and bioclast grainstone and packstone with rare mudstone and wackstone.
- 5- Sedimentological study showed that most of the limestone successions have same origin and most of them are not overturned but imbricated over each other.
- 6-All the allochems of the limestone successions are suffered from different degrees of micritization. Therefore, the main constituent, according to their abundance in successions are peloids, lithoclasts, ooids, bioclasts and in addition to some skeleton of algae and Forams.
- 7- All successions have nearly similar facies which includes grainstone and packstone with rare mudstone and wackstone of the above allochems. The cement material consists mostly of blocky cement and minor amount of matrix (lime mud).
- 8-The depositional environment was of high energy shallow platform of ramp setting. The facies analyses indicated that the middle part of the studied area (Koalos, Dostadara and Gali sections) was deposited in the mid-ramp while the type section and Tawella sections are deposited in inner and outer ramp respectively.
- 9-Generally the environment becomes shallower from extreme southeast toward extreme northwest of the studied area. This is also true for the vertical variation which becomes deep toward the top.
- 10-The tectonic setting consisted of extensional basin which is developed during the late phase of the Neo-Tethys opening.
- 11-The chemical analyses and distribution of CaO and MgO suggests that the majority of the limestones of the Lower part of the Qulqula Formation is of the low

Mg-calcite and with some argillaceous limestone type and calcite is the only major carbonate mineral present in these rocks.

12-The analytical result of the trace elements shows that they increase by increasing insoluble residues in the total rock analyses especially (Fe, Cr and Ni) but less affected on Sr due to its low content and diagenesis. So the total analyses of a bulk sample are not useful alone without special insoluble residue analyses or soluble carbonate part.

13-The distribution of MnO in all studied sections show the enrichment of MnO in one phase which indicates its low content in most samples and present both in insoluble residue and the carbonate fraction.

14- The negatively correlation coefficient relations between MgO and CaO conclude that the limestones in most of the sections are low Mg-Calcite. The high P₂O₅ Type Locality and Dostadara (1st Ridge), is due to the presence of apatite mineral which confirmed by MPA.

15-The X-Ray diffractograms for all bulk samples almost show a similar patterns which show clearly calcite as a main constituent mineral and also there was a noticeable variation in the intensity of kaolinite and quartz peaks and those of kaolinite were disappeared when the samples were heated to 550°C. Kaolinite is the only dominant clay mineral in the insoluble residues of the selected samples, It occurs in variable proportions, however kaolinite content is found to increase in Kaolos section and 3rd Ridge (towards the younger beds).

16-The cluster analyses of all limestone beds of all studied sections, which includes 60 samples with 18 geochemical variables explains 3 main groups: Limestone content, clay with I.R. content and trace elements.

17- Factor Analysis from all localities included in this study revealed seven factors affecting the total number of samples which is 60 samples; the main factor is carbonate factor which includes the presence of kaolinite mineral.

22- Another main factor indicating the presence of phosphate grains or apatite in the studied rocks and also there are indications of recrystallization, Mg-Calcite and diagenesis.

References

- Abdul-Hameed F. F. 1980.** Geochemistry, Petrography and Sedimentology of the Dhibban formation, at Sinjar, NW. Iraq (In Arabic). Unpublished MSc thesis, University of Mosul, 216p.
- Aitken, J. D., 1967.** Classification and environmental significance of cryptalgal limestones and dolomites, with illustrations from the Cambrian and Ordovician of Southwestern Alberta. *Jour. Sed. Pet.* Vol. 37, pp.1163-1178.
- Al-Barzinjy, S. T., 2005.** Stratigraphy and Basin analyses of Red Bed Series in NE-Iraq, Kurdistan Region, Unpublished Ph.D. thesis, University of Sulaimani. 167p.
- Al-Gailani, M. B., 1980.** Geochemical identification of Unconformities using semi-quantitative X-Ray Fluorescence analyses, *Journal of Sedimentary Petrology*, Vol.50, No.4, P. (1261-1270).
- Al-Hashimi, W. S., 1976.** Significance of Strontium distribution in some carbonate rocks in the carboniferous of North-umberland, England, *Journal of Sedimentology and petrology*, Vol.46, No.2, PP(369-376).
- Al-Haza'a, S. H. F., 1996.** Sedimentological and Geochemical studies of Zahra formation (Pliocene-Pleistocene) in the western and southern desert of Iraq. Unpublished MSc thesis, University of Baghdad. 108P.
- Al-Jawadi, A. F., 1978.** Mineralogical, Petrographical and Geochemical studies on Pila Spi formation from Northern Iraq, Unpublished MSc thesis, University of Mosul, 157P.
- Al-Jubouri, Z. A. and Al-Kawaz, H. A., 2005.** The Effect of Submergence on the Distribution of some Trace Element within the Recent Sediments at Mosul Lake.
- Al-Jubouri, Z. A., 1972.** Geochemistry, Origin and Diagenesis of some Triassic Gypsum deposits and associate sediments in the East-Midlands. Thesis presented for the degree of Ph.D., University of Nottingham.
- Al-Kufaishi, F. A. M., and Al-Rubaie, N. M. Z., 1986.** Petrography and Geochemistry of Jaddala formation in selected sections Northern Iraq. *Journal of the Geological Society of Iraq*, Vol.19, No.2, (7IGC).
- Al-Kufaishi, F. A. M., 1977.** A Geochemical Study on Sinjar limestone in a subsurface section (K-116). *Journal of the GSI*, Vol.X, pp (47-52).
- Al-Marsumi, A. H., 1980.** Geochemistry and Petrology of Lower Fars Evaporites in selected sections-NE Iraq (In Arabic) Unpublished MSc thesis, University of Baghdad, 172P.

Al-Rawi, S. M. and Al-Shihab, A. S., 2003. Application of Factor Analysis as a tool for Water Quality Management of Tigris River, within Mosul City. Jour. Sci. Vol. 10, No. 1, Geolo. Special Issue, pp. 56-64.

Al-Rawi, A. B. M., 1988. Petrology and Sedimentary Facies of Eocene Carbonate-Phosphatic Sequence (Damlouk member), Akashat Area Western-Desert, Iraq (in Arabic). Unpub. M. Sc. Thesis, Salahadeen Univ., p.147.

Al-Rubaie, N. M. Z. A., 1985. Geochemistry and Petrography of Jaddala formation in selected sections. Unpub. M. Sc. Thesis, Baghdad Univ.

Al-Sadooni, F. N., 1978. Sedimentology and Petroleum Prospects of Qumchuqa Group-Northern Iraq. Unpublished PhD thesis, University of Bristol, 325P.

Al-Ubaidi, S. S. H., 1984. Geochemistry, Mineralogy and Petrography of the argillaceous-carbonate rocks of the Lower Fars Formation at Butmah west area. Unpublished MSc thesis, University of Mosul.

Ali, S. S. and Ameen, D. A., 2005. Geological and hydrogeological study of the Zalim Spring, Sharazoor, and Sulaimaniya, Iraq. Iraqi Journal of Earth Science, V.5, No.1, pp.45-57.

Allen, A. P. and Allen, R. J., 1990. Basin Analyses Principles and Applications, Blackwell, 451p.

Ameen, B. M., 2008. Lithostratigraphy and Sedimentology of Qamchuqa Formation from Kurdistan Region, NE-Iraq. Unpublished Ph D. Thesis. University Of Sulaimani, 147p.

Ameen, M. A., 1979. Geochemistry and Mineralogy of Namurian sediments in the Pennine Basin, England. Unpublished Ph.D. thesis. University of Sheffield.

Asiedu, D. K., Suzuki, S., Nogami, K. and Shibata, T., 2000. Geochemistry of Lower-Cretaceous Sediments, Inner Zone of South West Japan, Constraints on Provenance and Tectonic Environment, Geochemical Jour., Vol. 34, pp. 155-173.

Aswad, K.J., 1999. Arc-continental collision in Northern Iraq as evidenced by the Mawat and Penjween Ophiolite Complexes. Raf. Jour. Sci. Vol.10, No.1, pp.51-61.

Babashekh, S. M. R., 2000. Hydrogeochemistry of Caves and Springs in Sangaw-Chamchamal area, Sulaimaniyah Governorate, NE-Iraq. Unpublished MSc thesis, University of Sulaimani, p.140

Basset, J., Denney, R. C., Jeffery, G. H. and Mendham, T., 1979. Vogel's Textbook of Quantitative Inorganic Analysis, 4th Edition. London. Longman. 925p.

- Barnes, R. L. and Jackson, J. A., 1980.** (eds.), *Glossary of Geology*, Second Edition, American Geological Institute, Falls Church, Vergina, 785 p.
- Bates, R. L. and Jackson, J. A., 1980.** (eds.), *Glossary of Geology*, Second Edition, American Geological Institute, Falls Church, Vergina, 785 p.
- Baush, W. M., 1968.** Outlines of distribution of Strontium in Marino limestone in Muller G. and Friedman G. M., (eds). Recent development in Carbonate Sedimentology in Central Europe. Springer Verlager, Berlin, pp. 106-115.
- Baziany, M. M. Q., 2006.** Sedimentology and stratigraphy of Qulqula Conglomerate Formation, Kurdistan region, NE-Iraq. Unpublished M. Sc. thesis, University of Sulaimani, 103.
- Baziany, M. M. and Karim, H.K., 2007.** A new concept for the origin of accumulated conglomerate, previously known as Qulqula Conglomerate Formation at Avroman-Halabja Area, NE-Iraq. Iraqi Bulletin of Geology and Mining, Vo.3, No.2., p. 33-41.
- Ben Ismail, M.H., and Mrabet, A., 1990.** Evaporite carbonate, and siliclastic transitions in the Jurassic sequences of southern Tunisia, *Sedimentary Geology* b , Vol.66, P.65-82.
- Bellen, R. C. Van, Dunnington, H. V., Wetzel, R. and Morton, D., 1959 .** Lexique Stratigraphique, International. Asie, Iraq, vol. 3c. 10a, 333 p.
- Blatt, H., Middleton, G., Murray, R., 1972.** Origin of Sedimentary Rocks; Prentice-Hall Inc., Englewood Cliffs, New Jersey. 634 P.
- Blatt, H., Middleton, G., Murray, R., 1980.** Origin of Sedimentary Rocks; Second Edition, Prentice-Hall Inc., Englewood Cliffs, New Jersey. 752 P.
- Blocker, A. B., Callendat, E. and Josephson, P. D., 1975.** Trace element and organic carbon content of surface sediment from Grand Travers Bay, Lake Michigan. *Geol. Soc. Am. Bull*, Vol. 86, pp. 1358-1362.
- Blomeier, D. G. and Reijmer. J. G., 1999.** drowning of the Lower Jurassic carbonate Platform: Jebel Bou Dahar, High Atlas, Morocco. *Facies*, Vol.40, pp.81-110.
- Bolton, C. M. G., 1955b.** Report on the geology and economic prospect of the Qala Dizah area Site Inv. Co. Report, SOM Library. No. 269, Baghdad.
- Bolton, C.M.G., 1958.** The Geology of Ranyia area. Site Inv Co. Unpubl. Report, SOM Library, Baghdad.
- Borch, V. C., 1965.** The distribution and preliminary geochemistry of modern carbonate sediments of the Coorong area, South Australia, *Geochim. Cosmochim. Acta.*, Vol.29, p p781-799.

- Buday, T. C., 1980.** Regional Geology of Iraq: vol. 1, Stratigraphy, I.I.M Kassab and S. Z. Jassim (Eds) D. G. Geol. Surv. Min. Invest. Publ. 445p.
- Buday, T. and Jassim, S. Z., 1987.** The Regional geology of Iraq: Tectonics' Magmatism and Metamorphism. I. I. Kassab and M.J. Abbas (Eds), Baghdad, 445 p.
- Cecil, C.B., 2004.** Eolian dust and the origin of sedimentary chert. Open-File Report, No.1089, USA Geological survey.11p.
- Chillinger, G. V., 1963.** Ca/Mg and Sr/Ca ratio of calcareous sediments as a function of Depth and Distance from Shore. Jour. Sed. Petrology. Vol. 33, pp236-237.
- Comery, A. L., (1973),** A first course in factor analysis, New York, Academic Press.
- Danner, W. R., 1985.** Origin of Bedded Radilarian Chert. Geol. Soc. Am., Abstr. Programs; Vol/Issue: 17; 98. annual meeting of the Geological Society of America; 28 Oct (1985); Orlando, FL, USA.
- Dapples, E. C., 1967.** Diagenesis of sandstone, in Larsen, G. and chilingier G. V. eds., Diagenesis in Sediments; Amsterdam, elsevier, 524p.
- Davies, J. C., 1973.** Statistica and Data analysis in Geology. John Wiley and Sons, Inc.New york.
- Davies, P. J., 1972.** Trace element distribution in reef and sub reef rocks of Jurassic age in Britain and Switzerland. Jour. Sed. Petrology. Vol. 39, pp183-194.
- De Boer, P. L., 1991.** Astronomical cycle reflected in sediment. *Zbl. Geol. Teil.* H.8, pp.911-930.
- Degens, E. T., 1965.** Geochemistry of Sediments. *A brief survey.* Prentice-Hall, Inc. Englewood Cliffs, N.J., 342p.
- Deurer, R., Forstnor, U., Schmoll, G., 1978.** Selective chemical extraction of carbonate-associated metals from recent lacustrine sediments. *Geochim. Cosmochim. Acta.*, Vol.42, p p.425–427.
- Dever, J. I., 1971.** Early diagenesis of clay minerals, *Rio American Basin, Maxico*, *jour. Sed. Petrol.*, Vol.41, pp 982-994.
- Doyle, P. and Bennett, M. R., 1998.** Interpreting paleoenvironments from fossils, in; *Unlocking the Stratigraphical Record (Advance in Modern Stratigraphy).* John Wiley and Sons, New york.
- Dunham, R. J., 1962.** Classification of carbonate rocks according to depositional texture: in Ham, W. E. (ed.), *Classification of rocks: a symposium*, A. A. P.G, no. 1, pp. 108-121.
- Dunnington, H. V., 1958 .** Generation, Migration and Dissipation of Oil in Northern Iraq. Arabian Gulf, Geology and Productivity. AAPG, Foreign Reprint Series No. 2.

- Dunoyer De Segozac, G., 1970.** The transformation of clay mineral during diagenesis and low grade metamorphism., *Sedimentology*, vol.15, p.282- 348.
- Einsele, G., 2000.** *Sedimentary Basin, Evolution, Facies and Sediment Budget.* Springer-Verlag Berlin,790 p.
- Embry A.F and Klovan J.E., 1971.** A late Devonian reef tract on north-eastern Banks Island ,N.W.T.: *Bulletin of Canadian Petroleum Geology*,V,19.P.730 -781.
- Feldmann, M, and McKenzie, J. A., 1998.** Stromatolite-Thrombolite associations in a modern environment, Lee Stocking Island, Bahamas. *Palaios*: April (1998):V13:No.2, pp.201 -212.SEPM, Society for Sedimentary Geology.
- Flugel E., 1982.** *Microfacies analyses of limestones*, Springer Verlag, Berline, 633 p.
- Folk , R. L. , 1974.** *Petrology of Sedimentary Rocks.* Hemhill Pub. Co. Texas, 182p.
- Fujnuki , T., 1970.** Study on the minor elements in Ryukyu limestone from Kikaijima Island, Kagoshima Prefecture, Japan-Bull, *Geol. Surv. Japan*, Vol. 21, No.5, pp. 27-40.
- Fyfe, W. S. and Bishoff, T. L., 1965.** The calcite-aragonite problem. Dolomitization and limestone diagenesis. A symposium Soc. Econ. Paleontologists, Mineralogists, Spec. Publ. vol. 13, pp. 3-13.
- Gale, A. S., 1995.** Cyclostratigraphy and correlation of the Cenomanian Stage in Western Europe. In: House, M. R. and Gale , A. S. (ed) *Orbital forcing time scales and cyclostratigraphy . AAPG special publication No. 85*, pp177-197.
- Glennie, K. W., 1970.** *Desert Sedimentary Environments.* Amsterdam, Elsvevier, 222p.
- Goldsmith, J. R., 1959.** Some aspect in geochemistry of carbonates. In a research in geochemistry. Abelson, p.t., John Wiley and Sons. Inc. Publ. New York. Vol.1, pp. 336-358...
- Goldschmidt, V. M., 1962.** *Geochemistry*, 3rd ed., Oxford art the Clareudon press., London. pp.730.
- Graf, D. L., 1960.** *Geochemistry of carbonate sediments and sedimentary carbonate*, 1-4 Illinois state Geol. Survey. Circ., Vol.297, p. 250.
- Graf, D. L., 1962.** Minor element distribution in sedimentary carbonate rocks, *Geochim. Cosmechim. Acta*, Vol.26, PP(849-856).
- Grotzinger J. P., Watters W. A., and Knoll A. H., 2000.** Calcified metazones thrombolite- stromatolite reefs of the terminal Proterozoic Nama Group, Namibia.*Paleobiology* ,Vo.26, No. 3 , pp.334-359.

- Haddad, S. N., 1980.** Geochemical and Mineralogical Study of selected sections of the Shiranish formation from Northern Iraq. Unpublished MSc thesis, University of Mosul, 157P.
- Haq, B. U., 1991.** Sequence stratigraphy, sea level change and significance for deep sea. spec. publs. int. ass. sediment, 12. p. 12-39.
- Hawkes, H. E. and Webb, H. K., 1962.** Geochemistry in Mineral Exploratin, 1st Edition. Harper and Row, Geosci. Series, New York, 425p.
- Hem, J. D., 1977.** Reaction of metal ions at surfaces of hydrous iron oxide. Geochem. et cosmochim. Acta. Vol. 41. PP.527-538.
- Heron, A. M. and Less, G. m., 1943.** The Zone of Nappes in Iraqi Kurdistan. Min. of Development. Unpubl. Report. SOM Library, No. 133.
- Hirst, D. M., 1962.** The Geochemistry of modren sediments from the Gulf of Paria-I. the relationship between mineralogy and the Distribution of major elements. Geochem. et cosmochim. Acta. Vol. 26. PP.309-334.
- Holland, C. H., 1998.** Chronostratigraphy (Global standard Stratigraphy): A personal Perspective, in: Unlocking the Stratigraphical Record (Advance in Modern Stratigraphy). John Wily & Sons, New York, Toronto.
- Hori, R.S; Cho, C; and Umeda, H., 1993.** Origin of cyclicity in Triassic-Jurassic radiolarian bedded cherts of the Mino accretionary complex from Japan, The Island Arc.
- Ingerson, E. 1962 ,** Problems of Geochemistry of Sedimentary carbonate rocks. Geochem., Chosmochim, ACTA, Vol.26, P(815-11)
- Ismail, S. A., 1996 ,** Mineralogy and Geochemistry of the clastic rocks in Amig Formation, Western Iraq. Unpublished Ph.D. thesis, University of Bghdadi.
- Jamil, A. K. and Hilaly, M. A., 1989.** Cluster and Factor Analysis of geochemical data of Najmah formation, Upper-Jurassic Western Desert-Iraq. Jour. Geol. Surv. And Minning(GEOSURV).
- Jassim, S. Z., Karim, S. A., Basi, M. A., Al-Mubarak, M. A. and Munir, J., 1984.** Final report on the regional geological survey of Iraq. Vol.3, Stratigraphy, GEOSURV, Baghdad, Lib, Unpub.Rep.No.1447. 498p.
- Jassim, S. Z. and Goff, J. C., 2006.** *Geology of Iraq*. Published by Dolin, Prague and Moravian Museum, Berno. 341p.
- Johnson, J. and Grotzinger, J. P., 2006.** Affect of Sedimentation on Stromatolite Reef Growth and Morphology, Ediacaran Omkyk Member (Nama Group), Namibia.

South African Journal of Geology; *June 2006; v. 109; No. 1-2; p. 87-96; Geological Society of South Africa (SAJG).*

Jovanovic, O. and Gabre, R., 1979. Results of sedimentological examination of specimens from the area of Kaolos Dam project–Iraq. GEOZAVOD, Belgrade. 120p.

Karim, S. A., 1975. Biostratigraphy of the Red Bed Series, Chuarta, NE-Iraq. *Jour. Geol. Soc. Iraq, special issue*, pp.147-156.

Karim, K.H., 2003. A conglomerate bed as a possible lower boundary of Qulqula Formation, from Chuarta-Said Sadiq area, NE Iraq. Kurdistan Academician Journal (KAJ), Vol.2.Part A.

Karim, K. H., 2004. Basin analyses of Tanjero Formation in Sulaimaniya area, NE-Iraq. Unpublished Ph.D. thesis, University of Sulaimani University, 135p

Karim, K.H., 2005. Some sedimentary and structural evidences of a possible graben in Mawat – Chuarta area, NE Iraq. *Iraqi Jour. Earth Science*, Vol.5, No.2, pp.9-18.

Karim, K.H. and Surdasy, A.M., 2005a. Paleocurrent analyses of Upper Cretaceous Foreland basin: a case study for Tanjero Formation, NE Iraq, *Jour. Iraqi Science*, Vol.5, No.1, pp.30-44.

Karim, K.H. and Surdasy, A.M., 2005b. Tectonic and depositional history of Upper Cretaceous Tanjero Formation, NE Iraq. *JZS (Journal Sulaimaniya University)*, Vol.8, No.1, p.47-62. .

Karim, K.H. and Surdasy, A.M., 2006. Sequence stratigraphy of Tanjero Formation, Sulaimanyia area, NE Iraq, *JAK*, Vol.4, No.1, pp.19–43.

Karim, K.H. and Baziany, M. M., 2007. Relationship between Qulqula Conglomerate Formation and Red Bed Series, at Qulqula area, NE Iraq. *Iraqi Jour. Earth Sciences*, Vol.7, No.1, pp.1-12.

Karim, K. H., Koyi, H. Qaradakh, A. I. and Fatah, A. I. 2007. Historical development of the present day lineaments of western Zagros Fold-Thrust Belt of Northeastern Iraq. *Iraqi Geological Journal* , Vol.40, No.1.

Kas-Yonan, S. A. H., 1989. Mineralogical, Geochemistry and properties, study of Palygorskite mineral and associated rocks and clays of Safra member-Late Maastrichtian in Ga'ara-Akashat are. Unpublished MSc thesis, University of Mosul. 167P.

Kebbekus, B. B., Metra, S. and Newark, N. J., 1997. Environmental Chemical Analysis. 330p.

Keith, M. L. and Degens, E. T., 1959. Geochemical indicators of marine and fresh-water sediments. In; *Research in Geochemistry*. pp. 38-61.

- Kenter, J. A. M., Harris, P.M. and Della Porta G., 2005.** Steep microbial boundstone-dominated platform margins – examples and implications. *Sedimentary Geology*, 178: 5-30.
- Kinsman, D. J. J., 1969.** Interpretation of Sr^{2+} concentration in carbonate minerals and rocks. *Jour. Sed. Petrology*. Vol. 39, pp. 606-609.
- Koyee, A. M. A., 2006.** Petrochemistry and Petrogenesis and Dating Analyses of Wallash Volcanics in Mawat -Chwarta area, NE-Iraq (In Arabic). Unpublished MSc thesis, University of Mosul, 100P.
- Krauskopf, K. B., 1959.** Sedimentary depositon of rare metals. *Economic Geol.* 50th Anniversary, pp. 411-463.
- Krauskopf, K. B. and Bird, D. K., 1995.** Introduction to Geochemistry. Mc Graw-Hill, New York. 650p.
- Kulp, J. L., Turekian, K. and Boyd, D. W., 1962.** Strontium content of limestones and fossils. *Bull. Geol. Soc. Am*, Vol.63, pp. 701-716.
- Lamar, J. E., and Thompson, K. B., 1956.** Sampling limestone and dolomite deposits for trace and minor elements. *Illinois State,. Geol. Surv. Cir.*, 221 p.18.
- Lehermann, D. J., Wei, J. and Enos, P., 1998.** Control of facies architecture of a large Triassic carbonate platform: The Great Bank of Guizhou, Nanpanjiang basin, south China, *Journal of Sedimentary Research*, Vol. 68, No. 2,pp. 311–326.
- Le Riche, H. H., 1959.** The distribution of certain trace elements in the Lower Lias of Southern England. *Geochim. et. Cosmochim. Acta.*, Vol.16, p p. 101-122.
- Lu, H., Matsumoto, R. and Watanabe, Y., 2000.** Major element geochemistry of the sediments from Site 997, Black ridge, Western Atlantic. *Proceeding of the Oclanic Drilling Programs, Scientific Results*, Vol. 164, p.147-b 149.
- Mc Bide, E., 1974.** Significant of colour in red, green, purple, olive, brown and grey beds of Defeuta Group, North-eastern Maxico. *Jour. Sed. Petrology*. Vol. 44, pp. 760-773.
- Mason, B., 1966.** Principles of Geochemistry. John Wiley and Sons. Inc. 3rd Edition, 330p.
- Maxwell J. A., 1968.** Rock and Mineral analysis, John Wiley and Sons., Inc. New York. 384p.
- Moglrabi, A., 1968.** A Trace element in carbonate of Foraker formation (Lower Permian) in North Central Oklahoma. *Oklahoma Geology Notes*, Vol.28, pp. 14-31.
- Murdoch, J. and Barnes, J. A., 1985.** Statistical Tables, Science, Engineering, Management and Business Studies. 2nd Edition, Cranfield Institute of Technology.

- Nicholls, G. D. and Loring, D. H., 1962.** The Geochemistry of some British carboniferous sediments. *Geochim. et. Cosmochim. Acta.*, Vol.26, p p. 181-223.
- Numan, N. M. S., 1997.** A plate tectonic scenario for the Phanerozoic Succession in Iraq. *Iraqi, Geol. Jour.* Vol.30, No. 2, p 85–110.
- Nichols, G. 1999.** Sedimentology and Stratigraphy, Blackwell Science. 354p.
- Nunna, R. R., Karim, M. K. and Hamza, R., 1981.** Geological study of the Kaolos Dam project. ZANKO (Scientific of University of Sulaimanyia), Vol.7, No.2, pp.43-66.
- Oliver N., Hantzpergue P., Gaillard C., Pittet B., Leinfelder R.R., Schmid D.U., and Pamela, J.W.G., 1998.** Sedimentary structures and depositional environments. Department of Geology, Georgia Perimeter College, Clarkston, GA 30121. 15pp.
- Parsons, M. Ralph, Engineering Company, 1957.** Groundwater Resource of Iraq, vol: 12, Sulaimaniya Liwa and area of north of Khaniqin.
- Pearce, J. A. and Cann, J. R., 1973.** Tectonic setting of volcanic rocks determined using trace elemnt analysis. *Earth Plant-Sci. lett.*, Vol. 19, pp. 290-300.
- Pettijohn, F. J., 1975.** Sedimentary Rocks, 3rd edit., Harper and Row Publ. Co., 627pp.
- Potter, P.E., Maynard, J. B. and Pryor, W.A., 1980.** Sedimentology of Shale: Study Guide and Reference Source, Springer-Verlage, 306 p.
- Pye, K., and Tsoar, H., 1987.** The mechanics and geological implications of dust transport and deposition in deserts with particular reference to loess formation and dune sand diagenesis in the northern Negev, Israel, *in* Frostick, L. and Reid, I., eds., Desert sediments: Ancient and modern: Geological Society [London] Special Publication no 35, p. 139-156.
- Rankhama, K. and Shahama, Th. G., 1950.** Geochemistry. Book University of Chicago. Press. 912p.
- Rao, C. P., 1986.** Geochemistry and Temperature-water carbonates, Tasmania, Australia, *Marine Geology*, 71, P(363-370). Elsevier Science Pbl. B. V. Amsterdam.
- Razuqi, W., 1980.** The properties of building materials. Internal report. Directorate General for Geological Survey and Mining, Baghdad-Iraq.
- Read, H. H., 1973.** Rutley's element of mineralogy. 26th Edition Thomas Murby and Co. 560p.
- Reading, H. G., 1986.** Sedimentary Environments and Facies. Blackwell scientific publications, Second edition, Oxford London Edinburgr. 612 p.
- Rechard, P. W. and Hawkes, H. E., 1958.** Adsorption of copper on quartz. *Geochim. et. Cosmochim. Acta.*, Vol.15, p p. 6-9.

- Reijers, T.J.A. and Hsu, K.L.J., 1985.** Manual of Carbonate Sedimentology: A Lexicographical Approach. 302p.
- Rose, A. W., Hawkes, H. E. and Webb, J. S., 1979.** Geochemistry and Mineral Exploration, 2nd Edition. Academic Press. London. 657p.
- Ronov, A. B., and Ermiskina, A. I. 1959.** Distribution of manganese in sedimentary rocks. Geochemistry. (USSR). (English transel), pp. 254-278.
- Runnel, D. D., and Schleicher, J. A., 1956** , Chemical composition of Eastern Kansan Limestone, Geological Survey, Kansas Bull, Vol.119, No.3, PP(83-103).
- Sadooni, F.N. and Alsharhan, A.S., 2003.** Stratigraphy and microfacies and petroleum potential of the Maudod Formation (Albian-Cenomania) in the Arabian Gulf basin. AAPG Bulleton, Vol.87. , No.10., pp. 1653-1680.
- Salim, A. A. and Duff, P. Mcl. D., 1974.** Carbonate facies in the Lower Carboniferous (Visen) of St. Monance, East five Scotland. Jour. Sed. Petrology. Vol. 44, pp. 806-815.
- Shapiro, R. S., 2000.** A comment on the systematic confusion of thrombolites. Palaios, V,15, pp.166-169,Tulsa.
- Shearman, D. J. and Shirmuhammad, N. H., 1969.** Distribution of Strontium in dolomites from the French Jura, Nature. Vol. 223, pp. 606-608.
- Siegel, F. R., 1960.** The effect of strontium on the aragonite-calcite ratio of Pleistocene corals. Jour. Sed. Pertology, Vol.30, pp.297-304.
- Siegel, F. R., 1961.** Variation of Sr/CaO ratios and magnesium content in recent carbonate sediment of northern Florida Keys area, Journal Sed. Pet. Vol.30, No.2, Positive(336-342).
- Sinjary, W. S., 2006.** Mineralogy and Geochemistry of Pirispiki formation-Northern Thrust zone –Iraq. Unpublished MSc thesis, University of Salahaddin, 137P.
- Sissakian, V. K., 1997.** Geological map of Arbeel and Mahabad Quadrangles. Sheets NJ-38-14 and NJ-38-15.State establishment of geological survey and mining.
- Sissakian, V. K., 2000.** Geological map of Iraq. Sheets No.1, Scale 1:1000000, State establishment of geological survey and mining. GEOSURV, Baghdad, Iraq.
- Sissakian, V. K., 2005.** The stratigraphy of the exposed cretaceous rocks in Iraq, as deduced from the result of the regional detail geological survey (Geoserve 1971-1996). Iraqi Bulletin of geology and mining..Baghdad. vol-1, No.1 pp.1-20.
- Smirnov, A. V. and Nelidov, V. P., 1962.** Report on 1: 200000 Prospecting correlation of Choarta -Sulaimaniya and Penjuin areas. Unpubl. Report, SOM Library, No. 290.

- Stanton, R. E., 1965.** Rapid Methods of Trace analysis for Geochemical Applications., Edward Arnold Pub. London, 96p.
- Steele, K. F. and Wanger, C. H., 1975.** Trace metal relationships in bottom sediments of a fresh water stream, the Buffalo river, Arkansas, Jour. Sed. Petrology., Vol. 45, pp. 310-319.
- Stephen, W. E., Watson S. W., Phillip, P. R. and Weir, J. A., 1975.** Element association and distribution through Lower Paleozoic graptolitic shale sequence in the Southern Upland of Scotland, chem. Geol., Vol. 16, pp. 269-294.
- Stocklin, J., 1968.** Structural history and tectonics of Iran: a review. American Association of Petroleum Geologists Bulletin 52, pp. 1229–1258.
- Stoody, K. D., Lewis, T. and Staintion, C. L., 1980.** Applied Statistical Techniques. John Wiley and Sons., London.
- Taha, Z.A., 2008.** Sedimentology of Late Cretaceous Formation from Kurdistan Region, NE–Iraq. Unpublished MSc thesis, University of Sulaimani, p.140
- Tahrani, K.K., 2006.** Stratigraphy of Iran, (in Persian) Tehran University Press.
- Tamish M., (1988),** Gromathematical and geochemical studies on Egyptian phosphorite deposits, Ph. D. Thesis, Technical Univ., Berlin, 97p.
- Tucker, M. E., 1991.** Sedimentary Petrology, an introduction to the origin of sedimentary rocks .Second edition. 260 p.
- Turekian, K. K., and Carr, M. H., 1960.** The Geochemistry of cromium, cobalt and nickel. Int. Geol. Congress-Norden, pp. 14-26.
- Turekian, K. K., and Imbrie, J., 1966.** The distribution of trace elements in deep sea sediments of Atlantic Ocean. Earth Planet. Sci. Lett., Vol. 1, pp. 161-168
- Turekian, K. K., and Kulp, J. K., 1956.** The Geochemistry of Strontium. Geochim. Cosmochim. Acta. Vol. 10, pp. 245-296.
- Turekian, K. K., and Wedepohl, K. H. 1961.** Distribution of the elements in some major units of the earth's crust. Geol. Soc. Am. Bull .Vol. 72, pp. 175-191.
- Van Hauten, , F. B., 1962.** Climate significunt of Red Beds in Narin A. E. M. Ed., Descriptive Paleoclimatology, New York. Interscience. pp. 89-139.
- Veizer, J. and Demovic, R., 1974.** Strontium as a tool in facies analysis, Jour. Sed. Petrology, Vol.44, pp. 93-115.
- Waddington, A.P.E., 1955.** Report on Geological survey of the Halabja area. Site Inv. Co. Report, SOM Library, NO. 266, Baghdad.
- Wallace, M. W., 1990.** Origin of dolomitization of the Barbowire, Canning Basin, Western Australia. Journal of the IAS, Vol.37, No.1, P.(105-122).

WalKer, T. R., 1967a. Colour of recent sediments in tropical maxico; A contribution to the origin of Red Bed; Geol. Soc. America. Bill., Vol. 79, pp. 917-920.

Walness, H.R., 1969. Limestone response to stress: Pressure solution and dolomitization. Journal of Sedimentary Petrology. Vol. **49**, No. 1. 437-462.

Waugh, B., 1970a . Petrology, Provenance and silica diagenesis of the Penrith sandstone (Lower Permian) of North West of England. Jour. Sed. Petrology, Vol.40, P.1226-1240.

Waugh, B., 1970b. Formation of quartz over growths in the Penrith sandstone (Lower Permian) of North West of England as revealed by sacnning microscopy. Sedimentology, Vol.14, P.309-320.

Werner W., 2002. Microbialite morphology, structure and growth: a model of the Upper Jurassic reefs of the Chay Peninsula (Western France).PALAEO Bulletin.193. pp.383-404

Weber, J. N., 1964. Trace element composition of Dolostones and Dolomitic and its bearing on the dolomitic problem. Geochim. Cosmochim. Acta., Vol.28, pp. 1817–1868.

Wigley, P., 1973. The distribution of strontium in limestones of Barbada, West Indies. Sedimentology., Vol.20, pp295- 304.

Wilson, J. L., 1975. Carbonate Facies in Geologic History. Spriger-Verlag,Berlin Heidelbreg New York , 471 p.

Wright, J., 2001. Making loess-sized quartz silt: Data from laboratory simulations and implications for sediment transport pathways and the formation of “desert” loess deposits associated with the Sahara: Quaternary International, v. 76/77, p. 7-19.

Younis, M.T., 1979. Geochemical and Mineralogical studies with Petrographical description of the Miocene Carbonate Rocks in the Eastern part of Jabal Alan, Northern Iraq, Unpublished MSc thesis, University of Mosul.

Appendixes

Appendix (A): Major oxide, Trace Element and Insoluble Residue content in the limestone bulk and insoluble residue samples from Qulqula Formation.

Table (A-1a): Major oxide, Trace Element and Insoluble Residue content in the limestone *bulk samples* from Qulqula Fm in 1st Ridge section.

S.No.	CaCO ₃ %	MgCO ₃ %	Other%	CaO%	MgO%	Al ₂ O ₃ %	SiO ₂ %	Fe ₂ O ₃ %	Na ₂ O%	K ₂ O%	MnO%	P ₂ O ₅ %	CO ₂ %	Co ppm	Cu ppm	Ni ppm	Pb ppm	Zn ppm	Sr ppm	Cr ppm	IR	Total%
5	82.87	17.13	0	43.71	7.30	2.95	4.49	0.16	0.09	0.01	0.01	0.05	42.26	30	6	34	30	16	360	70	10.21	101.08
6	78.23	21.77	0																			
7				40.88	7.60	4.35	5.75	0.11	0.05	0.01	0.01	0.03	40.38	20	8	50	26	44	532	74		99.24
8	73.03	26.97	0																			
9				41.98	8.39	4.16	4.51	0.17	0.03	0.02	0.01	0.04	42.09	28	10	64	34	26	490	76		101.47
10	73.55	26.45	0																			
11				41.19	8.41	3.97	4.52	0.08	0.01	0.01	0.01	0.04	42.03	30	8	54	28	24	350	50		100.32
12	72.76	27.24	0																			
13				40.66	9.31	4.05	4.54	0.09	0.01	0.01	0.01	0.04	42.07	32	8	50	30	30	420	50		100.85
14	71.52	27.71	0.77																			
15				37.81	9.05	6.24	7.06	0.17	0.03	0.04	0.01	0.04	39.54	130	10	40	26	28	270	80		100.05
16	67.41	30.28	2.31																			
17				44.8	6.56	2.04	4.50	0.23	0.12	0.04	0.01	0.05	42.31	100	12	46	34	20	410	100	12.01	100.73
18	74.88	24.44	0.68																			
19				41.08	6.81	5.67	6.66	0.10	0.01	0.01	0.01	0.03	39.67	110	8	54	30	16	340	30		100.11
20	74.61	25.39	0																			
21				46.82	2.42	4.23	6.68	0.13	0.01	0.05	0.01	0.03	39.38	102	10	36	26	20	370	40	8.51	99.81
22	95.7	4.3	0																			

Table (A-1b): Major oxide and Trace Element content in the *Insoluble Residue* samples from Qulqula formation in 1st Ridge section.

S.No.	CaO%	MgO%	Al ₂ O ₃ %	SiO ₂ %	Fe ₂ O ₃ %	Na ₂ O%	K ₂ O%	MnO%	P ₂ O ₅ %	Co ppm	Cu ppm	Ni ppm	Pb ppm	Zn ppm	Sr ppm	Cr ppm	Total%
5	1.15	0.16	41.68	53.48	1.55	0.21	0.57	1.14	0.44	230	26	234	130	216	60	870	100.55
17	1.25	0.33	38.32	57.34	1.52	0.39	0.64	0.05	0.53	1100	62	946	134	200	20	2100	100.82
21	0.42	0.19	29.17	66.56	1.13	0.07	1.74	0.03	0.32	902	25	220	110	205	980	845	99.96

Table (A-2a): Major oxide, Trace Element and Insoluble Residue content in the limestone *bulk samples* from Qulqula Fm in 2nd Ridge section.

S.N o.	CaCO ₃ %	MgCO ₃ %	Other %	CaO%	MgO%	Al ₂ O ₃ %	SiO ₂ %	Fe ₂ O ₃ %	Na ₂ O%	K ₂ O%	MnO%	P ₂ O ₅ %	CO ₂ %	Co ppm	Cu ppm	Ni ppm	Pb ppm	Zn ppm	Sr ppm	Cr ppm	IR	Total%
1	95.87	4.13	0	45.59	1.74	6.95	8.38	0.20	0.11	0.04	0.01	0.04	36.67	100	8	34	60	14	440	30	25.53	99.80
2																						
3	88.92	11.08	0	48.13	2.09	4.16	4.89	0.26	0.13	0.04	0.01	0.03	40.05	96	10	40	40	16	330	40		99.85
4																						
5	94.54	5.46	0	48.97	2.52	3.55	4.24	0.21	0.09	0.03	0.01	0.03	41.18	100	12	60	26	22	290	34		100.88
6																						
7	86.65	13.22	0.13	46.45	4.73	3.55	4.03	0.14	0.06	0.03	0.01	0.03	41.61	94	10	44	24	18	288	36		100.69
8																						
9	93.92	6.08	0	50.65	1.09	3.14	4.23	0.12	0.01	0.02	0.01	0.04	40.94	108	12	50	28	20	290	30		100.31
10																						
11	89.15	10.85	0	45.33	4.83	4.72	5.34	0.20	0.01	0.01	0.01	0.03	40.85	100	6	34	32	14	340	32		101.40
12																						
13	92.92	7.08	0	50.65	2.06	3.06	2.78	0.17	0.02	0.01	0.01	0.03	41.99	94	8	60	34	16	330	28		100.84
14																						
15	89.20	10.80	0	48.41	1.82	7.63	1.72	0.21	0.01	0.01	0.02	0.03	39.98	84	8	50	28	14	330	34		99.91
16																						
17	95.79	4.21	0	49.67	0.50	5.35	5.87	0.23	0.04	0.02	0.01	0.04	39.52	104	10	48	30	34	220	30	18.22	101.29

Table (A-2b): Major oxide and Trace Element content in the *Insoluble Residue* samples from Qulqula formation in 2nd Ridge section.

S.No.	CaO%	MgO%	Al ₂ O ₃ %	SiO ₂ %	Fe ₂ O ₃ %	Na ₂ O%	K ₂ O%	MnO%	P ₂ O ₅ %	Co ppm	Cu ppm	Ni ppm	Pb ppm	Zn ppm	Sr ppm	Cr ppm	Total%
1	1.01	0.19	40.63	55.31	2.70	0.07	0.09	0.02	0.07	210	24	77	580	94	40	330	100.22
17	0.63	0.12	41.78	52.32	3.22	0.39	0.54	0.66	0.13	3105	30	948	150	834	40	480	100.34

Table (A-3a): Major oxide, Trace Element and Insoluble Residue content in the limestone *bulk samples* from Qulqula Fm in 3rd Ridge section.

S.No	CaCO ₃ %	MgCO ₃ %	Othe r%	CaO%	MgO%	Al ₂ O ₃ %	SiO ₂ %	Fe ₂ O ₃ %	Na ₂ O%	K ₂ O%	MnO%	P ₂ O ₅ %	CO ₂ %	Co ppm	Cu ppm	Ni ppm	Pb ppm	Zn ppm	Sr ppm	Cr ppm	IR	Total%
1				43.66	4.71	5.27	6.04	0.37	0.34	0.02	0.01	0.04	39.39	106	14	42	30	18	380	38		99.90
2	73.64	25.48	0.88																			
3				48.83	2.52	3.36	4.08	0.18	0.03	0.00	0.01	0.03	41.07	110	8	34	22	16	520	42	9.49	100.20
4	75.00	8.94	16.06																			
5	76.41	23.59	0.00	46.87	4.18	3.29	4.51	0.09	0.01	0.01	0.01	0.03	41.34	106	6	30	26	18	300	32		100.39
6	79.11	20.89	0.00																			
7	73.55	24.96	1.49	44.21	6.30	2.91	3.21	1.75	0.04	0.05	0.02	0.03	41.57	102	10	32	22	24	360	26	3.52	100.15
8																						
9	80.79	19.21	0.00	44.07	5.31	4.84	5.77	0.31	0.07	0.03	0.01	0.03	40.38	86	16	40	24	18	480	44		100.90
10																						
11	82.51	16.21	1.28	42.12	5.84	2.76	3.36	5.98	0.05	0.07	0.02	0.03	39.42	84	12	38	28	44	380	26	5.23	99.70
12	72.86	21.55	5.59																			
13				40.21	6.73	6.20	7.50	0.27	0.16	0.05	0.02	0.03	39.90	82	10	60	22	28	320	32		101.12
14	78.28	17.38	4.35																			
15	81.73	18.27	0.00	46.17	4.21	4.16	4.54	0.17	0.09	0.04	0.02	0.04	40.83	100	12	30	24	18	330	34		100.32

Table (A-3b): Major oxide and Trace Element content in the *Insoluble Residue* samples from Qulqula formation in 3rd Ridge section.

S. N	CaO %	MgO%	Al ₂ O ₃ %	SiO ₂ %	Fe ₂ O ₃ %	Na ₂ O%	K ₂ O%	MnO%	P ₂ O ₅ %	Co ppm	Cu ppm	Ni ppm	Pb ppm	Zn ppm	Sr ppm	Cr ppm	Total%
3	0.42	0.30	43.99	51.31	3.21	0.30	0.66	0.11	0.07	2110	35	240	10	1250	20	2040	100.94
7	1.01	1.01	34.86	57.53	3.49	0.27	1.39	0.25	0.03	4522	20	215	42	920	40	726	100.48
11	0.92	0.98	30.56	62.58	2.97	0.26	1.24	0.24	0.03	985	95	132	64	1420	10	625	100.11

Table (A-4a): Major oxide, Trace Element and Insoluble Residue content in the limestone *bulk samples* from Qulqula Fm in 4th Ridge section.

S.N o.	CaCO ₃ %	MgCO ₃ %	Other %	CaO%	MgO%	Al ₂ O ₃ %	SiO ₂ %	Fe ₂ O ₃ %	Na ₂ O %	K ₂ O%	MnO%	P ₂ O ₅ %	CO ₂ %	Co ppm	Cu ppm	Ni ppm	Pb ppm	Zn ppm	Sr ppm	Cr ppm	IR	Total%
1				42.26	11.01	0.72	1.29	0.31	0.23	0.00	0.01	0.04	45.18	66	8	44	34	20	400	40	5.25	101.11
2	73.18	22.40	4.42																			
3				42.82	4.68	6.69	7.46	0.06	0.06	0.00	0.01	0.04	38.70	50	4	38	24	18	280	48		100.55
4	77.00	10.77	12.23																			
5	77.41	22.50	0.09	44.77	5.14	3.48	5.56	0.15	0.01	0.01	0.01	0.03	40.74	110	6	26	28	18	540	36		99.99
6	80.20	18.80	1.00																			
7	75.55	20.00	4.45	42.26	5.67	5.29	6.04	1.60	0.03	0.07	0.02	0.03	39.35	120	10	38	22	46	460	30		100.44
8																						
9	82.11	17.21	0.68	45.47	4.84	4.23	4.71	0.23	0.09	0.05	0.01	0.03	40.97	84	14	44	24	16	240	46		100.70
10																						
11	80.54	17.50	1.96	45.89	6.97	1.47	1.89	0.25	0.06	0.10	0.02	0.03	43.61	82	12	30	24	24	398	28	4.12	100.34
12	70.99	24.45	4.56																			
13				45.05	3.71	5.90	6.20	0.12	0.19	0.04	0.02	0.03	39.41	90	10	60	24	30	360	32		100.73
14	82.22	15.30	4.35																			

Table (A-4b): Major oxide and Trace Element content in the *Insoluble Residue* samples from Qulqula formation in 4th Ridge section.

S. N	CaO %	MgO%	Al ₂ O ₃ %	SiO ₂ %	Fe ₂ O ₃ %	Na ₂ O%	K ₂ O%	MnO%	P ₂ O ₅ %	Co ppm	Cu ppm	Ni ppm	Pb ppm	Zn ppm	Sr ppm	Cr ppm	Total %
1	1.32	0.56	46.10	50.37	2.08	0.55	0.17	0.13	0.04	306	28	442	102	110	20	840	101.51
11	1.18	0.51	45.05	49.71	2.12	0.32	0.58	0.27	0.03	482	112	230	84	124	40	428	99.93

Table (A-5a): Major oxide, Trace Element and Insoluble Residue content in the limestone *bulk samples* from Qulqula Fm in *Type Locality* section.

S.N o.	CaCO ₃ %	MgCO ₃ %	Other %	CaO%	MgO %	Al ₂ O ₃ %	SiO ₂ %	Fe ₂ O ₃ %	Na ₂ O%	K ₂ O%	MnO %	P ₂ O ₅ %	CO ₂ %	Co ppm	Cu ppm	Ni ppm	Pb ppm	Zn ppm	Sr ppm	Cr ppm	IR	Total%
1	79.17	5.99	14.85	45.33	0.76	1.32	13.10	0.46	0.98	0.29	0.03	1.94	36.40	110	18	32	28	62	450	34	16.12	100.70
2																						
3	94.59	5.41	0.00	48.13	1.99	0.83	8.77	0.09	0.01	0.01	0.07	0.03	39.94	70	8	30	22	36	190	28		99.90
4																						
5	94.02	5.98	0.00	49.81	1.06	1.55	8.17	0.07	0.01	0.01	0.02	0.05	40.24	64	10	20	26	38	290	38		101.04
6																						
7	93.70	6.30	0.00	48.27	3.63	2.91	3.20	0.09	0.01	0.01	0.02	0.05	41.84	74	8	20	20	34	280	26	8.12	100.09
8																						
9	93.21	6.79	0.00	50.09	2.54	2.83	3.16	0.07	0.01	0.01	0.01	0.05	42.07	70	8	18	18	20	310	22		100.89
10																						
11																						

Table (A-5b): Major oxide and Trace Element content in the *Insoluble Residue* samples from Qulqula formation in *Type Locality* section.

S. N	CaO%	MgO%	Al ₂ O ₃ %	SiO ₂ %	Fe ₂ O ₃ %	Na ₂ O%	K ₂ O%	MnO%	P ₂ O ₅ %	Co ppm	Cu ppm	Ni ppm	Pb ppm	Zn ppm	Sr ppm	Cr ppm	Total%
1	0.56	0.10	4.01	87.81	1.60	0.28	0.87	0.16	4.48	520	32	152	60	820	40	122	100.05
7	0.45	0.07	43.50	50.05	0.79	0.06	0.13	0.17	5.24	184	12	122	58	854	10	112	100.61

Table (A-6a): Major oxide, Trace Element and Insoluble Residue content in the limestone *bulk samples* from Qulqula Fm in *Kaolos section*

S. N	CaCO ₃ %	MgCO ₃ %	Other %	CaO%	MgO%	Al ₂ O ₃ %	SiO ₂ %	Fe ₂ O ₃ %	Na ₂ O%	K ₂ O%	MnO%	P ₂ O ₅ %	CO ₂ %	Co ppm	Cu ppm	Ni ppm	Pb ppm	Zn ppm	Sr ppm	Cr ppm	IR	Total%
1	71.35	20.37	8.28	41.56	7.96	4.19	4.12	1.65	0.02	0.40	0.03	0.05	41.30	80	10	20	22	24	250	30	10.62	101.32
2																						
3	78.44	18.20	3.36	43.66	4.78	4.18	6.38	1.22	0.02	0.16	0.03	0.04	39.47	94	14	40	26	16	220	34	12.12	99.97
4																						
5	88.21	11.79	0	47.85	3.38	3.25	4.76	0.06	0.01	0.01	0.02	0.04	41.24	88	6	20	22	26	250	32		100.67
6																						
7	77.2	22.8	0	44.77	6.90	2.31	4.25	0.18	0.02	0.06	0.02	0.17	42.66	86	8	34	28	14	230	28		101.37
8																						
9	89.53	10.47	0	45.05	4.66	4.35	5.26	0.44	0.01	0.10	0.04	0.13	40.44	82	16	90	20	20	490	42		100.55

Table (A-6b): Major oxide and Trace Element content in the *Insoluble Residue* samples from Qulqula formation in *Kaolos section*

S. N	CaO%	MgO%	Al ₂ O ₃ %	SiO ₂ %	Fe ₂ O ₃ %	Na ₂ O%	K ₂ O%	MnO%	P ₂ O ₅ %	Co ppm	Cu ppm	Ni ppm	Pb ppm	Zn ppm	Sr ppm	Cr ppm	Total%
1	0.9794	0.36	34.62	57.38	3.23	0.04	1.40	1.23	0.35	400	30	110	42	104	10	120	99.67
3	0.5877	0.40	41.95	52.46	3.51	0.05	0.67	0.49	0.13	880	44	160	52	98	15	110	100.37

Table (A-7a): Major oxide, Trace Element and Insoluble Residue content in the limestone *bulk* samples from Qulqula Fm in *KaolosZ* section

S.N o.	CaCO ₃ %	MgCO ₃ %	Other %	CaO%	MgO%	Al ₂ O ₃ %	SiO ₂ %	Fe ₂ O ₃ %	Na ₂ O%	K ₂ O%	MnO%	P ₂ O ₅ %	CO ₂ %	Co ppm	Cu ppm	Ni ppm	Pb ppm	Zn ppm	Sr ppm	Cr ppm	IR	Total%
2	69.35	22.37	8.28	40.16	7.79	4.18	7.32	1.48	0.02	0.40	0.03	0.04	40.02	77	8	22	88	75	320	50		101.50
5	70.42	20.20	9.38	43.52	4.26	5.50	6.15	1.33	0.02	0.14	0.03	0.04	38.80	90	24	55	20	10	200	30	12.12	99.82
7	80.21	8.79	11.00	49.25	2.70	2.10	4.46	0.07	0.01	0.01	0.03	0.04	41.59	80	8	28	20	36	240	42	10.62	100.32
9	72.20	26.80	1.00	42.26	5.24	3.82	8.34	0.19	0.02	0.07	0.01	0.10	38.88	806	8	30	48	24	233	22		99.04
12	82.50	17.47	0.03	45.05	3.67	4.72	6.31	0.45	0.01	0.11	0.05	0.13	39.35	80	18	92	25	40	660	52		99.95
14	75.13	24.41	0.46	42.26	4.96	6.05	8.25	0.37	0.01	0.12	0.03	0.12	38.57	92	10	99	28	32	600	30		100.82
17	72.13	20.11	7.76	42.68	3.33	6.05	10.34	0.47	0.01	0.09	0.06	0.11	37.12	84	15	89	22	18	390	40		100.33

Table (A-7b): Major oxide and Trace Element content in the *Insoluble Residue* samples from Qulqula formation in *kaolos* section

S.No .	CaO%	MgO%	Al ₂ O ₃ %	SiO ₂ %	Fe ₂ O ₃ %	Na ₂ O%	K ₂ O%	MnO%	P ₂ O ₅ %	Co ppm	Cu ppm	Ni ppm	Pb ppm	Zn ppm	Sr ppm	Cr ppm	Total %
5	0.59	0.38	42.04	51.69	3.52	0.05	0.07	0.49	0.14	840	40	190	82	120	21	100	99.11
7	1.09	0.35	34.43	57.38	3.23	0.04	1.49	1.06	0.37	450	31	120	45	104	20	220	99.53

Table (A-8a): Major oxide, Trace Element and Insoluble Residue content in the limestone *bulk samples* from Qulqula Fm in *Tawella section*.

S.N o.	CaCO ₃ %	MgCO ₃ %	Other %	CaO%	MgO%	Al ₂ O ₃ %	SiO ₂ %	Fe ₂ O ₃ %	Na ₂ O %	K ₂ O%	MnO%	P ₂ O ₅ %	CO ₂ %	Co ppm	Cu ppm	Ni ppm	Pb ppm	Zn ppm	Sr ppm	Cr ppm	IR	Total%
1	87.67	12.33	0.00	50.65	0.66	2.42	5.39	0.14	0.05	0.07	0.03	0.04	40.46	88	26	72	26	24	220	30	10.62	99.96
2	75.17	23.47	1.36																			
3																						
4																						
5	64.71	28.59	6.70	40.86	0.50	6.54	18.02	0.50	0.25	0.01	0.04	0.07	32.60	98	18	40	40	18	330	28	12.12	99.43

Table (A-8b): Major oxide and Trace Element content in the *Insoluble Residue* samples from Qulqula formation in *Tawella section*.

S.N o.	CaO%	MgO%	Al ₂ O ₃ %	SiO ₂ %	Fe ₂ O ₃ %	Na ₂ O%	K ₂ O%	MnO%	P ₂ O ₅ %	Co ppm	Cu ppm	Ni ppm	Pb ppm	Zn ppm	Sr ppm	Cr ppm	Total%
1	1.679	1.41	40.21	53.95	1.36	0.17	0.22	0.42	0.30	550	76	775	56	185	40	830	99.96
5	1.2593	1.58	38.89	55.73	1.50	1.15	0.04	0.13	0.76	208	78	120	90	118	22	105	101.11

Table (A-9a): Major oxide, Trace Element and Insoluble Residue content in the limestone *bulk samples* from Qulqula Fm in *Gali section*.

S.N o.	CaCO ₃ %	MgCO ₃ %	Other %	CaO %	MgO%	Al ₂ O ₃ %	SiO ₂ %	Fe ₂ O ₃ %	Na ₂ O%	K ₂ O%	MnO%	P ₂ O ₅ %	CO ₂ %	Co ppm	Cu ppm	Ni ppm	Pb ppm	Zn ppm	Sr ppm	Cr ppm	IR	Total%
1	75.5	12.37	12.13	39.18	3.78	5.12	16.74	1.44	0.01	0.28	0.03	0.04	34.87	67	9	32	80	70	330	55		101.55
3	90.5	5.20	4.30	48.55	3.43	1.91	3.79	1.35	0.03	0.11	0.03	0.05	41.84	80	14	45	22	15	100	38	10.20	101.13
4																						
5	85.21	8.79	6.00	47.85	3.02	4.18	4.89	0.11	0.01	0.01	0.03	0.04	40.84	77	8	20	20	32	244	42		101.03
7	77.2	10.80	12.00	43.66	3.45	5.33	9.77	0.15	0.01	0.07	0.01	0.05	38.02	706	10	44	40	28	230	20		100.63
9	89.5	8.47	2.03	48.69	2.82	2.08	4.39	0.18	0.01	0.12	0.07	0.10	41.28	70	16	110	20	40	660	54		99.83
10																						
11	90.13	7.41	2.46	52.05	1.39	1.51	1.83	0.30	0.01	0.10	0.04	0.12	42.36	72	8	120	38	32	680	20	8.20	99.82
12																						
13																						
15	78.13	14.41	7.46	45.05	3.47	5.48	7.14	0.30	0.01	0.24	0.02	0.18	39.13	82	10	99	40	33	700	38		101.13
16																						
17	92.11	7.11	0.78	49.67	1.68	2.27	4.78	0.45	0.01	0.08	0.05	0.10	40.80	80	15	88	22	28	490	30		99.96

Table (A-9b): Major oxide and Trace Element content in the *Insoluble Residue* samples from Qulqula formation in *Gali section*.

S. N	CaO%	MgO%	Al ₂ O ₃ %	SiO ₂ %	Fe ₂ O ₃ %	Na ₂ O%	K ₂ O%	MnO%	P ₂ O ₅ %	Co ppm	Cu ppm	Ni ppm	Pb ppm	Zn ppm	Sr ppm	Cr ppm	Total%
3	0.49	0.09	4.52	87.80	1.62	2.84	0.75	0.13	3.18	420	30	192	55	720	20	422	101.61
11	0.546	0.07	43.93	50.05	0.63	0.05	0.12	0.17	3.95	194	16	143	66	894	15	118	99.67

Appendix (B): XRD patterns of some black limestone powder bulk and insoluble residue samples illustrating the diffraction maximum pattern of Calcite and little Kaolinite & Quartz

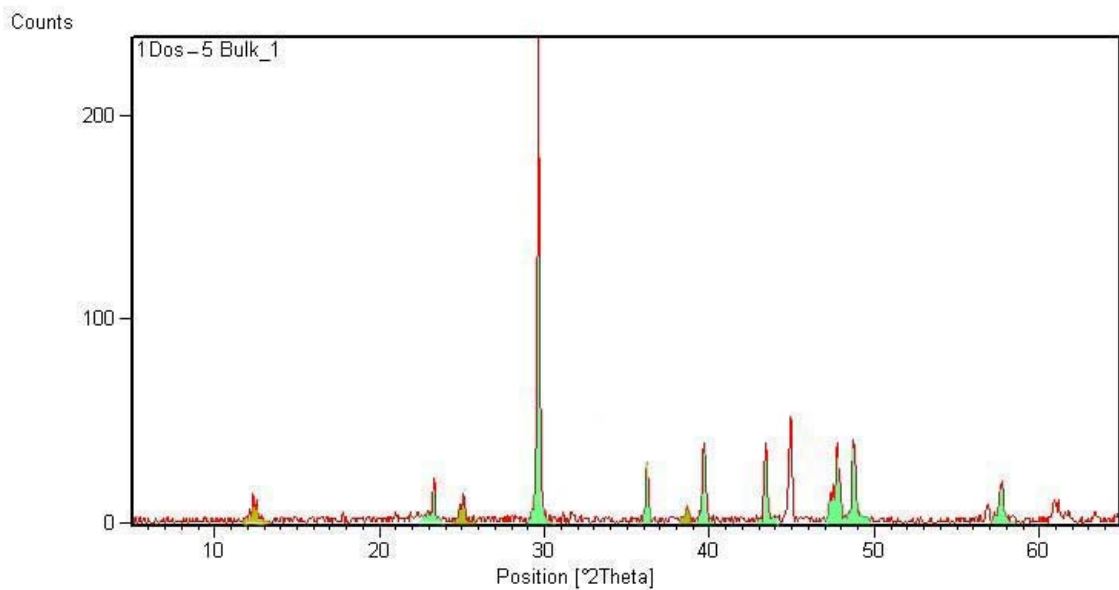


Fig (B-1): XRD patterns of black limestone powder bulk sample No.1Dos-5 at the bottom of the 1st Ridge illustrating the diffraction maximum pattern of Calcite and little Kaolinite.

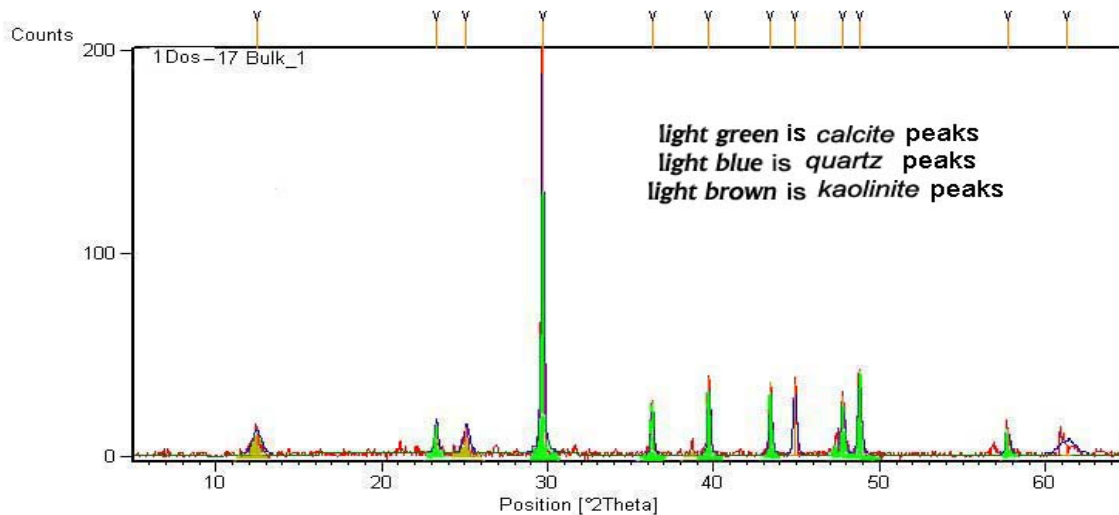


Fig (B-2): XRD patterns of black limestone powder *bulk sample No. 1Dos-17* at the middle of the 1st Ridge illustrating the diffraction maximum pattern of Calcite and little Kaolinite & Quartz. *bulk samples No.1Dos-5, No. 1Dos-21* showed nearly same composition and intensity.

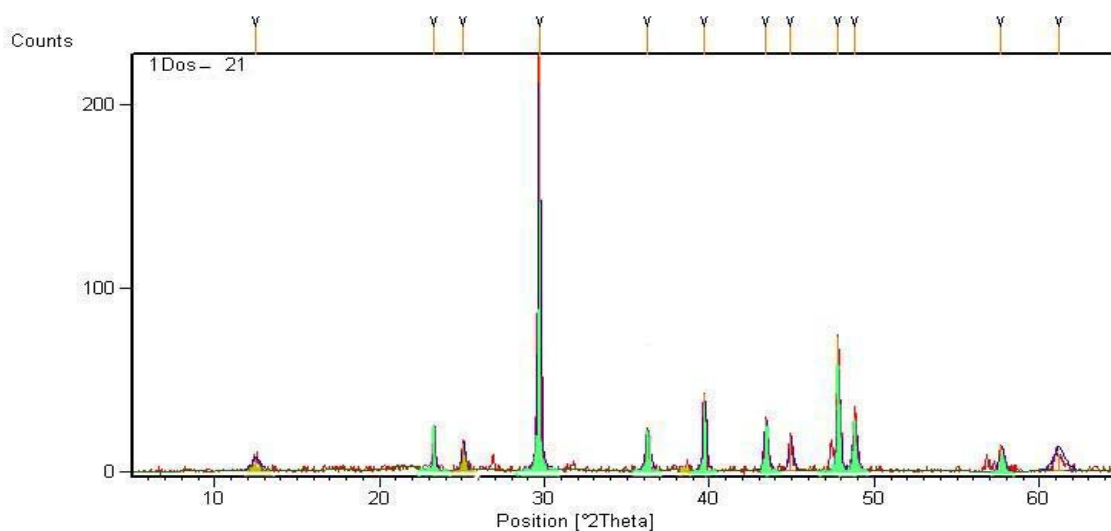


Fig (B-3): XRD patterns of black limestone powder **bulk sample No. 1Dos-21** at the top of the **1st Ridge** illustrating the diffraction maximum pattern of Calcite and little Kaolinite.& Quartz.

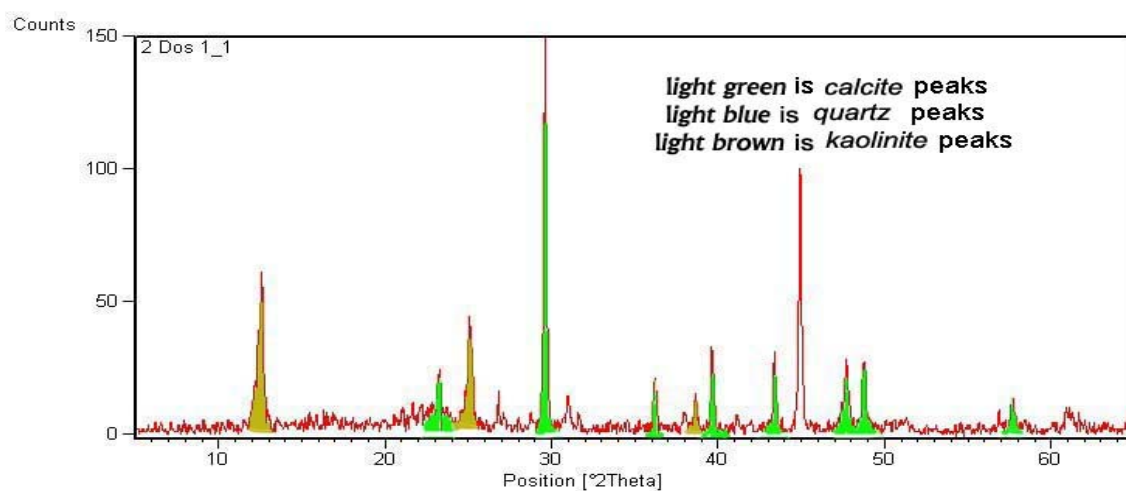


Fig (B-4): XRD patterns of black limestone powder **bulk sample No.2Dos-1** at the bottom of the **2nd Ridge** illustrating the diffraction maximum pattern of Calcite and little Kaolinite. & Quartz.

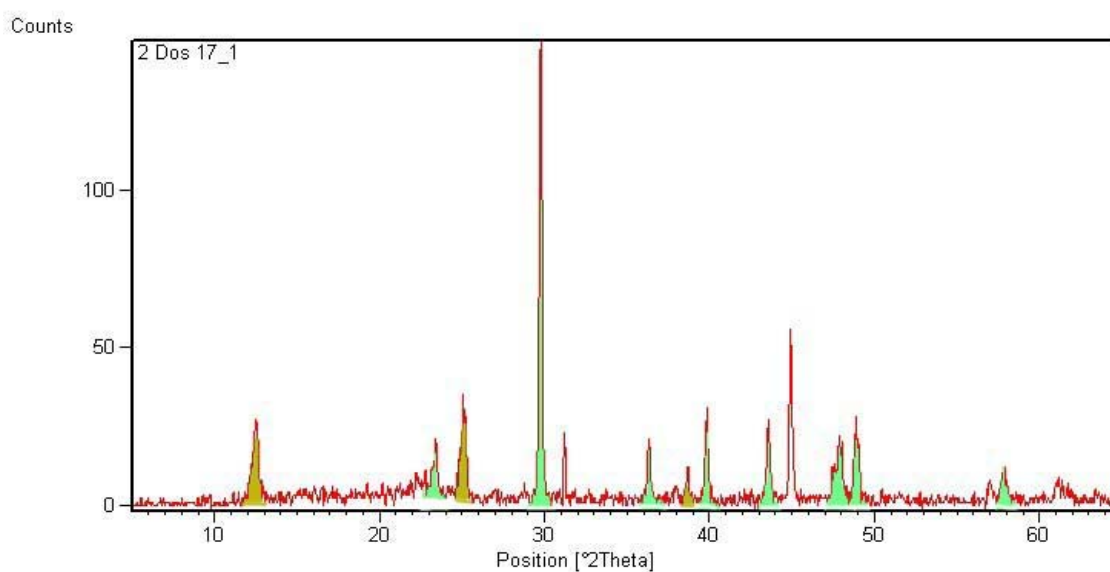


Fig (B-5): XRD patterns of black limestone powder **bulk sample No.2Dos-17** at the top of the **2nd Ridge** illustrating the diffraction maximum pattern of Calcite and little Kaolinite. & Quartz.

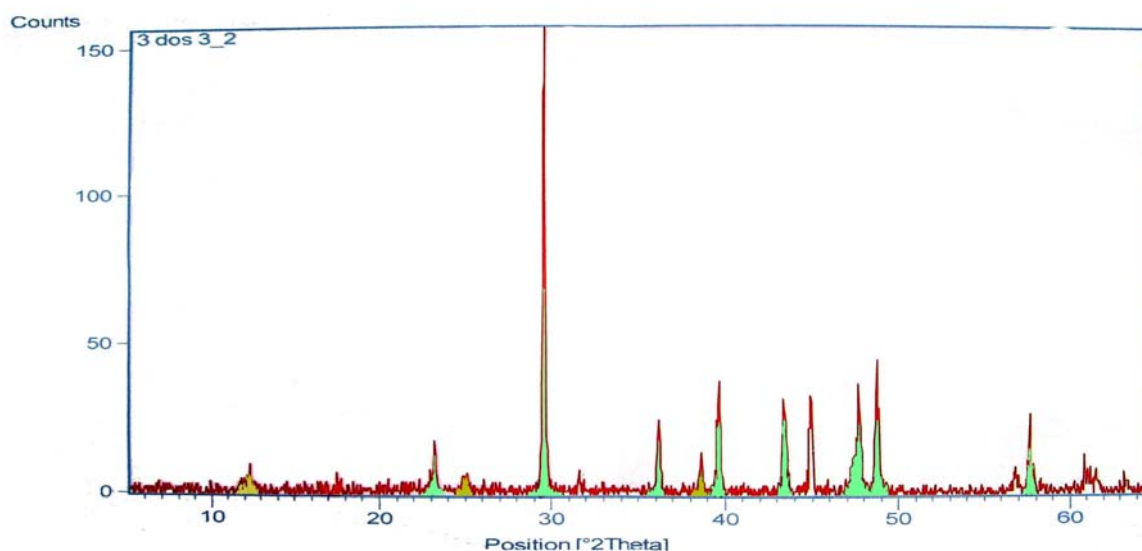


Fig (B-6): XRD patterns of black limestone powder **bulk sample No.3Dos-3** at the bottom of the 3rd Ridge illustrating the diffraction maximum pattern of Calcite and Quartz & little Kaolinite.

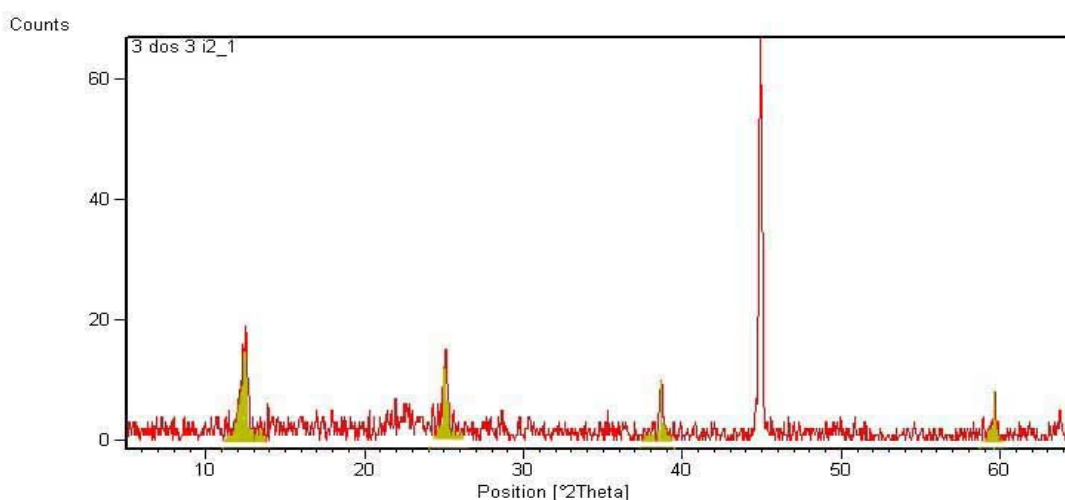


Fig (B-7): X-Ray Diffraction patterns of black limestone powder *IR sample No.3Dos-3* at the bottom of the 3rd Ridge illustrating the diffraction maximum pattern of Kaolinite.

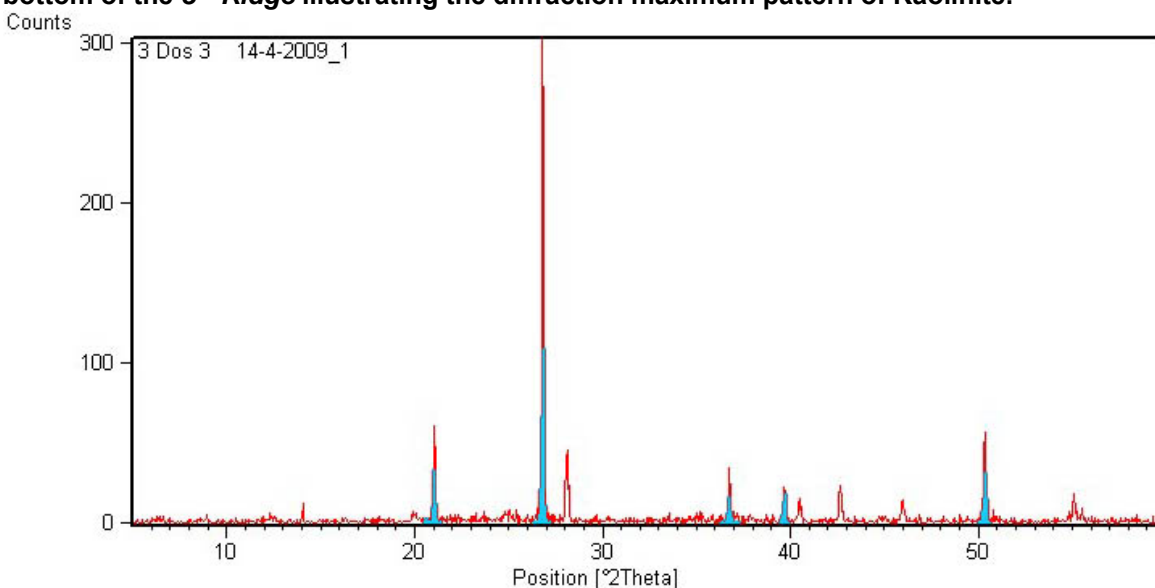


Fig (B-8): X-Ray Diffraction patterns of black limestone powder *IR sample No.3Dos-3, (Heated to 550°C)*, at the bottom of the 3rd Ridge illustrating the disappearance of Kaolinite.

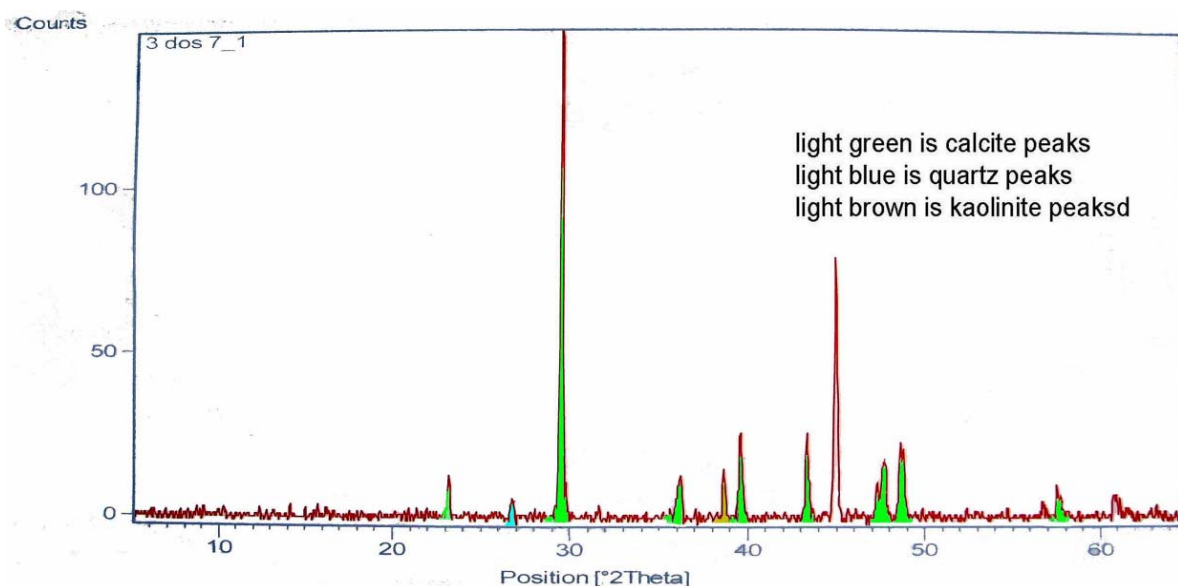


Fig (B-9): XRD patterns of black limestone powder *bulk sample No.3Dos-7* at the middle of the *3rd Ridge* illustrating the diffraction maximum pattern of calcite and little Quartz.

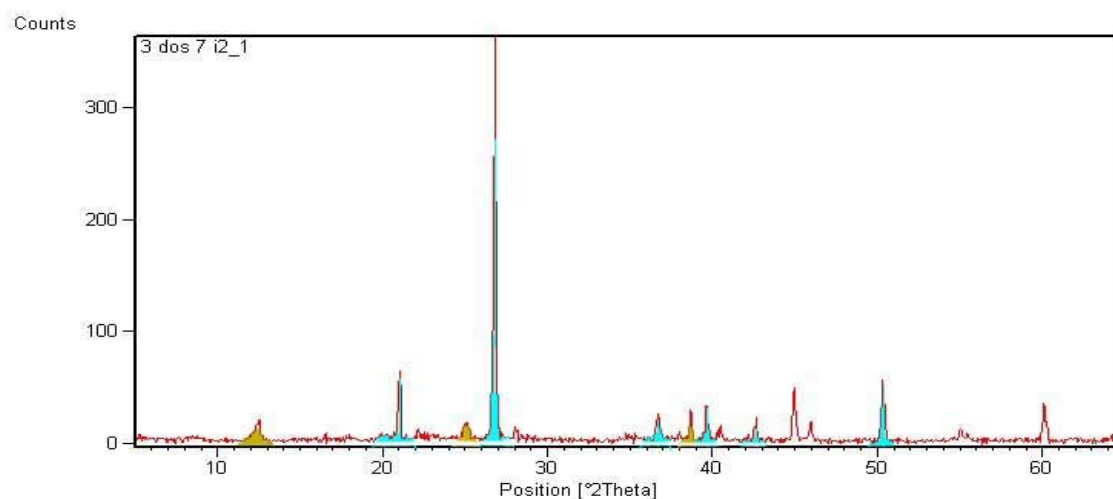


Fig (B-10): XRD patterns of black limestone powder *IR sample No.3Dos-7* at the middle of the *3rd Ridge* illustrating the diffraction maximum pattern of Quartz and little Kaolinite.

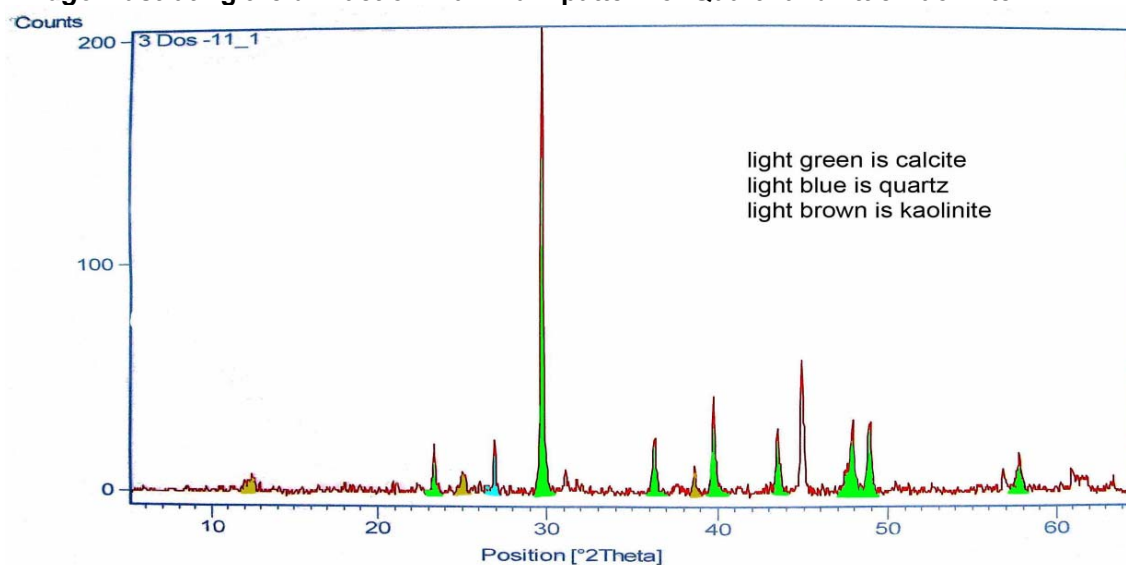


Fig (B-11): XRD patterns of black limestone powder *bulk sample No.3Dos-11* at the top of the *3rd Ridge* illustrating the diffraction maximum pattern of calcite and Quartz & little Kaolinite.

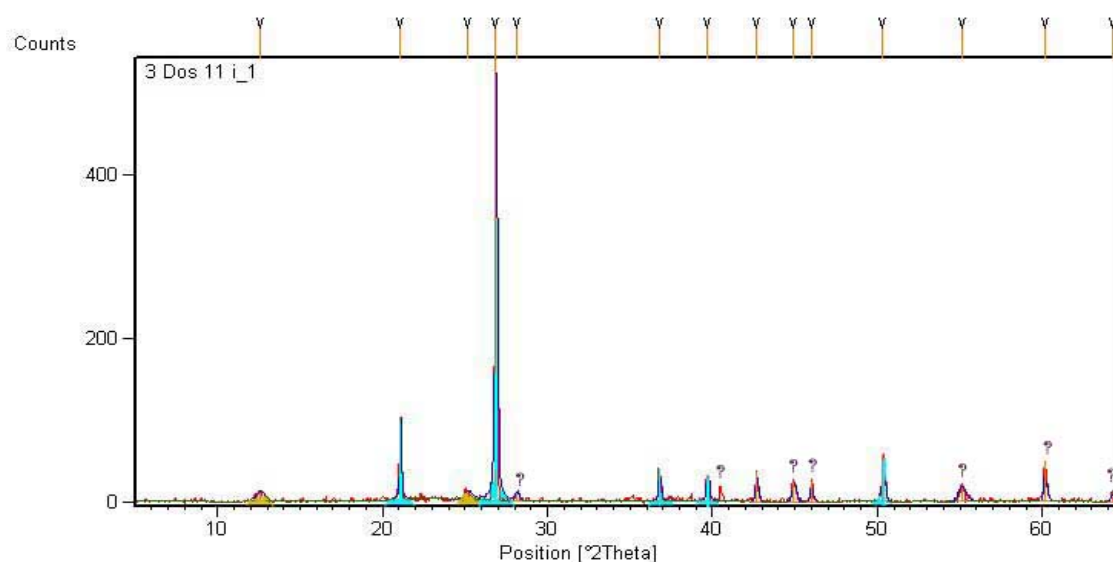


Fig (B-12): XRD patterns of black limestone powder *IR sample No.3Dos-11* at the top of the 3rd Ridge illustrating the diffraction maximum pattern of Quartz & little Kaolinite.

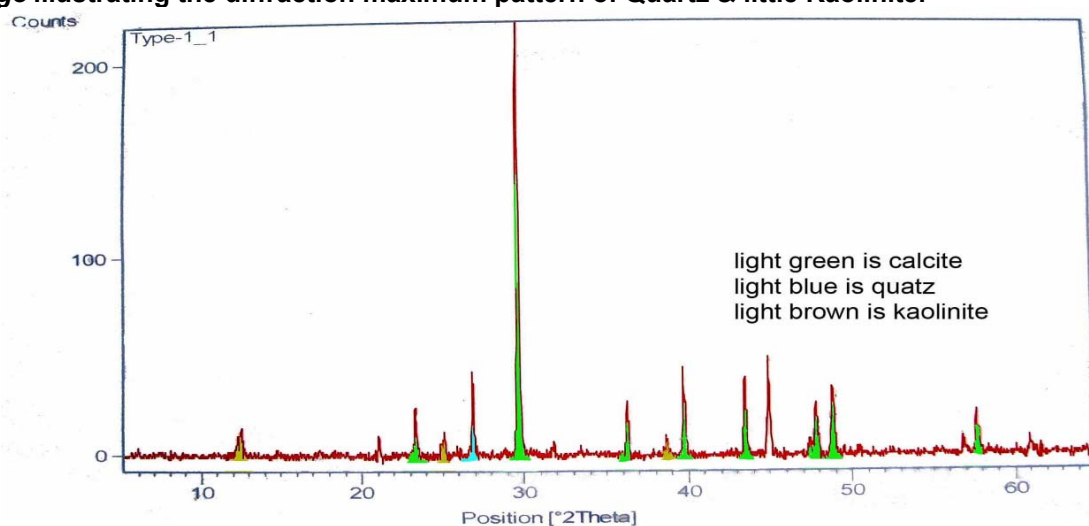


Fig (B-13): XRD patterns of black limestone powder *bulk sample No.Type-1* at the bottom of the Type Locality section illustrating the diffraction maximum pattern of Calcite, Quartz and little kaolinite

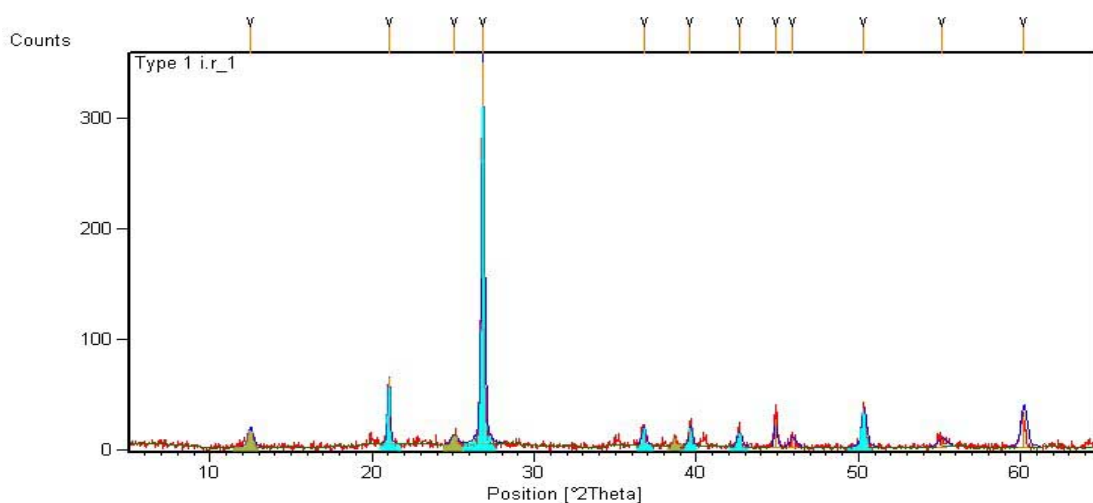


Fig (B-14): XRD patterns of black limestone powder *IR sample No.Type-1* at the bottom of the Type Locality section illustrating the diffraction maximum pattern of Quartz and little kaolinite.

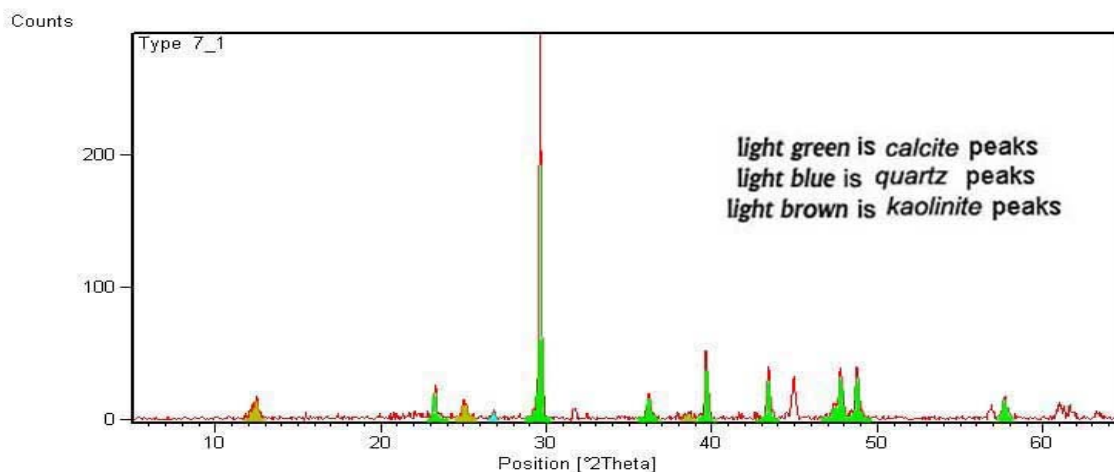


Fig (B-15): XRD patterns of black limestone powder *bulk sample No.Type-7* at the middle of the *Type Locality* section illustrating the diffraction maximum pattern of Calcite, Kaolinite and very little Quartz.

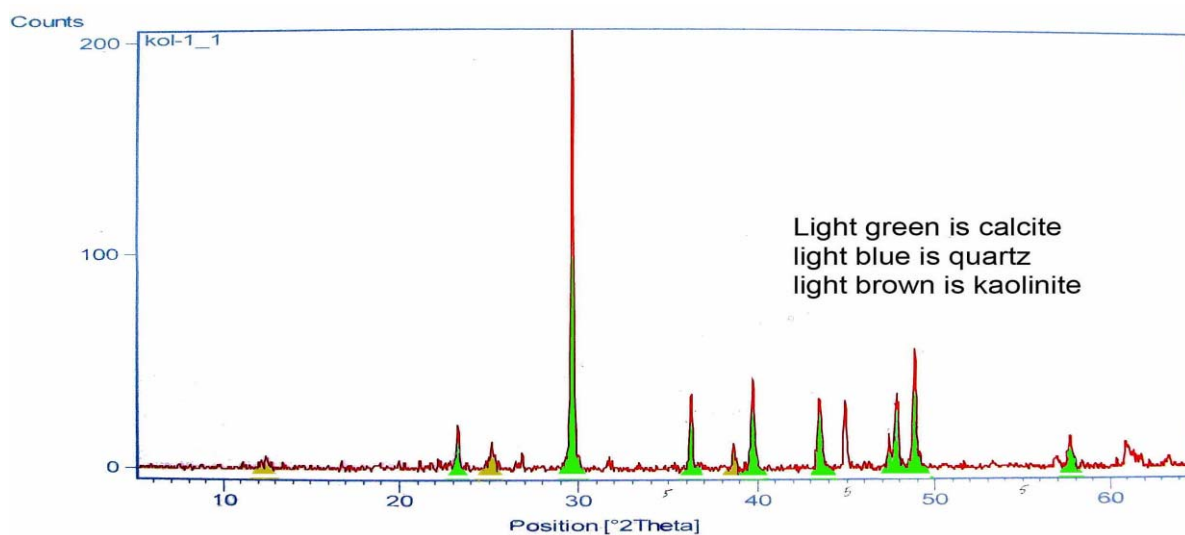


Fig (B-16): XRD patterns of black limestone powder *bulk sample No.Kol-1* at the bottom of the *Kaolose* section illustrating the diffraction maximum pattern of Calcite, and little Quartz & Kaolinite.

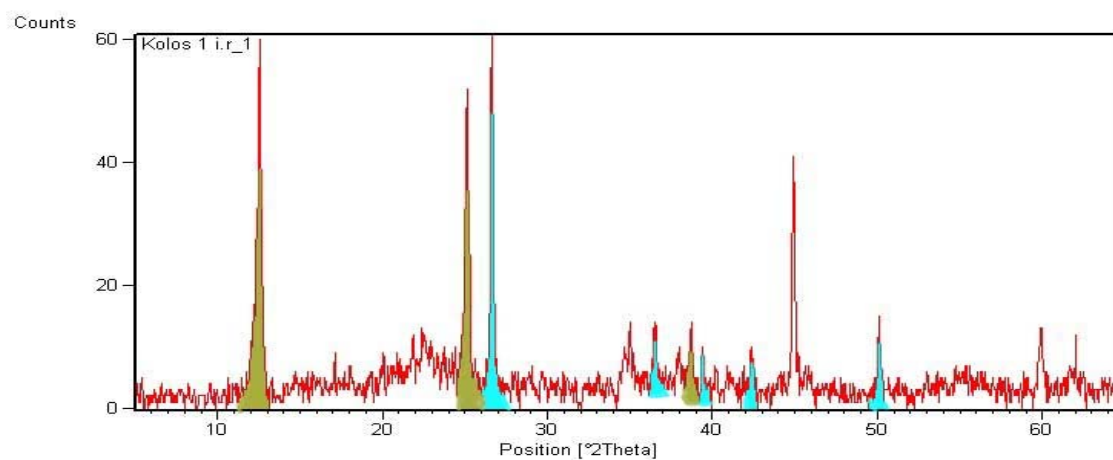


Fig (B-17): XRD patterns of black limestone powder *IR sample No.Kol-1* at the bottom of the *Kaolose* section illustrating the diffraction maximum pattern of Quartz and Kaolinite.

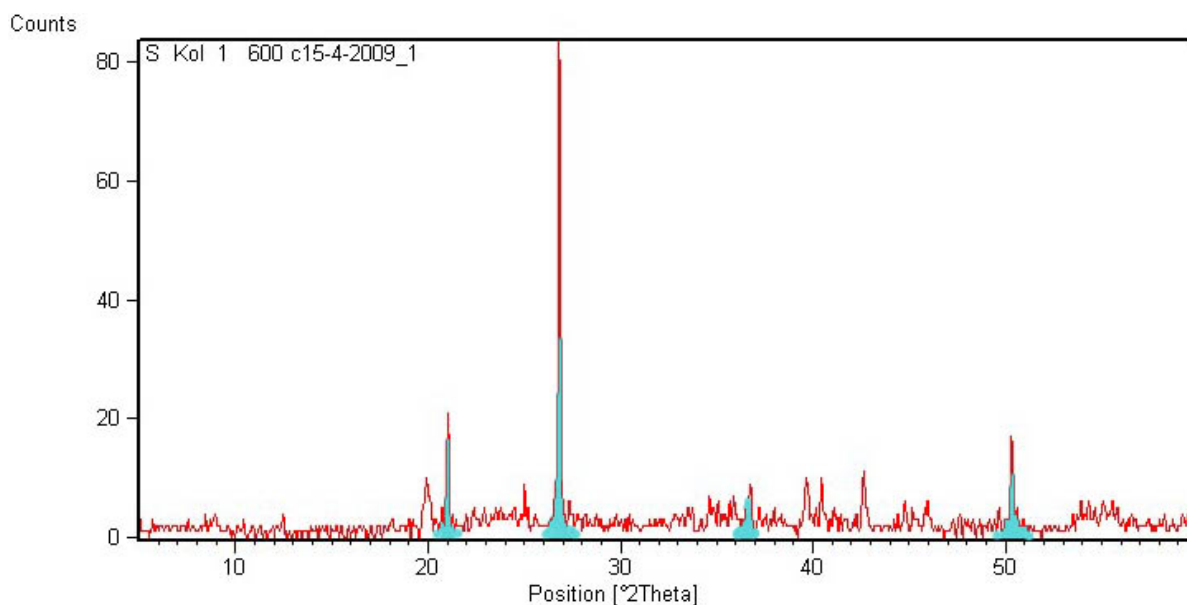


Fig (B-18): XRD patterns of black limestone powder *IR sample No. Kol-1*, (heated to 550°C), at the bottom of the *Kaolose* section illustrating the disappearing of Kaolinite..

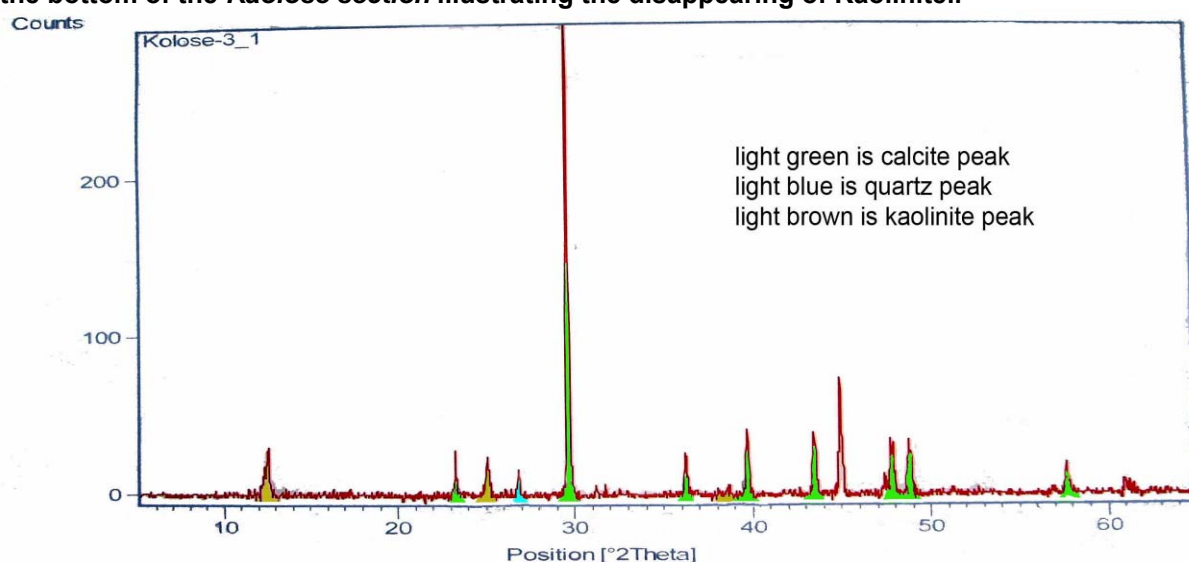


Fig (B-19): XRD patterns of black limestone powder *bulk sample no. Kol-3* at the bottom of the *Kaolose* section illustrating the diffraction maximum pattern of Quartz and Kaolinite.

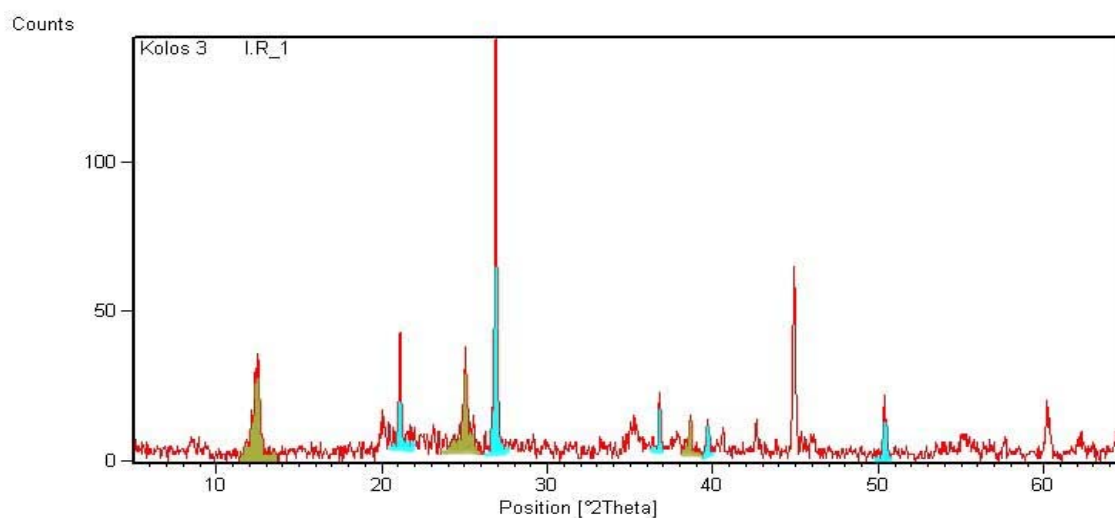


Fig (B-20): XRD patterns of black limestone powder *IR sample no. Kol-3* at the middle of the *Kaolose* section illustrating the diffraction maximum pattern of Calcite, and little Quartz & Kaolinite

**زانستی نیشوو و جیوکیمیای بهرده کلسه یهك له دواى یه که کانی
به شی خواره وهی پیکهاتهی قولقوله له هه ریمی کوردستان،
باکوری رۆژه لاتی عیراق**

نامه یه که

**پیشکەش کراوه به کۆلیجی زانست له زانکۆی سلیمانی وهك به شیکی
ته واوکه ر بۆ به دهست هیانانی دکتۆرای فه لسه فه
له زانستی جیۆلۆجی دا**

له لایهن

سه ردار محمد رهزا بابە شیخ

ماستەر له زانستی جیۆکیمیای دا – زانکۆی به غدا – 2000

به سه رپه رشتی

د. کمال حاجی کریم احمد

پروفسۆری یاریده ده ر

د. حبیب رشید حبیب

پروفسۆر

پوخته

بهشی خوارووی پیکهاتهی قولقوله دهرهکهویت له ناوچهی پالپوهنراوی باکوری رۆژهلاتی عیراق (ههریمی کوردستان) نزیک سنووری عیراق- ئیران. بهشی خوارووی پیک دیت له تییهکیشی زیاد له چوار نووتهشاخی بهردی کلس، که نهستووری ههر یهکیکیان زیاتر له (25) م دهییت، لهگهڵ ناوکاری نهستور له چینه بهردی سلیکا (چیرت) و شیلی کلسی. لیکۆلینهوه لهسهر نهم نووته شاخه بهرده کلسانه کراوه به زانستی جیوکیمییا و نیشتوووهکان له پینج بهشه ناوچهی دهرکهتوودا، بهشه ناوچهکان بریتین له دۆسته دهره، کهولۆس، شوینی بنچینهیی، تهویلله و گهلی. بهرده کلسهکان بهشیوهیهکی گشتی چین چین و دهنکۆلهی گهوره گهورهیان تییدا بهدی نهکریت که نهگهڕیتتهوه بو بنههرتی دهریای تهنکه قول، ههموو نهم بهرده کلسانه پیکهاتوون له دهنکۆلهی رۆشتوو لهگهڵ دۆخی وهک بهردی دهنکۆلهیی، بهردی قایم، کهمیک بهردی قورپن لهگهڵ قوری دهنکۆلهیی که پیکهاتوون له جوړیک یان زیاتر له دهنکۆله رۆشتوووهکانی وهک ووردی دریزکۆله و خر و پارچه بهرد لهگهڵ به بهردبوو که کاریگهری ووردبوون به پلهی جیاواز جیاواز لهسهریان دیاره.

بهشی ناوهراستی ناوچهی لیکۆلینهوه (دۆسه دهره و گهلی) نهستووری یان زیاتره و پیک دیت له بهردی دهنکۆلهی درشت له ناوچهکانی تر. له بهشه ناوچهی تهویللهدا بهرده کلسهکان زیاتر پیک دین له دهنکۆلهی دریزکۆله. لهکاتیکیدا له ناوچهی لیکۆلینهوهی تایپ لۆکالیتی (نزیک دی ی قولقوله) که بریتی یه له تهنها یهک نووته شاخ که پیکهاتوو له (نهگهڵ باوندستون). ماددهی پینبهستیش له بهردهکان دا پیک دیت بهشیوهیهکی سهرکی له قالبه پینبهست (بلوکی سمیت) وه بهشیکی زور کهم بریتی یه لهقوره کلس (لایم مهده).

بهشی خوارووی نهم پیکهاتهیه نهکهویتته سهر پیکهاتهی بالامبو و کویمیتان وه جیاونهبهوه به چینی کۆنگلومیرهیت (0.2 - 2) م نهستور، نهم لیکۆلینهوه یه دا سنووری خوارووی نهم پیکهاتهیه ناسرینراوه به جوړی تهکتونی کۆنگلومیرهیتته کهیش دوا لیکۆلینهوه گهڕینراوتهوه بو پیکهاتهی تانجهرو ههروهها زانراوه که لهگهڵ نهم کۆنگلومیرهیتته چهند چینیکی تهنک له پیکهاتهی شیرانش دهرکهوتوون که کهوتوونه ته ژیر بهشی خوارووی نهم پیکهاتهیه.

کۆنگلومیرهیتته که پیاونه کراوه به دریزایی 35 کم و لهوه نهچی که بهردهوامی ههبی بهدریزایی دووری یه که له کیلگه کهدا، له شاری سهید صادقوه تا شاری چوارتا (6 کم رۆژهلاتی شاری چوارتا)، کۆنگلومیرهیتته که بهشیوهیهکی ریک و زانسته چینی نهچیتته پال کۆنگلومیرهیتته کهی بهشی خوارووی پیکهاتهی تانجهرو (ماستریختیهن). نهم کۆنگلومیرهیتته لهرووی پیکهاتهی جیولۆجی یهوه له پیکهاتهی تانجهرو دهچی؛ ههردووکیان پیک دین له چیرتی رهنگاو رهنگ لهگهڵ پارچه بهردی کلس (لایمستون)، له بهرنهوه نهم دوو کۆنگلومیرهیتته یهک تهمن و یهک سهچاوهی بنههرتیان ههیه که نهگهڕینهوه بو پیکهاتهی تانجهرو که نیشتوو لهکاتهکانی کۆتایی کریتتهیشیهس تهنها جیاوازی یهک که ههبی له بهینیا نهوهیه که کۆنگلومیرهیتته کهی تانجهرو پیک دیت له دهنکۆلهی خر ترو چوونیهک تر وهک لهوهی که تاییهته بهم لیکۆلینهوهیه جیاوازی یه که نهگهڕیتتهوه بو نزیک له ناوچهی چاووگهوه. دهرکهوتنی پیکهاتهی شیرانش و چینه کۆنگلومیرهیتته کهی تانجهرو له ژیر پیکهاتهی قولقولهی رادیولارایتی نهگهڕیتتهوه بو لهوهی که پیکهاتهی قولقوله خزاوه ههگهراوهتهوه بهسهر نهوان دا.

بهشی سهرهوهی نهم پیکهاتهیه بهشیوهی تکتونی دهرهکهویت لهگهڵ یه که چینه بهرده نوێ ترهکان دا ههروهک و زنجیره چینی سوور، تانجهرو وه نیشتوووهکانی سهدهی چوارینی (کواتیرنری-کۆنگلومیرهیتته کهی بهمو) که خزاو و ههگهراونهتهوه بهسهر پیکهاتهی قولقوله دا.

ژینگهی نیشتنی نهم بهردانه بریتی یه له تهخته لیژییهکی کهم قوولی ووزه بهرز. شیکاری بارو دۆخهکانی نیشتن نهوه دهردهخن که بهشی ناوهراستی ناوچهی لیکۆلینهوه که (کهولۆس، دۆسه دهره و گهلی زهلان) نیشتوون له ناوهندی لیژیایی

يەكەدا ئەكاتىك دا ناوچەى تايپ لۆكالتى و تەوئىلە نىشتوون ئە ناوۋەو دەرەۋەى لىژاىى يەكەدا يەك ئەدۋاى يەك. بەشپۈەيەكى گشتى ژىنگەى نىشتن بەرەو كەم قوۋى ئەپوا تا ئە دوورتىن باشوورى رۇژھەلاتەۋە بەرەو دوورتىن باكوورى رۇژئاۋا برۋىن، بەلام بەستوونى كەم قوۋى دەپىت ئەبەشى ناۋەراست دا. جىگىربوونى تىكتۋى پىك ھاتوۋە ئە پانبوون و فراۋانبوونى نىزماى نىشتن كە زۆرگەشەى سەندوۋە ئە كاتەكانى دۇخى سەرەتايى نىوتىسس.

ئە نجامى شىكارى يە كىمىيائى يەكان ئەۋراستى يە دەرەخەن كە ھەر چوار زنجىرەكە يەك سەرچاۋەى بىنەرەتپان ھەبىۋاتە جىبابوونەتەۋە ئەيەك زنجىرە بەھۋى خلىسكان و ھەلگەرەنەۋە، ئەكۋتايى دا خزائە سەرپەكپان (imbrication). ئەمە ئەبەرەۋەى ئەشىكارە كىمىيائى يەكاندا ھىچ گۈرەنىكى يان ژمارەيەكى ناسروشتى تىپىنى ئەكراۋە.

شىكارى يەكانى (XRD) بۇ نىمۋنە تىكراىى يەكان و نىمۋنەى پاشماۋە نەتۋاۋەكان ۋادەرەكەۋن كە زۆرىنەى سەرەكى پىكەتەى بەردى كلىسى زنجىرەكان برىتى يە ئە مەعدەنى كالىسائت ئەگەل كەمپك ئە مەگنىسىوم كالىسائت ، كۋارتز وە كانۇلىنات .

P_2O_5 ئە شۋىنى بىنچىنەىى و دۈسەدەرە (لوۋتە شاخى 1) زىادبوونى پىۋەدىارە ئەبەرەۋەى مەعدەنى ئە پەتائت كە ئە شىكارى MPA دا دەرەكەۋتوۋە.

شىكارى ھىشۋىى Cluster Analysis تىكراى ناۋچەكانى لىكۋلىنەۋەكە، كەژمارەى 60 نىمۋنەۋ 18 سىفەتى جۈراۋجۈرى جىۋكىمىيائى گرتوۋەتە خۇ ئە سى گروۋپى ۋەك : بەردى كلىس ، بەردى قورپىن يا پاشماۋە نەتۋاۋەكان ۋە گروۋپى توخمە دەگمەنەكان.

شىكارى ھۈكارىيەكان Factor Analysis ى تىكراى ناۋچەكانى لىكۋلىنەۋەكە، ھەۋت ھۈكارى سەرەكى شىتەل كىرۋتەۋە كە بەزۋرى كارىگەرن ئە سەر 60 نىمۋنە، گىرەكتىنپان ناسرىنراۋە بە بە ھۈكارى كاربۋنەىت كە مەعدەنى كاۋۋلىناتى تىدا بەدى ئەكرىت. ھۈكارىكى تىرى گىرەك برىتىيە ئە بوونى دەنكۋەى فۇسفات يا مەعدەنى ئە پەتائت ، ھەرۋەھا بوونى نىشانەكانى دوۋبارەكرىستالېوون، Mg-Calcite ۋە شىتەل بوونەۋە Diagenesis

**جيوكيميائية ورسوبية الحجر الجيري المتعاقب في الجزء السفلي
لتكوين القوقولة في إقليم كردستان،
شمال شرق العراق**

رسالة

**مقدمة الى كلية العلوم- جامعة السليمانية كجزء من متطلبات نيل درجة
دكتوراه الفلسفة
في علم الأرض**

من قبل

**سه ردار محمد رضا بابه شيخ
ماجستير في الجيوكيمياء- جامعة بغداد، 2000**

بإشراف

**د. كمال حاجي كريم احمد
أستاذ مساعد**

**د. حبيب رشيد حبيب
أستاذ**

المستخلص

يقع الجزء السجلي لتكوين القولقولة في منطقة الفوالق الزاحفة في شمال شرق العراق (اقليم كوردستان) قرب الحدود العراقية الايرانية. هذا الجزء من التكوين يتكون من اكثر من اربعة تتابعات لصخور كلسية يصل سمك كل واحد منهما الى 25م والمتبادلة مع الحجر الصواني المتطبق السميك والطفل. كل من التتابعات الاربعة تتكون من الحجر الكلسي المتميز بالطباقية ذات البيئة البحرية الضحلة.

درست تتابعات الحجر الجيري رسوبيا" و جيوكيميائيا" في المقاطع الخمسة وهم دوسترة، كولوس، تايب لوكالتي، طويلة و كلي. جميع التتابعات لها نفس الصخرية حيث يحتوي على الحبيبات المنقولة يمثل الدمالق و السرئيات وقطع من الصخور والمتحجرات و بيئات الصخور الحبيبية والصلدة حيث تحتوي على نوع واحد أو أكثر من الحبيبات المنقولة المتأثرة بعمليات المكررة المختلفة. تتكون المادة الرابطة من سمنت كتلي مع قليل من الميكرات، و أيضا" هناك القليل من الصخور الطينية و واكستون.

يتكون الجزء الوسطي لمنطقة الدراسة اللتي تشمل مقطعين هما (دوسترة و كلي) و بسمك أكثر من 2.0-0.2 م. في الدراسة الحالية نوقش اصل طبقة المدملكات و استنتج على انها ترجع الى طبقات المدملكات لتكوين تانجرو، و كذلك تم التأكد من وجود شرائح من تكوين شيرانش مع المدملكات تحت الجزء السفلي لتكوين القولقولة. تم متابعة طبقة المدملكات لمسافة 30 كم من مدينة سيد السادق الي مدينة جوارتا الى الشرق من مدينة جوارتا تندمج (طباقيا و صخاريا) هذه المدملكات مع مدملكات الجزء السفلي لتكوين تانجرو ، لذلك ان المدملكات مشابهة لصخرية مدملكات تكوين تانجرو، حيث كليهما يتكونان من قطع من حجر الصوان (متعدد الالوان) وقطع من حجر الكلس. لذلك اعتبر ان المدملكات المذكورة لهما نفس الاصل والذي يرجع الى المسترخيتان، مع فرق واحد هو ان حبيبات مدملكات تكوين تانجرو لها تكور و فرز افضل من المدملكات المدروسة حاليا بسبب قرب الاخيرة من الصخور المصدر. ويرجع وجود تكوين شيرانش و المدملكات تحت تكوين قولقولة الراديولاريتي الي اندفاع تكوين القلقة فوق كل من تكوين شيرانش و المدملكات.

الجزء العلوي لهذا التكوين لها حدود واضحة و تكتونية مع وحدات طباقية متعددة حديثة العمر، كسلسلة الطبقات الحمراء، تانجرو و ترسبات العصر الرباعي (مدملكات بمو) زاحفين فوق تكوين القولقولة. البيئة الترسيبية لهذه الصخور هي ضحلة لمنحدر وذات الطاقة العالية ، والتحليل السحني لجزء الوسطي لمنطقة الدراسة تشمل المقاطع كولوس، دوسترة و كلي (زلان) تشير الى الترسيب في وسط المنحدر في حين مقطع التايب لوكالتي و طويلة ترسبا في جزئي الداخلي والخارجي حسب الترتيب و بصورة عامة بيئة الترسيب تتحول الى الضحلة من أقصى الجنوب الشرقي الى أقصى الشمال الغربي ، وهذه الحالة مطابقة للتغيرات العمودية اي تكون ضحلة باتجاه الأسفل او القاع.

الوضع التكتوني يتكون من تمدد حوض الترسيب حيث تطورت خلال بداية طور انفتاح النيو-تيش. نتائج التحاليل الكيميائية تشير الى تجانس وتشابه التتابعات الأربعة من حيث الأصل أي منفصلة من تتابع صخري واحد بسبب حدوث فوالق زاحفة و عكسية حيث زحفت الواحد فوق الثاني، وعدم وجود حالات شاذة و قوية او أرقام غير اعتيادية في النتائج الجيوكيميائية يؤكد على ذلك.

أظهرت نتائج تحاليل XRD لنماذج الكلية و الفضالة الغير ذائبة لكل المقاطع المدروسة بأن المعادن الرئيسية المكونة للصخور الجيرية (حسب نسبة التواجد) هي الكاسايت مع نسبة قليلة من Mg-calcite ، Quartz و Kaolinite ولأخرى وتم التأكد على المعدن كاؤولين بأختفاء قمته بعد حرق النموذج لدرجة 550 م°.

وجود معدن الأبتايت في بعض من نماذج مقطع التايب لوكالتي و دوسترة اكدت بواسطة التحليل MPA. التحليل العنقودي لكل النموذج عددها 60 نموذج وبأ استعمال 18 متغير فسرت ثلاثة مجاميع هم مجموعة الكالسايت الرئيسية ، معادن الطينية و الجزء المتبقي غير الذائب و المجموعة الأخيرة تشمل العناصر الشحيحة. أما التحليل العامل فميزت سبع مجاميع متأثرة بالعدد الكلي للنماذج وهي 60 نموذج، و العامل الرئيسي هه الكربونات المحتوي على نسبة قليلة من معدن الكاؤولينايت. العامل الرئيسي الآخر يدل على وجود حبيبات الفوسفات أو معدن الأبتايت، وهناك أيضا" عامل مهم يفسر عملية اعادة التبلور، citeMgO-Cal و عامل عملية Diagenesis .